



National Library
of Canada

Bibliothèque nationale
du Canada

Canadian Theses Service

Service des thèses canadiennes

Ottawa, Canada
K1A 0N4

NOTICE

The quality of this microform is heavily dependent upon the quality of the original thesis submitted for microfilming. Every effort has been made to ensure the highest quality of reproduction possible.

If pages are missing, contact the university which granted the degree.

Some pages may have indistinct print especially if the original pages were typed with a poor typewriter ribbon or if the university sent us an inferior photocopy.

Previously copyrighted materials (journal articles, published tests, etc.) are not filmed.

Reproduction in full or in part of this microform is governed by the Canadian Copyright Act, R.S.C. 1970, c. C-30.

AVIS

La qualité de cette microforme dépend grandement de la qualité de la thèse soumise au microfilmage. Nous avons tout fait pour assurer une qualité supérieure de reproduction.

S'il manque des pages, veuillez communiquer avec l'université qui a conféré le grade.

La qualité d'impression de certaines pages peut laisser à désirer, surtout si les pages originales ont été dactylographiées à l'aide d'un ruban usé ou si l'université nous a fait parvenir une photocopie de qualité inférieure.

Les documents qui font déjà l'objet d'un droit d'auteur (articles de revue, tests publiés, etc.) ne sont pas microfilmés.

La reproduction, même partielle, de cette microforme est soumise à la Loi canadienne sur le droit d'auteur, SRC 1970, c. C-30.

THE UNIVERSITY OF ALBERTA

LARGE CROSS SECTION TUNNELS IN SOFT GROUND

by

HEINRICH KARL HEINZ JR.

A THESIS

SUBMITTED TO THE FACULTY OF GRADUATE STUDIES AND RESEARCH
IN PARTIAL FULFILMENT OF THE REQUIREMENTS FOR THE DEGREE
OF DOCTOR OF PHILOSOPHY

DEPARTMENT OF CIVIL ENGINEERING

EDMONTON, ALBERTA

FALL, 1988

Permission has been granted to the National Library of Canada to microfilm this thesis and to lend or sell copies of the film.

The author (copyright owner) has reserved other publication rights, and neither the thesis nor extensive extracts from it may be printed or otherwise reproduced without his/her written permission.

L'autorisation a été accordée à la Bibliothèque nationale du Canada de microfilmer cette thèse et de prêter ou de vendre des exemplaires du film.

L'auteur (titulaire du droit d'auteur) se réserve les autres droits de publication; ni la thèse ni de longs extraits de celle-ci ne doivent être imprimés ou autrement reproduits sans son autorisation écrite.

ISBN 0-315-45773-2

THE UNIVERSITY OF ALBERTA

RELEASE FORM

NAME OF AUTHOR Heinrich Karl Heinz Jr.
TITLE OF THESIS Large Cross Section
Tunnels in Soft Ground
DEGREE FOR WHICH THESIS WAS PRESENTED Doctor of Philosophy
YEAR THIS DEGREE GRANTED Fall, 1988

Permission is hereby granted to THE UNIVERSITY OF ALBERTA LIBRARY to reproduce single copies of this thesis and to lend or sell such copies for private, scholarly or scientific research purposes only.

The author reserves other publication rights, and neither the thesis nor extensive extracts from it may be printed or otherwise reproduced without the author's written permission.

(SIGNED) 

PERMANENT ADDRESS:

Rua Francisco de Morais, 173/121

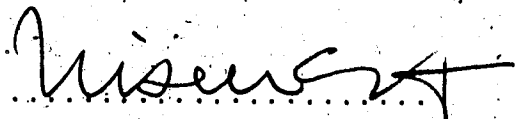
04714 São Paulo, SP - BRAZIL

DATED October 7.....1988

THE UNIVERSITY OF ALBERTA
FACULTY OF GRADUATE STUDIES AND RESEARCH

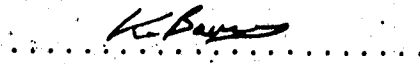
The undersigned certify that they have read, and recommend to the Faculty of Graduate Studies and Research, for acceptance, a thesis entitled *Large Cross Section Tunnels in Soft Ground* submitted by Heinrich Karl Heinz Jr. in partial fulfilment of the requirements for the degree of Doctor of Philosophy.

Dr. Z. Eisenstein

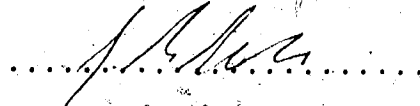


Supervisor

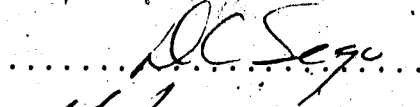
Dr. K. Barron



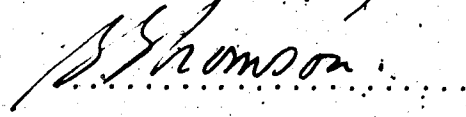
Dr. J.G. MacGregor



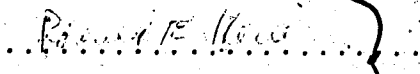
Dr. D.C. Sego



Dr. S. Thomson



Dr. R.E. Heuer



External Examiner

Date: September 16, 1988

ABSTRACT

Contemporary underground transit systems often require cross sections which are not adaptable to shield tunnelling. Due to the frequently large dimensions of these cross sections, which are normally situated at shallow depths and in soft ground, full face advance is not feasible because of ground control and construction requirements. In these large cross section tunnels, shotcrete is frequently used for initial support.

The thesis is aimed at reviewing the current practice of construction and design of these large tunnels and at formulating preliminary design concepts. Excavation schemes which have been frequently used in practice are reviewed and classified and selection criteria for choosing an appropriate scheme are outlined. A number of case histories are investigated and catalogued. The data collected from these field cases are presented in the form of empirical design recommendations, which have been developed for four distinct soft ground classes.

Aspects of tunnel stability are dealt with using a framework based on the Theory of Plasticity. Solutions based on the Upper and Lower Bound theorems are applied to the problem of selecting the construction procedure for a large cross section tunnel. The theoretical results are compared with results from model tests taken to collapse and from case histories of tunnel failures. It is verified that the

theoretical solutions provide reasonable estimates of the parameters at collapse in the model experiments. Comparison with actual field cases indicates that these solutions can be used in engineering practice provided appropriate factors of safety are employed.

A detailed review of a case history of a large cross section tunnel in coarse grained glacial soil is also included. Efforts are placed on relating tunnel behaviour to geological and geotechnical aspects. The field measurements obtained also serve as basis for checking the adequacy of the empirical recommendations derived.

ACKNOWLEDGEMENTS

I am indebted to my supervisor, Dr. Z. Eisenstein, for his support and guidance throughout this research programme. As well, I am grateful to Dr. S. Thomson, for his careful editing of the manuscript and for many positive suggestions. Appreciation is extended to the other members of my committee, for their review and constructive criticism.

The research was supported by grants from the National Sciences and Engineering Research Council of Canada to Drs. Z. Eisenstein and S. Thomson. I also wish to thank the Conselho Nacional de Desenvolvimento Científico e Tecnológico for personal financial support during part of the study.

C.P. Rail and Thurber Consultants Ltd. supplied geotechnical reports and information on the Rogers Pass Short Tunnel. Mr. J.G. Gehring provided a number of key references.

Fellow graduate students Flávio Kuwajima, José Napoleão and Tai Wong provided generous assistance at critical stages. André Assis, Júlio Alencar, Suzie Evison, Angela and João Küpper, Dwayne Tannant and Nobuyuki Yoshida also helped me in different ways. Special thanks are also due to Paulo Branco and Gerry Cyre, who assisted with the field instrumentation and to Arsenio Negro, who suggested the work on large cross section tunnels and encouraged me to pursue the Ph.D. programme.

Paulo Gomes provided a great deal of friendship at times when it was most needed. Our conversations during

endless miles of jogging contributed to keep this phase of my life in perspective. .

I also wish to express my deepest appreciation to my parents and sisters, who have always provided love, support and understanding.

Finally, and especially, I wish to thank my wife Ursula. Along with the usual praise accorded to spouses in acknowledgements for patience, typing, continued support, etc. (all of which she deserves), I am indebted to her for doing more than her share in the raising of our daughters Juliana and Lissa Maria while I was busy with "the thesis". Their affection is a source of continued inspiration.

TABLE OF CONTENTS

Chapter	Page
1. INTRODUCTION	1
1.1 Large Cross Section Tunnels.....	1
1.2 Objectives and Scope of this Thesis.....	2
1.3 The New Austrian Tunnelling Method (NATM).....	4
1.4 Ground-Support Interaction Concepts.....	5
2. OVERVIEW OF CURRENT PRACTICE	11
2.1 Introduction.....	11
2.2 Classification of Excavation Schemes.....	12
2.3 Selection Criteria of Excavation Scheme.....	16
2.3.1 Ground Conditions.....	17
2.3.2 Excavation Equipment	19
2.3.3 Cost Considerations	21
2.3.4 Local Traditions	23
2.3.5 Extent of Ground Movements	24
2.4 Case History: São Paulo Subway.....	25
2.4.1. Brief Description of the São Paulo Tunnel	26
2.4.2. Numerical Analyses	27
2.5 Empirical Recommendations.....	30
2.5.1 General	30
2.5.2 Existing Soil Classification Systems	32
2.5.3 Proposed Soft Ground Classification	34
2.5.4. Base Cases and Parameters Surveyed	39
2.5.5 Empirical Recommendations for Excavation and Support	47

2.6	Comments and Conclusions.....	48
2.6.1	General	48
2.6.2	Classification of Excavation Schemes.....	48
2.6.3	Settlement Behaviour.....	49
2.6.4	Empirical Recommendations.....	51
3.	SIMPLE SOLUTIONS FOR TUNNEL STABILITY.....	81
3.1	Introduction.....	81
3.2	Statement of the Problem.....	83
3.3	Fundamental Concepts.....	85
3.3.1	Stability Ratio	85
3.3.2	Load Factor and Factor of Safety.....	87
3.3.3	Bound Theorems of Plasticity.....	91
3.4	Lower Bound for the 3-D Tunnel Heading.....	98
3.4.1	Extension of Mühlhaus' (1985) Solution.....	99
3.4.2	Comparison with Undrained Model Tests.....	103
3.4.3	Comparison with Undrained Case Histories.....	108
3.4.4	Comparison with Drained Model Tests.....	111
3.4.5	Comparison with Drained Case Histories.....	114
3.5	Applications to Large Tunnel Problems.....	119
3.5.1	Estimates of Unsupported Length.....	119
3.5.2	Estimates of Critical Diameter.....	121
3.5.3	Discussion.....	126
4.	CASE HISTORY:MOUNT SHAUGHNESSY TUNNEL.....	152
4.1	Introduction.....	152
4.1.1	General	152
4.1.2	Scope of this Chapter.....	152
4.2	Description of the Field Case.....	154

4.2.1 Rogers Pass Project	154
4.2.2 Mount Shaughnessy Tunnel	154
4.2.3 Regional Geology and Glacial History	155
4.2.4 Background for Interpretation of Surficial Geology	156
4.2.5 Tunnel Setting	162
4.2.6 Site Investigation at West Portal	165
4.2.7 Soil Properties	167
4.2.8 Construction Details	187
4.3 Monitoring Program	188
4.3.1 Types of Instruments	190
4.3.2 Results and Interpretation of Instrumentation	194
4.4 Analysis of Field Results	200
4.4.1 Loss of Ground	200
4.4.2 Back Analysis of Displacements	202
4.4.3 Estimate of Loads from Displacements	200
4.5 Design Considerations	207
4.5.1 Prediction of Surface Settlements	208
4.5.2 Construction Procedure	209
4.5.3 Initial Support	210
4.6 Summary	212
4.6.1 Geological and Geotechnical Characterization ...	213
4.6.2 Instrumentation	213
4.6.3 Design Considerations	214
5. SUMMARY AND CONCLUSIONS	258
5.1 Introduction	258

5.2 Overview of Current Practice.....	259
5.3 Tunnel Stability.....	263
5.4 Mount Shaughnessy Tunnel.....	263
5.4.1 Geological and Geotechnical Characterization ...	265
5.4.2 Monitoring Program	266
5.4.3 Design	267
5.5 Suggestions for Further Studies.....	268
BIBLIOGRAPHY.....	270
APPENDIX A - Data from Case Histories	291
APPENDIX B - Settlement Points Readings	319
APPENDIX C - Multipoint Extensometers Readings	332

LIST OF FIGURES

Figure	Page
1.1 Relative size of large cross section tunnels and conventional shield tunnels (modified after Eisenstein and Sorensen, 1986)	8
1.2 Typical scheme for excavation of NATM in soft ground	9
1.3 Conceptual illustration of ground-support interaction	9
2.1 Illustration of invert closure distance in various excavation schemes	60
2.2 Effect of invert closure distance on settlements	60
2.3 Typical excavation schemes for large cross section tunnels	61
2.4 Ground control measures which have been used in addition to excavation schemes in Figure 2.3 (modified after Lechnitz and Kirschke, 1986)	62
2.5 Use of road header and hydraulic excavator in Munich, F.R.G. (modified after Hammer, 1978)	62
2.6 Comparison of excavation equipment frequently used in large cross-section projects	63
2.7 Comparison of excavation rates for schemes T2b and T3	64
2.8 Time spent on excavation stages of a T3 tunnel - At=88m ² (data from Kirschke and Weber, 1981)	65
2.9 Distribution of costs of large cross section tunnels in Bochum, F.R.G. (data from Laue, 1981)	65

2.10	São Paulo North Extension tunnel - geological profile (modified after Cruz et al., 1985)	66
2.11	Details of São Paulo North Extension tunnel (modified after Cruz et al., 1985)	67
2.12	Geotechnical profile used in the analyses	68
2.13	Finite Element mesh	69
2.14	Illustration of constitutive model used	69
2.15	Construction simulation sequences in Finite Element analyses	70
2.16	Comparison of settlement profiles from FEM simulations using different excavation schemes	71
2.17	Results of T2b simulation (curves) versus actual field readings (points)	71
2.18	Classification of empirical records in rock tunnelling (modified after Steiner and Einstein, 1980)	72
2.19	Definition of geometric and constructive parameters surveyed	72
2.20	Definition of typical support types in the tunnels surveyed (see Table 2.5)	73
2.21	Settlement trough represented by the error function (adapted from Clough and Schmidt, 1981)	74
2.22	Trough width parameter i versus tunnel depth in a normalized logarithmic diagram (after Heinz, 1984) ...	74
2.23	Illustration of variability of invert closure within an individual heading	75

2.24	Illustration of variability of depth of individual supported heading with no invert closed	76
2.25	Recommendations and example application for Class I - Stiff coherent homogeneous ground	77
2.26	Recommendations and example application for Class II - Stiff coherent heterogeneous ground	78
2.27	Recommendations and example application for Class III - Coarse grained cohesionless ground	79
2.28	Recommendations and example application for Class IV - Sandy cohesionless ground	80
3.1	Possible problems to be faced when planning a large cross section tunnel	135
3.2	Simplified model for analysis of tunnel heading	135
3.3	Observed collapse configurations for model tunnel headings in clay - $H/D=1.5$ (modified after Mair, 1979)	136
3.4	Influence of heading geometry on stability ratios at collapse (modified after Mair, 1979)	137
3.5	Influence of depth ratio on stability ratios at collapse* (modified after Mair, 1979)	138
3.6	Two dimensional representation of tunnel heading	138
3.7	Illustration of correspondence between Load Factor and settlements (modified after Atkinson and Potts, 1977)	138
3.8	Observed variation of crown settlement with load factor for six model tunnels (modified after Mair et al., 1985)	139

3.9	Observed variation of dimensionless crown displacement versus factor of safety (modified after Negro, 1988)	139
3.10	Geometry for 2D lower bound solution	140
3.11	Geometry for 2D upper bound solution	140
3.12	Illustration of Mohr circle at failure in upper bound solution (modified after Seneviratne, 1979)	141
3.13	Bound solutions compared to results of model experiments by Atkinson and Cairncross (1973)	141
3.14	Mühlhaus sphere approximation for the tunnel heading (original does not include internal support pressure)	142
3.15	Hollow sphere subject to uniform external and internal stresses (modified after Timoshenko and Goodier, 1970:394)	142
3.16	Lower bound stability solutions versus results of model tests taken to collapse ($L/D=0$)	143
3.17	Lower bound stability solutions versus results of model tests taken to collapse ($L/D \neq 0$)	143
3.18	Factor of safety versus H/D for undrained model tests reported in Table 3.1	144
3.19	Factor of safety versus L/D for undrained model tests reported in Table 3.1	144
3.20	Comparison of unfactored lower bound calculations with data from actual case histories in Mexico City ..	145
3.21	Comparison of factored lower bound calculations with data from actual case histories in Mexico City	145

3.22	Factor of safety versus H/D for drained tests reported in Tables 3.3 and 3.4	146
3.23	Factor of safety versus H/D for drained tests by Gudehus and Melix (1986) using residual strength parameters	146
3.24	Predicted lining radial stresses for single tunnel and measured stresses in twin tunnels in Frankfurt subway (modified after Chambosse, 1972:72 and Negro, 1988:1232)	147
3.25	Illustration of dependency of critical diameter on H/D and L/D - UNDRAINED CASE	148
3.26	Illustration of dependency of critical diameter on H/D and L/D - DRAINED CASE	149
3.27	Illustration of effect of cohesion and friction angle on drained lower bound (H/D=2)	150
3.28	Summary of lower bound solutions for application in large cross section tunnels	151
4.1	Location of Rogers Pass Project	226
4.2	Model for interpretation of upland valleys which have been subject to glaciation (modified after Boulton and Deynoux, 1981)	227
4.3	Main physiographic features of the study area	228
4.4	Longitudinal profile under Trans-Canada Highway (modified after Piteau and Associates, 1982)	229
4.5	Histogram for natural moisture contents at the study area	230

4.6	Dependence of moisture content on silt-clay content for soils at the study area	230
4.7	Plasticity chart showing coarse grained supraglacial diamictons, Edmonton tills, and soils at the study area (adapted from Sladen and Wrigley, 1983)	231
4.8	Textural diagrams showing differentiation between various types of glacial sediments (a: study area; b: modified after Derbyshire and Love, 1986)	232
4.9	Shear strength from recompacted samples of soils at the study area (tests by Thurber Consultants Ltd., 1983b)	233
4.10	Chart for estimating Equivalent Strength of rockfills (S) based on uniaxial compressive strength and particle size (modified after Barton and Kjaernsli, 1981)	233
4.11	Chart for estimating Equivalent Roughness (R) of rockfills based on porosity, origin of the materials and degree of roundedness and smoothness of particles (modified after Barton and Kjaernsli, 1981)	234
4.12	Chart for estimating friction angle of materials of glaciofluvial origin	235
4.13	Chart for estimating friction angle of materials of morainic origin	235
4.14	Variation of normalized modulus with normalized confining pressure (data from triaxial tests by Thurber Consultants Ltd., 1983b)	236

4.15	Void ratio versus modulus number for natural and compacted coarse grained soils (data from Table 4.7)	237
4.16	Correlation between void ratio and modulus number for natural coarse grained soils (data from Table 4.7)	237
4.17	Illustration of procedure for correcting the dynamic moduli to static values	238
4.18	Typical excavation sequence	239
4.19	Tunnel cross section with lining detail	239
4.20	Location of all instruments in plan	240
4.21	Typical instrumented section	241
4.22	Calculation procedure for inclined extensometers	242
4.23	Illustration of placement of strain gauges	242
4.24	Zoning of instrumented area according to magnitude of surface settlements after bench excavation	243
4.25	Final surface settlements in Zones I, II and III	244
4.26	Typical subsurface settlement behaviour close to the tunnel crown (Zones I and II)	245
4.27	Subsurface settlement profile : ME1	246
4.28	Subsurface settlement profile : ME2	246
4.29	Subsurface settlement profile : ME3	247
4.30	Horizontal displacements measured at slope indicator SI-3	248
4.31	Strains in the steel ribs vs. distance to excavation bench	249
4.32	Loss of ground versus position of excavation face ...	250

4.33	Sequence of calculations on proposed method for estimating E and K_0	251
4.34	Application of proposed method for estimating E and K_0 to the case of the Mount Shaughnessy tunnel	252
4.35	Best fit K_0 -E from Boundary Element analyses	253
4.36	Surface settlements predicted using empirical recommendations versus actual readings	254
4.37	Finite element mesh for lining analyses	255
4.38	Results of plane strain, elastic finite element analyses - lining is represented by isoparametric beam elements	256
5.1	Illustration of T2b scheme of staged excavation (modified after Hochmut et al., 1987)	269
5.2	Illustration of T3 scheme of staged excavation (modified after Hochmut et al., 1987)	269
B.1 to B.24	Evolution of surface-settlement with time - SP21 to SP24	320-331
C.1 to C.32	Longitudinal distribution of displacements from multipoint extensometers 1 to 5	333-348

LIST OF TABLES

Table	Page
2.1 Tunnelman's soft ground classification as described by Peck (1969)	53
2.2 Soil groups defined by Peck (1969)	55
2.3 Large cross section tunnels surveyed	56
2.4 Geometric parameters surveyed	57
2.5 Support characteristics of tunnels surveyed	58
2.6 Settlement performance of tunnels surveyed	59
3.1 Data from Cambridge undrained model tests taken to collapse	129
3.2 Data from actual case histories in Mexico City	130
3.3 Data from Cambridge drained model tests taken to collapse	131
3.4 Data from Karlsruhe drained model tests taken to collapse	132
3.5 Data from actual drained cases reported by Stroh and Chambosse (1973)	133
4.1 Subdivisions of late Quaternary events and deposits in British Columbia Southern Interior (based on Fulton, 1984)	215
4.2 Some typical properties of soils in glaciated upland valleys	216
4.3 Properties of natural soils from major dam projects in British Columbia	217
4.4 Field dry densities from Thurber Consultants Ltd. (1983b)	218

4.5	Some procedures for empirical determination of drained friction angle of coarse drained soils	219
4.6	Deformability parameters from multistage triaxial tests by Thurber Consultants Ltd. (1983b)	220
4.7	Summary of data collected for void ratio versus modulus number correlation	221
4.8	Summary of data from seismic velocity lines at West Portal (data from Pitt and Associates, 1982: Figures 7, 8 and 9)	222
4.9	Comparison between estimated and measured soil properties (values shown are average for Units 1 and 2 in Figure 4.3)	223
4.10	Schedule of readings for ground instruments	224
4.11	Loss of ground expressed as a percentage of tunnel volume - comparison with NATM case histories (data from Heinz, 1984)	225
A.1. to A.25	Data from case histories 1 to 25	292-316
A.26	Commonly used welded wire steel mesh sizes (adapted from Beton Kalender, 1981)	317
A.27	Commonly used steel sets (modified after Maidl, 1984:354)	318

LIST OF PLATES

Plate	Page
1.1 Excavation of a large cross section tunnel with side galleries (from 'U-Bahn Linie 8.1', reproduced with permission of the U-Bahn Referat - München)	10
4.1 Study area: looking northward along Mount Shaughnessy Tunnel alignment	257
4.2 Aspect of excavation of West Portal	257

LIST OF SYMBOLS

a	Tunnel radius
c	Cohesion
c_u	Undrained shear strength
e, e_0	Void ratio
f	Factoring value for soil strength
i	Settlement trough width parameter
k	Coefficient of permeability
m.c.	Moisture content
n	Modulus exponent (Equation 4.2)
q_u	Uniaxial compressive strength of soil
s	Rib spacing
t	Thickness of shotcrete lining
u	Ground displacement at tunnel perimeter
A_h	Area of the top excavated heading
A_t	Total excavated area
D	Tunnel diameter
D'	Sphere diameter in Mühlhaus' (1985) solution
D_m	Equivalent diameter of the critical excavation portion (defined in Section 2.5.4, Chapter 2)
D_{max}	Critical opening diameter above which instabilities could occur
E	Young's modulus
F_s	Factor of safety
G	Shear modulus
H	Soil cover above tunnel crown

H'	Soil cover above hollow sphere in Mühlhaus' (1985) solution
H _t	Height of non circular tunnel
K ₀	Coefficient of earth pressure at rest
L	Distance between excavation face and point where shotcrete invert is closed (invert closure distance)
L _a	Length of one excavation round
L _f	Final invert closure distance in a multiple stage excavated tunnel
L _h	Length of top heading within critical excavation portion defined by D _m
LL	Liquid limit
OCR	Overconsolidation ratio
PL	Plastic limit
PI	Plasticity index
\bar{S}	Dimensionless surface settlement defined by Equation 2.1
S _c	Crown settlement
S _s	Surface settlement
U	Dimensionless displacement at tunnel crown defined by Equation 3.7
V _l	Loss of ground
ε	Engineering strain
φ	Friction angle
γ	Engineering shear strain
γ	Bulk density

γ_d	Dry density
λ_p	Function of soil friction angle in Mühlhaus' (1985) original solution (Equation 3.21)
ν	Poisson's ratio
ρ	Mass density
σ	Normal stress
σ_c	Rock uniaxial compressive strength
σ_m	Mean normal stress
σ_{r0}	Initial radial stress at tunnel perimeter
σ_s	Surface pressure
σ_t	Tunnel internal pressure
σ_{tc}	Tunnel internal pressure at collapse
σ_u	Function of soil friction angle and cohesion in Mühlhaus' (1985) original solution (Equation 3.22)
σ_r, σ_θ	Normal stresses in (r, θ) directions
$\sigma_1, \sigma_2, \sigma_3$	Principal stresses ($\sigma_1 \geq \sigma_2 \geq \sigma_3$)
τ	Shear stress
$\bar{\tau}, \tau_f$	Mobilized shear strength

Notes: The list above is not exhaustive, but includes most of the parameters used in this thesis. A prime against the parameter (e.g., σ') normally denotes values based on effective stresses or strains. Compressive stresses and strains are taken as positive, except where noted otherwise.

1. INTRODUCTION

1.1 Large Cross Section Tunnels

Contemporary underground transit systems often require cross sections which are not adaptable to shield tunnelling. Due to the frequently large dimensions of these cross sections, which are normally situated at shallow depths and in soft ground, full face advance is not feasible because of ground control and construction reasons. Ground deformation and face stability are controlled by "staged excavation", which consists of sequentially driving smaller, specially arranged, individual headings hence avoiding full-face excavation.

Figure 1.1 illustrates the relative size of large cross section tunnels with respect to conventional shield tunnels. Within the scope of this thesis, 'large' cross sections are defined as those whose continuous (i.e., without intermediate pillar support) cross sectional excavated area exceeds 60m^2 . This definition includes most double track highway, railway and subway tunnels, subway stations and some single track railway tunnels. Most large cross section tunnels currently have total excavated areas up to 150m^2 (Hochmut et al., 1987). Plate 1.1 illustrates the sequence of excavation and lining placement in a large cross section tunnel.

The design of such underground structures is a relatively new subject, particularly when shotcrete is employed as initial or final support. Although a number of

papers has been published on this topic during the past fifteen years, the vast majority is concerned with experiences gained in specific cases and just a few actually deal with design issues of general technical interest. Furthermore, many of these reports are found in the German literature and are not readily accessible to the practicing engineer in North America.

1.2 Objectives and Scope of this Thesis

The present work is aimed at reviewing current practice of construction and design of large cross section tunnels in soft ground and at formulating preliminary design concepts. This is carried out in three essentially distinct studies, which are presented in Chapters 2, 3 and 4.

Attention is initially given to collecting and organizing information from actual case histories which could reflect current tunnelling practice. Theoretical studies based on simple models were also carried out in order to investigate the significance of the variation of parameters such as the tunnel geometry and the soil mechanical properties in the design process. An attempt was made to summarize both empirical and analytical findings in forms easily useable by practitioners.

The data collected from actual field cases is organized and evaluated in Chapter 2. Schemes which have been frequently used in practice are reviewed and classified and selection criteria for choosing an appropriate scheme are

outlined. A brief review of concepts associated with classification systems for tunnel design is also included and empirical recommendations aimed at the design of large cross section tunnels in soft ground are proposed. A number of case histories are revised and catalogued.

Chapter 3 is devoted to the investigation of simple solutions for estimating some of the parameters of interest in the design and construction of large cross section tunnels. Aspects of tunnel stability are dealt with using a framework based on the Theory of Plasticity. Solutions based on the Upper and Lower Bound theorems are applied to the problem of selecting the construction procedure for a large cross section tunnel. Results from model tests and from a few actual tunnels are set against the theoretical results.

Chapter 4 presents a detailed review of a case history of a large cross section tunnel in soft ground which was instrumented by the author during the course of this research. Efforts were placed on relating tunnel behaviour to geological and geotechnical aspects. The field measurements obtained also served as basis for checking the adequacy of the solutions derived in other chapters.

Chapter 5 summarizes the findings of this research project, emphasis being placed on practical implications on current design procedures. Recommendations for further research are also outlined.

1.3 The New Austrian Tunnelling Method (NATM)

Excavation and support of a large cross section tunnel in soft ground, as defined above, is often referred to as an application of the New Austrian Tunnelling Method (NATM). The term NATM was introduced by Rabcewicz (1963) and is related to the existence of ancient tunnelling methods to which several national names were applied (e.g., Austrian method, Belgian method, etc.).

The NATM is a procedure for excavating tunnels which is adaptable to ground conditions varying from hard rock to soft ground. Support is provided by suitable combinations of shotcrete, steel ribs and anchors. Excavation by the NATM in soft ground frequently makes use of a heading and bench procedure, illustrated in Figure 1.2. Within an individual heading in soft ground, the support is erected immediately after excavation and closed to a full ring as close as possible to the excavation face. This is aimed at maintaining the face stability and minimizing the soil displacements.

The NATM is frequently presented as a 'philosophy' instead of a tunnelling method, which includes design, construction and performance monitoring in an integrated manner. An in-depth assessment of this philosophy is not attempted in this thesis, where the term NATM (or SEM - Sequential Excavation Method, proposed by Eisenstein and Sorensen, 1986, 1987) is used to define any tunnel constructed with 'non-shield' techniques and shotcrete

linings. A thorough discussion of the NATM is presented by Brown (1981).

1.4 Ground-Support Interaction Concepts

A concept which is frequently associated with the NATM, but is by no means an exclusive feature of this method, is that of mobilization of the strength of the surrounding ground and consequent reduction of the short term loads in the lining. This concept is perhaps best understood from an analysis of ground-support interaction diagrams, a tool which was frequently used by Rabcewicz (1963) and his co-workers in order to explain the NATM concepts. Figure 1.3 is an attempt to illustrate this concept, which has been the subject of continual investigation at the University of Alberta in recent years (Eisenstein et al., 1981a, Kaiser, 1981; Eisenstein et al., 1984; Eisenstein and Branco, 1985b; Wong, 1986; Negro, 1988).

For simplicity, it is assumed in Figure 1.3 that a deep circular tunnel is being excavated in a ground mass subjected to a hydrostatic stress field. This problem is axisymmetric thus the stresses and displacements in the ground around the tunnel and in the support elements will not vary along the tunnel perimeter. As the tunnel excavation progresses, the original existing radial support pressure (P_0 in Figure 1.3b) is gradually reduced, stresses being redistributed part to the ground and part to the support. As this support pressure is reduced, radial deformations (u) will occur at the tunnel

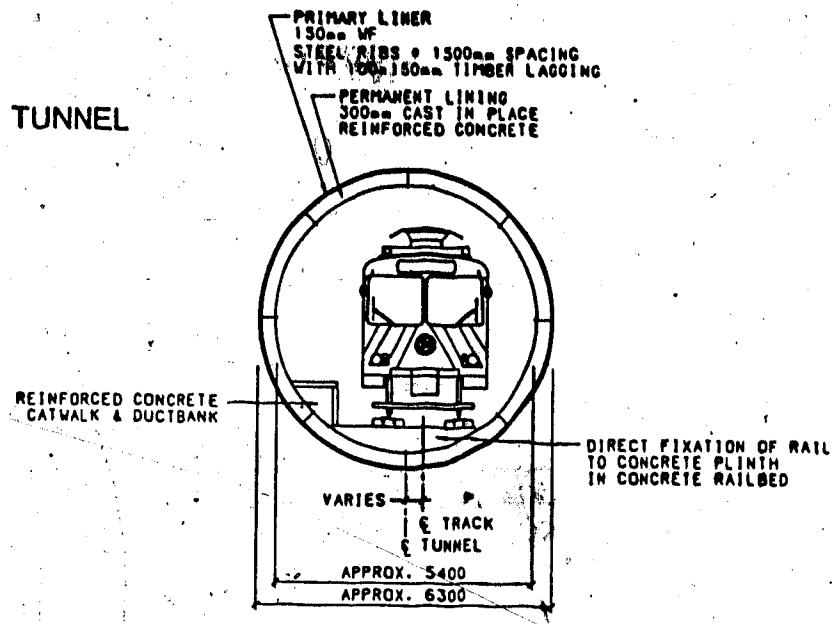
perimeter and the pressure-displacement behaviour will follow the ground characteristic curve (also known as 'ground response curve' or 'ground reaction curve'), shown in Figure 1.3b. This concept is of importance for interpretation of the load-displacement behaviour around tunnels and will be discussed subsequently in this thesis.

Figure 1.3b also shows a support characteristic curve (also support reaction line or support reaction curve). As the ground supporting pressure is reduced, this support element will deform and attract load. In deep rock tunnels, it is desirable to mobilize the strength of the rock to a certain extent, minimizing the loads which will be carried by the support. In this case, it would be appropriate to delay the support installation and a displacement u_d will occur, as shown in Figure 1.3b. In shallow soft ground tunnels, the concept of allowing a pressure relief is generally not applicable because this will necessarily increase the displacements around the tunnel and at the surface. In order to minimize settlement, it is important that the support be installed as close as possible to the tunnel face, where an unavoidable displacement u_0 has already taken place, as shown in Figure 1.3b.

If sufficient displacement is allowed, a condition of "loosening" has been said to occur. Within the conceptual framework presented above, this would mean that the ground reaction curve passes through a point of minimum support pressure and starts to show an ascending branch. Based on an

extensive review of the literature, Negro (1988:Section 3.2.3) suggests that such a condition would occur only in non-cohesive granular soils at large deformations (typically 1 to 2% of the tunnel diameter). Negro further argues that such displacements would generally be in excess of those which normally develop in properly constructed urban tunnels, defining therefore a condition of 'good ground control'. This terminology will be used subsequently in this thesis (Chapter 3).

T.B.M. TUNNEL



DOUBLE TRACK CAVITY

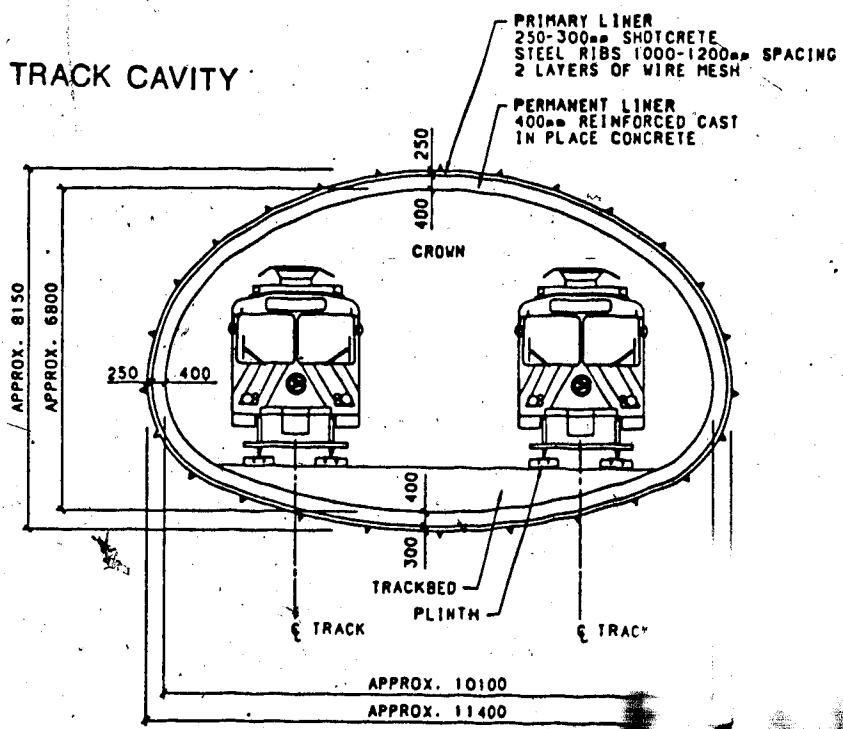


Figure 1.1 Relative size of large cross section tunnels and conventional shield tunnels (modified after Eisenstein and Sorensen, 1986)

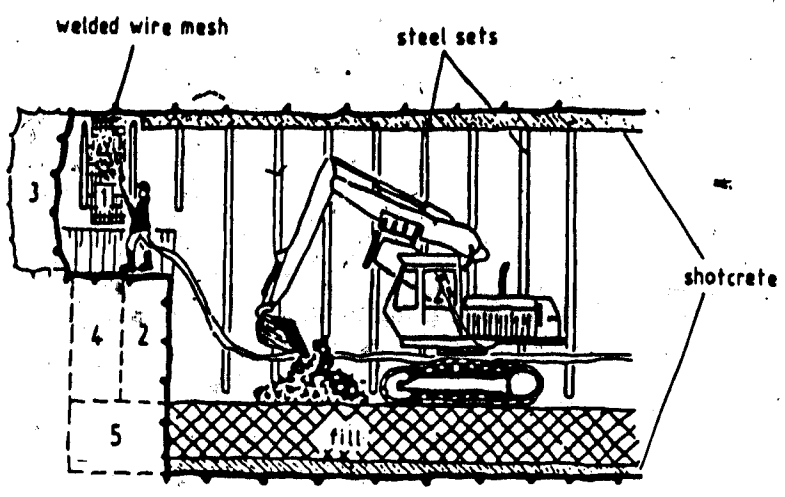


Figure 1.2 Typical scheme for excavation of NATM in soft ground

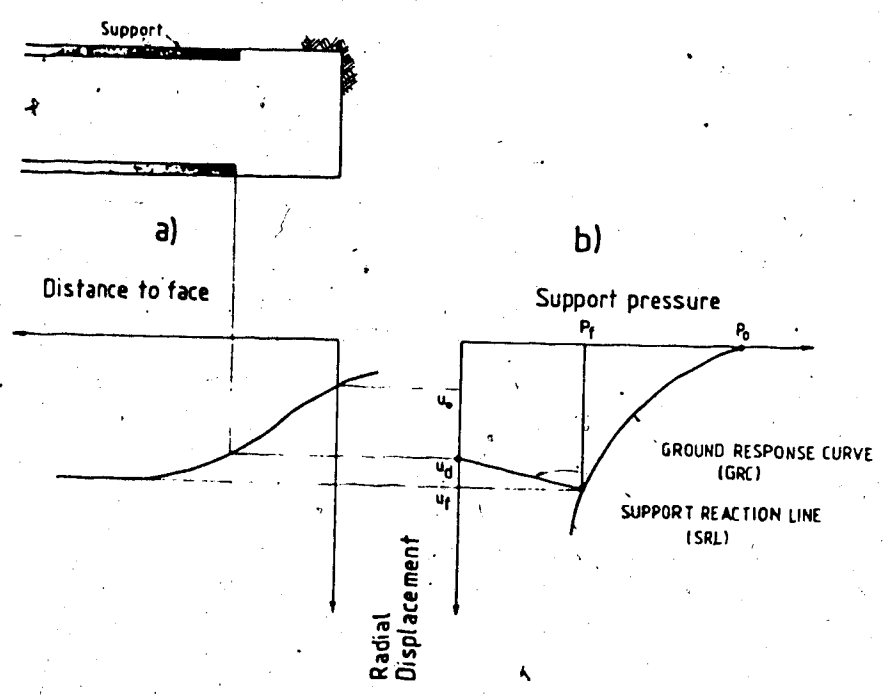


Figure 1.3 Conceptual illustration of ground-support interaction

Landeshauptstadt München

U-Bahn-Referat

Postanschrift: Postfach, 8000 München 1

Landeshauptstadt München U-Bahn-Referat Postfach 8000 München 1

Viktualienmarkt 13

Zimmer 218

Telefon Durchwahl 233/5110

Ihr Zeichen

Ihre Nachricht vom 26.12.1983

Unser Zeichen 89-V I-0

München 11. Januar 1984

Herrn
H. Heinz jr.
Dept. of Civil Engineering
University of Alberta
Edmonton, Alberta
T6G 2G7

K a n a d a

Betreff

Buch "Bau der Linie 8/1"

Anlagen

Sehr geehrter Herr Heinz,

wir sind gerne bereit, Ihnen die Reproduktion der von Ihnen genannten Fotos zu gestatten. Es wird jedoch Wert auf eine Quellenangabe beim jeweiligen Bild gelegt.

Wir überreichen 2 weitere Exemplare unseres Buches "Bau der Linie 8/1" sowie die Broschüre "Moderner Tunnelbau bei der Münchner U-Bahn" als Geschenk.

Abschließend wünschen wir Ihnen für Ihre Arbeit viel Erfolg.

Mit freundlichen Grüßen,

Im Auftrag

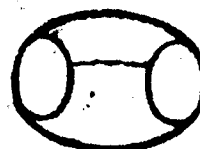
Wehe

Wehe
Ltd. Verwaltungsdirektor

*Copyright permission
for page 10*



SIDE GALLERIES



TOP HEADING



FULL CROSS SECTION

Plate 1.1 Excavation of a large cross section tunnel with side galleries (from 'U-Bahn Linie 8.1; reproduced with permission of the U-Bahn Referat - München)

2. OVERVIEW OF CURRENT PRACTICE

2.1 Introduction

When an engineering practitioner faces a problem that is relatively new to the profession and for which well established procedures do not yet exist, one of his natural concerns is to learn from experiences that others have had with a similar problem. The design of large cross section tunnels in soft ground is a problem that falls into this category. Despite the paucity of specific design methods, a fair amount of useful information regarding particular case histories is available in the international technical literature. In this chapter, attention is focussed on collecting and organizing data from these case histories.

From the literature review, the most frequently used excavation schemes are reviewed and classified and criteria for selection of the most efficient scheme are outlined. A relatively simple numerical model is then used for comparison and evaluation of ground displacements induced by different excavation schemes and for an analysis of a recent case history. Finally, an attempt is made to synthesize information collected from various case histories in the form of empirical design recommendations for large cross section tunnels in soft ground. Such guidelines are intended to allow preliminary estimates of the construction parameters and support quantities by relating them to a description of

ground conditions without the use of an explicit analytical model.

2.2 Classification of Excavation Schemes

As pointed out by Széchy (1973:669), "it is a long established procedure to excavate the tunnel's cross section not in full face at once, but in smaller parts by the driving of smaller, specially arranged individual headings". In fact, early attempts to classify these multiple stage tunnelling methods were presented as early as the 19th century (Rziha, 1874; Drinker, 1878), by attaching national names to them (e.g., Belgian Method, German Method, etc.).

More recently, such classifications have been related mainly to tunnels which use shotcrete as initial support, frequently generalized as applications of the NATM or SEM, introduced in Chapter 1. This method, reviewed by Heinz (1984) with respect to applications in urban areas, is a highly flexible and adaptable tunnelling approach and, as such, it allows a great variety of staged excavation techniques, which will be classified in the following sections. The classification presented is derived from schemes that have been used in practice.

An initial distinction should be made with respect to the distance between the face of the excavation and the point where the final invert is closed. In urban areas, concern with excessive ground movements and possible damage to nearby structures requires that this distance should be minimized.

On the other hand, in non-urban tunnels, excavated in good ground conditions, this requirement is frequently relaxed.

In the latter case, schemes such as that shown in Figure 2.1a are normally the first choice, since the use of one or more headings will allow the contractor to reach higher rates of advance. In tunnels of short length, it might be advantageous to the contractor to first fully excavate the top heading portion (i.e., until the 'break-through' is reached) and later proceed with the lower bench or benches. This procedure has been adopted, for instance, in the Mount Shaughnessy Tunnel, described in Chapter 4, as well as in tunnels of the Hannover-Würzburg express line of the German Federal Railways, currently under construction (Leichnetz and Kirschke, 1986).

As ground conditions deteriorate or as the tunnel approaches sensitive areas where excessive movements might endanger nearby structures, a temporary invert on the top heading might become necessary (Figure 2.1b). In this case, some material will be lost but it has been argued that productivity will not be significantly affected (Leichnetz and Kirschke, 1986). This scheme has been used for the recent German railway tunnels referred to above, as well as for urban tunnels in heavily populated areas (Cruz et al., 1985; Matsusita and Shimizu, 1986).

In urban areas or even non-urban areas where poor ground conditions may compromise the stability of the opening, it is necessary to close the invert as soon as possible and as

close as possible to the excavation face (Figures 2.1c and 2.1d). The excavation and support system is, therefore, much stiffer.

The adverse effect of increasing the final invert closure distance (L_f) is illustrated in Figure 2.2, where surface settlements from several urban tunnels excavated by the NATM are plotted against L_f . Field measurements from case histories reported later in this chapter have been added to data by Heinz (1984). All settlements were normalized as per procedure described by Oteo and Sagasetta (1982), in order to minimize discrepancies due to different tunnel geometries and soil properties. Figure 2.2 shows a tendency of the surface settlement to increase as L_f increases. However, the trend shown for single track urban tunnels is more marked and the large tunnels present reasonably good performances with much larger final invert closure distances. This is likely due to the fact that the excavation of these large sections is performed in stages, frequently with a temporary invert closed within a stage, which allows a better ground control.

Excavation schemes which have been more frequently used for continuous cross sections (i.e., without intermediate pillars) in urban areas¹ are presented in Figure 2.3. The classification shown in this figure is an extension of that presented previously (Heinz, 1984). The modifications were

¹Scheme T1a is a variation which differs from scheme T1b and T1c solely due to the longer invert closure distance. It is more frequent in non urban tunnels.

deemed necessary due to the large amount of new technical information on large cross section soft ground tunnels that recently became available (e.g., ITA, 1986).

The symbols used for classifying the excavation schemes are formed by the letter T, (for "type"), followed by a number, which represents the number of excavation stages fully embraced by a shotcrete ring, termed "cells" by Lessmann (1986). The numbers inside the cross sections in Figure 2.3 correspond to the sequence of excavation and are presented along with the ranges of total excavated cross sectional area (A_t) observed in the cases surveyed and the approximate percentages of the individual excavation steps with respect to A_t . Some basic information on example case histories is also included.

The review of tunnels presented is by no means exhaustive and more details will be presented later in this chapter. However, a few trends may be derived from the information presented. For example, it is observed that one single step of face advance seldom exceeds 40% of the total cross sectional area. A trend towards a larger number of stages as the cross sectional area increases is also apparent. This probably reflects concern with tunnel stability and surface settlements, since all tunnels listed were constructed in urban areas. Also, the literature review suggests that schemes T2b and T3 (with one or two side galleries) are given preference in urban areas with unfavourable groundwater conditions (see Section 2.3).

It should also be pointed out that although the cases reviewed previously by Heinz (1984) indicated that these large tunnels were predominantly driven in stiff cohesive soils, recent Japanese cases demonstrate that this conclusion is no longer valid. Tunnels such as those described for instance by Horiuchi et al. (1986), represent applications in significantly less favourable ground conditions, such as cohesionless sands below the groundwater table. Some of the features of these relatively new developments are outlined in Section 2.5.

2.3 Selection Criteria of Excavation Scheme

Selection of an excavation scheme involves a number of considerations, some of which are subjective in nature and thus difficult to assess. The topic has already been addressed by various authors (e.g., Krischke and Weber, 1981; Heinz, 1984; Negro et al., 1984; Laabmayr and Swoboda, 1986; Lessmann, 1986), and a brief attempt is made herein to extend and synthesize relevant criteria. It is recognized that the relative importance of each factor involved may vary from case to case and no rigid rules for selection of an appropriate excavation scheme can be established. The following items present a review of what are believed to be the main governing factors and are intended to provide a brief insight into the topic.

2.3.1 Ground Conditions

The geotechnical properties of the ground mass have a major influence upon tunnel face stability and on the magnitude of induced settlement. In general, an increasing number of excavation stages (and a consequent decrease of excavated cross sectional area for a single step) will normally lead to a safer face advance and smaller settlements. From the works by Horiuchi et al., (1986) and Hochmut et al. (1987), it may be inferred that preference will be given to T3 schemes (with two side galleries) for tunnels with cross sectional areas above 90m^2 . Empirical and analytical criteria for selecting the maximum excavation size will be discussed subsequently in this thesis.

When evaluating stability, it is also important to remember that in stiff fissured soils strength may decrease with increasing sample size. Stability during construction of an underground opening in this type of soil would become even more critical as its size increases. As suggested by Eisenstein and Thomson (1978), geotechnical studies in these soils must consider a soil mass rather than extrapolation of results from small samples. It is believed that insitu tests and field mapping may be necessary tools in such investigations. Further insights into the stability problem are given in Chapter 3.

Also, a few case histories investigated were excavated through sandy, gravelly and even bouldery soils, where conventional sampling and testing techniques are not usually

applicable. In these cases, the use of large diameter auger holes (e.g., \varnothing 900mm) is believed to be an appropriate tool to inspect the condition of the ground insitu (Heuer, 1985; Smirnoff and Lundin, 1985). The degree of cementation of the grains, which is of fundamental importance for an evaluation of the "stand-up-time" of the ground, could then be evaluated¹. The stand-up-time is known, from practical experience, to be directly related to the unsupported length or width of the opening (e.g., Deere et al., 1969). It may be assumed, therefore, that it will directly influence the choice of the number of stages to be used in a given large tunnel.

In some cases ground water lowering from the surface is feasible. In other cases, however, it is preferable to drain the soil from inside the tunnel. This normally requires the use of smaller excavation sections since the presence of ground water may reduce considerably the stand-up-time of the ground. In some sections of the Munich underground transit system perched water tables and some highly permeable horizons showing artesian water pressures were found (Krischke and Weber, 1981; Hochmüt et al, 1987). These aspects lead to the selection of types T2b and T3 excavation schemes, with the side galleries excavated in advance to drain the soil mass before the main section was excavated.

¹ The stand-up-time was defined by Terzaghi (1950), as "the time that elapses between the exposure of an area at the roof of the tunnel and the beginning of noticeable movements of the ground above this area".

Also, by excavating a side drift in advance, a better examination of the ground conditions is possible and may be used to optimize subsequent construction stages, thus fulfilling some of the requirements for application of an observational approach (e.g., Eisenstein and Branco, 1985a).

Other recent applications in the Munich and Vienna underground transit systems (e.g., Weber, 1987; Deix and Gebeshuber, 1987), have shown that compressed air is often used in order to control groundwater inflow. This is generally the case where piezometric heads are high and the large pumping volumes involved make it difficult to lower the groundwater by means of deep wells. Several other additional ground control measures were frequently mentioned in connection with the case histories examined. They are briefly summarized in Figure 2.4 and while none of them appear to be specifically connected with any of the schemes in Figure 2.3, it appears that a combination of them is frequently chosen as an alternative to an increase in the number of excavation stages or a reduction in the invert closure distance.

2.3.2 Excavation Equipment

The practitioner normally faces decisions concerning the need for certain equipment, its availability and related costs. Economically feasible NATM excavation in soft rocks, for example, appears to require the use of "road headers", also known as "part face tunnelling machines". On the other hand, excavation in softer material can be carried out with

the aid of conventional hydraulic excavators ("backhoes"). The road headers are equipped with powerful rotating cutting heads, sometimes with an individual conveyor belt, allowing high rates of advance. The cutting head is rotated and forced against the excavation face in order to cut the soil in pieces for easier removal. Several manufacturers claim that very small cross sections (down to 5m^2) may be handled by these machines, which seem appropriate, for example, for schemes of the T3 type, when small side galleries may be required.

Krischke and Weber (1981) suggest that the choice of an excavation scheme may also be conditioned by the available machinery. For a T3 type tunnel with 90m^2 cross section, each side gallery, as well as the top heading (stage 3 in Figure 2.3) would have about 20m^2 , which would likely require the use of roadheaders. On the other hand if the tunnel has 150m^2 of cross section the side galleries will have about 30m^2 , which is approximately the size of a regular, single track, subway tunnel. In this case, hydraulic excavators may be used.

Figure 2.5 illustrates the use of both a roadheader and a conventional hydraulic excavator in a large cross section tunnel in Munich, with about 100m^2 of excavated area (Hammer, 1978). Reviews of available excavation equipment and their selection may be found in several publications (Hammer, 1978; Lessmann, 1980; Maidl, 1984). A complete review falls beyond

the scope of the present work. Figure 2.6 presents a brief comparison between roadheaders and hydraulic excavators.

2.3.3 Cost Considerations

The overall cost of tunnelling appears to be, first, a function of the rate of advance and, only second, related to the costs of ground support. Focussing only on the staged excavation problem, one may assume that preferences will be given to schemes leading to high rates of advance with a possible allowance for some support savings. The total costs are also known to be highly dependent on the length of the contract section (Klawe and Schreyer, 1979).

The only available comparisons of advance rates in similar ground conditions were for the tunnels in Munich, namely between the T2b and T3 types. The T2b scheme has been described as a development of the T3 type which allowed higher advance rates (Laabmayr and Swoboda, 1986; Lessmann, 1986). This is confirmed by data reported by Krischke and Weber (1981) which is summarized in Figure 2.7. Krischke and Weber (op. cit.) were also able to evaluate the average time spent on different stages of excavating and placing the initial shotcrete support for a running meter of a T3 type tunnel with about 90m² of excavated cross section. Their results are summarized in Figure 2.8 and show that the excavation and support of the top heading of the T3 scheme (stage 3 in Figure 2.8) takes a considerable portion of the

total time, especially when this stage represents only about 20% of the total excavated volume. This possibly reflects the great care exercised during excavation of this stage. It has been observed by the writer that sliding beams are used at the crown, possibly reflecting a concern with the longitudinal support in the early stages of construction, when the shotcrete is not fully hardened and the ring is not closed. As will be shown subsequently in this chapter, the excavation of this stage is responsible for a considerable portion of the surface settlement.

No comparison between advance rates achieved by the schemes T2a and T2b has been found. Cruz et al. (1985) report an average advance rate of 1m per day for a tunnel with 77m² cross section driven in a Tertiary stiff fissured clay with minor groundwater inflow. Krischke and Weber (1981) report an average of 1.7m/day for a T2b tunnel with 88m², driven under slightly less favourable conditions in terms of groundwater inflow. Since in the case reported by Cruz et al. (1985) the construction crew was probably less experienced (they reported the first large cross section NATM tunnel constructed in Brazil), it appears that the two procedures (i.e., T2a and T2b) could yield comparable rates of advance if executed in similar ground conditions by experienced personnel.

Also, if one assumes that in large tunnels (about 80-90m² of area or larger), the contractor would give preference to schemes allowing two relatively widely spaced excavation

fronts to proceed simultaneously (Leichnetz and Krischke, 1986), one might speculate that the T2 schemes (Figure 2.3) might be preferred to schemes T1b or T1c in terms of advance rate in urban areas.

Regarding the total costs of large cross section tunnels, very little published information has been found. Laue (1981) evaluated the distribution of total costs for subway tunnels in the city of Bochum, F.R.G. (Figure 2.9). While his findings are strictly valid only for those particular conditions (very shallow tunnels in heterogeneous ground, generally soft to stiff marls), they do provide an insight into the percentages of the total cost that are ascribed to each construction stage. In this instance, for double track tunnels, excavating, supporting and placing the final concrete liner share more or less the same proportion. In stations, however, the final concrete liner is responsible for a greater component of the total cost.

2.3.4 Local Traditions

A recognized factor which might influence the selection of a staged excavation scheme is the "tradition" factor. Methods which have been successfully used in the past normally tend to gain an acceptance that assures their continuity. These traditions may also be carried over to other locations by consultants or contractors.

In the São Paulo tunnel reported by Cruz et al. (1985) for instance, the T3 scheme was initially proposed, possibly

due to previous successful applications in Southern Germany. The T2a scheme was finally adopted and was successful, since the excavation was completed ahead of schedule. The use of traditional methods may appear practical but may also have the effect of not allowing innovative techniques to be attempted.

2.3.5 Extent of Ground Movements

In urban areas, limiting settlements which may cause structural damage to surface and subsurface utilities is a major concern. In general, not only the magnitude of the surface settlement but also the slope of the surface settlement depression caused by tunnelling are the prime factors to be considered. It is apparent that for the same tunnel cross section, increasing the number of excavation stages, with immediate application of shotcrete forming a load bearing ring, will reduce the amount of surface settlement. This is supported by data reported by Krischke and Weber (1981), who also verified that increasing the number of excavated cells led to a flattening of the surface settlement depression (i.e., a wider trough). It is also important to point out that the longitudinal distortions (i.e., along the excavation axis) verified for these T2b and T3 tunnels of the Munich subway were very small, of the order of 1:1500 to 1:6000.

Laabmayr and Swoboda (1986) published a comparison between the T1b and T2b schemes by means of Finite Element

analyses which they claim is substantiated by field measurements. Their results indicate that the loss of ground ahead of the face is larger for the T1 scheme and that the application of the T2b scheme allows a pronounced reduction of surface settlement. The stiffer scheme is also better in terms of increasing face stability.

2.4 Case History: São Paulo Subway

The relative amount of settlement provoked by different schemes could not be assessed through the review of case histories since, in general, only one scheme is used within a single project. If the scheme is changed during construction (e.g., Krischke and Weber, 1981), this is generally due to a significant change in ground conditions and, hence a comparison is no longer valid.

This absence of actual performance data can be compensated for by the use of numerical models. In order not to lose touch with reality, however, it is important that results derived from these models are compared with actual field data. In the following, simple finite element numerical analyses are used to compare the amount of surface settlement generated by different excavation schemes. The results are checked with field measurements taken in a large cross section tunnel and reported by Celestino et al. (1985) and Cruz et al. (1985). The results introduced herein complement those previously published by Eisenstein et al. (1986).

2.4.1. Brief Description of the São Paulo Tunnel

This double track subway tunnel has an excavated area of about 77m² over a length of 194m. Construction took place between January and August of 1984, using a conventional hydraulic excavator and jackhammers. The local soils were sediments of the São Paulo Tertiary formation, namely a stiff fissured silty clay (E=50 to 100MPa, SPT=20 to 50), underlying a fine clayey sand deposit. The area is densely populated and the tunnel passes under several 2-3 storey buildings.

Figure 2.10 illustrates the geological profile including two perched water tables. Dewatering prior to tunnel construction was undertaken just at the extremes of the tunnel. Except in the portions where the overburden was extremely low, which correspond to 25% of the total length, no ground treatment was applied. Thus, ground control for this tunnel depended mainly on a multiple stage excavation technique.

The T3 scheme (with side galleries) was originally proposed in design. Several reasons which are reported by Cruz et al. (1985) led to construction using scheme T2a. As additional precautionary measures, a central support core and a temporary invert closure on the top heading portion were adopted (Figure 2.11a). The distance between the excavation of heading and bench was initially specified as 12m maximum. This distance was eventually increased up to 40m in the central portion due to operational reasons, an expedient

supported by evaluation of field instrumentation. The average excavation progress was 3m/day for the heading and 6m/day for the bench, yielding an overall average of about 1m/day (Cruz et al., op. cit.).

Lining placement was carried out in two stages. The first stage took place immediately after each excavation round and included spraying of a 3cm stabilizing layer of shotcrete, placement of a first layer of welded wire mesh (Q283:Ø6mm in 10x10cm grid; 4.48kg/m²), followed by installation of polygonal steel sets (18" spaced 0.6 to 1.0m). The total shotcrete thickness in this stage was 25cm. In the second stage, shotcrete and a second wire mesh with the same specifications as the first were applied (20cm close to the portals and 15cm in the central portion). This layer constituted the definitive inner lining and was sprayed after deformations were considered stable. This case is quoted as being the first subway tunnel in soil using shotcrete as the final support.

The tunnel was instrumented and monitored. A typical layout of the instrumented sections is presented in Figure 2.11b. A total of 16 instrumented sections were installed, consisting primarily of surface levelling and deep settlement points. Internal convergence measurements and levelling of the roof were also carried out.

2.4.2. Numerical Analyses

The primary objective of this section is to analyze, using the Finite Element Method (FEM), the relative amount of surface settlement provoked by three different staged excavation schemes. It is recognized that the excavation of a large cross section tunnel is a truly three-dimensional process. However, three-dimensional analyses are very complex and would demand a considerable effort, as shown by Heinz (1984). A simple two-dimensional analysis, regardless of its limitations, allows an estimate of the relative performance of different construction schemes in terms of ground movements.

The analyses are aimed at comparing settlements due to excavation of a tunnel 12m wide and 9m high with about 80m² of cross sectional area. The soil cover above the tunnel crown is taken as 10m. These dimensions are fairly close to those found in the São Paulo tunnel reported above. A comparison is intended for three constructions schemes, namely types T1b, T2a and T3, as defined in Figure 2.3. The assumed geotechnical profile is depicted in Figure 2.12. The properties adopted are also shown and correspond roughly to those reported for the São Paulo Tertiary sediments.

Finite Element Simulation

All analyses employed the general purpose program ADINA (Bathe, 1978; ADINA Engineering, 1984). The mesh used is shown on Figure 2.13. The stress-strain behaviour of the soil was represented by ADINA's von Mises model with isotropic

hardening. The value of the yield stress was chosen as the value of the uniaxial compressive strength of the soil ($q_u = 2c_u$) and the hardening modulus was arbitrarily taken as $E/10$, where E is the modulus of the elastic portion of the stress-strain curve (Figure 2.14). This model was chosen from those available in ADINA at the time the analyses were conducted, since it was considered capable of reproducing aspects of actual soil behaviour. Successful use of this model in geotechnical analyses has been reported by Dysli and Fontana (1982). The shotcrete lining was represented by beam elements and assumed to behave linearly elastically with $E = 10\text{GPa}$ and $\nu = 0.25$. The thickness of the inner wall of the side galleries (scheme T3), as well as of the temporary invert in the T2b scheme was assumed to be 15cm, while the thickness of the external wall was taken as 25cm. The tunnel construction simulation sequence is illustrated in Figure 2.15. Modelling criteria follow recommendations by Heinz (1984).

Results of Comparative Analyses

Figure 2.16 shows the settlement profiles obtained for the three excavation schemes. The settlements occurring during the top heading excavation (step 2 for schemes T1b and T2a and step 4 for scheme T3) are also shown. It is seen that these represent a significant portion of the total settlement and in the case of the T3 scheme they practically coincide with the final values. It may also be observed that the T3

scheme has a better performance in terms of maximum surface settlement and of maximum distortion, while the T2b performance falls within that of the other two, but closer to the T1 maximum.

Figure 2.17 shows the result of the numerical analysis for scheme T2a, this time plotted against the field readings. A good agreement is observed despite the several simplifications adopted, what suggests that a first approximation of such complex excavation schemes may be obtained from simple two-dimensional techniques. It should be pointed out, however, that the accuracy of finite element analyses is also highly dependent on factors such as the density of the mesh, position of the bottom rigid boundary, etc. (Heinz, 1984). The close match could, therefore be viewed as fortuitous.

2.5 Empirical Recommendations

2.5.1 General

In hard rock tunnelling, "classification systems" have become a popular solution for establishing a design based on past experience. A classification system may be essentially described as an empirical design approach derived from a collection of prototype observations. Support requirements and/or construction procedures are related to certain classes of rock mass conditions for which observations are available. These procedures appear to be applicable when there is insufficient data to establish an explicit analytical model,

for example before construction, when there is limited geological information. It has also been argued (Brady and Brown, 1985:77) that classification systems may be used when the behaviour of the rock surrounding the excavation is so complex that it is not amenable to engineering analysis using existing techniques.

A detailed review of several empirical methods for rock tunnelling is presented by Steiner and Einstein (1980). Examination of this fairly extensive publication shows that many rock classifications include some sort of "soil class". This possibly reflects the fact that in certain areas the distinction between soft ground and rock is arbitrary. In Continental Europe, for instance, soft ground is frequently considered just another rock, which is softer and involves a distinct class of problems (Deere et al., 1969:I-3).

The existing rock classifications which include a soil class are, however, of limited use if one is concerned exclusively with soft ground tunnelling, since they were mainly developed for specific ground conditions and from a limited number of observations. They lack, therefore, the necessary detail for differentiating between several soft-ground classes. This may lead to the same design parameters for classes of soil which are widely distinct.

The behaviour of large cross section tunnels in soft ground is likely complex and therefore not amenable to simple solutions. At the same time, there seems to be enough case histories information published so that a classification

system taking account of this previous experience would probably be welcome. Combining information concerning a soil and tunnel geometry with such a system, the practitioner could establish a preliminary design.

2.5.2 Existing Soil Classification Systems

Despite the existence of a fair number of classification systems for soils, most of them were developed for roads and runway projects and are not directly applicable to tunnel design. An example is the Unified Soil Classification (UCS), which is widely used in North America and is recommended for identification and classification of soils in the Canadian Building Code (CGS, 1985). The UCS is reviewed in many soil mechanics textbooks and its framework is generally attributed to Casagrande (1948), who also reviewed several other classification systems. The basic problem with all these classifications is that they do not describe the soil in its natural state, which is an essential requirement for tunnelling purposes. In sands, for instance, a slight cementation between the particles, usually not detectable through conventional sampling, will often dictate the difficulty of tunnelling.

Other classification systems which do include information about the soil insitu are the German "Classification of Loose Rocks for Excavation Purposes" (DGEG, 1979) and the British "Guide to Site Identification and Description of Coarse, Fine and Organic Soils" (Bell,

1983). However, they are clearly not directed toward tunnel design, although some of the included features may be useful when evaluating the possible behaviour of the ground during tunnelling.

To the author's knowledge, a single soft ground tunnel classification system, proposed by Terzaghi (1950), is referred to in the literature. This classification is behaviouristic, in the sense that it attempts to describe the soil as it behaves during tunnelling. While it might be appropriate to characterize conditions effectively encountered during excavation, it is not directly related to intrinsic ground properties and may not be applicable in the design stage (OMTC, 1976). Terzaghi (op. cit.) refers to this classification as the "Tunnelman's Ground Classification" and suggests that several classes may be differentiated using the stand-up-time as criterion. Table 2.1 summarizes its main features, mainly as interpreted by Peck (1969).

A subdivision of soil types which is perhaps more appropriate for the present study was used by Peck (1969) in his state-of-the-art report on tunnels and excavations in soft ground. Peck (op. cit.) reviewed a number of case histories, from widely different geographic-cultural areas. Peck placed these tunnels in four broad classes, according to the soil characteristics of interest to tunnelling, namely "cohesionless granular soils", "cohesive granular soils", "non-swelling stiff to hard clays" and "soft to stiff saturated clays". Both typical soil types and possible

behaviour during tunnelling were outlined, and are summarized in Table 2.2.

This classification may be criticized on grounds that the classes are only broadly related to intrinsic soil properties. Also, Peck's description of tunnelling methods, not included in Table 2.2, is perhaps a little out of date. Nevertheless, it has the merit that it is usually a simple matter to classify a new case history into any of these four ground classes. As such, it was taken as background for the classification introduced in the following items.

2.5.3 Proposed Soft Ground Classification

A number of case histories of large cross section tunnels in which shotcrete was used as initial support, were analyzed based on information contained in technical papers and reports. The tunnels evaluated were constructed in fairly different geographical, cultural and socio-economic areas and, as such, construction practices may have been influenced by factors other than the ground characteristics, for instance those outlined in Section 2.3. Moreover, the majority of the reports reviewed lacked a consistent soil mechanics approach for the description of the ground.

For these reasons, and also because it was verified that the excavation procedures and support quantities were affected by an environmental factor, namely the existence or lack of nearby structures, a definition of classes based on quantitative parameters did not prove practical. Instead, a

simpler subdivision of ground types, which according to Steiner and Einstein (op. cit.) would fall into "Type B" or "Qualitative Direct Methods" for tunnels in rock, was preferred. In the existing rock tunnel empirical methods which belong to this category, the ground conditions and/or the ground behaviour are described qualitatively and are directly (i.e., not through an estimated "rock load") related to an excavation procedure and support requirements, as illustrated in Figure 2.18.

Soft Ground Classes

Most of the cases reviewed would fall into the "cohesive granular" and "non swelling stiff to hard clays" groups advanced by Peck (1969) and summarized in Table 2.2. A few, however, belonged to Peck's "cohesionless granular soils" group. No reports were found of large cross section tunnels excavated in soft clays, although at times these may have been present in a non-dominant fashion.

The influence of features such as fissures or joints in the ground mass in the construction procedure and support quantities could not be assessed. It is believed however, that the good lining-soil contact usually provided by the rapid application of the shotcrete will be sufficient to increase safety and to prevent the development of loosening zones around the opening (see Negro, 1988:114 for a more extensive discussion). Also, in all cases where a combination of piezometric pressures and ground permeability could cause

problems during excavation (e.g., flowing ground - Table 2.1), the groundwater level was either lowered well in advance or was drained through the tunnel during construction. In exceptional cases (e.g., large reservoirs of available water and highly sensitive structures nearby), dewatering was not feasible and alternative techniques such as the use of compressed air or freezing were used (e.g., Deix and Gebeshuber, 1987; Krischke and Weber, 1987). In summary, most of the cases reviewed are believed to have been excavated in fairly firm ground¹.

In the following, soil displaying any sort of "bond" between particles is termed "coherent", a term which seems appropriate to encompass both fine grained and coarse grained soils and apparently coined by Deere et al. (1969). Also, it was felt convenient to adopt the term "heterogeneities" in connection, for instance, with mixed-face conditions. Heterogeneities frequently referred to in the case histories examined, which seem to have influenced the construction procedure and/or the support quantities were:

- a) presence of weaker layers at the excavation face, for example softer clayey beds within cohesive granular soils (e.g., Bauernfeind et al., 1978);
- b) presence of lenses of cohesionless sands or gravels at the excavation face which could be running or flowing

¹ Babendererde (1985) suggests that for the shotcrete method to be applied, the ground must be able to remain unsupported for at least 1.5 hours after a 1m advance. Non cohesive soils would have to be somehow improved to meet these requirements.

depending on the groundwater conditions (e.g., Krischke and Weber, 1981);

c) ground where stiff and soft¹ layers would be present alternately (e.g., Jagsch et al., 1974; Deix and Gebeshuber, 1987).

Four classes of soil were found appropriate for a classification of the cases studied:

Class I: Stiff coherent homogeneous ground

This group includes "cohesive granular" and "non swelling stiff to hard clays" of Table 2.2, in which the geotechnical properties of the geological units in the vicinity of the tunnel were consistently favourable. In other words, no heterogeneities, as defined above, were encountered. In terms of the Tunnelman's Classification, these soils could be generally classified as firm.

Class II: Stiff coherent heterogeneous ground

This would be essentially "stiff coherent ground", as described above, but with geological anomalies present in varying degrees. The presence of thick softer beds could, for example, be responsible for a marked non uniform loading of

¹ Moduli consistently reported in the cases reviewed suggest that a quantitative boundary differentiating the stiff from the soft soils would be about $E=30\text{MPa}$. Since, however, the E value is known to be dependent on the test procedure, which could not be assessed in most cases, care should be exercised, when applying the present classification, in judging what is actually a soft soil.

the liner, as demonstrated by Wittke (1984). Also, the presence of lenses of sand which could run or flow into the tunnel would probably require a more careful excavation sequence.

Class III: Coarse grained coherent ground

Some case histories were found of tunnels in ground which contained a considerable amount of coarse grained particles. Although it is believed that at least a portion of these soils presented some degree of cementation, which would allow unsupported face advance followed by immediate application of shotcrete, measures such as the use of forepoling in the crown area were consistently reported in these tunnels. This probably reflects a concern with the possibility of soil runs in these locations, with direct implication in the loss of ground and in the crew's safety. Although a rigid guideline for establishing which gravelly or bouldery soils would fall into this category could not be established, it was verified that, for the cases examined, the dominant soil had at least 30% in weight of particles with average diameter larger than 60mm, i.e., of cobbles and boulders according to CGS (1985). Also, it is believed that the maximum silt-clay content of these soils was below 15%.

Class IV: Sandy cohesionless ground

Some recent Japanese tunnels were excavated in sands described as cohesionless except for some cohesion due to

capillarity. These sands were fairly dense and generally had an N(SPT) value of around 30. However, due to its running characteristics, extra precautions had to be taken in order for the excavation to proceed. For example, in all cases forepoling in the form of steel plates was used above the springline. Also, in extreme cases where the sands would rapidly run after exposed by excavation, a chemical resin coating which solidified in about 5 minutes was applied before the shotcrete, in order to prevent the material from running into the tunnel (Horiuchi et al., 1986).

2.5.4. Base Cases and Parameters Surveyed

Twenty five case histories were reviewed based on literature reports and complementary unpublished material obtained from correspondence with the authors. In order to make the information collected readily accessible, tunnel and soil parameters considered of relevance for design were collected and organized into a microcomputer based Database Management System (DBMS). In simple terms, a DBMS allows a large quantity of information to be stored, accessed and retrieved efficiently. A detailed summary of each case history reviewed, as contained in the DBMS, is included in Appendix A and should be viewed as a complement to the information presented below. It is considered prudent that anyone interested in using the following information for design purposes, should study the base cases (Appendix A) individually. This is suggested by Steiner and Einstein

(1980) with respect to use of all rock classification systems.

Parameters Surveyed

In addition to the soft ground class to which the tunnel belonged, a further factor, which was verified as exerting a strong influence in the support type and in the construction sequence adopted, was the presence or not of nearby structures. Essentially two situations were encountered, namely tunnels in non-urban areas and tunnels in urban areas. Also, it was verified that some urban tunnels, more specifically those situated under or close to highly sensitive structures (e.g., old historical buildings, important railways), deserved special attention. These areas are, accordingly, designated as "sensitive urban area" in the data that follows.

Relevant construction parameters and support quantities were also collected (Tables 2.3 and 2.4). Figure 2.19 illustrates the geometric parameters surveyed, whereas in Figure 2.20 the types of lining more frequently encountered are described. It should be pointed out that the excavation parameters presented in Figure 2.19 refer mainly to the most critical excavation portion in the cross section, usually the top heading in the largest cell. For the sake of clarity, the following guidelines have been adhered to:

- a) Schemes T1: L is the final invert closure distance (L_f), D_m corresponds to the full cross section.

- b) Scheme T2a: L and D_m correspond to the top heading.
- c) Scheme T2b: L and D_m correspond to the first cell (i.e., steps 1 and 2 in Figure 2.3).
- d) Scheme T3: L and D_m correspond to the central portion (steps 3, 4 and 5 in Figure 2.3).

A geometric parameter surveyed which is not illustrated in Figure 2.19 but is listed in Table 2.4 is the ratio between the area of the top heading in the largest cell (A_h) and the total excavated area (A_t). It was obtained directly from values reported or measured on available drawings. Although approximate, these values are believed to be indicative of the size limits for safe excavation of each heading.

Table 2.6 presents, for the cases in which sufficient data was available, performance indices which compare the volume of surface settlement caused by excavation of the full tunnel (V_s) with the volume (per lineal meter) of the tunnel (V_{tn}). The V_s values were calculated assuming that the surface settlement trough could be approximated by an error function (such as that shown on Figure 2.21) as outlined in the Schmidt-Peck theory (e.g., Clough and Schmidt, 1981). Other assumptions are listed in Table 2.6. In the present context, the index V_s/V_{tn} is included as tentative to provide basic guidelines on the settlement behaviour that could be expected for each soft ground class. It should be pointed out that the procedures usually used for estimating the trough width parameter i , used to calculate the V_s value, may not be

fully applicable to large tunnels, as shown in Figure 2.22. This is not regarded as a serious shortcoming in the present work, since the calculated V_s values are mainly compared among large cross section tunnels.

Also given in Table 2.6 are values of a dimensionless surface settlement, introduced by Oteo and Sagaseta (1982):

$$\bar{S} = \frac{E S_s}{\gamma D^2} \quad [2.1]$$

where E is the soil modulus of elasticity, S_s is the maximum surface settlement, γ is the soil unit weight and D is the average diameter. This parameter is thought to provide a better basis for estimates of settlements than the V_s/V_{tn} ratios, at least in stiff soils, but it is realized that accurate soil parameters are not always available. Hence preference might be, in certain cases, given to the use of V_s/V_{tn} .

The data collected, which is considered relevant for the definition of parameters of each soft ground class, are summarized in Tables 2.3 to 2.6. It is recognized that the number of cases examined is statistically limited and may be biased due to the fact that 'non-successful' ventures are seldom reported in sufficient detail. Notwithstanding all these considerations, some important observations can be made. It is believed that their validity may be reinforced in the future by means of a large number of field observations.

in a variety of ground conditions. The points realized from an examination of Tables 2.3 to 2.6 are:

Regarding Construction Parameters

It is apparent that the parameter L/D_m , which is the ratio between the invert closure distance and the equivalent diameter of the opening (these may correspond only to a portion of the tunnel, as described above) is more a function of the environment in which the tunnel was built than of the soft ground class (Figures 2.23a and 2.23b). The same conclusion can be derived for the parameter $L_h/(A_h/A_t)D$, which indicates the dimensionless depth with which the top heading is excavated (Figure 2.24). These observations are an initial indication that, for tunnelling purposes, the soils in the soft ground classes did not present marked differences.

Regarding Figure 2.23a, it should be pointed out that although it would appear that all tunnels in Class III soils (i.e., coarse grained coherent) were built using fairly large invert closure distances, this is not actually verified. Inspection of Table 2.4 will show that, in fact. Two of the three cases of Class III for which L/D_m was available (cases 10 and 25), were non-urban tunnels, which is responsible for the longer invert closure distances. However, still with respect to Figure 2.23a, it is observed that tunnels in Class IV (i.e., sandy cohesionless soils) do have surprisingly high L/D_m ratios. All four cases examined in this class (cases 19,

20, 21, and 22) were Japanese tunnels excavated in fairly dense sands and although cases 20, 21 and 22 are located in urban areas, it is possible that the structures existing in their vicinity were not significantly sensitive. Also, it has to be pointed out that Japanese practice, as shown in the cases analyzed, appears to favour longer invert closure distances, associated with other ground control techniques such as extensive forepoling by steel plates in the upper portion of the tunnel and ground anchors. Although extensive use of anchors was made in early NATM tunnels in soft ground, their effectiveness as a support aid has been questioned (Schulz and Edeling, 1972; Laabmayr and Weber, 1978). In recent soft ground tunnels built in West Germany anchors have been totally dismissed (Höchmut et al., 1987) and their apparent effectiveness in the Japanese tunnels certainly deserves further attention.

Inspection of Tables 2.3 and 2.4 also shows that the rib spacing (s) and length of one excavation round (L_a) do not vary much and, in fact, could be estimated as varying from 0.8m to 1.2m in most cases, regardless of the type of soil. Observations carried out in smaller diameter NATM tunnels (Heinz, 1984; Kuwajima, 1988) show that the rib spacing is normally shortened when the tunnel excavation passes near sensitive structures. This is seen as a way to minimize some of the displacement around the tunnel by stiffening the support, without however increasing the lining thickness, which could generate cracking problems (Müller, 1978). The

parameter L_a is believed to have been in most cases, equal to one rib spacing, regardless of the type of soil, location of the tunnel, or geometry.

Regarding the Settlement Performance


From inspection of Table 2.6, it is realized that the vast majority of cases of large cross-section tunnels examined fall below the limit $V_s = 1.5\% V_{tn}$ which may be considered good performance. Possible bias exists due to the fact that cases where excessive displacements occurred are seldom reported in detail but, it is apparent that values of V_s/V_{tn} of 1.5% or less may be achieved under normal circumstances (i.e., firm soils, experienced workmanship). Also, it is noticeable that non-urban tunnels (cases 10, 18, 19 and 25) present V_s/V_{tn} values consistently higher than urban tunnels, what can be probably related to the more relaxed construction procedure with which these tunnels are executed.

Regarding Initial Support Quantities

The initial support types which were more frequently used in the cases reviewed (Table 2.5), are schematically illustrated in Figure 2.20. It did not prove practical to present the specifications for the various components of the shotcrete support (e.g., steel ribs, welded wire mesh) in this figure. This is because the tunnels, coming from a variety of geographical-cultural areas, presented an

accordingly varied range of these components. Detailed information may be found in some of the individual tunnel files, presented in Appendix A. Some general information, given in recent review papers by Duddeck et al. (1984), Lechnitz and Kirschke (1986) and Hochmut et al. (1987), may also be considered to complement that given in Figure 2.20 and Table 2.5. The following observations are believed to be applicable to large cross section tunnels with total excavated areas up to 150m²:

a) Steel Sets



The main function of the steel sets is to provide support and assure the safety of the excavation crew before the shotcrete is fully hardened. It also serves as an aid in controlling the excavation profile during construction (Maidl, 1984:113). Light GI and TH profiles¹ are normally preferred, but lattice girders have also had increasing use. Hochmut et al. (1987) favour the use of lattice girders due to their lower weight, smaller spray shadows (and therefore an improved bond with the shotcrete) and also a reduction of the lining permeability, which is particularly significant when compressed air is used. Lechnitz and Kirschke (1986), however, refer to these members as highly sensitive to transport and report occasional breakage at

¹ Details of steel sets commonly used are included in Appendix A.

welding points, hence they favour the use of heavier steel profiles.

b) Reinforced Shotcrete

The thickness of the shotcrete lining in the majority of cases investigated was 20 to 30cm, which is in agreement with standards described by Hochmut et al. (1987). In West Germany, concrete quality B25 (nominal 28 day cube compressive strength 25N/mm^2) is required, plus an early strength of 5N/mm^2 after 6 hours. Regarding the shotcrete thicknesses (t), the following minimum reinforcement, in the form of welded wire mesh, is quoted by Duddeck et al. (1984) for large cross section tunnels with an excavated area up to 140m^2 :

$t < 20\text{cm}$: 1 external layer of Q188 ($1.88\text{cm}^2/\text{m} - 3.01\text{kg/m}^2$: $\varnothing 6.0\text{mm}$ in $150 \times 150\text{mm}$ openings)

$t \geq 20\text{cm}$: 2 (external and internal) layers of Q188

The steel employed in the mesh should be BSt 500/550 ($f_y = 550\text{ N/mm}^2$). The minimum shotcrete cover is usually set to 3cm on both sides. The mesh should overlap at least 2 openings ($\approx 30\text{cm}$) circumferentially and 1 opening ($\approx 15\text{cm}$) longitudinally.

2.5.5 Empirical Recommendations for Excavation and Support

In an attempt to summarize the experience collected in the case histories reported above, excavation parameters and support quantities believed appropriate for

each soft ground class are summarized in Figures 2.25 to 2.28. It is necessary to reiterate that the information provided is intended for preliminary design only, and considerable care should be exercised when extending this past experience to future applications. Numeric values shown represent values or ranges found in the cases surveyed (Tables 2.3 to 2.6).

Figures 2.25 to 2.28 also include layouts of example tunnels for each of the ground classes. Details shown are for the excavation scheme and the initial support measures in cases considered to be conservative in each ground class.

2.6 Comments and Conclusions

2.6.1 General

The current state-of-the-art of soft ground tunnelling includes tunnels of large cross sectional area. Tunnels with up to 150m² of excavated cross section and no intermediate pillars for permanent support have been constructed in a variety of ground conditions using variations of the New Austrian Tunnelling Method (NATM). Initial support, in all the cases reviewed, was provided by suitable combinations of shotcrete, steel ribs and welded wire steel meshes.

2.6.2 Classification of Excavation Schemes

In order to control ground deformation and maintain face stability in such works, use is made of "staged excavation". This consists of avoiding full face advance by s

driving smaller, specially arranged headings. Although an unlimited number of staged excavation schemes may be envisaged, there appears to be a tendency to rely on some typical layouts. These were reviewed and classified.

Selection criteria for the excavation scheme were examined but no rigid rules could be established, since the choice of a scheme appears to depend on numerous factors which are not always controlled by the geotechnical engineer. For tunnels with more than about 90m², constructed under unfavourable conditions (e.g., urban areas and/or the necessity of draining the ground from inside the tunnel), preference appears to be given to T3 schemes, where initial advance makes use of side galleries. An alternative scheme, with use of one side gallery only (T2b) is apparently preferred for smaller cross sections under the same circumstances.

2.6.3 Settlement Behaviour

An insight into the settlement behaviour during construction of large cross section tunnels was obtained using simplified numerical techniques. Two-dimensional finite element analyses were carried out to compare the relative performance of three construction schemes. The results of these analyses were compared with field measurements from an actual case history. It was seen that, despite several simplifications introduced in the analyses, aspects of field

behaviour could be reproduced hence reinforcing the validity of these studies.

It was verified, through these numerical studies, that the T3 staged excavation scheme (with side galleries) is superior to heading and bench schemes (T1b and T2a) in terms of maximum surface settlement generated. This is attributed to the sequence of excavation and support placement in the T3 scheme, where the temporary linings in the side galleries are stiff inclusions which contribute to the reduction of settlement. The slope of the settlement trough for scheme T3 was also found to be flatter, confirming assertions by Krischke and Weber (1981). No significant difference in terms of settlement performance was verified between schemes T2a and T1b, but it is recognized that this might be related to the simplified two-dimensional behaviour assumed in the analyses. Information presented by Laabmayr and Swoboda (1986) suggests that the use of schemes with two cells (i.e., headings fully enclosed by a shotcrete ring) such as the T2b may reduce considerably the settlements which occur ahead of the excavation face.

Excavation of the top heading of all three schemes evaluated was shown to be responsible for a significant amount of the total settlement. Review of a few case histories shows that excavation and support of this portion is carried out with special care. Use of sliding beams in the crown area, as well as of temporary hydraulic supports was made in certain instances. Another measure frequently used

was a central support core in the heading portion. Construction times evaluated for a particular case history also show that excavation and support of the central heading portion is responsible for about 50% of the total time spent in the construction of one meter of tunnel. This confirms that excavation of this portion is carried out with extreme care.

2.6.4 Empirical Recommendations

Data from a number of case histories of large cross section tunnels was collected in the literature and through personal correspondence with authors and companies. In order to make this information more useable, all cases studied were classified into four soft ground classes. It is believed that a new tunnel could be placed in one of these classes using engineering judgement.

The average support quantities determined for each ground class were not found to differ significantly. However, a noticeable variation was verified in the construction parameters, depending on the environment in which the tunnel was built (i.e., non urban, urban and sensitive urban).

Summary figures were presented for each ground class and are expected to enable at least a preliminary determination of construction procedures and initial support quantities. This information, although believed attractive, should only be used with judgement and possibly in conjunction with more refined analytical models, provided sufficient information is

available. It is believed that the classification proposed could be expanded as increasing experience with large cross section tunnels in soft ground becomes available.

Table 2.1 Tunnelman's soft ground classification as described by Peck (1969)

CLASSIFICATION	BEHAVIOUR DURING TUNNELLING	TYPICAL SOIL TYPES	FURTHER REMARKS
FIRM	<p>A heading may be advanced several feet, either by hand or by machine, without immediate support. Tunnelling can be accomplished without danger of collapse because there is adequate time for the erection of the initial support.</p>	<p>Stiff clays and cemented or cohesive granular materials when not subjected to high insitu stresses.</p>	
RAVELLING	<p>Chunks or flakes of material in the upper part of the working face may fall into the heading some time after they are exposed. The action is progressive and may lead to open cavities above the tunnels or even to sinkholes at the surface. The raveling can be prevented if at least moderate support is provided at an early stage, before loosening becomes extensive.</p>	<p>Slightly cohesive sands, silts and fine sands gaining their strength from apparent cohesion; residual soils with relict structure from the parent rock.</p>	<p>1) If raveling is permitted to start, loss of the heading may occur during construction or seriously unbalanced or non-uniform loadings may develop against the lining even after the passage of considerable time. 2) Seepage forces caused by the flow of water toward the working face may increase the tendency to ravel. Hence, there might be instances where raveling ground may be transformed to firm by pre-drainage.</p>
RUNNING	<p>Materials run from any unsupported face until a stable pile is built up at the angle of repose. Soil above the roof needs to be supported by, for example, poling boards.</p>	<p>Perfectly cohesionless materials such as dry sand or clean loose gravel.</p>	<p>1) Running soil may slope into the heading and may bury the lower part of a conventional shield, stopping its progress and leading to an extensive hand excavation to free machine.</p>

Table 2.1 Tunnelman's soft ground classification (contd.)

CLASSIFICATION	BEHAVIOUR DURING TUNNELLING	TYPICAL SOIL TYPES	FURTHER REMARKS
FLOWING	Soil advances like a thick liquid into the heading and may eventually fill all of the tunnel. Tunnelling through such materials cannot be usually accomplished satisfactorily unless the materials are first transformed into ravelling or firm ground (e.g., drainage, compressed air, chemical grouting).	Ravelling or running ground when seepage pressures are permitted to develop. Usually silt, sand or gravel without enough clay content to create a significant cohesion. Highly sensitive clays may flow when disturbed.	
SQUEEZING	Ground slowly squeezes into the tunnel without any signs of fracturing and without any perceptible increase in water content. Can be tunnelled successfully by hand methods if the rate of squeeze is not excessive.	Very soft to medium clays. Rate of squeezing will depend on the insitu stresses.	<ol style="list-style-type: none"> 1) Construction may be facilitated by the use of air pressure. 2) Materials are frequently impervious so construction performance may not be significantly enhanced by drainage.
SWELLING	Like squeezing ground moves slowly into the tunnel but the movement is associated with a very considerable volume increase of the ground surrounding the tunnel.	Heavily overconsolidated clays with a Plasticity Index in excess of about 30.	

Table 2.2 Soil groups defined by Peck (1969)

GROUP	TYPICAL SOIL TYPES	REMARKS
Cohesionless granular soils	Silts, sands or gravels which are cohesionless except for capillarity	<p>a) Tunnelling through such materials can be carried out only by complete protection of the top, sides and face of the excavation (e.g., forepoling).</p> <p>b) If the materials are dense and the construction procedures are expertly carried out so that no runs occur, loss of ground and settlements are usually negligibly small.</p>
Cohesive Granular Soils	Clayey sands, sandy clays, cohesive silts, residual soils possessing a cohesive bond, marls.	<p>a) Initial tangent modulus relatively high, often strain weakening behaviour under low confining stresses.</p> <p>b) Well executed tunnels in these materials are usually accompanied by very modest or negligible loss of ground.</p>
Non-swelling Stiff to Hard Clays	Clayey tills, stiff clays.	<p>a) Unless they possess a well-developed secondary structure, these soils are unlikely to ravel or to be adversely influenced by seepage toward the opening.</p> <p>b) Loss of ground usually negligibly small.</p>
Soft to stiff saturated clays	Sensitive clays, glacial clays.	<p>a) Although completely undisturbed masses of such clays may possess considerable rigidity due to the presence of bonds between particles, disturbances due to tunnelling are usually great enough to break these bonds.</p> <p>b) Loss of ground usually significant.</p>

Table 2.3 Large cross section tunnels surveyed

CASE#	TUNNEL	LOCATION	YEAR	PURPOSE	AREA(m ²)	SCHEME	H/D	MAIN REFERENCE
1	Baulos A2 #1	Bochum, FRG	1973	2 track subway	64	T1b	0.6-1.4	Jagsch et al. (1974)
2	Baulos A2 #2	Bochum, FRG	1973	2 track subway	64	T1c	0.6-1.4	Jagsch et al. (1974)
3	Hasenbuck	Nürnberg, FRG	1972	2 track subway	75	T1a	<2.5	Bauernfeind (1984)
4	Lorenzkirche #1	Nürnberg, FRG	1976	station (1 track)	65	T1b	1	Bauernfeind et al. (1978)
5	Lorenzkirche #2	Nürnberg, FRG	1976	station (1 track)	65	T1b	1	Bauernfeind et al. (1978)
6	Rothenburgstrasse	Nürnberg, FRG	1979	2 track subway	85	T1b	0.7	Bauernfeind et al. (1986)
7	Grigny #1	Paris, France	1974	2 track subway	80	T1b	0.8-1.6	Egger (1975)
8	Grigny #2	Paris, France	1974	2 track subway	80	T2a	0.8-1.6	Egger (1975)
9	Butterberg	Osterode, FRG	1978	2 track railway	90	T1b	<2.5	Duddeck et al. (1981)
10	Sinnberg - South Portal	N of Würzburg, FRG	1981	2 track railway	138	T1a	<1.5	Harpi/Gals (1983)
11	Martinstrasse	Essen, FRG	1983	station	132	T3	<0.5	Stadt Essen (1981)
12	North Extension	Sao Paulo, Brazil	1984	2 track subway	77	T2a	<2.5	Cruz et al. (1985)
13	Baulos 9/18.2	Munich, FRG	1976	2 track subway	106	T3	0.7-1.7	Laabmayr/Weber (1978)
14	Unidentified	Munich, FRG	1979	2 track subway	88	T3	<2.5	Krischke/Weber (1981)
15	Unidentified	Munich, FRG	1979	2 track subway	88	T2b	<2.5	Krischke/Weber (1981)
16	Genegic T2b	Munich, FRG	1986	2 track subway	64	T2b	<2.5	Hochmut et al. (1987)
17	Viventogasse	Vienna, Austria	1987	2 track subway	64	T2b	0.9	Deix/Gebeshuber (1987)
18	Hiraiashi No.1	N of Tokyo, Japan	1978	2 track railway	90	T1b	0.14-0.65	Mussger (1981)
19	Kokubu	Matsudo, Japan	1984	drainage	60	T1b	0.6-2.3	Fujimori et al. (1985)
20	Kuriyama - Yagiri #1	Tokyo, Japan	1984	2 track railway	73	T2a	1.0-1.4	Horiuchi et al. (1986)
21	Kuriyama - Yagiri #2	Tokyo, Japan	1984	station	90	T3	0.4-1.2	Horiuchi et al. (1986)
22	Narita Airport Section 9	Tokyo, Japan	1983	station	90	T3	0.7	Imaki et al. (1984)
23	Hokushin #1	Kobe, Japan	1985	2 track railway	130	T2a	1.27	Matsusita/Shimizu (1986)
24	Hokushin #2	Kobe, Japan	1985	2 track railway	70	T1b	1.27	Matsusita/Shimizu (1986)
25	Ran-Hokke	Noboribetsu, Japan	1981	2 track railway	70	T2a	2	Miyazaki (1982)

NOTE'S:

* Probable year of completion

** H/D = Soil cover above crown / Equivalent diameter of the full cross-section

Table 2.4 Geometric parameters surveyed

CASE#	TUNNEL	CLASS	W(m)	Ht(m)	Dm(m)	L(m)	Lh(m)	La(m)	Ah/At(m)
1	Baulos A2 #1	Urban+	10.2	8.5	9.03	11.0	2.0	1.0	0.30
2	Baulos A2 #2	Urban+	10.2	8.5	9.03	4.0	0.8	0.5-0.8	0.15
3	Hasenbuck	Urban	11.0	7.5	9.77	>50		1.0-1.5	0.52
4	Lorenzkirche #1	Urban+	9.6	8.4	9.10	2.6	1.6	0.8	0.30
5	Lorenzkirche #2	Urban+	9.6	8.4	9.10	2.6	1.2	0.6-0.8	0.30
6	Rothenburgerstrasse	Urban	13.2	7.5	10.40	12.0	3.0	3.0	0.40
7	Grigny #1	Urban	10.4	9.3	16.09			0.8-1.2	0.25
8	Grigny #2	Urban	10.4	9.3	8.10			0.8-0.9	0.25
9	Butterberg	Urban	11.7	10.1	10.70	10.0	4.0		0.26
10	Sinnberg - South Portal	Non Urban	15.5	11.0	13.26	50.0	20-50		0.40
11	Marinstrasse	Urban	15.9	10.1	9.84	20.0	5.5	1.0	0.16
12	North Extension	Urban	11.5	8.5	7.40	8.0	2.5-3.0	1.0	0.23
13	Baulos 9/18.2	Urban	11.4	8.2	9.01	10.5	10.0	1.0	0.22
14	Unidentified	Urban	13.1	8.3	7.82		2.0-4.0	0.8-1.0	0.25
15	Unidentified	Urban	13.1	8.3	7.48		2.0-4.0	0.8-1.0	0.20
16	Generic T2b	Urban	9.0	8.5	6.38	6.0	2.0-4.0	1.0	0.18
17	Vivonogasse	Urban+	9.5	8.5	6.38	5.0	3.0	1.0	0.24
18	Hiratashi No.1	Non Urban	11.4	10.0	10.70	25.0	10.0	0.8-1.2	0.25
19	Kokubu	Non Urban	8.6	8.3	8.74	20.0		0.9	0.26
20	Kuriyama - Yagiri #1	Urban	10.2	8.7	7.00			1.0	0.05
21	Kuriyama - Yagiri #2	Urban	12.4	8.9	6.15			0	0.05
22	Narita Airport Section 9	Urban	13.4	11.2	9.41	15.0	2.5	1.0	0.07
23	Hokushin #1	Urban+	10.4	8.5	9.44	20.0		0.8	0.27
24	Hokushin #2	Urban+	10.4	8.5	7.00		3.0-6.0	0.8	0.65
25	Ran-Hokke	Non Urban	9.7	8.5	9.44	40-60	10-20	1.0-1.2	0.31

- NOTES:
- 1) L = distance between face and first invert closure (except in T3 schemes)
 - 2) Lh = length-supported but with no invert closure (usually initial top heading)
 - 3) La = unsupported advance ("round length")
 - 4) Dm = equivalent diameter of critical portion. (see guidelines in text)

Sensitive Urban Area

Table 2.5 Support characteristics of tunnels surveyed

CASE#	TUNNEL	Crown		SUPPORT TYPE Sides		Floor		s (m)
		Type	t (cm)	Type	t (cm)	Type	t (cm)	
1	Baufos A2 #1	B	25	B	25	C	25	1.0
2	Baufos A2 #2	B	25	B	25	B	25	0.5-0.8
3	Hasenbuck	A	15-20	A	15-20			1.0-1.5
4	Lorenzkirche #1	A	20	A	20	C	25	0.8
5	Lorenzkirche #2	A	20	A	20	A	25	0.6-0.8
6	Rothenburgerstrasse	A	20	A	20	(A)	25	0.8
7	Grigny #1	B	20	B	20	G	135	0.8-1.2
8	Grigny #2	B	30	B	30	G	135	0.8-0.9
9	Butterberg	F	30	B	30	C	30	1.0
10	Sinnberg - South Portal	F	30	B	30	C	50	0.8
11	Martinstrasse	B	25	B	25	D	15	1.0
12	North Extension	B	25	B	25			1.0
13	Baufos 9/18.2	B	30	B	30	C	30	1.0
14	Unidentified	B	25	B	25	C	25	1.0
15	Unidentified	B	25	B	25	C	25	1.0
16	Generic T2b	(B)	20	(B)	20	(C)	20	1.0
17	Vivendgasse	(B)	25	(B)	25	C	25	1.0
18	Hiraiashi No.1	F	25	(B)	25	C	28	1.0
19	Kokubu	F	20	B	20	G	50	0.8-1.2
20	Kuriyama - Yagiri #1	F	20	(A)	20	G	70	0.9
21	Kuriyama - Yagiri #2	F	20	(A)	20	G	70	1.0
22	Narita Airport Section 9	F	20	(A)	20	G	70	1.0
23	Hokushin #1	F	20	(A)	20	(D)	20	1.0
24	Hokushin #2	F	20	(A)	20	(A)	20	0.8
25	Ran-Hokke	F	20-25	C	20-25	G	40	1.0-1.2

NOTES:
 () Probable value
 For a description of support types see Figure 2.20

Table 2.6. Settlement performance of tunnels surveyed.

CASE#	TUNNEL	AREA(m ²)	D (m)	H (m)	Max S	Vs (m ³ /m)	Vs/Vtn (%)	ESs/Gama.D2
1	Baulos A2 #1	64	9.03					
2	Baulos A2 #2	64	9.03	13	17.6	0.39	0.61	
3	Hasenbuck	75	9.77	5	34	0.42	0.56	1.780
4	Lorenzkirche #1	65	9.1					
5	Lorenzkirche #2	65	9.1					
6	Rothenburgerstrasse	85	10.4	7	20	0.31	0.36	0.820
7	Grigny #1	80	10.09	12	48	1.02	1.28	
8	Grigny #2	80	10.09					
9	Butterberg	90	10.7	13.5	13	0.31	0.34	0.961
10	Singberg - South Portal	138	13.26	13.7	80-200	2.06-5.08	1.49-3.68	
11	Martinstrasse	132	12.96					
12	North Extension	77	9.9	11				
13	Baulos 9/18.2	106	11.62	8	19.5	0.39	0.51	0.660
14	Unidentified	88	10.59		10	0.17	0.16	0.530
15	Unidentified	88	10.59	16	50			
16	Generic T2b	64	9.03		50	1.33	1.51	3.180
17	Vivendogasse	64	9.03					
18	Hiraiashi No.1	90	10.7	3.5	110	1.22	1.36	0.700
19	Kokubu	60	8.74	20	29	0.88	1.47	0.950
20	Kuriyama - Yagiri #1	73	9.64	10	41.8	0.77	1.05	
21	Kuriyama - Yagiri #2	90	10.7	10	66.5	1.28	1.42	
22	Nanta Airport Section 9	130	12.87	8.3	72	1.33	1.02	
23	Hokushin #1	70	9.44					
24	Hokushin #2	70	9.44					
25	Ran-Hokke	70	9.44	20	15.2	0.47	0.67	

NOTES:
 * Equivalent diameter with respect to full cross section
 ** Soil cover above crown at instrumented section
 $I=(C+D)/2$ = trough width parameter

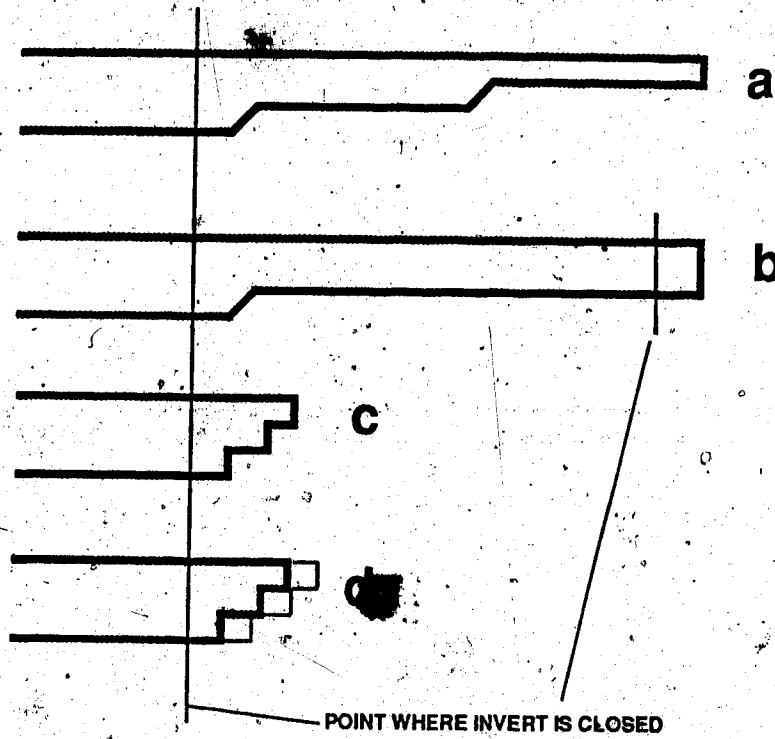


Figure 2.1 Illustration of invert closure distance in various excavation schemes

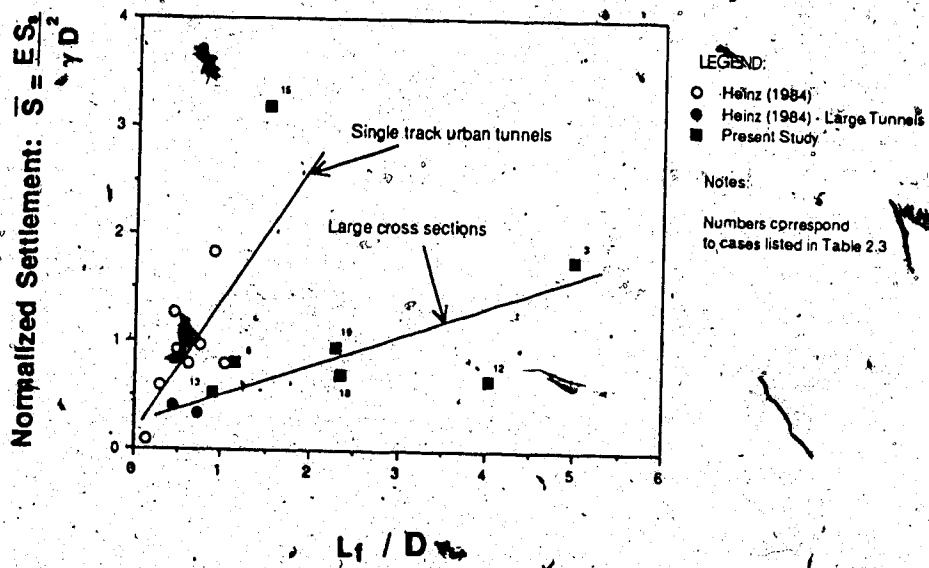


Figure 2.2 Effect of invert closure distance on settlements


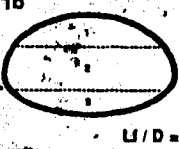


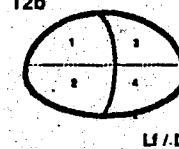
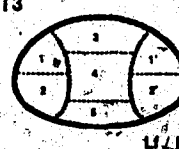
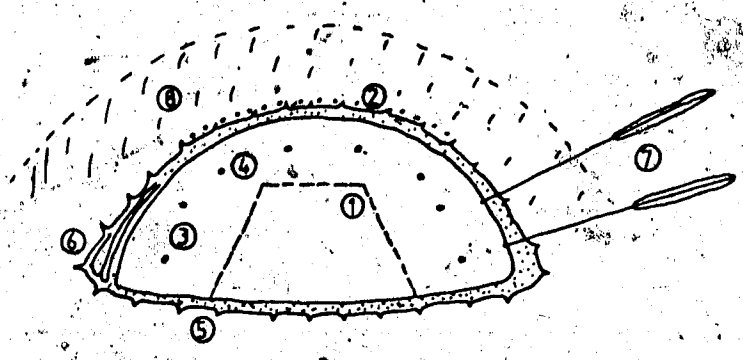
TYPE OF STAGED EXCAVATION	CROSS SECTION (m ²)	EXAMPLE OF APPLICATION	% TOTAL AREA (2)
<p>T1a</p>  <p>L/D=3</p>	70-138 (N=3)	NÜRNBERG (Müller/Bauernfeind, 1977) At=75m ² - 2 track subway SOFT SANDSTONE E=80-160MPa, Ø'=30-45° (4) (Case #3 in Table 2.3)	1 = 50% 2 = 40% 3 = 30%
<p>T1b</p>  <p>L/D=1-2</p>	64-90 (N=9)	NÜRNBERG (Bauernfeind et al., 1978) At=65m ² - 2 track subway SOFT SANDSTONE E=80-160MPa, Ø'=30-45° (4) (Case #3 in Table 2.3)	1 = 35% 2 = 45% 3 = 20%
<p>T1c</p>  <p>L/D=3</p>	64 (N=1)	BOCHUM (Hochmüt et al., 1974) At=64m ² - 2 track subway SOFT TO STIFF MARLS E=10-100MPa, Ø'=25° (Case #1 in Table 2.3)	1 = 17% 2 = 24% 3 = 17% 4 = 24% 5 = 18%
<p>T2a</p>  <p>L/D=4</p>	70-130 (N=5)	SÃO PAULO (Cruz et al., 1985) At=77m ² - 2 track subway STIFF SILTY CLAY E=50-100MPa, SPT 20-50 (Case #12 in Table 2.3)	1 = 60% 2 = 40%
<p>T2b</p>  <p>L/D=3</p>	64 (N=3)	MUNICH (Hochmüt et al., 1987) At=64m ² - 2 track subway STIFF SANDY CLAYEY MARLS (+water-bearing sands) E=90-200MPa, Ø'=25°	1 = 20% 2 = 30% 3 = 20% 4 = 30%
<p>T3</p>  <p>L/D=5</p>	88-132 (N=4)	TOKYO (Horiuchi et al., 1986) At=90m ² - Subway station FINE SANDS (Uncemented) Water bearing, Ø'=25° (Case #21 in table 2.3)	1 = 11% 1' = 11% 2 = 11% 2' = 11% 3 = 17% 4 = 20% 5 = 19%
<p>Notes:</p> <p>(1) Schemes T2a, T2b and T3 have temporary shotcrete walls</p> <p>(2) Approximate values derived from the cases examined</p> <p>(3) L corresponds to final invert closure in the full section</p> <p>D is the "equivalent diameter", calculated from cross section area</p> <p>(4) Dominant soil properties estimated at tunnel axis level</p> <p>(5) N = number of cases examined (see Table 2.3)</p>			

Figure 2.3 Typical excavation schemes for large cross section tunnels



- 1 - Central Support Column
- 2 - Forepoling (spiles or steel plates depending on type of soil)
- 3 - Drainage through face
- 4 - Grouting through face
- 5 - Temporary shotcrete invert (used with a smaller heading, not necessarily T2a scheme)
- 6 - "Elephant foot"
- 7 - Anchors (current use in Japanese tunnels in dense sands)
- 8 - Arch with improved ground properties (e.g., grouting, freezing)

Notes:
 a) Pre-construction dewatering and compressed air not shown
 b) Numbering does not imply order of preference

Figure 2.4 Ground control measures which have been used in addition to excavation schemes in Figure 2.3 (modified after Lechnitz and Kirschke, 1986).

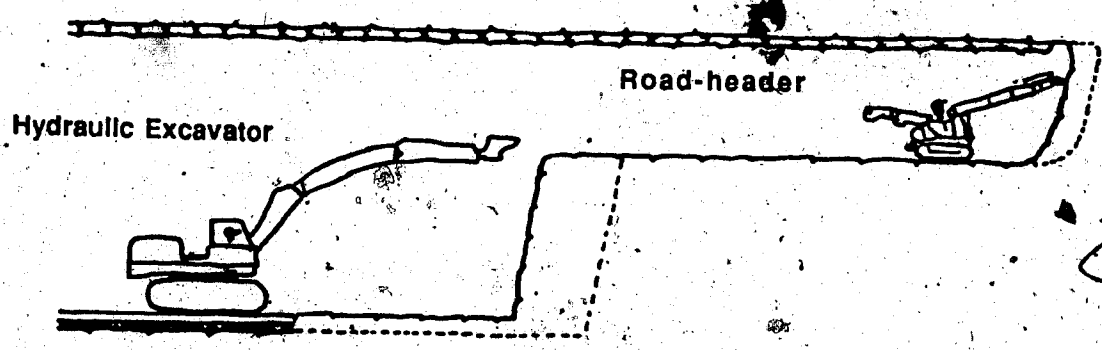


Figure 2.5 Use of road-header and hydraulic excavator in Munich, F.R.G. (modified after Hammer, 1978).

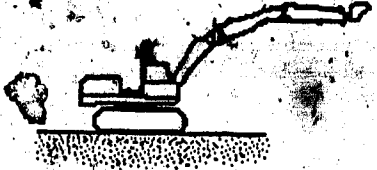
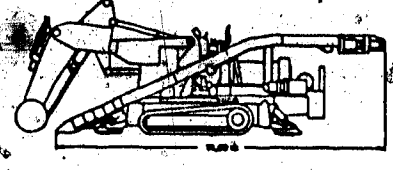
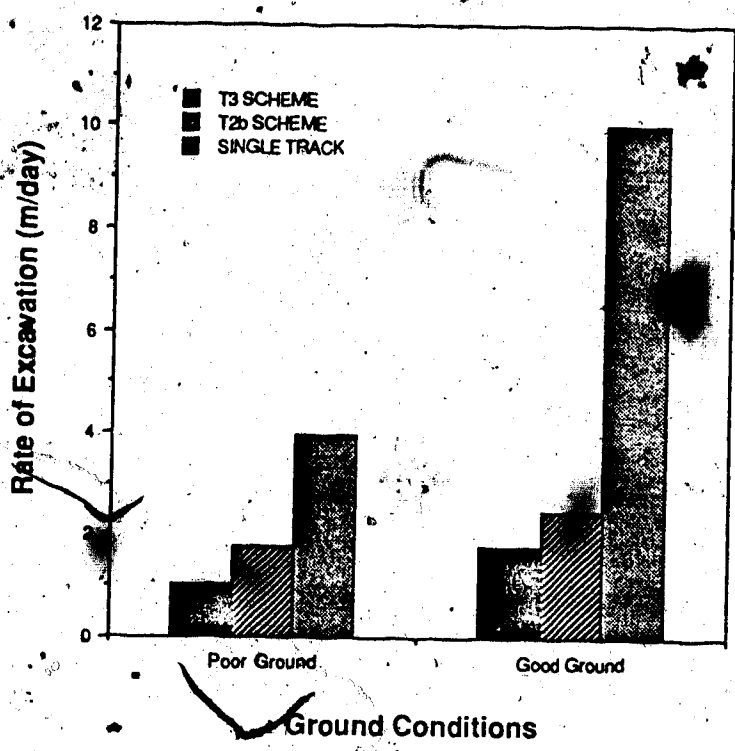
<p style="text-align: center;">Hydraulic Excavator</p> 	<p style="text-align: center;">Road-Header</p> 
<p>APPLICABILITY:</p> <ul style="list-style-type: none"> - soft to stiff soils 	<p>APPLICABILITY:</p> <ul style="list-style-type: none"> - stiff soils, soft rocks
<p>ADVANTAGES:</p> <ul style="list-style-type: none"> - conventional equipment (availability of equipment + operators) - used in works other than tunnels - relatively low cost 	<p>ADVANTAGES:</p> <ul style="list-style-type: none"> - higher rates of advance - practically independent of tunnel size and shape - cross sections of 4-5m² may be excavated - muck removal facilitated when equipped with conveyor belt
<p>DISADVANTAGES:</p> <ul style="list-style-type: none"> - unfeasible in very small cross sections - requires interruption of excavation and additional equipment for muck removal 	<p>DISADVANTAGES:</p> <ul style="list-style-type: none"> - high initial costs - low availability

Figure 2.6 Comparison of excavation equipment frequently used in large cross-section projects



Notes:

SINGLE TRACK: Maximum rates quoted by Distelmeier (1980) for NATM tunnels

Poor Ground: Fast Ravelling at Crown

Good Ground: Firm at Crown

Figure 2.7 Comparison of excavation rates for schemes T2b and T3

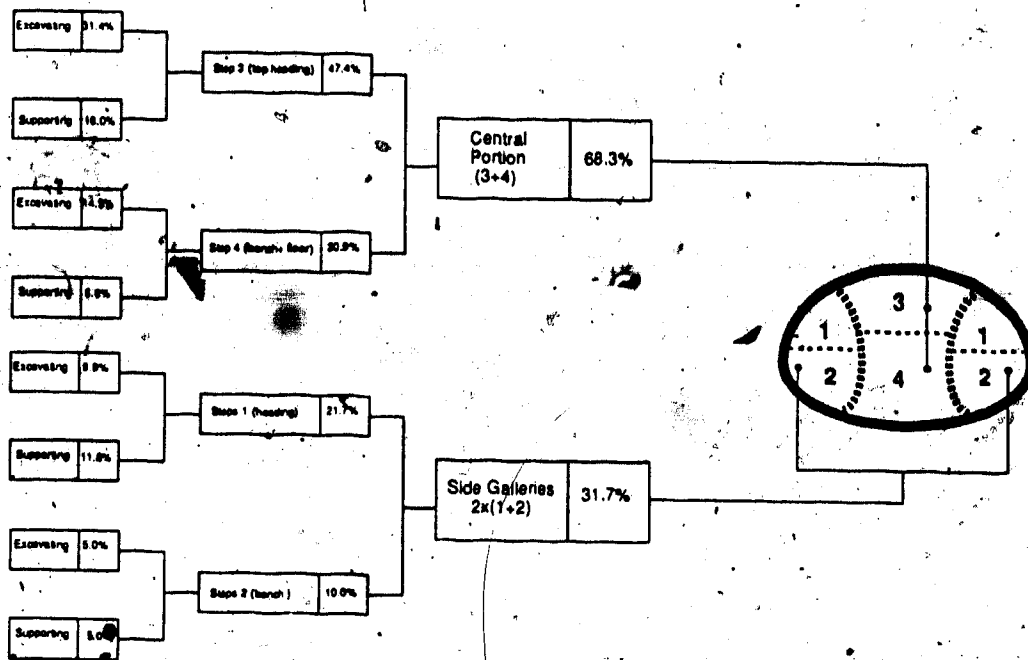


Figure 2.8 Time spent on excavation stages of a T3 tunnel - At=88m² (data from Kruschke and Weber, 1981)

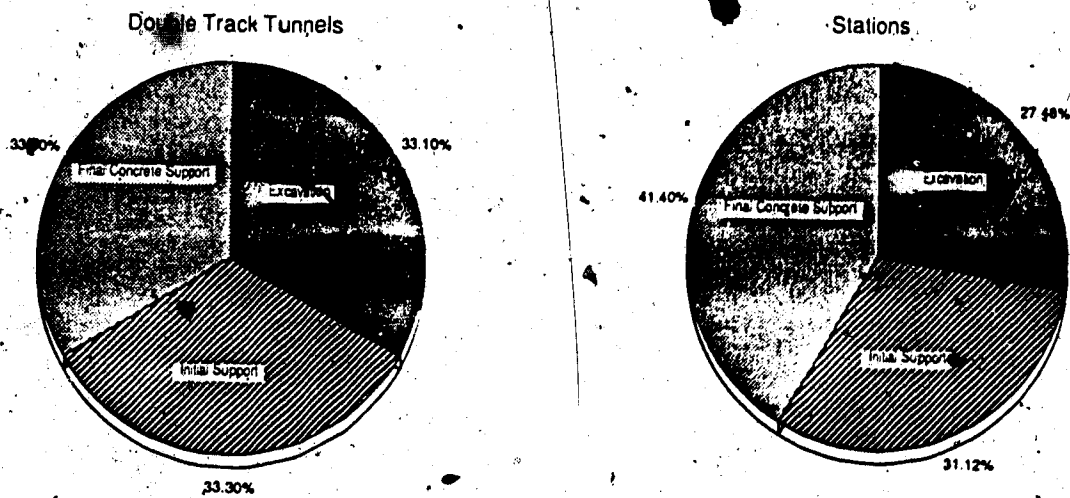
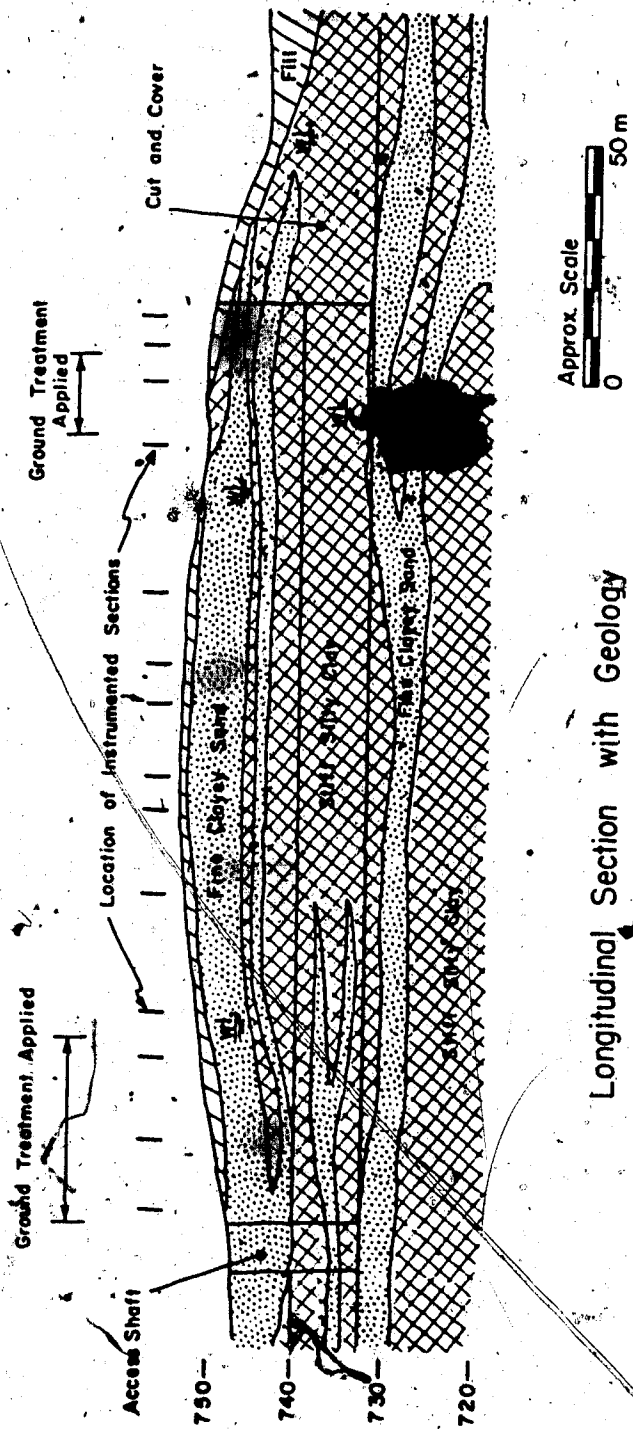
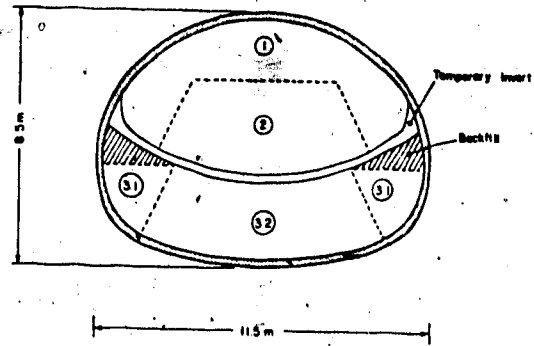


Figure 2.9 Distribution of costs of large cross. section tunnels in Bochum, F.R.G. (data from Laue, 1981)

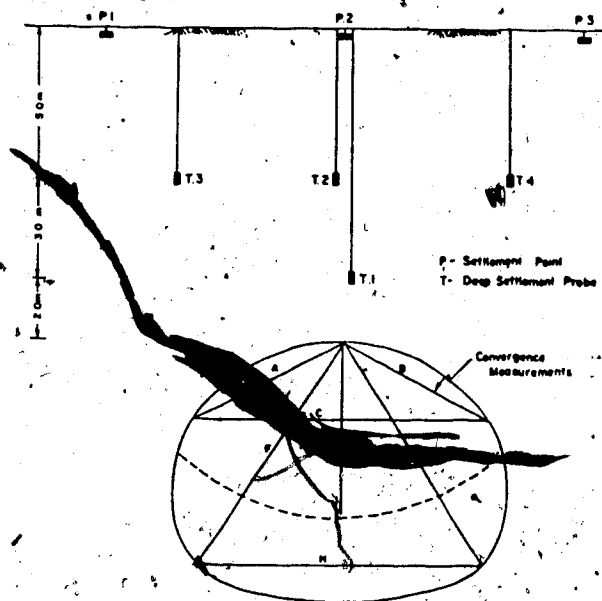


Longitudinal Section with Geology

Figure 2.10 São Paulo North Extension tunnel - geological profile (modified after Cruz et al., 1985)



a) Sequence of Excavation



b) Typical Instrumented Section

Figure 2.11 Details of São Paulo North Extension tunnel
(modified after Cruz et al., 1985)

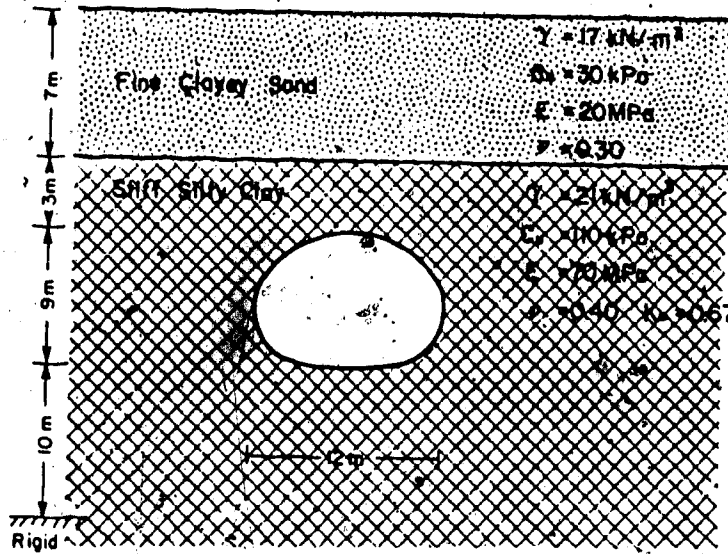


Figure 2.12 Geotechnical profile used in the analyses

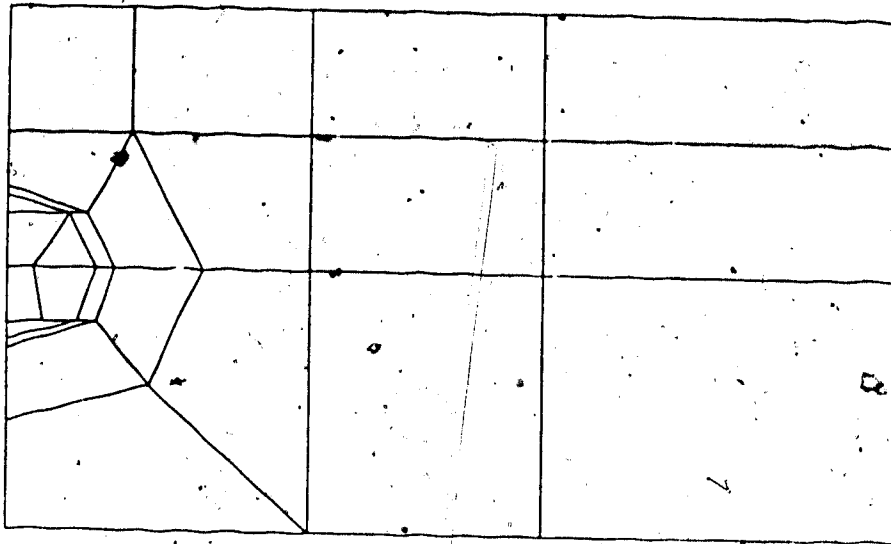


Figure 2.13 Finite element mesh

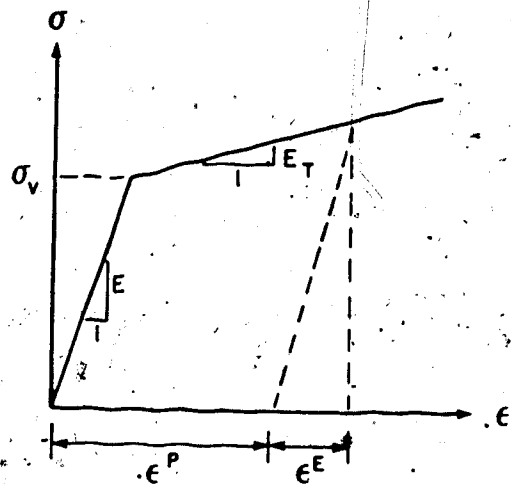
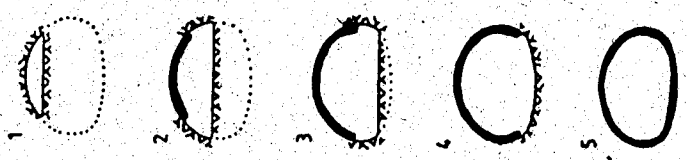


Figure 2.14 Illustration of constitutive model used

T1b



T2a



T3

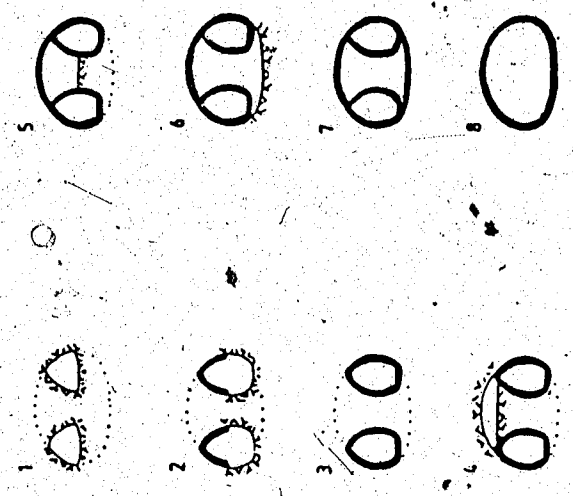


Figure 2.15 Construction simulation sequences in finite element analyses

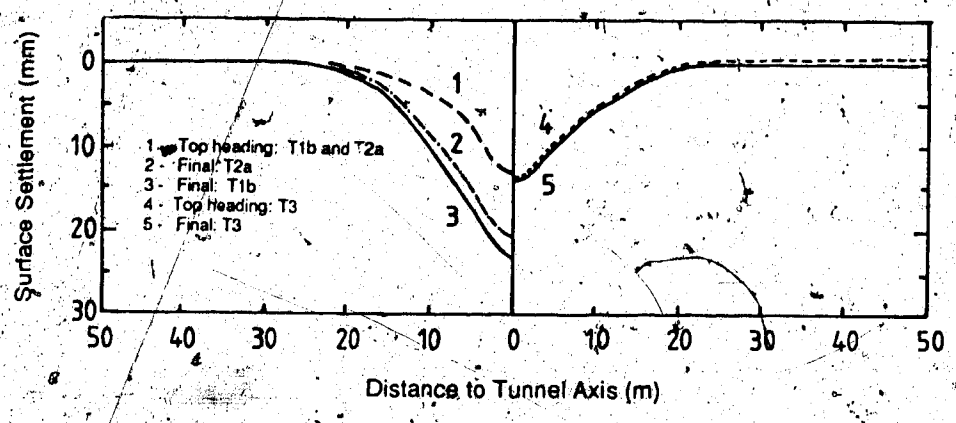


Figure 2.16 Comparison of settlement profiles from FEM simulations using different excavation schemes

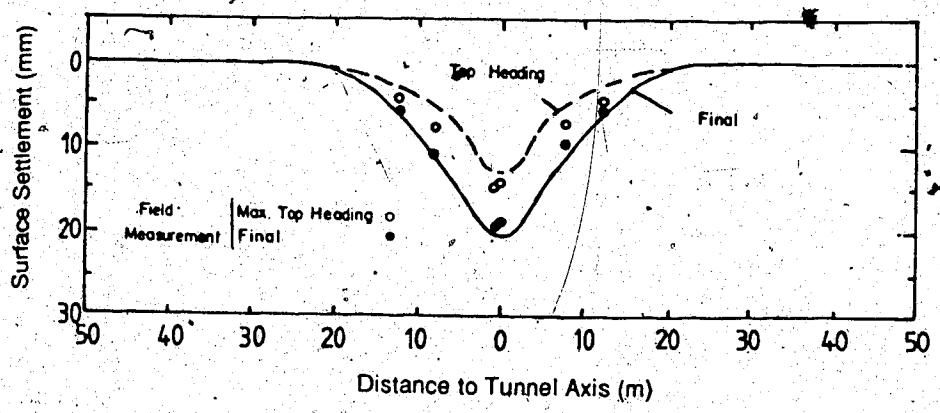


Figure 2.17 Results of T2b simulation (curves) versus actual field readings (points) - São Paulo North Extension Tunnel

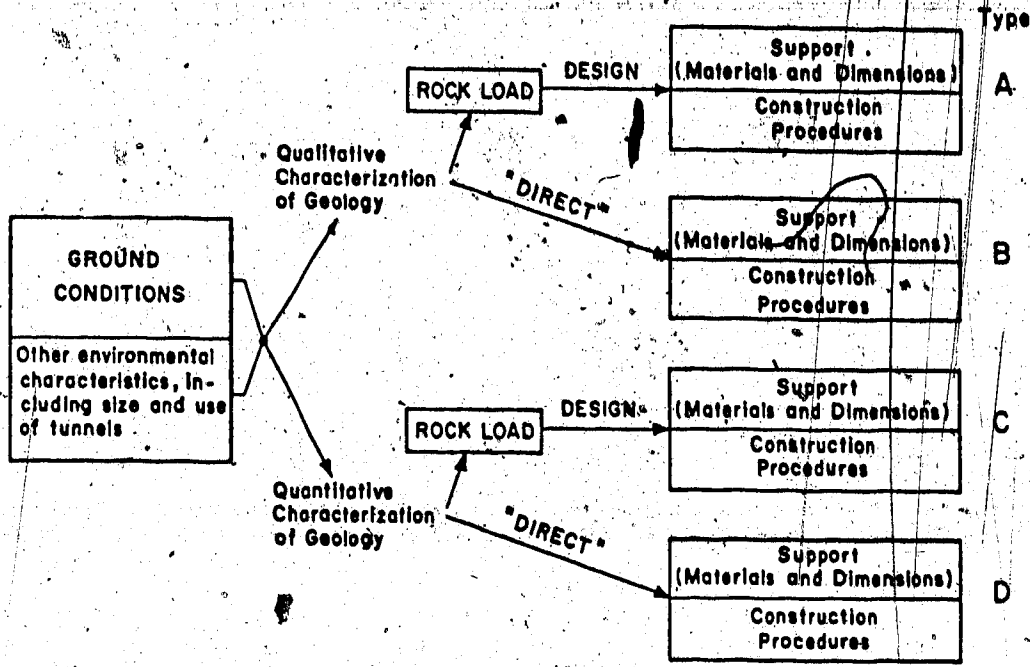


Figure 2.18 Classification of empirical methods in rock tunneling (modified after Steiner and Einstein, 1980)

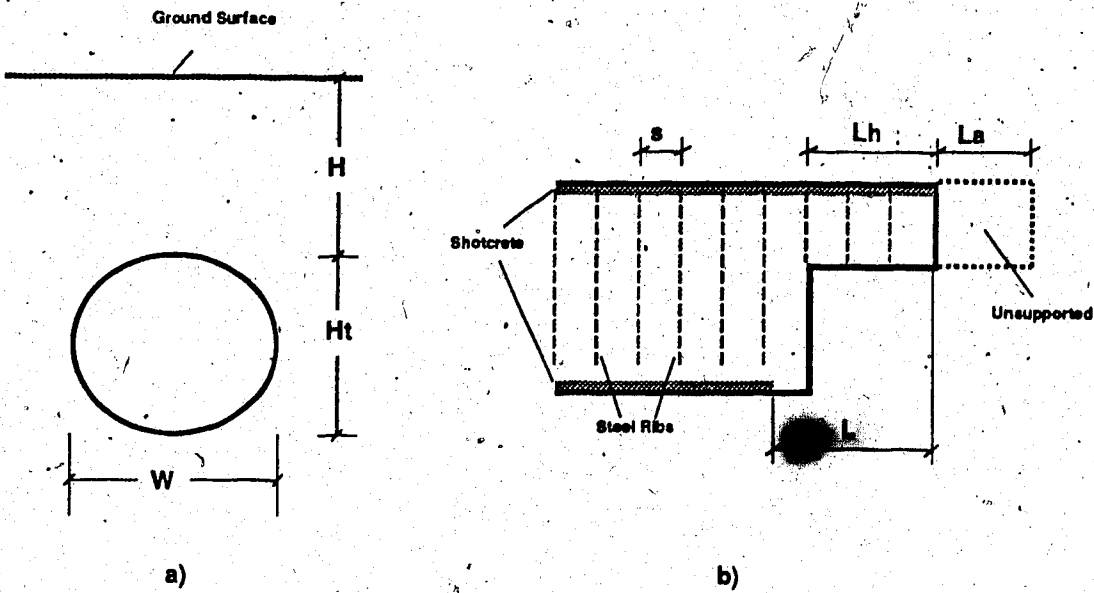


Figure 2.19 Definition of geometric and constructive parameters surveyed

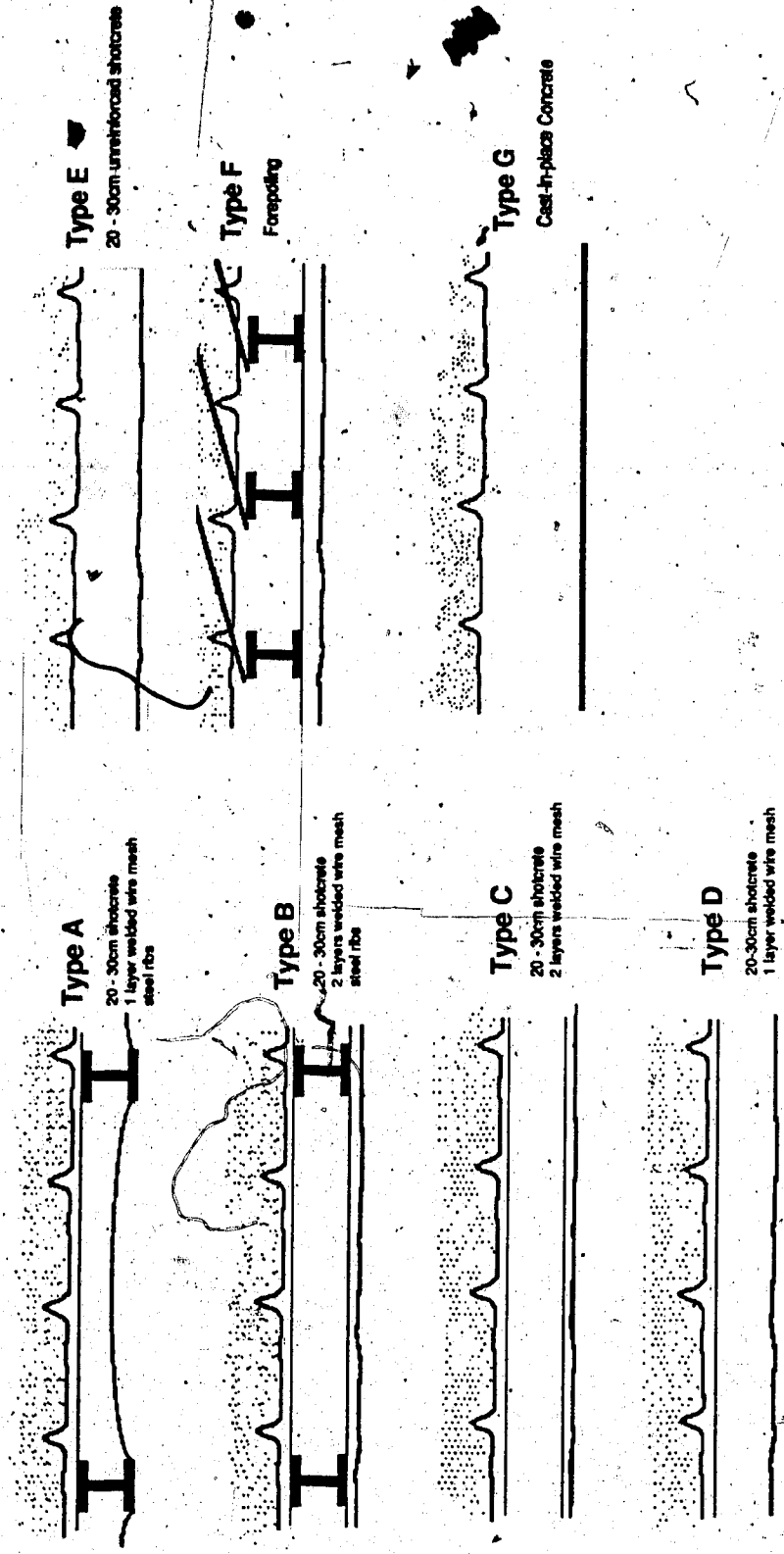


Figure 2.20 Schematic representation of typical support types in the tunnels surveyed (see Table 2.5 and Table A.27)

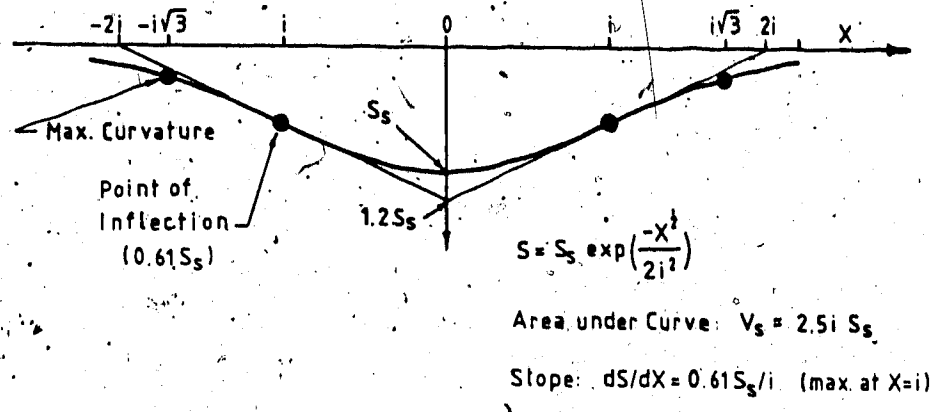


Figure 2.21 Settlement trough represented by the error function (adapted from Clough and Schmidt, 1981)

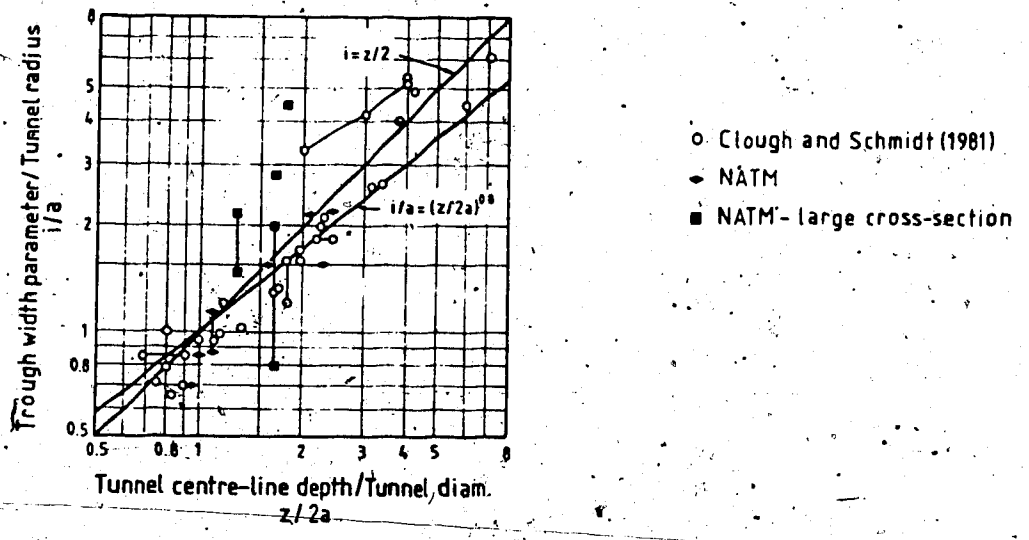


Figure 2.22 Trough width parameter i vs. tunnel depth in a normalized logarithmic diagram (after Heinz, 1984)

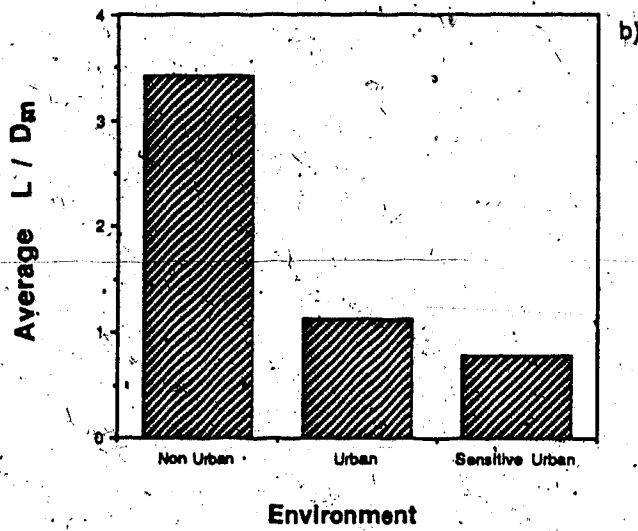
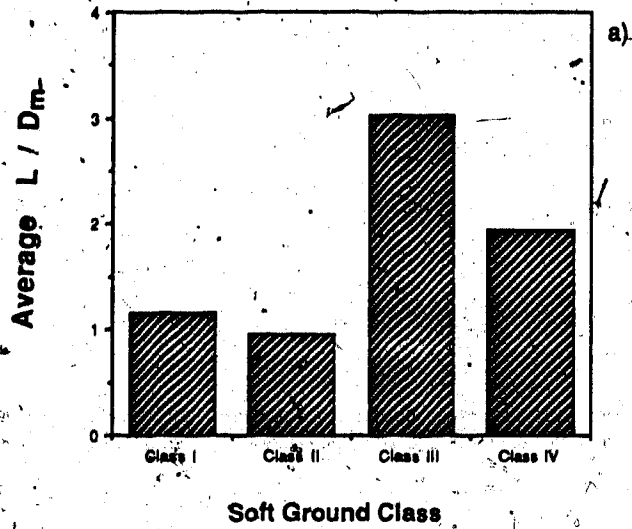


Figure 2.23 Illustration of variability of invert closure within an individual heading

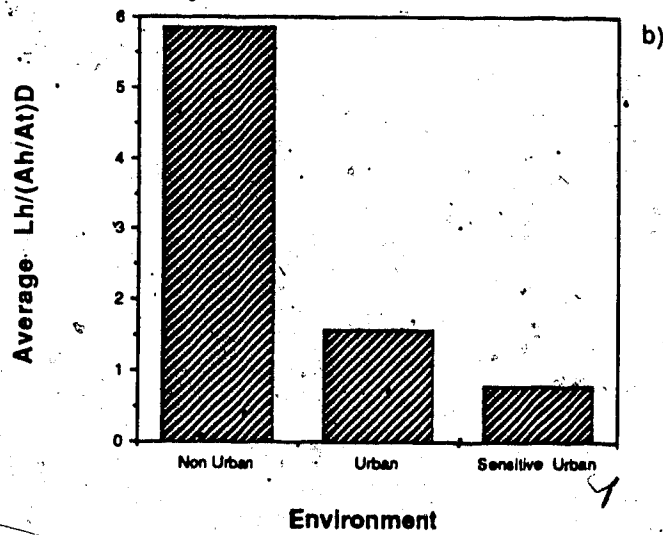
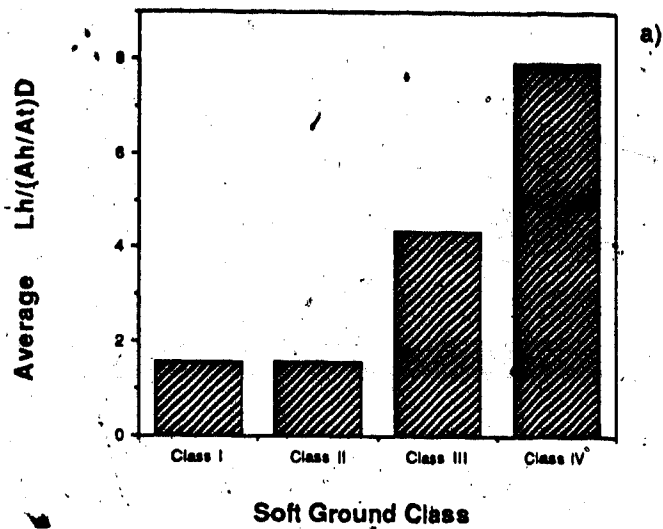


Figure 2.24 Illustration of variability of depth of individual supported heading with no invert closed

Class I: Stiff coherent homogeneous ground

Parameter	Non Urban Area	Urban Area	Urban Sensitive Area
$A_h/A_c - \%A_c$	-	0.2 - 0.5	0.3
L/Dm	-	1.0 - 2.0	0.3
$L_a - s$ (m)	-	1.0	0.8
$L_h / (\%A_c \cdot D)$	-	0.7 - 4.0	0.6
V_s/V_{tn} (%)	-	0.1 - 0.6	-
\bar{S}	-	0.5 - 0.7	-

Notes: 1) Numeric values derived from cases examined
 2) For meaning of parameters see list of symbols

MARTINSTRASSE STATION (Essen, F.R.G.) - Case 11

	Shotcrete	Mesh	Steel Ribs
Floor	15 cm	1 x Q188	-
Sides+Crowns	25 cm	2 x Q188	TH21/29
Intern. Wall	15 cm	2 x Q188	TH16

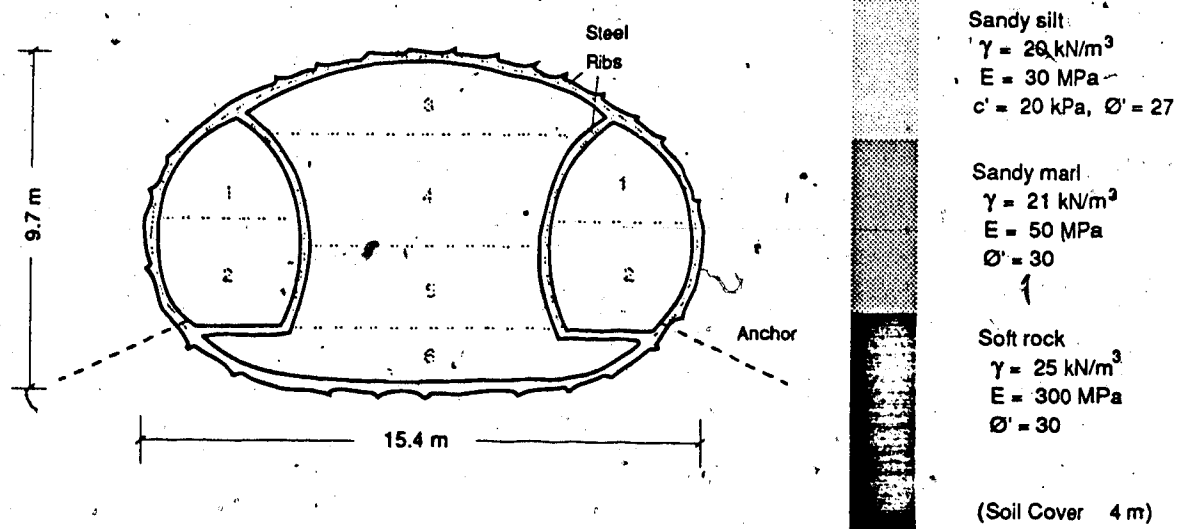


Figure 2.25 Recommendations and example application for Class I - Stiff coherent homogeneous ground

Class II: Stiff coherent heterogeneous ground

Parameter	Non Urban Area	Urban Area	Urban Sensitive Area
$A_h/A_t = \%A_t$	0.25	0.18 - 0.25	0.15 - 0.24
L/D_m	2.3	0.9	0.3 - 0.8
$L_a = s$ (m)	1.0	0.8	0.6
$L_h / (\%A_t \cdot D)$	3.7	1.6	0.4 - 1.4
V_s/V_{cn} (%)	1.4	1.3 - 1.5	0.6
\bar{S}	-	-	-

Notes: 1) Numeric values derived from cases examined
 2) For meaning of parameters see list of symbols

BAULOS A2 TUNNEL (Bochum, F.R.G.) - Case 2

	Shotcrete	Mesh	Steel Ribs
Floor	25 cm	(2 x Q188)	TH 29/58
Sides+ Crown	25 cm	(2 x Q188)	TH 29/58

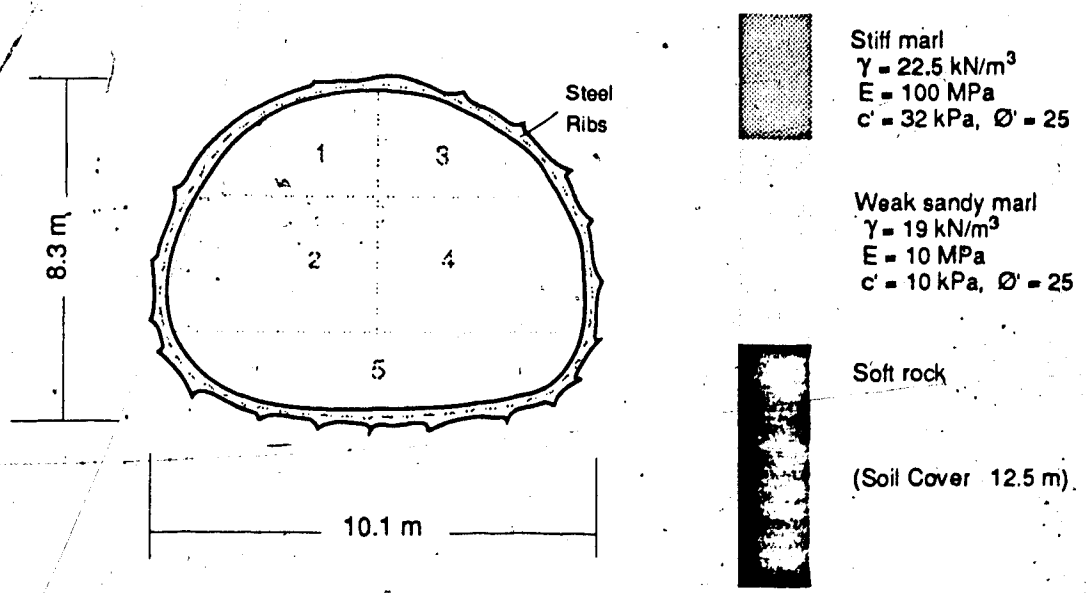


Figure 2.26 Recommendations and example application for Class II - Stiff coherent heterogeneous ground

Class III: Coarse grained coherent ground

Parameter	Non Urban Area	Urban Area	Urban Sensitive Area
$A_h/A_c = \%A_c$	0.3 - 0.4	0.25	0.25
L/D_m	3.5 - 5.5	0.9	-
$L_a = s$ (m)	1.2	1.0	0.8
$L_h / (\%A_c \cdot D)$	5.0-6.5	1.4	0.7
V_s/V_{tn} (%)	1.5 - 4.0	0.3	-
\bar{s}	-	1.0	-

Notes: 1) Numeric values derived from cases examined
 2) For meaning of parameters see list of symbols

BUTTERBERG TUNNEL (Osterode, F.R.G.) - Case 9

Shotcrete $t = 30$ cm
 Steel ribs GI 130 spaced $s = 100$ cm at crown and walls
 2 layers of welded wire mesh: min $f_e = f_e' = 4.5$ cm²/m (> at bending moment concentrations)
 Spilling at crown

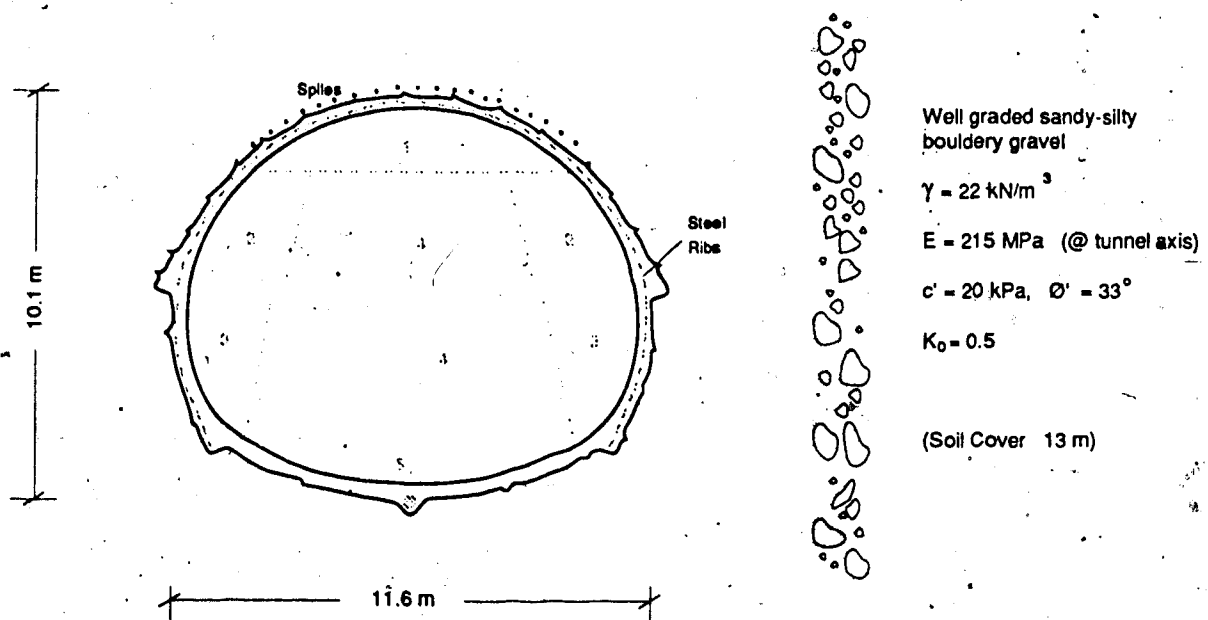


Figure 2.27 Recommendations and example application for Class III - Coarse grained coherent ground

Class IV: Sandy cohesionless ground

Parameter	Non Urban Area	Urban Area	Urban Sensitive Area
$A_h/A_t = \%A_t$	0.25	0.6	-
L/D_m	2.3	1.6	-
$L_a = s$ (m)	1.0	0.8	-
$L_h/(\%A_t \cdot D)$	7.9	-	-
V_s/V_{tn} (%)	1.5	1.2	-
\bar{S}	1.0	-	-

Notes: 1) Numeric values derived from cases examined
2) For meaning of parameters see list of symbols

KOKUBU TUNNEL (Matsudo, Japan) - Case 19

Shotcrete $t = 20$ cm

Steel ribs $H = 125$ spaced $s = 90$ cm at crown and walls

2 layers of welded wire mesh: 1st $\emptyset 3.2 - 50 \times 50$, 2nd $\emptyset 6.0 - 50 \times 50$

Forepoling by steel plates 1600 mm long at crown area

Anchors as per figure below

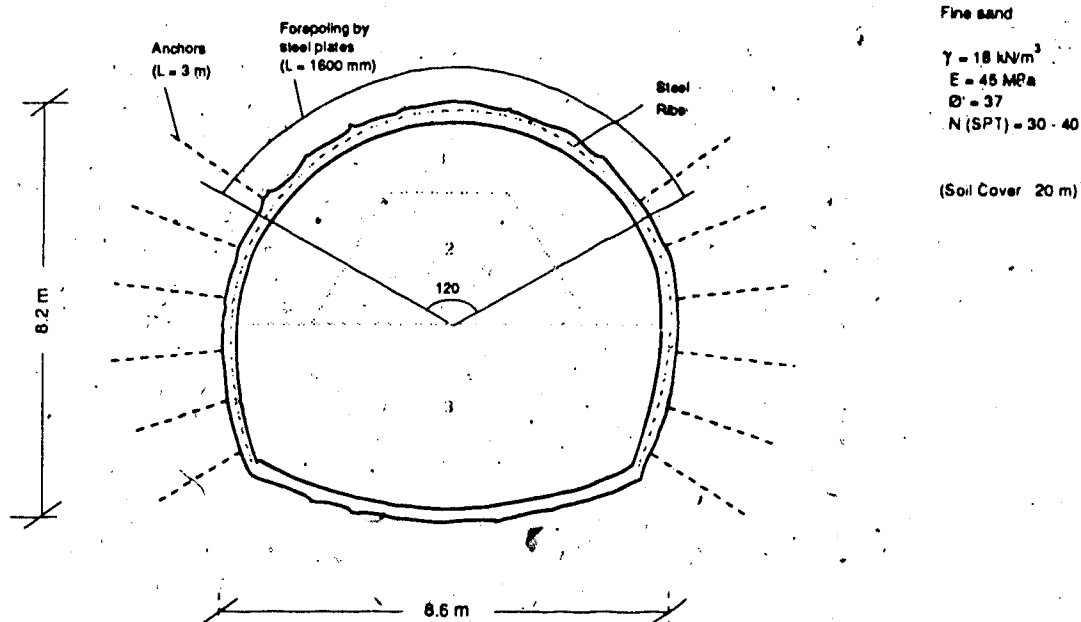


Figure 2.28 Recommendations and example application for Class IV - Sandy cohesionless ground

3. SIMPLE SOLUTIONS FOR TUNNEL STABILITY

3.1 Introduction

The last two decades have witnessed major accomplishments in geotechnical modelling through numerical techniques such as the Finite Element Method (FEM). It is important to realize, however, that the FEM is not a general solution, as pointed out by Wroth and Houlsby (1985:37) in their general report to the 1985 ICSMFE:

"...there has been recently a trend towards the almost universal use of the finite element method, often in wholly inappropriate circumstances. In combination with complex constitutive models the method becomes expensive and inefficient, and can lead to results on which no reliance should be placed. In addition, there is the drawback that physical insight into the problem may be lost".

In engineering practice, the ability of the FEM to analyze complex problems such as the tunnel excavation is frequently limited due to several factors. To cite a few:

- 1) The cost of computer time required for an appropriate analysis is frequently prohibitive. This is especially critical in the analysis of tunnel behaviour close to the face, which requires three-dimensional modelling (e.g., Heinz, 1984).
- 2) The relevant soil properties must frequently be obtained from a relatively small number of simple laboratory or insitu tests, which are unlikely to provide sufficient input for a highly complex model. This is due to factors such as the scatter of the data

which may exist due to geological variations of the samples, sample disturbance, etc. (Wroth and Houlsby, op.cit.).

3) At present, use of the FEM to model geotechnical problems where failure is approached is not a straightforward task. For example, the collapse of a geotechnical structure is frequently associated with the formation of narrow shear bands, which seem to form in an unpredictable manner (e.g., Wroth and Houlsby, 1985:42; Mühlhaus, 1985:37). Modelling such soil behaviour poses considerable difficulties which are currently the subject of research at the University of Alberta, (Wan et al., 1988).

For these reasons, simpler solutions, based on sound theoretical principles but containing convenient simplifications, are often favoured in practice. In Geotechnical Engineering, several of these simple solutions have been traditionally associated with limit analysis (e.g., slope stability and bearing capacity problems). This type of analysis is solely concerned with the equilibrium of soil masses and does not take deformations into account. The soil properties required are essentially the strength parameters, which may be total (c_u) or effective (c', ϕ'), depending on whether a total or effective stress analysis will be conducted.

In this chapter, solutions associated with limit analysis will be examined, aimed at facilitating estimates of

practical significance to the design of large cross-section tunnels. More specifically, solutions based on the bound theorems of plasticity will be applied to the problem of choosing an excavation procedure for these tunnels, based essentially on the geometry of the problem and on the soil properties.

3.2. Statement of the Problem

Given a large cross section tunnel to be excavated, questions arise regarding which excavation sequence should be used for the given soil conditions. Two particular questions that might require consideration, as illustrated in Figure 3.1, are:

- 1) Given a required cross sectional area, what is the maximum heading size that may be safely excavated?
- 2) What is the maximum length of tunnel that can be excavated without support?

While a decision may be controlled by non-geotechnical factors such as those outlined in Section 2.3, it is also possible that access to some simple procedures which would enable the engineer to carry out sensitivity analyses and evaluate several possibilities. Such procedures would complement the empirical design recommendations of the previous chapter.

The choice of a suitable excavation sequence for a given case may be viewed from a stability perspective. Adoption of this approach means that the risk of failure of the tunnel

heading during construction has to be assessed and the construction sequence chosen so that a reasonable margin of safety is available. However, the problem of estimating deformations is ignored which will yield simpler solutions, desirable from an engineering perspective.

It is proposed that this problem be treated using the simplified model depicted in Figure 3.2, where σ_t is an eventual temporary tunnel support pressure (e.g., applied by compressed air or by the shotcrete support at the heading), H is the cover above crown, D is the tunnel diameter and L is the distance from the excavation face to the point where the structural support is activated.

It has been verified by model tests (e.g. Casarin and Mair, 1981) that the stability of the heading is governed mainly by its geometry, which may be expressed in terms of dimensionless ratios H/D and L/D (defined in Figure 3.2). Depending mainly on these two parameters, conditions at collapse could be similar to those shown on Figure 3.3, which shows sketches from actual model tests by Mair (1979).

It should be pointed out that in further discussions presented in this chapter, reference will be made to undrained and drained tunnel stability. The distinction between these two states is rigorously associated with the rate of tunnel advance and the rate of pore pressure dissipation under given boundary conditions (e.g., Negro, 1988:246). In order to render the problem tractable, it will be assumed hereafter that for clayey soils, tunnel excavation

will be considered to take place under undrained conditions hence stability should be carried out in terms of total stresses using the soil undrained strength (c_u). By the same token, tunnelling in coarse grained soils can be considered drained and its stability should be evaluated in terms of effective stresses with effective strength parameters (c' , ϕ'). Care must be taken, however, in the case of clayey soils containing layers of coarse grained material, which may accelerate the rate of consolidation so that conditions will not be fully undrained.

3.3 Fundamental Concepts

3.3.1 Stability Ratio

Broms and Bennermark (1967) postulated that the stability of a tunnel face could be evaluated by an expression of the form:

$$N = \frac{\sigma_v - \sigma_t}{c_u} \quad [3.1]$$

where σ_v is the total vertical stress in the ground at the tunnel axis level and σ_t an eventual uniform tunnel pressure, due, for example, to the use of compressed air. The parameter c_u represents the undrained shear strength in the zone adjacent to the exposed tunnel face and N is termed the "stability number" (also "stability ratio" or "overload factor"). Expression 3.1 is frequently rewritten as:

$$N = \frac{[\sigma_s - \sigma_t + \gamma (H + D/2)]}{C_u} \quad [3.2]$$

where σ_s represents an eventual uniform pressure applied at the ground surface, γ is the soil unit weight and H and D are geometric parameters defined in Figure 3.2.

Through analyses of a number of stable and unstable tunnel case histories, Broms and Bennermark (op.cit.) verified that instability occurred at values of $N \geq 6$. This value is often regarded as the possible onset of face instability, but the validity of this assertion for tunnels with small cover to diameter ratios has been questioned (e.g., Schmidt, 1969, Ward and Pender, 1981). Broms and Bennermark studies were chiefly aimed at investigating the intrusion of clay at depth into vertical openings and are rigorously comparable only to cases where the soil cover/diameter ratio is large and the L/D ratio is equal to zero. Further research by workers at the University of Cambridge (e.g., Casarin, 1977; Mair, 1979; Kimura and Mair, 1981) has dealt with cases where $L/D \neq 0$.

Several results of tunnel model tests reported by Mair (1979:116) have shown that small changes of L/D , notably in the range $0 < L/D < 1$, have a marked effect on heading stability. This is illustrated in Figure 3.4, which also shows the line representing the criterion by Broms and Bennermark (op.cit.). It is seen that this criterion (i.e., onset of instability for $N \geq 6$) is conservative for L/D

ratios of less than about 0.5 in the cases reported. It should also be noticed that the stability numbers depicted in Figure 3.4 represent collapse conditions effectively obtained and are therefore represented by the symbol N_c . The same model test results are shown in an alternative form in Figure 3.5, in order to illustrate the dependence of N_c on the soil cover to diameter ratio (H/D). These results indicate that for shallow tunnels with H/D varying between 1 and 3, the stability numbers at collapse can vary from about 3 to 8, depending on L/D .

It should be stressed that the curves depicted in Figures 3.4 and 3.5 were constructed exclusively from experimental results. Results of the Cambridge research summarized by Davis et al. (1980), Gunn (1984) and Mair et al. (1985) also show that attempts have been made to solve this problem theoretically, but complete success has only been achieved for the particular cases of $L/D=0$ or $L/D=\infty$. In the case of $L/D=\infty$, the problem is reduced to that of a two-dimensional cavity supported by a uniform internal pressure σ_t (Figure 3.6). These solutions are approached in more detail in the following paragraphs.

3.3.2 Load Factor and Factor of Safety

In most tunnel model tests which will be reviewed, the tunnel pressure (σ_t) was initially set approximately equal to the overburden stress in the soil at the level of the tunnel axis, i.e.:

$$\sigma_t = \sigma_v = \gamma(H + D/2) + \sigma_s \quad [3.3]$$

where σ_s may be zero, as for example in most centrifuge tests reported by Mair (1979). During the tests, σ_t was reduced gradually and displacements monitored through x-ray techniques until the tunnel collapsed.

In order to relate soil displacements to the loading conditions at various test stages, Atkinson and Potts (1977) introduced the concept of "load factor" (LF), which is important for estimating a safety margin and may be written:

$$LF = \frac{\sigma_v - \sigma_t}{\sigma_v - \sigma_{tc}} \quad [3.4]$$

where σ_v is the overburden stress at the tunnel axis, σ_t is the current support stress during the test and σ_{tc} is the value of σ_t at which collapse occurs. Atkinson and Potts (op.cit.) also suggest that the load factor may be regarded as the reciprocal of the factor of safety against collapse:

$$LF = \frac{1}{F_s} \quad [3.5]$$

It should be noticed that when σ_t is equal to σ_v (i.e., before excavation), LF is zero ($F_s = \infty$) and when σ_t is reduced to σ_{tc} , LF is equal to one ($F_s = 1.0$). For the case of undrained loading, another useful form of the load factor is

obtained by introducing the stability number (Equation 3.1).

In this case:

$$LF = \frac{\frac{\sigma_v - \sigma_t}{c_u}}{\frac{\sigma_v - \sigma_{tc}}{c_u}} = \frac{N}{N_c} \quad [3.6]$$

where N is the current stability number during the test and N_c is the stability number at collapse.

Mair et al. (1981) suggested that, for a given soil there appears to be a promising relationship between load factor and settlement. This relationship is of great practical significance and becomes apparent from an inspection of Figures 3.7 and 3.8. Figure 3.7 shows the distribution of vertical settlement along the centerline and along the soil surface above a model tunnel in dense sand (void ratio $e=0.52$, $H/D \cong 1.5$, $L/D = \infty$), at two different load factors. Figure 3.8 shows normalized crown settlement versus the load factor for a variety of centrifuge tests on tunnels at different cover to depth ratios. Both figures illustrate the relationship between the load factor and the settlements and, in fact, Figure 3.8 may be interpreted as a form of the ground reaction curve introduced in Chapter 1.

Negro (1988) summarized considerable data from the Cambridge experiments which confirms the relationship between load factor and ground displacements. Negro further introduced a dimensionless displacement:

$$U = \frac{uE_0}{D\sigma_{r0}}$$

[3.7]

where u is the radial displacement at a point on the tunnel perimeter (e.g., at the crown), E_0 is an initial tangent soil modulus of elasticity, σ_{r0} is the initial radial stress at this point (e.g., the vertical insitu stress at the crown) and D is the tunnel diameter. The E_0 and σ_{r0} values are introduced either in a drained or undrained form, depending on the type of analysis to be conducted.

Based on the information provided by several Cambridge researchers, Negro (1988:74) was able to plot the dimensionless displacement at the crown versus the factor of safety given by equation 3.5 at various stages of the tests. This data showed remarkably little scatter and a definite trend, independent of the tunnel depth, the type of test (i.e., drained or undrained) and the type of soil, although the final collapse was attained sooner in terms of displacements for stiffer soils (Negro, 1988:73).

Based on analysis of this data (reproduced in Figure 3.9), Negro suggested that U values greater than 1.8 will generally represent a near collapse condition, whereas "good ground control" is attained for U values typically 1.0 or less. Negro associated this latter value to a loss of ground of about 1.0% of the tunnel volume, a value frequently adopted for prediction of settlements caused by shield tunnels (e.g., Attewell, 1978:881). The $U=1.0$ value would be

associated with factors of safety ranging from about 1.2 (stiff soils) to 2.0 (soft soils), a range which also seems to encompass the factor of safety in actual tunnels (Negro, 1988:1297).

Despite the fact that the preceding conclusions were derived from model tests, where a relatively good control over the soil properties and the boundary conditions is normally the rule, these concepts are thought to have important practical implications. For instance the equation for the load factor (equation 3.4) may be rewritten as

$$LF = \frac{1 - \frac{\sigma_t}{\sigma_v}}{1 - \frac{\sigma_{tc}}{\sigma_v}} \quad [3.8]$$

If the possibility of establishing relationships between the load factor LF (or the factor of safety F_s) and the displacement U, as in Figure 3.9 is accepted, then a rough estimate of the loads acting on the tunnel, based only on readings of settlements and on plasticity solutions, could be made. This concept is discussed subsequently in this thesis.

3.3.3 Bound Theorems of Plasticity

Solutions for tunnel stability problems may be obtained using the upper and lower bound theorems of the theory of plasticity, which are described in several textbooks (e.g., Chen, 1975). According to the theory of plasticity, the

collapse loads of a particular configuration of loading on a perfectly plastic body is unique. This collapse load, which may not be exactly determinable, may be bracketed by use of these theorems, which may be stated as follows (Atkinson, 1981):

Lower Bound Theorem

"If there is a set of external loads which are in equilibrium with a state of stress which nowhere exceeds the failure criterion for the material, collapse cannot occur and the external loads are a lower bound to the true collapse loads".

Upper Bound Theorem

"If there is a set of external loads and a mechanism of plastic collapse such that the increment of work done by the external loads in an increment of displacement equals the work done by the internal stresses, collapse must occur and the external loads are an upper bound to the true collapse loads".

These theorems are used to ease calculations by ignoring some of the conditions of equilibrium and compatibility, required for the theoretically possible determination of the collapse loads of a structure. By ignoring the equilibrium condition, one may calculate an upper bound to the collapse load, such that if the structure is loaded to this value, it must collapse. Similarly, by ignoring the compatibility conditions, one may calculate a lower bound to the collapse load, so that if the structure is loaded to this value, it cannot collapse.

It should be cautioned that application of these theorems to geotechnical problems implies that the stress-strain behaviour of the soil is assumed to be either rigid or elastic, until it reaches yield stress level, where it

continues to shear with no change in volume. Real soils frequently show departures from this idealized behaviour, particularly dense sands and stiff clays, at low stress levels. The latter may show some strain softening. It has been argued, however, that the assumption of perfect plasticity is acceptable for soils if the yield stress level is chosen to represent the average stress in an appropriate range of strain (e.g., Chen, 1975:16). Another point is that these theorems, particularly the lower bound one, cannot be proved theoretically for the case of drained loading, where ultimate soil behaviour is known to yield an angle of dilation (ψ) different from the friction angle (ϕ). This aspect is discussed by Davis (1968), Atkinson (1981:116) and Negro (1988:1089) and it appears to be a general consensus that although some of the theoretical plasticity assumptions may be violated, the results of upper and lower bound calculations are acceptable approximations, even for the case of drained loading of a soil.

It has also been suggested (Calladine, 1969:94) that although these theorems are very powerful for solution of plasticity problems, their power is not fully evident until examples of their use are examined. Several applications to geotechnical problems are presented by Chen (1975) and Atkinson (1981). Since examples of application to tunnels appear to be few and are mostly restricted to unpublished works, it is felt appropriate that some simple cases be

presented at this point. This is intended to clarify aspects of bound solutions approached later in this chapter.

It is proposed to find the collapse tunnel pressure for the problem depicted in Figure 3.6. For simplicity, the soil is assumed weightless ($\gamma=0$) and the loading is provided by a uniform surface pressure σ_s . It is further assumed that loading takes place under drained conditions.

Lower Bound Calculation

It is assumed that there is a condition of radial symmetry of the stress field around the tunnel, so that the problem can be approximated to that of a thick cylinder subject to uniform external and internal pressures (Figure 3.10). Under these assumptions the equilibrium condition for the stresses on an element at a radius r from the tunnel axis becomes (Timoshenko and Goodier, 1970):

$$\frac{d\sigma_r}{dr} + \frac{(\sigma_r - \sigma_\theta)}{r} = 0 \quad [3.9]$$

A lower bound solution also requires that the failure criterion is not violated so that at the onset of failure (σ_r is the minor principal stress):

$$\sigma_\theta = \frac{1 + \sin \phi}{1 - \sin \phi} \sigma_r + \frac{2c \cos \phi}{1 - \sin^2 \phi} \quad [3.10]$$

By combining equations 3.9 and 3.10 one obtains the following differential equation:

$$\frac{1 - \sin \phi}{2} \frac{d\sigma_r}{(\sin \phi \sigma_r + c \cos \phi)} = \frac{dr}{r} \quad [3.11]$$

and solving it with the boundary conditions:

$$\sigma_r = \sigma_t \quad \text{at} \quad r = \frac{D}{2} \quad [3.12]$$

$$\sigma_r = \sigma_s \quad \text{at} \quad r = \frac{D}{2} + H \quad [3.13]$$

one obtains:

$$\frac{\sigma_s + c \cot \phi}{\sigma_t + c \cot \phi} = \left(2 \frac{H}{D} + 1\right)^{\frac{2 \sin \phi}{1 - \sin \phi}} \quad [3.14]$$

For the particular case where σ_s is maintained constant while σ_t is reduced until the tunnel collapses (e.g., case of Cambridge static tests), equation 3.14 may be rewritten as:

$$\sigma_s - \sigma_t = (\sigma_s + c \cot \phi) \left[1 - \left(2 \frac{H}{D} + 1\right)^{\frac{-2 \sin \phi}{1 - \sin \phi}} \right] \quad [3.15]$$

This equation reduces to equation 5 by Atkinson and Cairncross (1973) if one substitutes the somewhat unconventional notation employed by those authors. Although the equation has been derived assuming an isotropic stress field ($\sigma_h = \sigma_v = \sigma_s$) outside the axisymmetric region, it has been

suggested that, the same approach can be used to find solutions for any value of K_0 (Seneviratne, 1979:77).

Upper Bound Calculation.

A simple collapse mechanism chosen for illustration of an upper bound calculation is shown in Figure 3.11. It is assumed that τ_f is constant along the vertical failure surfaces so that comparing the work done by the internal stresses with the work done by the external loads during sliding of the block ABA'B' results in:

$$2 \bar{\tau}_f y W = (\sigma_s - \sigma_t) 2 d W \quad [3.16]$$

Using geometrical relationships in Figure 3.11 this equation can be converted into:

$$\frac{\sigma_s - \sigma_t}{\tau_f} = \frac{H}{R \sin \alpha} + \frac{1 - \cos \alpha}{\sin \alpha} \quad [3.17]$$

In order to find the minimum value of $(\sigma_s - \sigma_t)$, equation 3.17 is differentiated with respect to α , resulting in:

$$(\sigma_s - \sigma_t) = 2 \bar{\tau}_f \sqrt{\frac{H}{D} \left(1 + \frac{H}{D}\right)} \quad [3.18]$$

The average shear stress along the failure surfaces is taken as the average of shear strengths at the tunnel perimeter and at the surface, determined from the Mohr circle at these locations (Figure 3.12):

$$\bar{\tau}_t = \frac{1}{2} \frac{\sin \phi}{1 - \sin \phi} (\sigma_s + \sigma_c + 2c \cot \phi) \quad [3.19]$$

If $c=0$, this equation becomes identical to equation 5.3 by Seneviratne (1979), who solved this problem for a cohesionless material. By combining equations 3.19 and 3.18, one obtains the upper bound solution.

Comparison with results of model tests

In order to portrait the ability of these solutions to bracket collapse loads, the theoretical values are compared in Figure 3.13 to results of model tests presented by Atkinson and Cairncross (1973). The properties involved in the calculations are shown in Figure 3.13 and a description of these drained tests is found in the original paper. The experimental results tend to lie between the upper and lower bound calculations, as expected. Also, it is apparent that these test results tend to be closer to the lower bound curve. This indicates that, for this case, the lower bound represents a better approximation of the exact solution than the upper bound.

It should be noted that upper bound solutions have been shown, in general, to yield poorer results than the lower bound. This is attributed to the fact that satisfactory upper bound mechanisms need to be carefully refined and, as such, the solutions also become more complex and impractical (Davis

et al., 1980; Melix, 1987). This is especially critical in the case of three-dimensional mechanisms, presented for example by Casarin (1977). For this reason, and also because it is the lower bound which will yield a theoretically "safe" prediction of the collapse load, only lower bounds will be explored further in this work.

3.4 Lower Bound for the 3-D Tunnel Heading

In this section, a lower bound for the three-dimensional tunnel heading (Figure 3.2) is introduced. Undrained solutions for the particular case where $L/D=0$ (tunnel lined up to the face) have been known to exist for some time (Davis et al., 1980). Recently Mühlhaus (1985) developed a solution valid for any L/D and for both drained and undrained loading. This solution will be presented in some detail for the following reasons:

- 1) The original paper contained typographic mistakes in several sections, which were rectified through correspondence with the author (Mühlhaus, 1986:personal communication).
- 2) The notation employed by Mühlhaus (1985) is somewhat obscure, thus rendering the solution, which is actually quite simple, unattractive to a practitioner.
- 3) In its original form, the solution does not allow the inclusion of an internal pressure (σ_t in Figure 3.2) which is required for a rigorous comparison between Mühlhaus's solution and the model tests results which

will be analyzed in the following sections. Also, σ_t may be viewed as an approximation of the average stresses acting on an actual support. An attempt to extend Mühlhaus solution for $\sigma_t \neq 0$ has also been presented by Mélix (1987:6), but appears to be in error.

3.4.1 Extension of Mühlhaus' (1985) Solution

The "extended Mühlhaus solution" (i.e., including the internal tunnel pressure σ_t), assumes that the unsupported tunnel heading of length L may be replaced by a sphere of diameter D' , as shown in Figure 3.14. Within this sphere there is an all-round stress σ_t . External loads are provided by uniform surface pressure σ_s and γ is assumed to be zero.

Drained Solution

Similar to the case treated in Figure 3.10, this problem can now be approximated as a hollow sphere subject to uniform external and internal pressures (Figure 3.15). The condition of spherical symmetry yields the following equation of equilibrium (Timoshenko and Goodier, 1970:395):

$$\frac{d\sigma_r}{dr} + 2 \frac{(\sigma_r - \sigma_\theta)}{r} = 0 \quad [3.20]$$

Again, a lower bound solution requires that the failure criterion is not violated so that equation 3.10 should be introduced in equation 3.20. Also, the following

substitutions are made at this point, in order to be consistent with the original paper (Mühlhaus, op.cit.):

$$\lambda_p = \frac{1 + \sin \phi}{1 - \sin \phi} \quad [3.21]$$

$$\sigma_u = \frac{2 c \cos \phi}{1 - \sin \phi} \quad [3.22]$$

This results in the following differential equation:

$$\frac{1}{2} \frac{d\sigma_r}{\sigma_r (1 - \lambda_p) - \sigma_u} = \frac{dr}{r} \quad [3.23]$$

which solved with the boundary conditions (see Figure 3.13):

$$\sigma_r = \sigma_t \quad \text{at} \quad r = \frac{D'}{2} \quad [3.24]$$

$$\sigma_r = \sigma_s \quad \text{at} \quad r = \frac{D'}{2} + H' \quad [3.25]$$

yields:

$$\frac{(1 - \lambda_p)\sigma_s - \sigma_u}{(1 - \lambda_p)\sigma_t - \sigma_u} = \left(2 \frac{H'}{D'} + 1\right)^{2(\lambda_p - 1)} \quad [3.26]$$

The following geometrical relationships are now introduced, in order to replace the fictitious parameters H' and D' by H , D , and L (see Figure 3.14):

$$D'^2 = L^2 + D^2 \quad [3.27]$$

$$\frac{D'}{2} + H' = \frac{D}{2} + H \quad [3.28]$$

Using equations 3.27 and 3.28 one may rewrite equation 3.26 as:

$$\frac{(1 - \lambda_p)\sigma_s - \sigma_u}{(1 - \lambda_p)\sigma_t - \sigma_u} = \left[\frac{(1 + 2 \frac{H}{D})}{\sqrt{\frac{L^2}{D^2} + 1}} \right]^{2(\lambda_p - 1)} \quad [3.29]$$

or:

$$\left[\frac{(\lambda_p - 1)\sigma_s + \sigma_u}{(\lambda_p - 1)\sigma_t + \sigma_u} \right]^{\frac{1}{(\lambda_p - 1)}} = \frac{(1 + 2 \frac{H}{D})^2}{\frac{L^2}{D^2} + 1} \quad [3.30]$$

which may be re-arranged as:

$$\frac{L}{D} = \sqrt{\frac{(1 + 2 \frac{H}{D})^2}{\left[\frac{(\lambda_p - 1)\sigma_s + \sigma_u}{(\lambda_p - 1)\sigma_t + \sigma_u} \right]^{\frac{1}{(\lambda_p - 1)}}} - 1} \quad [3.31]$$

For the particular case where $\sigma_t=0$, this equation reduces to equation 4.5 by Mühlhäus (1985:50). Also, if the substitutions given by equations 3.21 and 3.22 are employed, equation 3.31 becomes:

$$\frac{L}{D} = \sqrt{\frac{(1 + 2 \frac{H}{D})^2}{\left(\frac{\sigma_s + c \cot \phi}{\sigma_t + c \cot \phi}\right)^{\frac{1 - \sin \phi}{2 \sin \phi}}} - 1} \quad [3.32]$$

Undrained Solution

The solution for undrained loading is similar and essentially, the Mohr-Coulomb failure criterion equation has to be rewritten as:

$$\sigma_\theta = \sigma_r + 2 c_u \quad [3.33]$$

where c_u is the undrained shear strength. The differential equation which is equivalent to equation 3.23 now becomes:

$$\frac{d\sigma_r}{dr} = \frac{4 c_u}{r} \quad [3.34]$$

and integrating with the same boundary conditions (i.e., equations 3.24 and 3.25) one obtains:

$$\sigma_s - \sigma_t = 4 c_u \ln\left(2 \frac{H'}{D'} + 1\right) \quad [3.35]$$

and again, using the geometrical relationships given by equations 3.27 and 3.28, yields:

$$\frac{\sigma_s - \sigma_t}{4c_u} = \ln \left[\frac{(1 + 2 \frac{H}{D})}{\sqrt{\frac{L^2}{D^2} + 1}} \right] \quad [3.36]$$

Re-arranging this equation, the following expression is obtained:

$$\frac{L}{D} = \sqrt{\left[\frac{1 + 2 \frac{H}{D}}{e^{\frac{(\sigma_s - \sigma_t)}{4c_u}}} \right]^2 - 1} \quad [3.37]$$

which reduces to equation 4.6 by Mühlhaus (1985:50), if $\sigma_t=0$. Although the solutions given by equations 3.32 and 3.37 were derived for the case where gravity was ignored, information presented by Mühlhaus (1985:50) suggests that replacing σ_s by $\sigma_s + \gamma(H+D/2)$ would still result in a valid approximation. In order to evaluate the consequences of this assumption and of the solutions, results given by these theoretical approximations will now be compared with existing fully lined ($L/D=0$) solutions, to results of model tests and to actual tunnel failures. This has not been done by Mühlhaus (op.cit.) and it seems to be an approximate manner to assess these lower bound solutions.

3.4.2 Comparison with Undrained Model Test Results

It is interesting to note that for the case where $L/D=0$, equation 3.36 becomes mathematically identical to the lower bound solution given by equation 9 of Davis et al. (1980),

who assumed that at the fully lined tunnel heading there is a hemispherical cap with an internal isotropic stress field σ_t . Davis et al. (op.cit.) present another solution for the case of $L/D=0$, assuming an axisymmetric stress field similar to that adopted for the plane strain circular tunnel, shown on Figure 3.10.

In Figure 3.16, the results given by these equations are compared to those of model tests by Casarin (1977:Table 4.1) and Mair (1979:Table 6.1), which are summarized in Table 3.1. In order to include all these results, which were conducted in soils with different undrained strengths, on the same plot, equation 3.36 is expressed as a function of the stability number, defined by equation 3.1:

$$N = 4 \ln \left[\frac{(1 + 2 \frac{H}{D})}{\sqrt{\frac{L^2}{D^2} + 1}} \right] \quad [3.38]$$

It should be noted that the value of the stability number given by this equation is in reality a lower bound for the stability number at collapse (N_c). Figure 3.16 shows that, for the case of $L/D=0$, using equation 3.38 would yield predictions of N_c which are close to the experimental values, but generally on the safe side. In other words, estimating the collapse tunnel pressure through equation 3.38 would yield values above those actually encountered in actual failures. This is a conservative result from a design

perspective. Also presented in Figure 3.16 are the "thick cylinder" lower bound given by Davis et al. (1980), which is safer than the extended Mühlhaus solution for $H/D > 0.86$, but appears to be farther from an exact solution. An upper bound solution derived by Mair (1979) is clearly remote from the collapse values (Figure 3.16).

In Figure 3.17, results given by equation 3.38 are plotted for $L/D \neq 0$ and compared again with results of model tests reported by Casarin (op.cit.) and by Mair (op.cit.). It is observed that the extended Mühlhaus solution still provides appropriate estimates of the stability number at collapse for all the values of L/D investigated. It appears, however, that as L/D increases this solution becomes excessively conservative, especially for low H/D ratios. This is explained by inspection of Figure 3.14, which shows that for large L/D values, the sphere approximation for the tunnel heading becomes inaccurate.

Also, if one accepts the trend apparent from the experimental results of Mair (op.cit.) as representative of an exact collapse solution, it may be speculated that equation 3.38 could provide unsafe results for H/D values larger than those investigated in the model tests. It is possible, therefore, that for undrained loading, the extended Mühlhaus solution could only be appropriate for cases with H/D values up to about 3. Fortunately, it is in this range that most practical cases of interest to the present study are encountered.

Perhaps a more appropriate manner of visualizing the potential of the solution derived to evaluate collapse loads would be through the concepts of load factor and factor of safety, introduced in Section 3.2.2. One may compute, for a specific case, the ratio N_c/N , which is equal to the factor of safety defined by equations 3.5 and 3.6. The factor of safety may be written as:

$$F_s = \frac{N^{LB}}{N} \quad [3.39]$$

In the above expressions, it is suggested that the lower bound stability number (NLB) may be viewed as an "available" N (i.e., N_{ava}), which divided by the "required" stability number (N_{req}) will yield a factor of safety similar to those normally used in limit equilibrium analyses. In other words:

$$F_s = \frac{N_{ava}}{N_{req}} \quad [3.40]$$

If one admits that a safe estimate of the collapse load is given by the lower bound solution (e.g., equation 3.38), values of F_s given by equation 3.40 would represent safe estimates for the cases where the tunnel actually collapsed. If collapse did not occur, this is not necessarily valid. For example, if a test did not collapse when N_{req} was increased to 4.0, with the lower bound solution yielding $N_{ava}=4.5$, it could still have failed with, say, $N_{req}=4.2$ and the estimate

would have been unsafe. This enhances the value of the collapsed laboratory model experiments reviewed herein for the understanding of tunnel stability problems.

Table 3.1 summarizes data from a number of the Cambridge experiments, including those reviewed to this point. It also includes the values of N_{ava} calculated by equation 3.38. Figures 3.18 and 3.19 relate the value of the factor of safety to the H/D and L/D parameters respectively. It is observed that, for these undrained tests, the estimates through the extended Mühlhaus lower bound are generally safe. In other words, if one's task was to specify an allowable unsupported length of the tunnel (L) in order to avoid collapse, it would be safe to do this through either equation 3.38 or equation 3.37. A trend for this solution to be safer as L/D increases and H/D decreases, as apparent from Figures 3.16 and 3.17, is no longer apparent in these plots, but the number of test results is fairly limited and more research would be needed in order to evaluate possible trends.

Also, some of the model test results fall very close to the line where $F_s=1.0$ and a few of the estimates are unsafe. These discrepancies could be ascribed, for instance, to the soil properties effectively encountered in the model tests. Even under these relatively controlled conditions, factors such as anisotropy, rate of loading, stress paths to failure and experimental errors could have influenced these predictions (for example, see discussions by Mair, 1979:38). It is perhaps for this reason that authors such as Atkinson

and Mair (1981) and Gudehus and Mélix (1986) have advocated the adoption of partial factors of safety for the soil strength parameters used in this type of analysis. The use of partial factors of safety instead of global factors of safety is favoured due to differences in the accuracy with which different strength parameters are determined. For example, the parameter c' , defined as the cohesion intercept in terms of effective stresses, is usually much more variable than the effective friction angle ϕ' and plays a dominant role in tunnel stability problems. This will be discussed subsequently in this thesis.

3.4.3 Comparison with Undrained Case Histories

It would seem appropriate to check the lower bound solution derived previously against actual tunnel failures. Regrettably, unfortunate experiences are seldom published with the clearness necessary for elaborating an appropriate analysis. In the following, a few field cases, which were judged reasonably documented, will be discussed.

It should be pointed out that in actual cases, the tunnel collapse pressure is not known and, in general, the only value of N_{req} that can be established precisely is that in effect before the tunnel is excavated. Evaluating the factor of safety (equation 3.40) using this initial stability number and N_{ava} given by the lower bound is probably conservative. This is because the tunnel excavation process

leads to a stress release, associated with the ground reaction curve concept, introduced in Chapter 1.

Mexico City Tunnels

A number of tunnels excavated in Mexico City's saturated clays are described by Moreno and Schmitter (1981). A summary of geometry and location, material properties and a description of instabilities effectively observed is presented for several shafts and tunnels (only tunnels will be analyzed herein). From this data, it is possible to obtain all the necessary input for application of equation 3.38, with the exception of the L/D ratio.

The shields used in these Mexico City tunnels had a ratio of length to diameter (L/D) of about one. The actual L/D ratio to be used depends on the length of the shield in contact with the soil, which is not readily determinable. Mair (1979:140) argues that the L/D in these cases will generally exceed zero, on account of the shield being shoved forward only after a certain advance of the heading excavation. For these tunnels in soft clay, it seems reasonable to assume that the L/D ratio will fall somewhere between 0 and 1.0 and evaluation of stability was carried out for both L/D values.

The data provided by Moreno and Schmitter (1981), as well as the lower bound values of the stability number (N_{ava}) are summarized in Table 3.2. The data collected is from cases where failures were observed, as well as from cases with no

problems. For these latter cases, an $F_s < 1$ does not necessarily represent a safe estimate, since there is an unknown margin for collapse to occur. Of greater interest are the cases where actual failures were observed.

The ten cases presented in Table 3.2 are plotted in Figure 3.20, together with the lower bound solutions for $L/D=0$ and $L/D=1$, determined from equation 3.38. If one assumes the region below the H/D vs. N curve for $L/D=1.0$ (worst possibility) as being safe, it is observed that in at least two cases (2 and 5), this assumption would have been unsafe (although in case 2 the failure may have been caused by the rupture of a pipe above the tunnel). While this could be viewed as a deficiency of the proposed solution, it is also possible that the actual field conditions may show departures from the idealized boundary conditions (e.g., c_u varying with depth, $K_0 \neq 1$, local non-homogeneities in the deposits, etc.). It should also be considered that in these field cases, defining what represents a collapse condition is more difficult than in the case of model tests. This enhances the fact that considerable judgement should be exercised when applying the theory to natural situations.

A different approach would be to seek safer estimates by establishing an allowable stability number (N_{all}), determined after factoring the undrained shear strength (c_u). If one multiplies the c_u value by a factor f ($f < 1$) and recalculates σ_t through equation 3.36, a new value σ_t' is found, which is higher than the σ_t obtained for the full c_u . It can be

demonstrated that the value σ_t' will be equal to σ_t multiplied by the reciprocal of the factor f (i.e., $1/f$). In practical terms, this means that the N_{all} using the factored c_u will be equal to N_{ava} multiplied by f . For illustration, Figure 3.21 presents the same points as Figure 3.20, but with values of N_{all} instead of N_{ava} . These new curves were obtained by dividing the c_u value by a factor of two¹, suggested as a minimum by Gudehus and Mélix (1986). It is observed that in this case safe estimates would be obtained for nearly all tunnels.

3.4.4 Comparison with Drained Model Tests

The data from drained model tests is relatively meager compared to that from undrained cases. Results which will be examined are from static model tests reported by Casarin (1977), carried out in overconsolidated kaolin, and from Gudehus and Mélix (1986), who used a dry uniform sand mixed with a small amount of kaolin. Casarin's tests were carried out at the University of Cambridge (U.K.), and Gudehus and Mélix conducted their work at the University of Karlsruhe (F.R.G.). As in the undrained tests reported previously, the collapse was achieved by decreasing the air pressure (σ_t) inside a flexible rubber bag which lined the unsupported heading (L in Figure 3.2).

¹ Gudehus and Mélix (1986) justify the adoption of a partial factor of safety of two for the cohesion due to the uncertainties in its determination and due to the catastrophic consequences of a tunnel heading failure. They seem to suggest, however, that further research is needed for establishment of this factor.

In Casarin's tests, the initial tunnel pressure was set equal to an externally applied surface load (σ_s), whereas in Gudehus/Mélix tests, this initial pressure was set to σ_s plus the self weight of the soil above the tunnel. Casarin (1977:41) reports that a drained condition was achieved by allowing sufficient time between decrements of σ_t for the generated water pressures to dissipate. In Gudehus and Mélix (1986), the soil was virtually dry, so that a drained assumption is reasonable. Other details may be found in the original references.

All parameters relevant to the application of the drained lower bound solution (i.e., equation 3.32) are summarized in Tables 3.3 (Casarin's data) and 3.4 (Gudehus and Mélix's data). Inspection of these tables reveals that the values of L/D calculated by the lower bound solution for Casarin's results were mostly safe. In other words, if one were to specify a maximum unsupported length of the heading using the lower bound equation, for the conditions of these tests, the calculations would be conservative, except in one case. Analysis of Table 3.4 shows that this does not hold true for the results from Gudehus and Mélix (op.cit.), where adoption of the lower bound solution would lead to unsafe estimates of L/D.

Alternatively, one could calculate the value of σ_t which would ensure a "no collapse" situation for the L/D ratio at failure in these tests. These values, obtained by inserting L/D at collapse into equation 3.32, are also given in Tables

3.3 and 3.4, as is the factor of safety (F_s), calculated from equations 3.4 and 3.5. These results are summarized in Figure 3.22, which suggests that the drained lower bound solution yields results which are close to an exact solution (within 30% of $F_s=1$), but that could lie either on the safe or on the unsafe side. Similar mixed results are mentioned by Negro (1988:1096), who suggested that the lower bound approach may not provide safe estimates of the collapse load for frictional materials. Alternatively Negro (1988:1101) suggested that the deformation in the soil prior to collapse may have an effect on the collapse pressure. In any case, these discrepancies, which are not unreasonable in geotechnical terms, enhance the necessity of common sense when applying these plasticity solutions.

In Figure 3.23, the results of Gudehus and Mélix (op.cit.) are shown again, this time with the adoption of the residual strength parameters for the sand-clay mixture ($c'=0.14\text{kPa}$ and $\phi'=29^\circ$, obtained from Mélix, 1987:23). The factors of safety are now much closer to one, which shows that the value of the cohesion has a marked influence on the results obtained from these lower bound solutions. It must also be remembered that the value of the c' intercept calculated in practice may be an essentially mathematical effect caused by a curve fitting procedure (e.g., Bolton, 1979:73).

Atkinson and Mair (1981) recommend the use of $c'=0$ in these plasticity calculations but it must not be forgotten,

however, that in certain soils (e.g., cemented sands) there may be an actual cohesion which must be counted upon if an unsupported heading is to be excavated. In any case the drained lower bound solution, given by equation 3.32, illustrates the effect that even a small amount of cohesion has on the excavation of an unsupported heading. For instance for $\sigma_t=0$ (fully unsupported heading), a value of $c=0$ will render the solution (Equation 3.32) indeterminate, which may be interpreted physically as the impossibility of tunnelling under these conditions without additional ground control measures.

3.4.5 Comparison with Drained Case Histories

No records of tunnel failures that could be used to substantiate the validity of the lower bound solution were found in the literature. However, a number of reasonably well documented cases of NATM excavated tunnels, where a good record of settlement is available, may be used to illustrate aspects of the present research, more specifically of the validity of the concepts discussed in Section 3.3.2 (Load Factor versus displacements). The cases described were published by Stroh and Chambosse (1973) and reviewed by Heinz (1984:39).

All tunnels were excavated in Frankfurt clay, whose properties have been extensively investigated and were summarized by Katzenbach (1981). The fact that dewatering was initiated months before tunnel excavation and the constant

presence of pervious calcareous layers and sand layers in the natural ground favours the choice of drained behaviour.

A peculiar feature of these tunnels is that they represent the first applications of the NATM in urban areas. As such, attempts were made to calibrate construction parameters with varying degrees of success. Based on comments made by Stroh and Chambosse (1973), it is believed that, in at least some of these tunnels, a failure condition was approached. All measurements presented herein were obtained in adjacent contract sections and, at least as a first approximation, the soil conditions can be considered similar. This approach was also adopted in Katzenbach's (1981) finite element analyses of these tunnels.

The data collected by Stroh and Chambosse (1973) is summarized in Table 3.5. Also listed are the soil properties used in the present calculations, derived from Katzenbach's (1981:68) summary. It should be pointed out that all cases which are examined here were excavated using a heading and bench procedure. However, in specifying the length of the unsupported heading to be used in the present study, the influence upon stability of the shotcrete in the top heading and of the bench were neglected. This is considered, for practical purposes, to be on the safe side. Also, the values of the ratio L/D calculated by the drained lower bound solution (equation 3.32) were determined using the worst strength parameters in the range presented by Katzenbach ($c'=10\text{kPa}$ and $\phi'=18^\circ$ instead of the average parameters

$c'=20\text{kPa}$ and $\phi'=20^\circ$). This is perhaps slightly conservative, but reasonable from a design perspective, if one bears in mind that the soil properties were determined from conventional triaxial tests on small samples and are intended to represent a field situation.

Inspection of Table 3.5 shows that the calculated L/D ratios, approach, for some cases, the actual L/D's. Furthermore, it is noted that for these cases, the dimensionless crown displacement U , calculated from expression 3.7, is always greater than unity. For the cases where the actual L/D is much less than that calculated (e.g., cases II and III), U is less than unity. This agrees with Negro's (1988) suggestion that, in this case, good ground control conditions no longer exist and failure is being approached (see Section 3.3.2).

The values of the loss of ground, expressed as a percentage of the tunnel volume and calculated through Cording and Hansmire's (1975) widely used correlation, are also given in Table 3.5. Similarly to the case of U reported above, it is seen that for the cases where the lower bound values of L/D are close to those actually used, the loss of ground V_1 is always greater than 1% of the tunnel volume. This is a value commonly used in practice for prediction of settlement under good control conditions and it seems reasonable to assume that for $V_1 > 1\%$, a situation which is close to failure will be encountered. It must also be remembered that these considerations assume that the lower

bound solution, yields results which are close to the exact collapse solution. This seems reasonable from analysis of records of model tests reported earlier in this chapter.

Another tentative conclusion that might be reached from an analysis of Table 3.5 refers to the L/D ratios to be used in practice. It would appear that in order to limit the loss of ground, the results from the lower bound solution should be reduced by a factor of at least two. This would yield L/D ratios which are more in line with those surveyed in Chapter 2. However, the number of cases analyzed is limited and data from other prototypes would be necessary in order to verify these conclusions.

A final observation regards the analysis of the data from Stroh and Chambosse (1973) within the framework discussed in Section 3.3.2. Taking only the sections corresponding to Case I in Table 3.5¹, one may attempt to determine the load factors LF from the dimensionless displacements U, through use of Figure 2.8 by Negro (1988) which is reproduced as Figure 3.9.

Using the U values given in Table 3.5, values of the load factor corresponding to Negro's bounds are obtained. These load factors are then inserted into equation 3.8, with σ_{tc} estimated by the extended lower bound solutions for the respective L/D's. The ranges of σ_t/σ_v which are shown on

¹ This is a case history (Romerberg Tunnel) which has been extensively reviewed in the literature (e.g., Chambosse, 1972; Heinz, 1984; Negro, 1988) and for which reasonable records of support loads exist.

Table 3.5 are obtained. These σ_t/σ_v ratios may be viewed as a rough approximation of the radial stress acting on the tunnel support for the measured displacements, and could then be compared to field measurements.

In Figure 3.24 the range of radial stresses obtained through the above procedure is compared to actual measurements. These readings were obtained with contact pressure cells of the Glötzl type, installed between the soil and the shotcrete in twin tunnels driven simultaneously and about two diameters apart (center to center). The radial stresses may have, therefore, been affected, particularly at the springline level between the tubes ($+90^\circ$ in Figure 3.24). Also shown in Figure 3.24 are estimates of the radial stress obtained by Negro (1988), which are based on a more refined method, derived from finite element parametric studies.

It is seen that the range of radial stresses obtained through the approximate procedure fit reasonably well within the large scatter shown by the field measurements. Also, the average radial stress calculated is slightly lower than the values obtained by Negro (1988), but this is not considered unreasonable. These results suggest that a rough estimate of the loads acting on the liner could be obtained through the extended Mühlhaus lower bound solution, using the assumptions previously described. Also, it appears that U values greater than 1.0 will be associated with relatively low stresses on the lining, which is consistent with the ideas put forward by

Negro (op. cit.) and illustrated through the concept of ground reaction curve introduced in Chapter 1.

3.5 Applications to Large Tunnel Problems

3.5.1 Estimates of Unsupported Length

Design diagrams could be easily produced for estimating the L/D ratio knowing H/D and the soil properties. However, given the simplicity of equations 3.32 and 3.38, such charts would probably be of limited use, since the expressions can be easily programmed for a pocket calculator. In summary, in addition to the assumptions inherent in the theory, it seems appropriate to stress a few points concerning the applicability of the solutions derived.

3.5.1.1 Undrained Lower Bound

The undrained lower bound solution, when compared to results of model tests, provided estimates which were generally on the safe side. This is in agreement with the theory presented in Section 3.3.3 and suggests that, at least for the ranges of parameters investigated (e.g., $0.5 < H/D < 3.0$), this solution could be used to determine the maximum unsupported length within an individual heading.

However, when compared to a few case histories, the solution yielded mixed results, which may be attributed to possible field departures from the assumptions in the theory. This enhances the fact that considerable judgement should be used when applying the theory to natural situations. It is

thought that the inclusion of partial factors of safety, to be applied to the undrained strength c_u , would be a reasonable expedient, as has already been suggested by several authors (e.g., Atkinson and Mair, 1981; Gudehus and Mélix, 1986). Gudehus and Mélix (op.cit.) propose that the value of the cohesive strength should be divided by a factor of at least two and applying this factor to some actual cases (Section 3.4.3) appears to provide reasonable results. However, the field data evaluated is sketchy and any conclusions regarding the appropriateness of this factor of two will require considerably more research.

Another point that may be noted is that equation 3.37 may yield impractical results if the value of c_u is increased to high values such as those associated with very stiff soils. For instance for $H/D=2.0$, $\gamma=20\text{kN/m}^3$, $D=6.0\text{m}$ and $c_u=60\text{kPa}$, an L/D of about 1.0 is found. Increasing c_u to 240kPa and keeping the other parameters constant, L/D becomes 3.5, which is well above values used in practice. Therefore, for these stiffer and possibly fissured soils, it would appear of great importance to consider, besides the factor of safety, an operational strength of the soil mass, which could be estimated through methods such as those described by Lo (1970).

3.5.1.2 Drained Lower Bound

Comparison with results of a limited number of model tests furnished results which were not necessarily safe, but

were close to the exact values. This could be due to the fact that the theory is not strictly valid for drained situations, but it should also be noted that the value of the cohesion necessary for a mathematical solution of equation 3.32 is critical. For instance, for $\sigma_t=0$ and $c=0$, this solution becomes indeterminate. This result reflects the impossibility of tunnelling with zero support in fully cohesionless ground.

In the analysis of the results by Gudehus and Mélix (1985), choosing a residual cohesion, which was about 25% of the peak value, provided a ~~sensible~~ improvement of the estimates. This suggests that the value of the drained cohesion to be used in these solutions should be picked with extreme care and, again, the adoption of partial factors of safety may be required. Adopting $c'=0$, as suggested by Atkinson and Mair (1981), seems unduly conservative and, in fact, would mean the impossibility of excavating any heading with no support.

Another point that may be noted is that, in equation 3.32, as H/D becomes large, L/D increases in an unreasonable fashion and no longer conforms to the model depicted in Figure 3.14. Also, this perhaps means that for deeper tunnels, deformation may control rather than stability.

3.5.2 Estimates of Critical Diameter

As suggested in Section 3.2, another problem that might arise in preliminary design stages concerns the maximum heading size that may be safely excavated. Reducing the

problem to that of an equivalent, circular opening, one may refer to the "critical diameter" (D_{max}), in analogy with the concept of critical depth of an excavation (e.g., Bjerrum and Eide, 1956). For a given soil, openings with a diameter above this critical diameter (D_{max}) would be at the onset of collapse, depending on the values of H/D and L/D .

3.5.2.1 Undrained Case

Davis et al. (1980) provided solutions for a plane strain opening (i.e., $L/D=\infty$) subject to an internal pressure σ_t , in a gravitational stress field ($\gamma \neq 0$). Their undrained solutions are expressed as

$$N = f \left(\frac{\gamma D}{c_u}, \frac{H}{D} \right) \quad [3.41]$$

where $\gamma D/c_u$ and H/D are dimensionless factors and N is the stability number defined previously. Davis et al. (1980), by analysis of their Figure 8, suggest that onset of instability will occur at $\gamma D/c_u \geq 2$. Re-analyzing the same figure by Davis et al. (op.cit.), Ward and Pender (1981) suggest that the limiting factor would be $\gamma D/c_u = 1$, which corresponds to a zero support pressure in Davis et al. diagram. In this manner, instability would be imminent in a 1m diameter tunnel in very soft clay ($c_u=20\text{kPa}$) and in a 7.5m tunnel in stiff clay ($c_u=150\text{kPa}$).

The preceding values may be taken as rules of thumb for delineating the scheme of excavation to be used in a large cross section tunnel in soil. For instance, in the São Paulo case history analyzed in the previous chapter, the equivalent diameter of the top heading was about 7.5m. With the soil properties given in Figure 2.12, one obtains $\gamma D/c_u = 1.43$, which lies in the range delimited by the recommendations by Davis et al. (1980) and Ward and Pender (1981).

The extended Mühlhaus lower bound solutions presented in this chapter allow verification of these simple rules under conditions where L/D may vary, as opposed to the relatively conservative $L/D = \infty$ which is built into the solution by Davis et al. (1980). Rearranging equation 3.36, it may be easily shown that, for $\sigma_t = 0$:

$$\frac{\gamma D}{c_u} = \frac{4 \ln \left[\frac{(1 + 2 \frac{H}{D})}{\sqrt{\frac{L^2}{D^2} + 1}} \right]}{(\frac{H}{D} + \frac{1}{2})} \quad [3.42]$$

Results of this equation are plotted in Figure 3.25 and illustrate the limiting ratio $\gamma D/c_u$ is dependent on both L/D and H/D . The area under the curve in Figure 3.25 corresponds to a safe domain. The suggested values by Davis et al. and Ward and Pender are also depicted and seem to correspond roughly to Equation 3.42 for values of $L/D=1$ and $L/D=2$ respectively and for usual values of H/D . The curve for $L/D=0.5$, not shown

on Figure 3.25, may yield non-conservative results, and it seems that, for practical purposes, the rule-of-thumb by Ward and Pender (op.cit.), expressed as $D_{max} = c_u / \gamma$, would provide the most conservative results, except for H/D less than about one, where equation 3.42 (with $L/D=2$) would be more appropriate. Perhaps as a more appropriate alternative, equation 3.42 could be used with the actual L/D values, but in this case considerable judgement should be exercised in the choice of c_u , with an appreciation of its variability and perhaps with consideration of partial factors of safety, as discussed previously in this chapter.

3.5.2.2 Drained Case

It may be argued that the collapse of a tunnel heading will usually be a sudden event and hence it would be appropriate to characterize the strength of the ground by its undrained shear strength c_u , as discussed by Davis et al. (op.cit.). There might be circumstances, however, when use of a drained approach may be more appropriate. For instance in the case of cemented, predominantly coarse grained soils, it seems likely that both the cohesion and the friction will contribute to stability. Re-arranging equation 3.30, with $\sigma_s = \gamma(H+D/2)$ and $\sigma_t = 0$, one may find the equivalent of equation 3.42 for the drained case:

$$\frac{\gamma D}{c} = \frac{\left[\frac{(1 + 2 \frac{H}{D})}{D} \right]^{\frac{4 \sin \phi}{1 - \sin \phi}} \sqrt{\frac{L^2}{D^2} + 1}}{(\frac{H}{D} + \frac{1}{2}) \tan \phi + 1} \quad [3.43]$$

Figure 3.26 shows, for the case of $\phi=20^\circ$, the variation of $\gamma D/c$ as H/D increases, for two values of L/D . As expected, this figure shows that the critical diameter, for a given γ/c ratio, will be larger, the closer the lining is installed to the face. One may also estimate the "required cohesion" (a term used by Gudehus and Mélix, 1986) for a certain tunnel to be excavated. For instance with $\gamma=20\text{kN/m}^3$, $\phi=20^\circ$, $D=6\text{m}$ and $H=12\text{m}$, the cohesion required to prevent instability would be about 40kPa for $L/D=2$ and about 20kPa for $L/D=1$. This enhances the necessity of an accurate determination of the cohesion for analysis of tunnel stability problems.

The angle of friction to be used in equation 3.43 also has a significant effect, as shown in Figure 3.27, but the cohesion is probably more important. For instance, for the same example referred to above, a decrease in the friction angle from 30° to 20° , which can be considered significant, will increase the value of the required cohesion from 70kPa to 100kPa, which is comparatively not as significant. In any case, it should be pointed out once more that values of the cohesion which represent more than a simple effect of curve fitting will be required for these stability analysis.

3.5.3 Discussion

In this chapter, lower bound plasticity solutions were derived which were aimed at evaluating the three dimensional stability of a tunnel heading. Although these solutions were expected to provide safe estimates of the various parameters in question (L/D , N_c , etc.), the theoretical results, when compared to findings from model experiments, were found to be reasonably close to the collapse values of these parameters. It appears, therefore, that these lower bounds yield results which are close to the exact solutions, which is possible, according to the theoretical considerations outlined in Section 3.3.

Ways were shown in which these lower bound solutions could be applied to the problem of evaluating the critical values of the unsupported length (L) close to the tunnel face, as well as of the critical diameter (D_{max}), beyond which instabilities could occur. For clarity the expressions, which relate these parameters to the geometry and to the soil properties, are summarized in Figure 3.28.

Comparison between the theoretical values and observations made in actual tunnels indicate that use of these solutions for practical cases is only warranted if considerable judgement is used in the selection of the strength parameters. Use of partial factors of safety has already been suggested by several authors (e.g., Atkinson and Mair, 1981; Gudehus and Mélix, 1986) and may be the way to deal with the uncertainties regarding the operational

strength parameters. Based on the studies reported in this chapter, it is recommended that the cohesive strength to be used in these lower bound equations should be divided by a factor of 2 to 4. Factoring the friction angle appears to be less critical and dividing the $\tan\phi$ by 1.5, as suggested by Gudehus and Mélix (op. cit.), could be taken as an initial suggestion. It is felt, however, that more research is needed in this area and papers such as those by Bolton (1981) and Ovesen (1981) could be used as a starting point for future work. Alternatively, global factors of safety, as used in conventional slope stability analyses, may also be used. Based on the data evaluated in this chapter (e.g., Figure 3.9) it appears that a global F_s of 1.5 to 2.0 would ensure a condition of good ground control (see discussion in Negro, 1988).

On the other hand, it may be argued that the solutions derived are of limited application in practical engineering, where constraints such as those discussed in Section 2.3 in the previous chapter may prevail. Also, these solutions are not as versatile as the FEM, in the sense that features such as heterogeneities in the natural ground could be more easily implemented in the latter. Design should not be carried out solely based on these solutions, just as it would probably be unwise to design exclusively with the Finite Element Method (FEM). The greatest merit of these lower bound equations lies in their simplicity and it is believed that they could be

used to complement the empirical recommendations presented in Chapter 2, in preliminary design stages.

Table 3.1 Data from Cambridge undrained model tests taken to collapse

Reference	H/D	L/D	N _{req}	N _{ava}	F _s
Casarin (1977:Table 4.1)	0.33	0.00	3.75	2.03	0.54
"	1.19	0.00	4.85	4.87	1.00
"	1.20	0.00	5.30	4.90	0.92
"	1.28	0.47	4.20	4.68	1.11
"	1.21	1.00	3.30	3.53	1.07
Mair (1979:Figure 6.16)	1.20	0.00	5.90	4.90	0.83
"	1.50	0.00	7.10	5.55	0.78
"	2.30	0.00	7.80	6.89	0.88
"	3.00	0.00	9.00	7.78	0.86
"	3.40	0.00	9.00	8.22	0.91
"	3.50	0.00	7.40	8.32	1.12
Mair (1979:Table 6.1)	3.00	0.50	7.80	7.34	0.94
"	1.50	0.50	6.10	5.10	0.84
"	3.00	0.92	6.90	6.56	0.95
"	1.50	1.00	5.30	4.16	0.78
"	3.00	2.00	5.70	4.56	0.80
"	1.50	2.00	4.40	2.33	0.53

Notes:
 N_{req} = N effectively acting during test
 N_{ava} = N calculated through lower bound solution (Equation 3.38)

Table 3.2 Data from actual case histories in Mexico City

Case Project	H/D	N ¹ _{req}	Obs. ²	L/D=0		L/D=1			
				N _{ava}	F _s	N _{ava}	F _s	N _{all}	F _s
1 S5-S6	3.58	16.5	BF	8.40	0.51	7.01	0.42	3.51	0.21
2 Consulado	2.00	4.2	MF	6.44	1.53	5.05	1.20	2.53	0.60
3 2 de Abril	3.33	3.4	NP	8.14	2.39	6.76	1.99	3.38	0.99
4 M.Gonzales	3.40	4.3	NP	8.22	1.91	6.83	1.59	3.42	0.79
5 Obrero Mundial	3.73	4.7	MP	8.54	1.82	7.16	1.52	3.58	0.76
6 Cuitlahuac	2.67	4.3	NP	7.39	1.72	6.00	1.40	3.00	0.70
7 La Raza I	2.48	3.3	NP	7.14	2.16	5.75	1.74	2.88	0.87
8 La Raza II	3.22	3.2	NP	8.03	2.51	6.64	2.08	3.32	1.04
9 Central Collector	2.67	6.2	MP	7.39	1.19	6.00	0.97	3.00	0.48
10 Central Interceptor	4.33	4.1	NP	9.07	2.21	7.69	1.88	3.85	0.94

Notes:

- (1) Given by Moreno and Schmitter (1981:31)
- (2) Terminology employed in the original paper:
 - BF=Big Failure
 - MF=Minor Failure
 - NP=No Problems
 - MP=Minor Problems
- (3) Failure possibly due to rupture of adjacent pipe
- (4) N_{all} obtained by factoring the undrained shear strength ($f=0.5$)

Table 3.3 Data from Cambridge drained model tests taken to collapse

Test	H/D	(L/D) _c	σ_s (kPa)	σ_t (kPa)	(L/D) ^{LB}	σ_t^{LB} (kPa)	F_s
A	0.84	∞	140	50	1.65	-	-
B	0.73	0.15	140	0	0.00	8.57	0.94
C	0.60	0.00	140	0	0.00	11.75	0.92
D	0.60	0.00	140	5	0.00	16.48	0.91
E	0.62	1.01	140	25	0.82	33.53	0.93
F	0.57	1.54	140	35	0.95	86.54	0.51

Soil: Overconsolidated Kaolin ($c'=0, \phi'=26.1^\circ$)

Source: Casarin (1977:table 4.1)

Table 3.4 Data from Karlsruhe drained model tests taken to collapse

Test	H/D	(L/D) _c	σ_s (kPa)	σ_t (kPa)	(L/D) ^{LB}	σ_t^{LB} (kPa)	F_s
49	1.00	1.00	5.09	0.30	1.72	-0.63	1.19(1.05)
51	1.00	1.00	7.12	0.90	1.78	-0.51	1.23(1.12)
55	0.50	1.00	4.41	0.50	1.01	0.47	1.01(0.87)
59	0.50	1.00	6.41	1.70	0.47	1.02	1.14(1.03)
64	0.50	0.50	5.40	0.00	0.70	-0.28	1.05(0.93)
69	0.50	0.50	0.00	0.70	0.75	-0.07	1.07(0.97)
80	1.50	1.00	7.79	0.20	2.13	-0.82	1.13(1.04)

Soil: Uniform sand with minor amount of Kaolin ($c' = 0.55 \text{ kPa}$, $\phi'_{res} = 29^\circ$, $c'_{res} = 0.14 \text{ kPa}$)

Source: Gudehus and Melix (1986) - only cases with tunnel pressure decreased

Notes: (1) Includes gravity effects

(2) Values in italics calculated with residual strength parameters

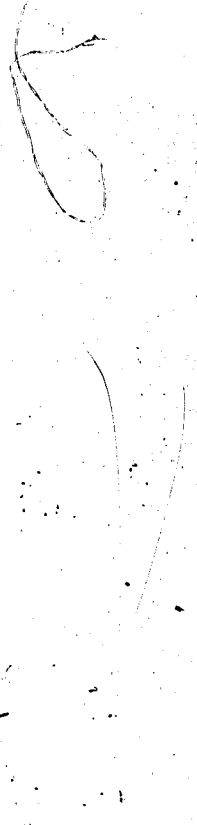


Table 3.5 Data from actual drained cases reported by Stroh and Chambosse (1973)

Case	I	II	III	I-2	I-4	I-7
H(m)	11.5	13.0	12.5	11.5	11.5	11.5
D(m)	6.4	6.7	6.7	6.4	6.4	6.4
S_c (mm)	61	42	34	59	70	52
U	1.34	0.78	0.66	1.30	1.54	1.15
V_L (%)	1.40	0.92	0.74	1.36	1.61	1.20
H/D	1.80	1.94	1.80	1.80	1.80	1.80
L/D	0.78	0.45	0.22	0.63	0.78	0.63
σ_v (kPa)	272	302	293	271	272	272
(L/D) LB	0.80	0.81	0.79	0.80	0.80	0.80

Notes:

- (1) S_c = final radial displacement at crown
- (2) U = dimensionless radial displacement at crown (eqn. 3.7)
- (3) V_L = loss of ground expressed as a percentage of tunnel volume
(through correlation by Cording and Hansmire, 1975)
- (4) σ_v = vertical insitu stress at tunnel axis
- (5) Soil Properties from Katzenbach (1981:68):
 $\gamma=18.5\text{kN/m}^3$, $c'=10\text{kPa}$, $\phi'=18^\circ$, $E_0=30\text{MPa}$ at crown level
- (6) LF values represent ranges obtained from U through Figure 2.8 by Negro (1988)
- (7) σ_t/σ_v obtained from Equation 3.8 with LF given above and σ_{tc} determined through extended Mülhhaus lower bound (drained)

Table 3.5 (contd.)

Case	I	II	III	I-2	I-4	I-7
LF _{upper}	0.56	-	-	0.55	0.61	0.53
σ_t/σ_v	0.44	-	-	0.45	0.39	0.47
σ_t (kPa)	120	-	-	136	106	128
LF _{aver}	0.69	-	-	0.68	0.74	0.66
σ_t/σ_v	0.31	-	-	0.32	0.26	0.34
σ_t (kPa)	84	-	-	97	71	93
LF _{lower}	0.90	-	-	0.89	0.94	0.87
σ_t/σ_v	0.10	-	-	0.11	0.06	0.13
σ_t (kPa)	27	-	-	33	16	35

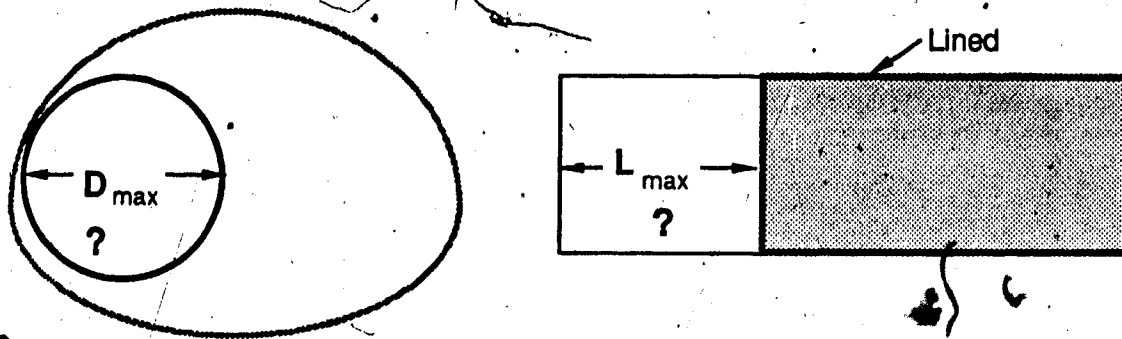


Figure 3.1 Possible problems to be faced when planning a large cross section tunnel

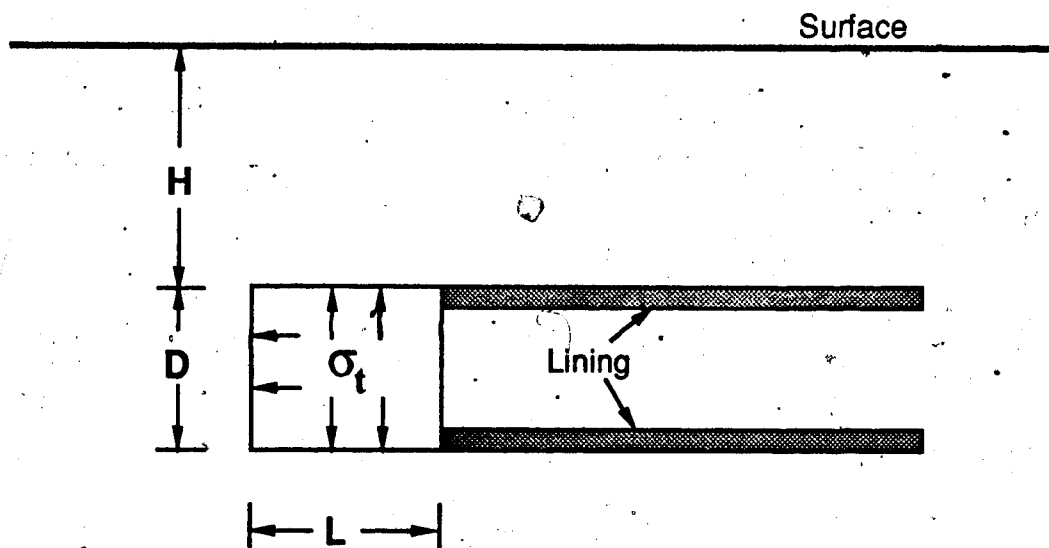
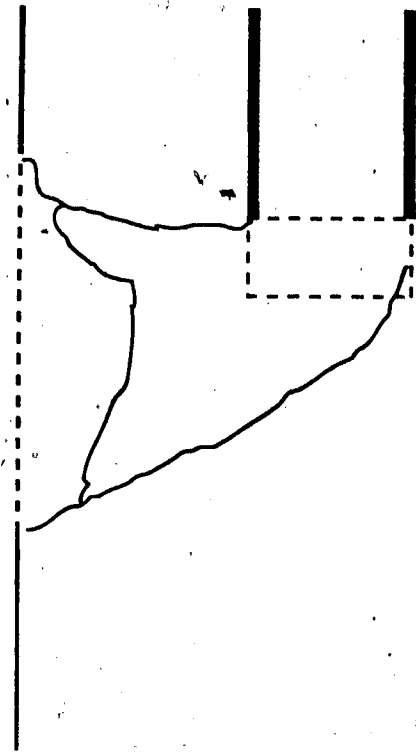
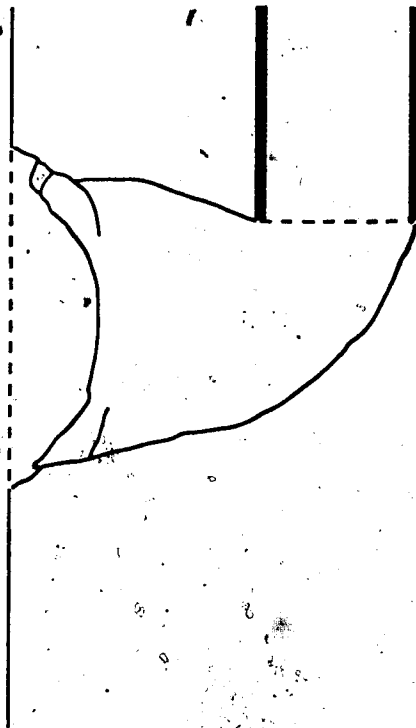


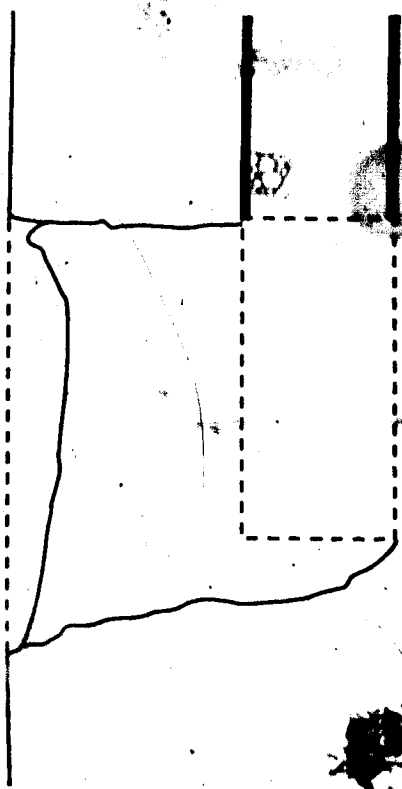
Figure 3.2 Simplified model for analysis of tunnel heading



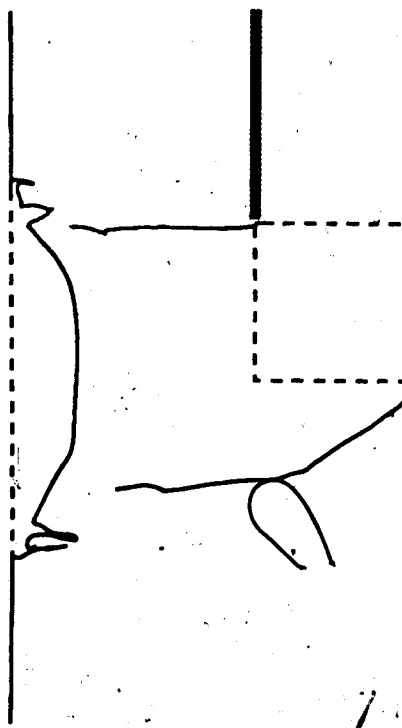
$L/D = 0.5$



$L/D = 0$



$L/D = 2.0$



$L/D = 1.0$

Figure 3.3 Observed collapse configurations for model tunnel headings in clay - $H/D=1.5$ (modified after Mair, 1979)

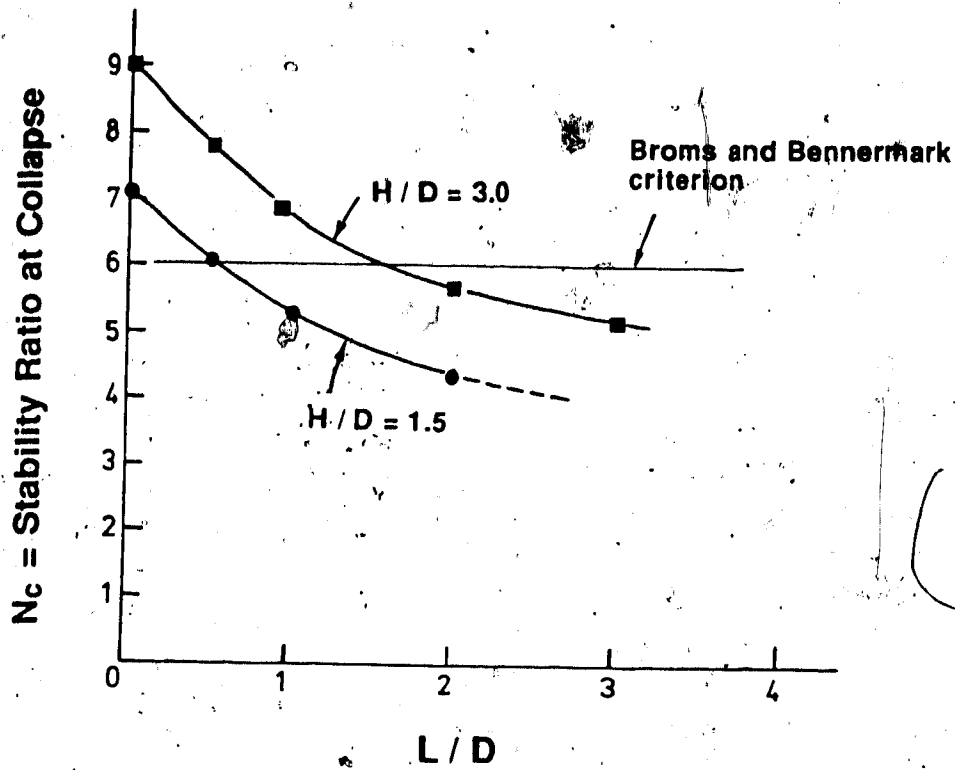


Figure 3.4 Influence of heading geometry on stability ratios at collapse (modified after Mair, 1979)

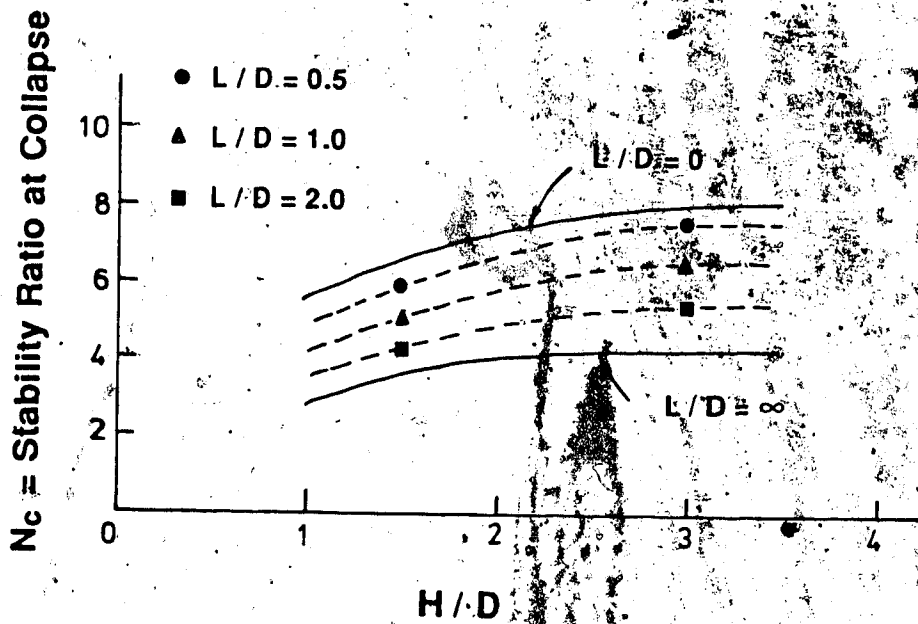


Figure 3.5 Influence of depth ratio on stability ratios at collapse (modified after Mair, 1979)

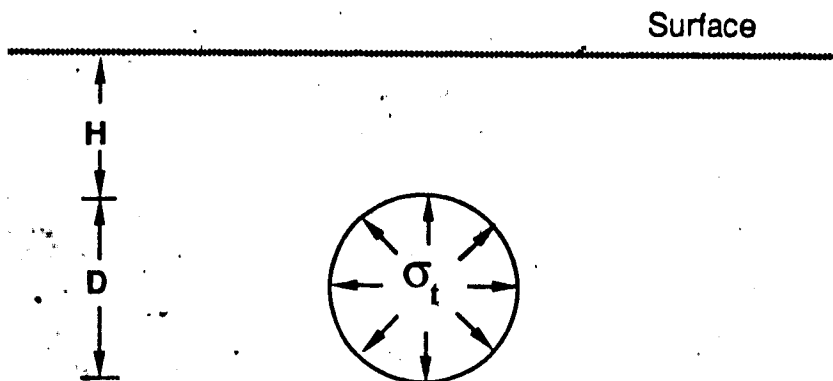


Figure 3.6 Two dimensional representation of tunnel heading

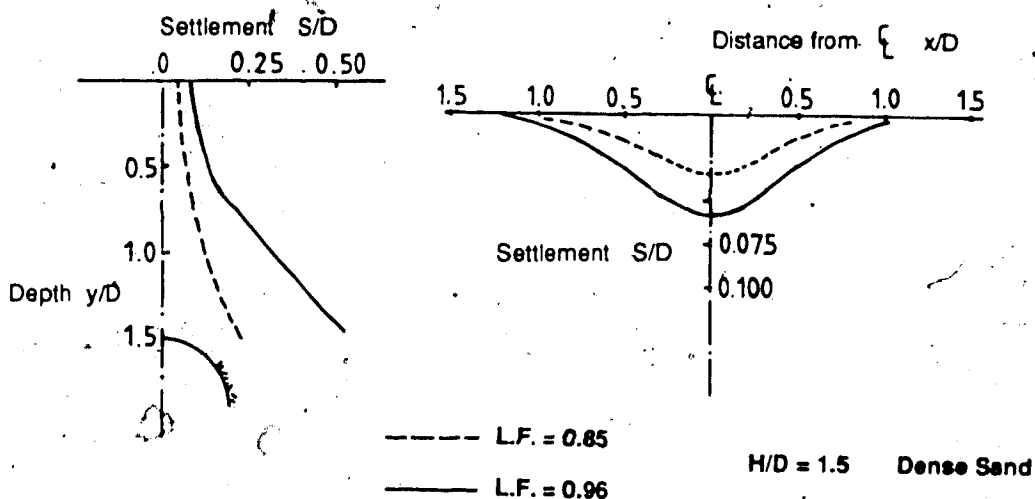


Figure 3.7 Illustration of correspondence between Load Factor and settlements (modified after Atkinson and Potts, 1977)

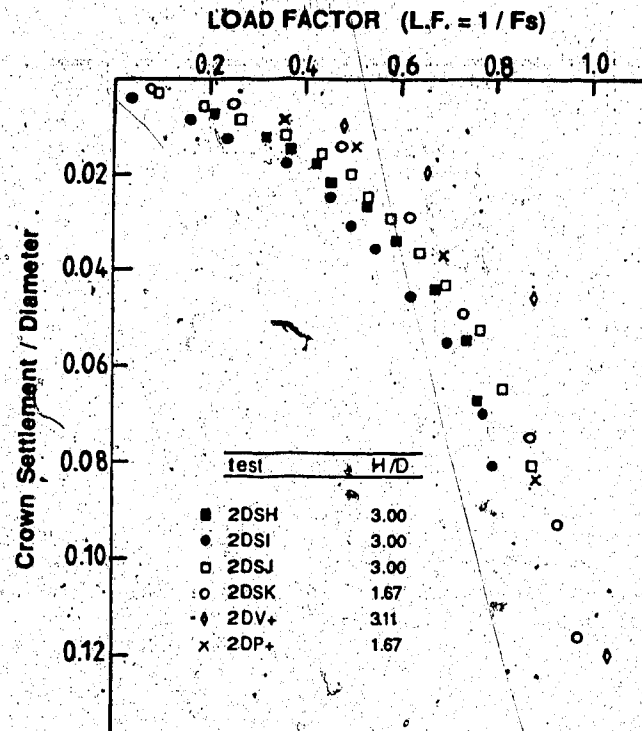


Figure 3.8 Observed variation of crown settlement with load factor for six model tunnels (modified after Mair et al., 1985)

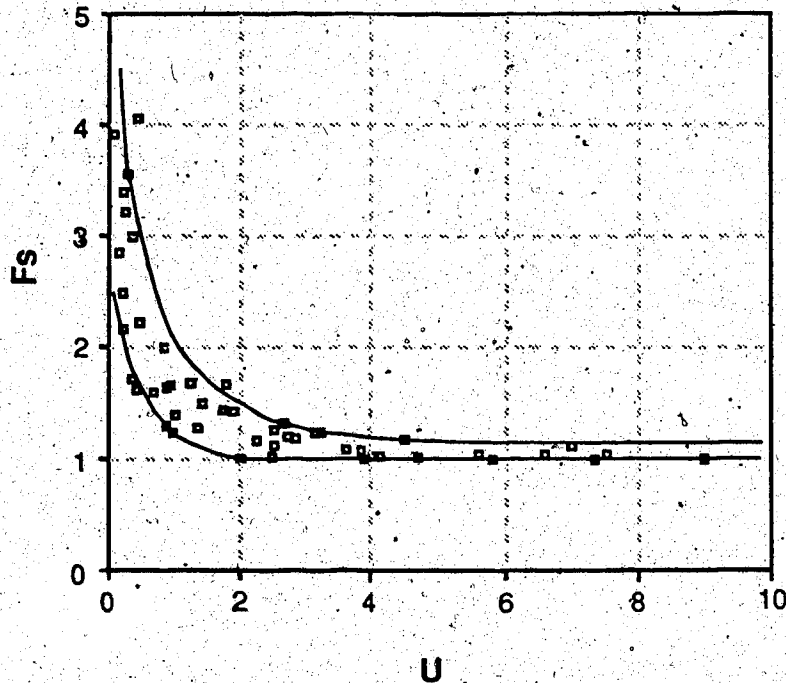


Figure 3.9 Observed variation of dimensionless crown settlement versus factor of safety (modified after Negro, 1988)

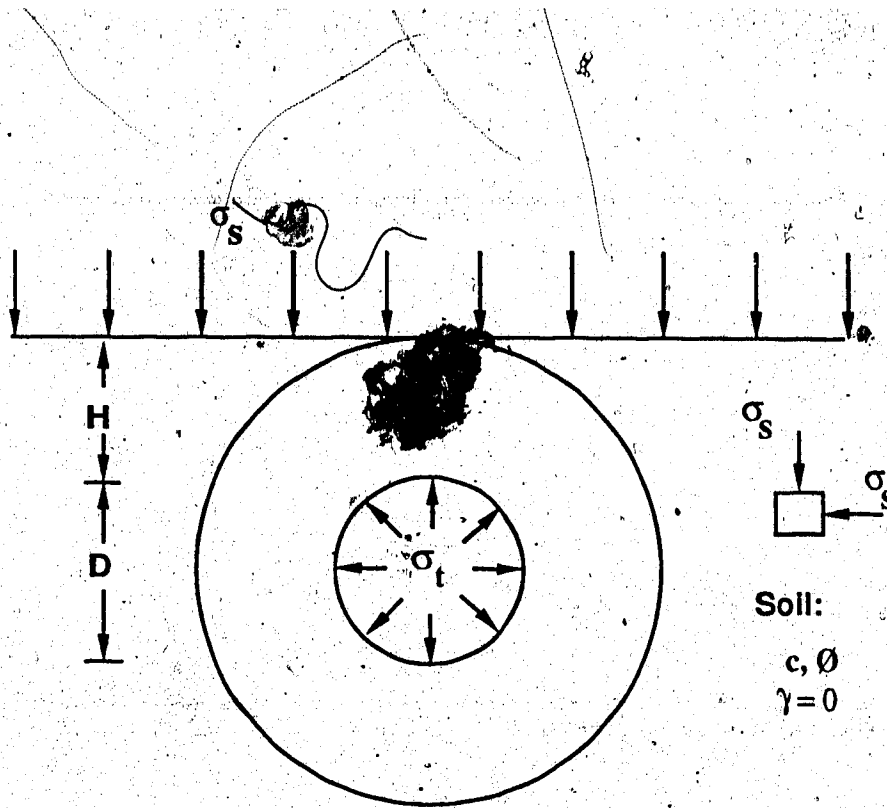


Figure 3.10 Geometry for 2D lower bound solution

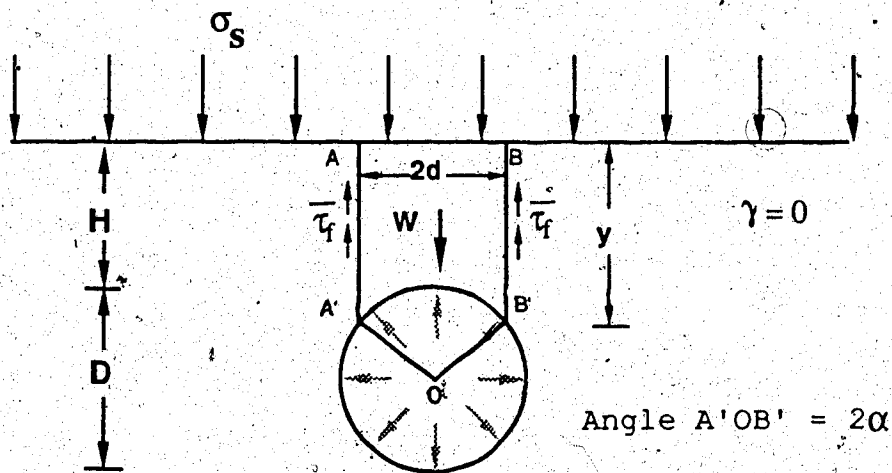


Figure 3.11 Geometry for 2D upper bound solution

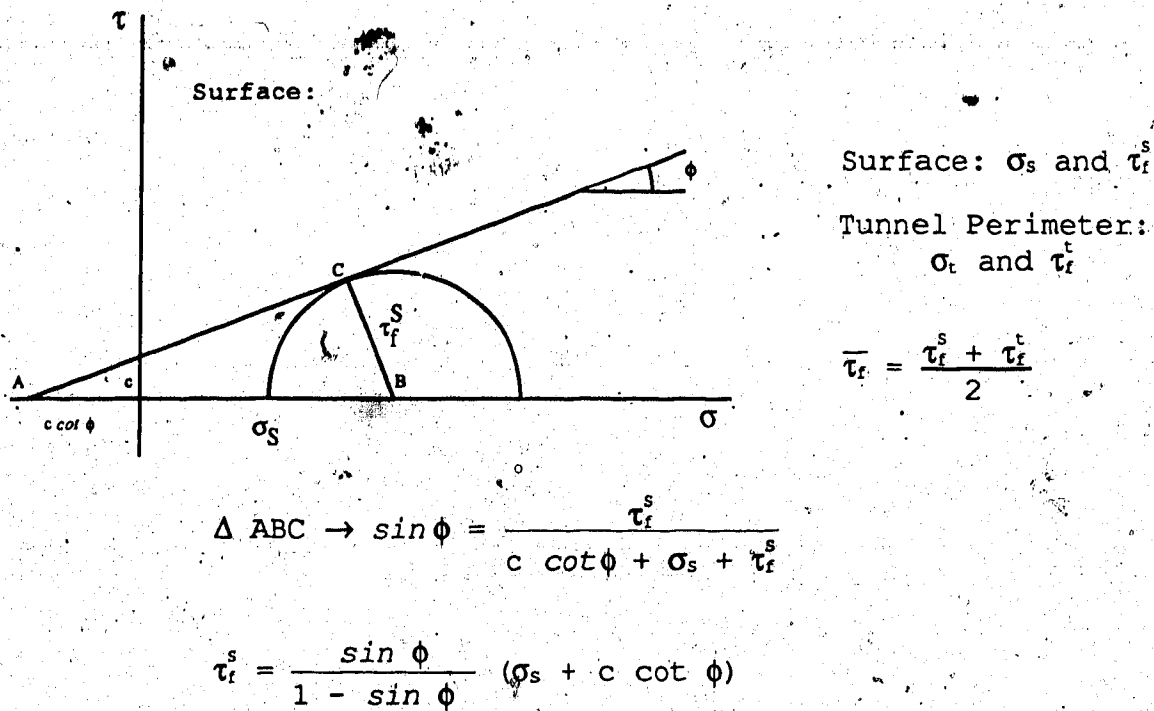


Figure 3.12 Illustration of Mohr circle at failure in upper bound solution (modified after Seneviratne, 1979)

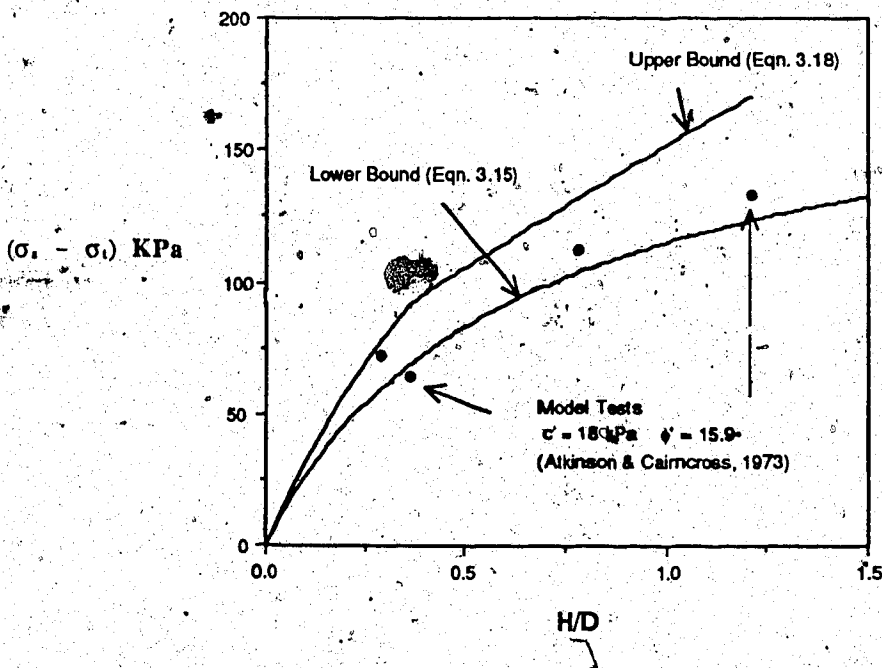


Figure 3.13 Bound solutions compared to results of model experiments by Atkinson and Cairncross (1973)

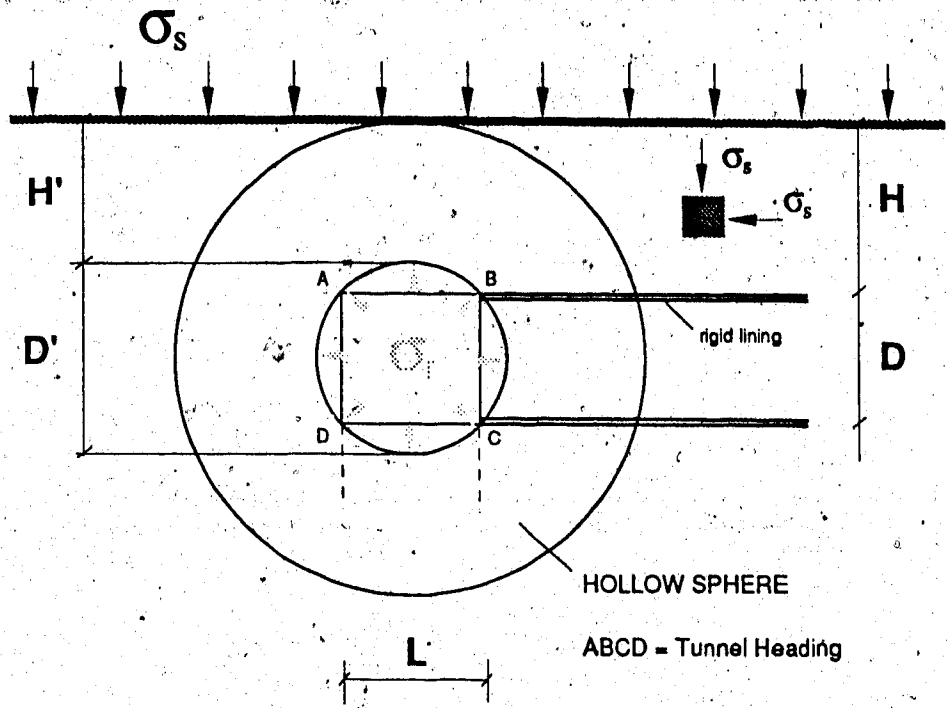


Figure 3.14 Mühlhaus sphere approximation for the tunnel heading (original does not include internal tunnel pressure)

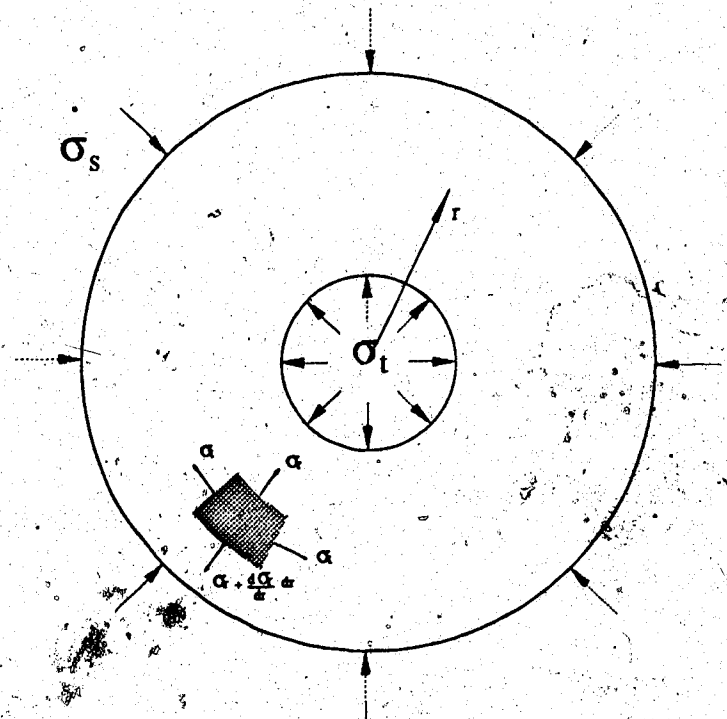


Figure 3.15 Hollow sphere subject to uniform external and internal stresses (modified after Timoshenko and Goodier, 1970:394)

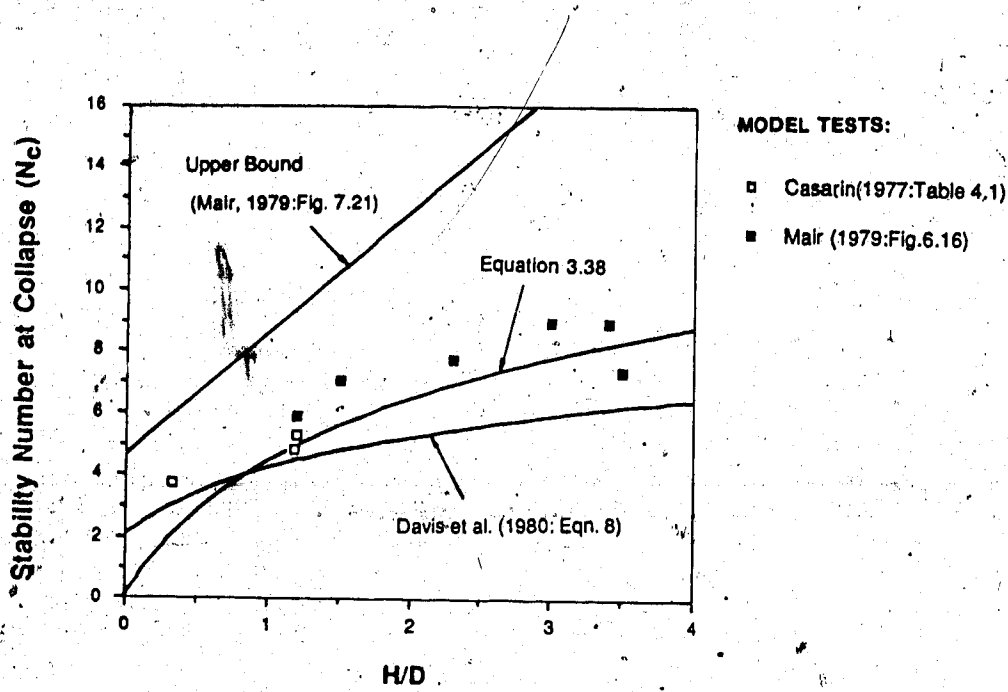


Figure 3.16 Lower bound stability solutions versus results of model tests taken to collapse ($L/D=0$)

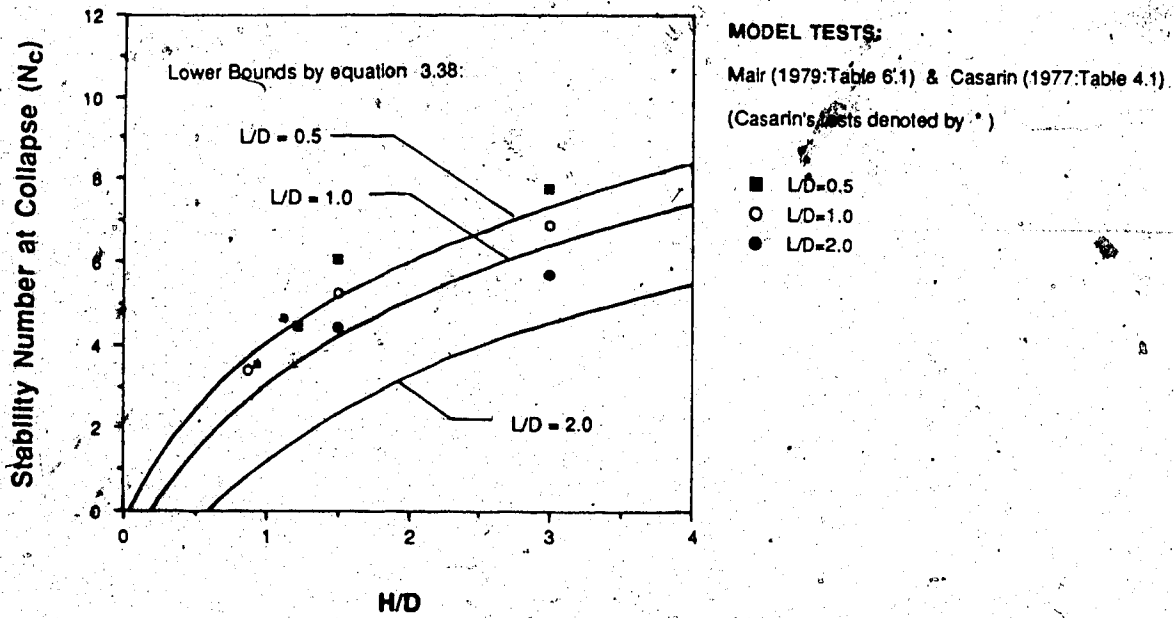


Figure 3.17 Lower bound stability solutions versus results of model tests taken to collapse ($L/D \neq 0$)

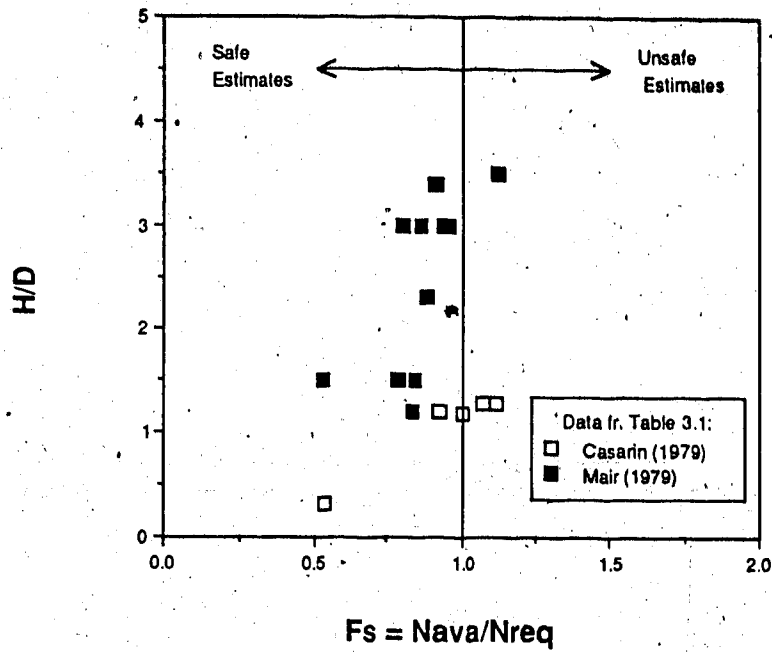


Figure 3.18 Factor of safety versus H/D for undrained model tests reported in Table 3.1

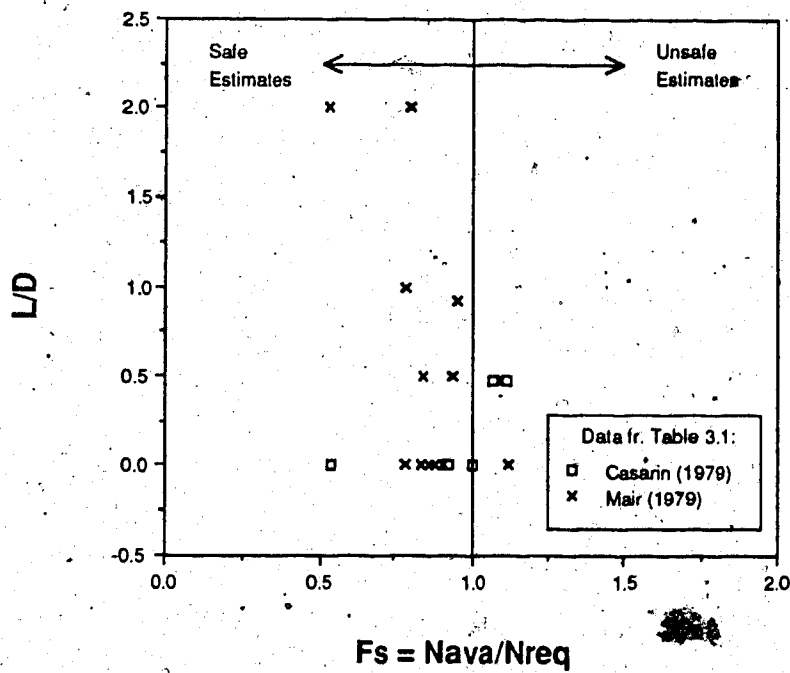


Figure 3.19 Factor of safety versus L/D for undrained model tests reported in Table 3.1

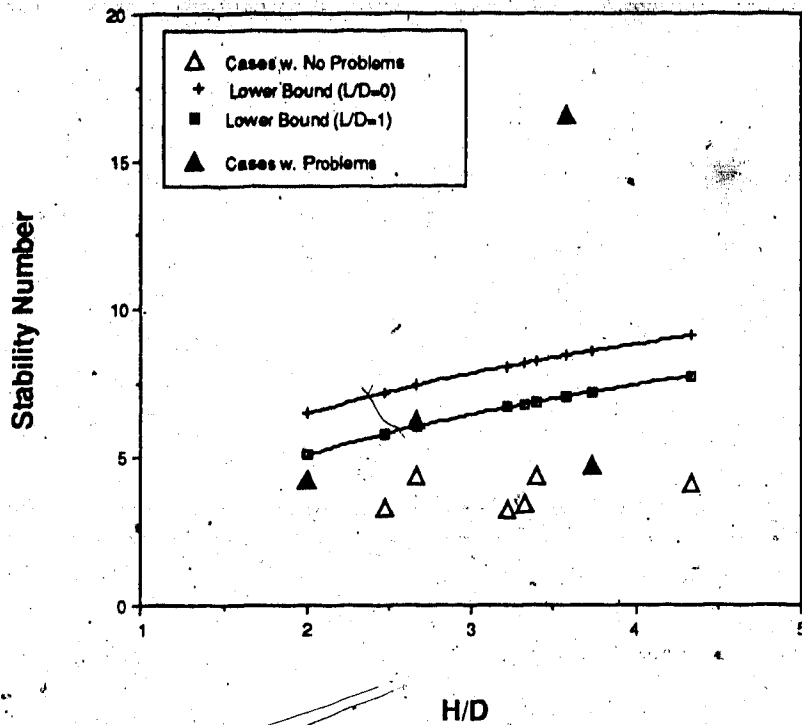


Figure 3.20 Comparison of unfactored lower bound calculations with data from actual case histories in Mexico City

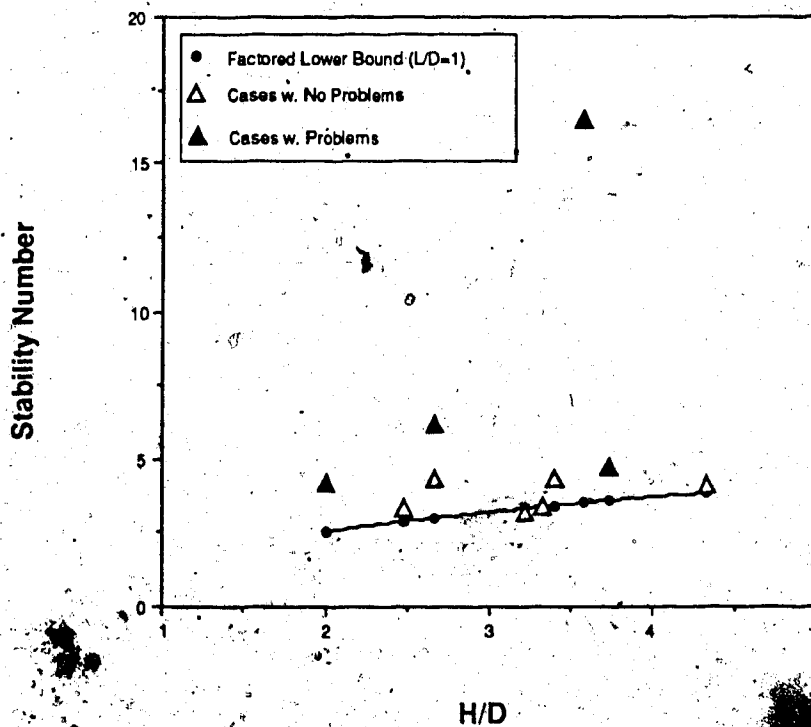


Figure 3.21 Comparison of factored lower bound calculations (L/D=1) with data from actual case histories in Mexico City

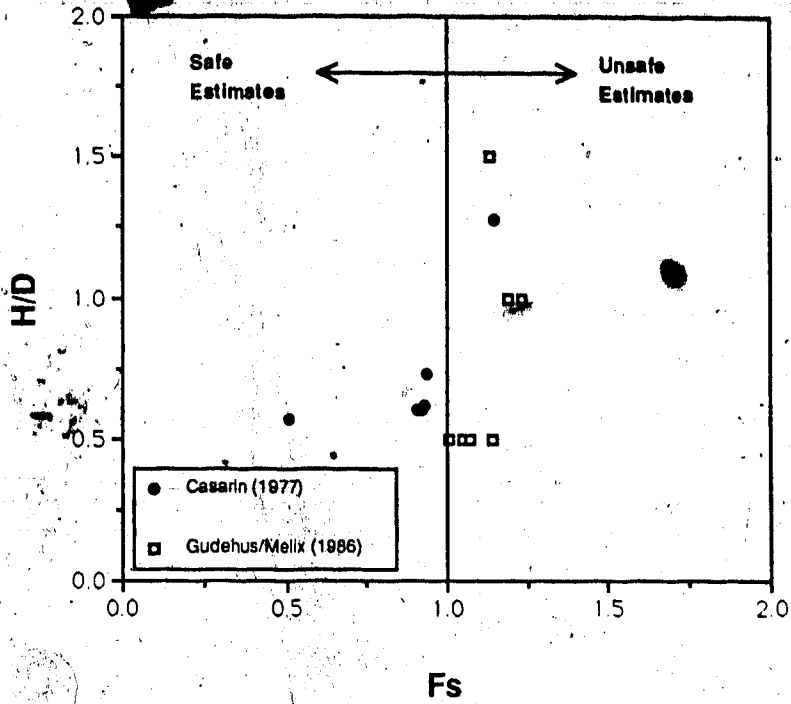


Figure 3.22 Factor of safety versus H/D for drained tests reported in Tables 3.3 and 3.4

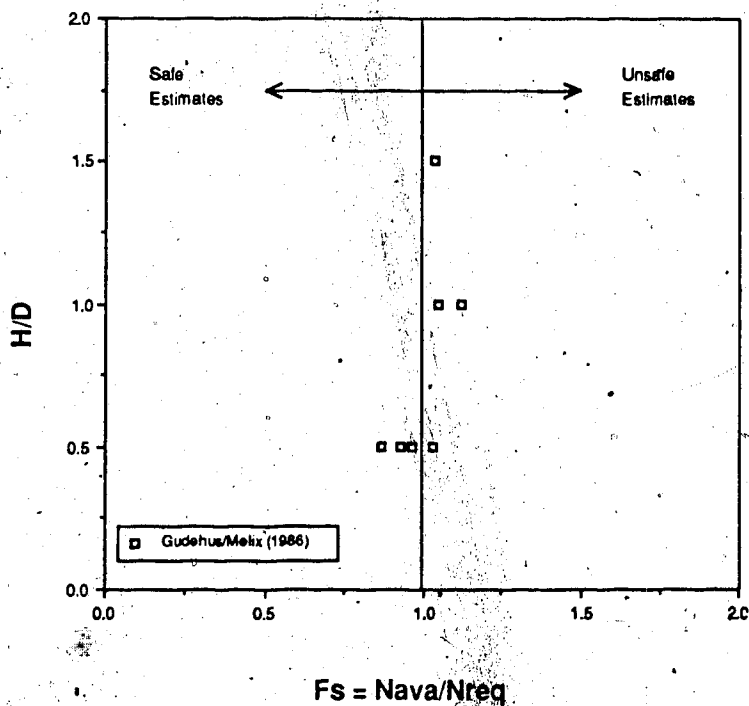


Figure 3.23 Factor of safety versus H/D for drained tests by Gudehus and Melix (1986) using residual strength parameters

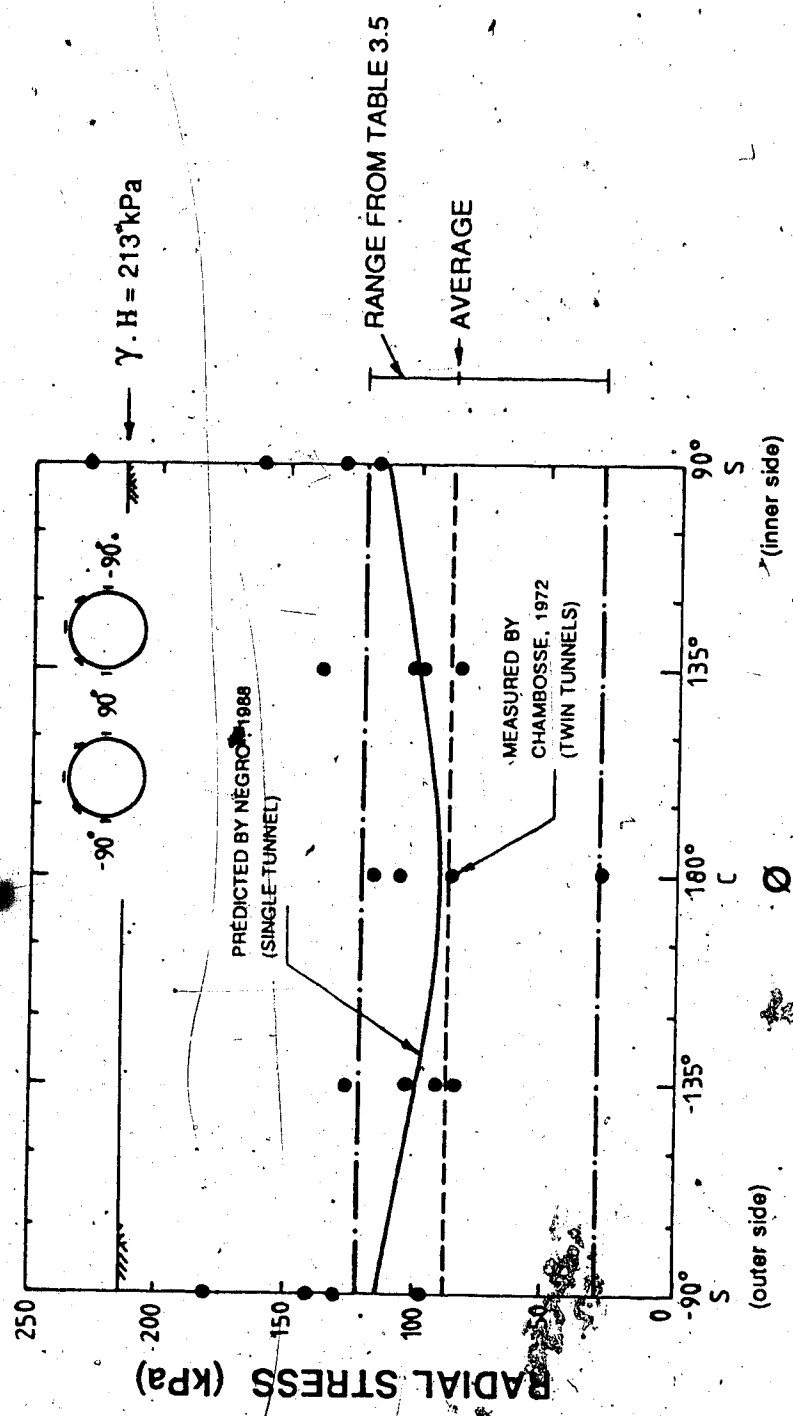


Figure 3.24 Predicted lining radial stresses for single tunnel and measured stresses in twin tunnels in Frankfurt subway (modified after Chamboisse, 1972:72 and Negro, 1988:1232)

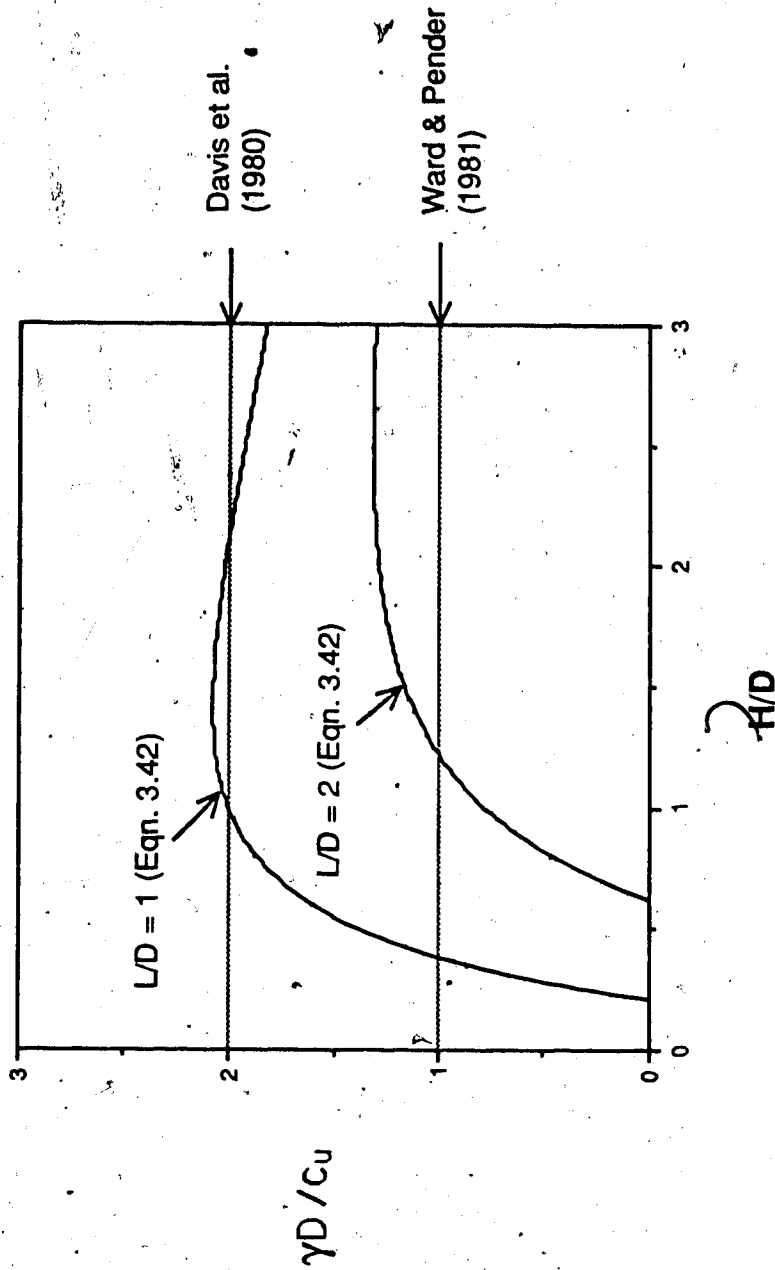


Figure 3.25 Illustration of dependency of critical diameter on H/D and L/D - UNDRAINED CASE

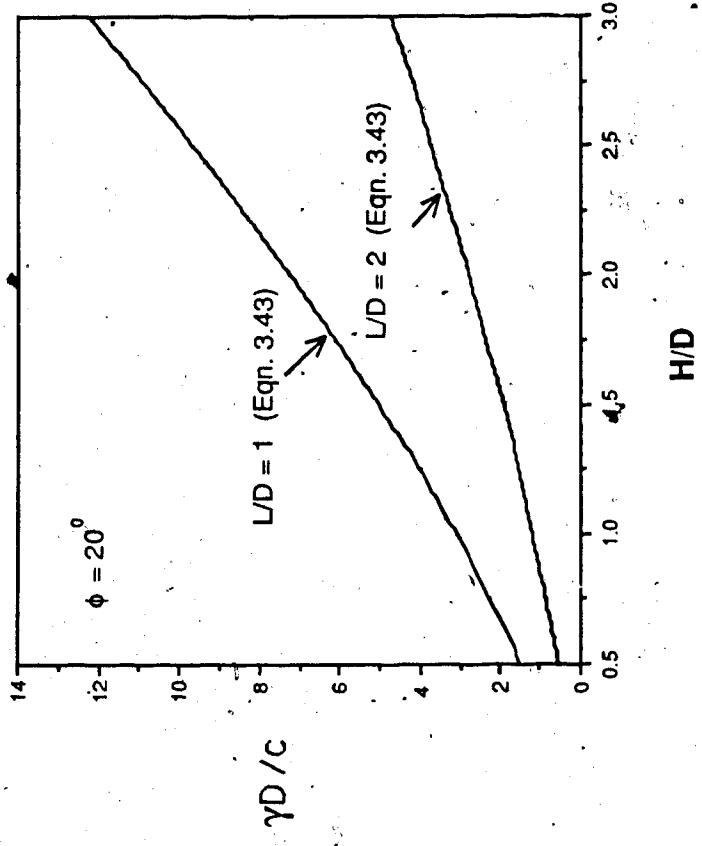


Figure 3.26 Illustration of dependency of critical diameter on H/D and L/D - DRAINED CASE

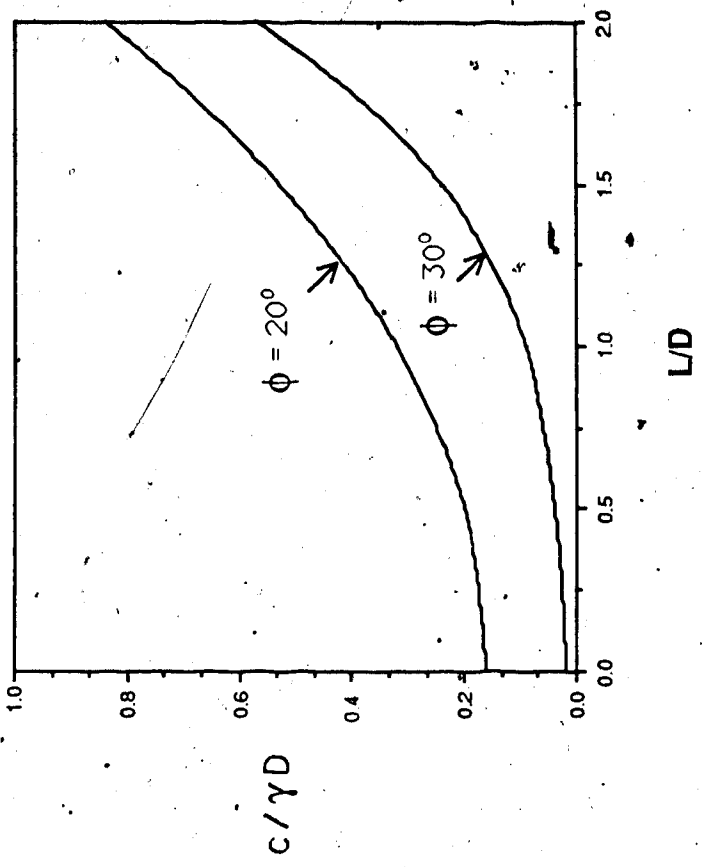


Figure 3.27 Illustration of effect of cohesion and friction angle on drained lower bound

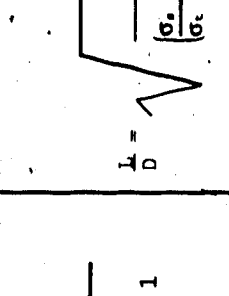
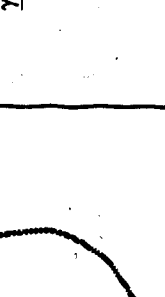
Type of Problem	Undrained Solution	Drained Solution
 <p>Lined</p> <p>L_{max} ?</p>	$\frac{L}{D} = \sqrt{\left[\frac{1 + 2 \frac{H}{D}}{e^{\frac{2c}{\gamma D}}} \right]^2 - 1}$	$\frac{L}{D} = \sqrt{\frac{(1 + 2 \frac{H}{D})^2}{\left(\frac{\sigma_v + c \cot \phi}{\sigma_t + c \cot \phi} \right)^2 \sin^2 \phi} - 1}$
 <p>D_{max} ?</p>	$\frac{\gamma D}{c_u} = \frac{4 \ln \left[\frac{(1 + 2 \frac{H}{D})}{\sqrt{\frac{L^2}{D^2} + 1}} \right]}{\left(\frac{H}{D} + \frac{1}{2} \right)}$	$\frac{\gamma D}{c} = \frac{\left[\frac{(1 + 2 \frac{H}{D})}{\sqrt{\frac{L^2}{D^2} + 1}} \right]^{\frac{2 \sin \phi}{1 - \sin \phi}}}{\left(\frac{H}{D} + \frac{1}{2} \right) \tan \phi + 1}$

Figure 3.28 Summary of lower bound solutions for application in large cross section tunnels

4. CASE HISTORY: MOUNT SHAUGHNESSY TUNNEL

4.1 Introduction

4.1.1 General

This chapter focuses on the geotechnical behaviour of the Mount Shaughnessy Tunnel (Rogers Pass Short Tunnel). This railway tunnel has geometrical characteristics which depart somewhat from the cases reviewed in Chapter 2. The section which is analyzed does, however, contain features which enable this case to be classified as a large cross section soft ground tunnel. The tunnel, which has an excavated cross sectional area of about 64m^2 , was excavated by a heading and bench procedure which could be characterized as type T1a (Figure 2.3, Chapter 2). Also, the section in question was excavated in soft ground and under a major highway thus concerns with settlement and stability were comparable to those faced in urban environments. Analysis of this case history is considered capable of providing data for verification of some of the findings from the previous chapters, as well as yielding conclusions which could be of general interest in the design and analysis of large cross section tunnels.

4.1.2 Scope of this Chapter

The initial sections of this chapter characterize the Mount Shaughnessy Tunnel Project, with emphasis placed on a relatively detailed geological and geotechnical

characterization of the tunnel site. The reasons for emphasizing this point are twofold:

1) Proper knowledge of the geotechnical characteristics of the site was deemed necessary in order to fit this case history into the frameworks outlined in previous chapters. Due to difficulties in sampling and testing the soil at the site, the geological characterization provided valuable assistance.

2) The geological and geotechnical characterization of the site provide insights which may become of value in future projects to be carried out in similar mountainous environments. Benson et al. (1985) for instance, describe a study of potential sites for expansion of the British Columbia railway system which could benefit from results of the present study.

Further sections of this chapter are concerned with field instrumentation, which was installed and monitored during the course of this study. Analysis of this monitoring data was undertaken and simplified analytical techniques, derived from numerical studies, were developed in order to assess the ground deformation parameters and their influence on tunnel performance. Finally, the empirical recommendations introduced in Chapter 2 are applied to this case history. Although these recommendations were not actually used in the project, a brief comparison is made between this empirical design and that which was actually used.

4.2 Description of the Field Case

4.2.1 Rogers Pass Project

The formidable chain of mountains that constitutes the Selkirk Range, British Columbia (B.C.), has always been a natural barrier to transportation routes. Deep winter snows¹ and avalanches were a threat to railway travellers through Rogers Pass until construction of the 8km Connaught Tunnel, completed in 1916. Although this tunnel is still in service, modern requirements led the owners of the tunnel, CP Rail, to undertake an extensive grade reduction and line duplication program.

The Rogers Pass Project, currently under construction, will create a double track line over 34km, including two tunnels totalling about 17km. The longer of these is the Mount MacDonald Tunnel, 14.7km long, which will be the longest railway tunnel in North America. East of this tunnel is the Mount Shaughnessy Tunnel (Rogers Pass Short Tunnel), which is the subject of this research. A general review of tunnelling activities at Rogers Pass was published by CP Rail (1985). The location of the project is shown in Figure 4.1.

4.2.2 Mount Shaughnessy Tunnel

This is a single track, 1.8km long tunnel, which, at its southerly end, passes under the Trans-Canada Highway, a vital road link through the mountains. This area is termed the

¹ Winter snow falls of up to 17,200 mm have been recorded at Rogers Pass (Mollard and Janes, 1984).

'West Portal', to concur with the overall direction of the railway. Although most of the tunnel is located in rock, the sections close to the portals were excavated in unconsolidated, bouldery deposits, whose nature is described in subsequent sections.

4.2.3 Regional Geology and Glacial History

The Selkirk Range is one of the interior mountain ranges of B.C. and comprises folded and faulted meta-sedimentary rocks. In the study area, the characteristic rocks are mainly phyllites and quartzites of Proterozoic and lower Paleozoic age. A detailed account of the bedrock geology of the area is given by Wheeler (1963).

British Columbia was intensely glaciated during the Pleistocene and evidence exists for at least four Quaternary glaciations. During the last major ice advance, generally referred to as the Fraser Glaciation, it is believed that, with the exception of scattered small nunataks, the Cordillera was totally ice covered (Fulton, 1984). During each of these glaciations the Cordilleran Ice Sheet is thought to have originated in the high areas which presently support glaciers. At the end of each glacial period, the Cordilleran Ice Sheet decayed by downwasting and complex frontal retreat (Clague, 1981). The actual pattern of deglaciation in a specific area depended on complex interrelationships of physiographic factors hence generalization is not possible.

The Quaternary geology of Rogers Pass has not been studied in detail¹. However, investigations on the late Quaternary geology of a wider physiographic area, termed B.C. Southern Interior (Holland, 1964) were presented by Fulton (1968), Fulton and Smith (1978), Clague (1981) and Fulton (1984). Based on stratigraphic studies supported by radiocarbon analyses, these authors attempted to identify major subdivisions of late Quaternary events and associated deposits, a summary being presented in Table 4.1. One should add that a radiocarbon date reported from near the downstream end of the Beaver River (GSC-1457), at about 30km from the tunnel indicates deglaciation before 10,000 years B.P. (R.J. Fulton, 1987, written personal communication).

4.2.4 Background for Interpretation of Surficial Geology

Geological assessment of sites located in mountainous areas such as that of this study may be a difficult task. Landforms and associated soil deposits, resulting from

¹ The author has searched a number of publications and technical reports, consulted with a number of known authorities and has come to the conclusion that no substantial surficial geology or geotechnical studies were carried out in the area of interest, prior to commencement of activities linked to the Rogers Pass Project. This is attributed to the fact that the area has been a National Park for about a century, resource development being therefore very limited. Among those consulted Drs. J.J. Clague and R.J. Fulton (Geological Survey of Canada), Dr. N. Rutter (University of Alberta), Dr. J.M. Ryder (Vancouver) and Mr. B. Thomson (Geomorphologist, Ministry of Environment and Parks, Victoria) should be mentioned. Some general information, of limited interest to this study, was published by Camsell (1914) and Daly (1915). A more recent work by Achuff et al. (1984) emphasizes vegetation and wildlife characteristics, but includes a very complete land classification map, derived from airphoto and field studies.

complex sequences of glacial erosion and deposition, are frequently modified by postglacial processes and their remnants are hidden beneath more recent deposits and a dense forest cover. Criteria for identifying vestiges of these glacial forms have been discussed by Chinn (1979).

On the other hand, observations made on contemporary glacial environments have enabled geologists to recognize a number of typical sedimentary models which may be used to interpret ancient glacial environments (e.g., Boulton and Paul, 1976; Boulton and Deynoux, 1981; Derbyshire and Love, 1986). Each of these models displays an assemblage of dominant landforms where major types of sediments, which may be recognized by their facies, are known to occur. The use of similar models in connection with the interpretation of geotechnical complexities has already been discussed by Morgenstern and Cruden (1979) and is attempted in the present study¹.

4.2.4.1 Model for Glaciated Upland Valleys

The model which is considered useful for the interpretation of glacial sequences in upland valleys is illustrated in Figure 4.2. In valleys which have been free of ice for some time, the principal features will be

¹At this point, it should be noted that at the time this study was initiated the report by Thurber Consultants Ltd. (1983a), which contains a detailed geomorphological investigation, was not known to the author. The use of available sedimentary models was seen as an approach to complement the evaluation of the local geomorphic features.

concentrated along the valley margins. Along the valley floor, glacial features are often destroyed or buried by meltwater streams and recent geomorphic activity. The dominant geomorphic processes and associated landforms which appear to be linked with this model are (Boulton and Eyles, 1979; Boulton and Deynoux, 1981; Derbyshire and Love, 1986):

1) Weathering and failure of the flanking slopes is the predominant source of debris as material falls onto the glacier and is transported either englacially (i.e., within the ice mass) or supraglacially (i.e., on the glacier surface), depending on whether it falls in the zone of accumulation or in the zone of ablation of the glacier. Owing to the relatively short transportation distances and lack of particle contact, this material tends to escape the rounding and comminution processes that normally operate upon basal or englacial debris (Boulton and Eyles, 1979). It will, therefore, create a very coarse grained 'supraglacial morainic till' (Boulton and Paul, 1976), which accumulates at the valley sides and may form very large lateral moraines¹.

2) Blocking of the natural drainage and interruption of mass wasting processes by the valley glacier will produce genetically complex ice contact accumulations which are sometimes classified as kame terraces (Figure

¹ Authors such as Kerschner (1981) have pointed out that under certain circumstances, substantial amounts of material in lateral moraines may also be derived from subglacial sources.

4.2). These may contain glaciofluvial and glaciolacustrine sediments and material derived from the local slope. These deposits are often multilayered and may contain beds of lower strength glaciolacustrine silts and clays which may be of engineering concern. Due to the unstable nature of the ice-supported topography and of the drainage system, which is subject to sporadic high water discharges, these sediments may intermix with the supraglacial morainic till and differentiation is frequently very difficult (Boulton and Eyles, 1979). The grain size distribution, for instance, is not significantly different from supraglacial morainic till.

3) Immediately after deglaciation, the soils in lateral moraines and kame terraces were made available for erosion by streams and slope forming processes. While large amounts of this material were transported downslope and formed colluvial fans (Eyles, 1983), a considerable portion was also introduced into stream systems at very high rates. As a result, the fluvial sediment transporting system became heavily loaded and poorly integrated, resulting in the occurrence of many alluvial fans and cones (Church and Ryder, 1972).

4.2.4.2 Geotechnical Characteristics

Due to the variety and complexity of the sedimentation processes occurring in upland glaciated valleys, it is not always possible to interpret the deposits with respect to

their genesis. Some authors, especially those working in modern glacial environments, do not consider re-sedimented deposits as tills, as pointed out by Levson (1986). For this reason, preference is frequently given by geologists to the descriptive term 'diamicton'¹ rather than the term 'till'², when referring to deposits such as those found in upland glaciated valleys.

In the present study, soils created by the geomorphic processes described above will be referred to as 'coarse grained supraglacial diamictons' (after Eyles, 1983). This term is probably broad enough to encompass most of the soils found along the lower slopes of glaciated upland valleys. A fundamental difference between these materials and subglacially-derived debris is in terms of grain size. The latter normally suffer traction at the glacier-bed interface, which produces comminution and generates a relatively high proportion of fines. Coarse grained supraglacial diamictons, on the other hand, present a minor silt-clay content, generally below 15%, which is one of their most distinguishing geotechnical characteristics (Boulton and Eyles, 1979; Eyles, 1983).

A review of the literature has shown a limited availability of field data on these supraglacial diamictons,

¹ The term diamicton is defined as 'any non-sorted or poorly sorted sediment that contains a wide range of particle sizes' (Levson, 1986:10).

² Till is defined as 'a sediment that has been transported and deposited by or from glacial ice, with little or no sorting by water' (Levson, op.cit.).

which may be related to difficulties in sampling and testing. Characteristics which are believed to be of geotechnical importance were collected from a few published studies and are summarized in Table 4.2. Table 4.3 presents another summary of properties, collected from published papers on some major dam sites in British Columbia. Although insufficient information on the geology of these sites was obtained which would warrant their classification as supraglacial diamictons, the properties shown were obtained in mountainous sites and are not substantially different from those presented in Table 4.2. Moreover, these properties were obtained for engineering purposes and it may be argued that they are more reliable than those in Table 4.2, which are related to geological studies of a rather general nature.

From analysis of the properties presented in Tables 4.2 and 4.3 it is apparent that the bulk density of the soils examined by Boulton and co-workers (column 1 in Table 4.2) and Eyles (column 2 in Table 4.2), which was likely derived from observations in recent glacial settings, is lower than that reported in the remaining cases. These same soils are reported as normally consolidated by those authors. It may be speculated that the higher densities in the more ancient deposits are due to phenomena which might have occurred after deposition. For instance, the reworking by water is known to provoke a densifying effect in such coarse-grained materials (see, for instance, Sherard et al., 1963 on the compaction of rockfills). Also, there appears to be a variety of processes

in upland glaciated valleys which may be responsible for some overconsolidation of the deposits, such as successive advances of the glacier and removal of overburden by slope movements.

4.2.4.3. Comments

It may be appreciated that there are a variety of processes which may have acted during and after the geomorphic development of upland glaciated valleys. Although a genetic distinction between various types of deposits is, at least in principle, possible (facies criteria are discussed by Boulton and Deynoux, 1981), this was not considered feasible in the present study, which was aimed mainly at investigating the engineering behaviour of a tunnel.

Also, the study area is heavily forested, which makes interpretation of airphotos and ground access difficult and sampling and testing are hindered by the bouldery nature of the soils. Moreover, the lack of good exposures and probable complexity of the deposits renders stratigraphic correlations difficult to establish. For these reasons, it is believed that setting the study site within the preceding framework, however idealized this may be, will provide a first approximation of the possible range of soil properties.

4.2.5 Tunnel Setting

The tunnel site is on the western side of the Purcell Trench, a topographic feature which separates the Selkirks from the Purcell Mountains. At this location, the trench is occupied by the Beaver River, in a classical glaciated U-shaped valley (Plate 4.1). Another significant feature in the area is Connaught Creek¹ which flows through a steep sided valley trending about N75°W and which is at the East entrance to Rogers Pass (Figure 4.3). Connaught Creek Valley lies about 150m higher than Beaver River, which led Daly (1915:4) to identify it as a hanging valley. Snow and sludge avalanches are frequent in this area and mudflows of great proportions have been reported in this valley as recently as 1983 (Achuff et al., 1984). Close to the Mount Shaughnessy West Portal, Connaught Creek is carving a canyon in the bedrock, the site of a series of waterfalls (Bear Falls).

The instrumented sections are located in the vicinity of the West Portal (figure 4.3). The alignment of the tunnel trends N51°W at this portal, changing to N10°E along most of its length. The overall surface slope perpendicular to the tunnel alignment ranges from 16 to 25°. However, at the West Portal, the natural slope was steeper (about 40°). The vegetation in the area consisted mainly of coniferous trees, up to 30m in height, covering most of the slopes.

The project area appears to conform to the upland valley sediment system described in the preceding section. For

¹ Formerly identified as Bear Creek, in early maps and reports such as those by Camsell (1914) or Daly (1915).

instance, the majority of the deposits on the valley walls along the tunnel route (Plate 4.1) appear to be remnants of lateral moraines and kame terrace complexes. This conclusion is based on analysis of airphotos obtained from the National Airphoto Library (Scale 1:12000, flown in 1973) and is partially supported by Thurber Consultants (1983).

Figure 4.3 presents the major geomorphic units in the area of interest. It is seen that the West Portal area is located in what is believed to be a distinct geomorphic unit (designated as Unit 2), a conclusion based mainly on topographical evidence and on the fact that the soils in this unit appear to be more bouldery and with a lesser silt-clay content than those of Unit 1. The location of this unit allows for the possibility that part of the material in this unit came from the adjacent Connaught Valley, and was deposited in the form of a large fan, at the break in slope where Connaught Creek enters the Beaver River Valley. Also, it should be pointed out that the upper portion of the slope above the West Portal appears to be the site of an ancient landslide of very large proportions, as identified by Mollard and Janes (1984:68). It is likely that at least a portion of the soils at the West Portal area are actually remnants of this slide.

A slightly different view is offered by Thurber Consultants Ltd. (1983a) with respect to Unit 2 in Figure 4.3. They contemplate that a minor readvance of an ice lobe down Gupola Creek, a tributary of the Beaver River 15km.

downstream of the tunnel site, occurred around 7,500 years B.P., damming the Beaver River and creating a large lake that covered the entire area. At the same time, another ice lobe moved down the Beaver River Valley, almost as far as the instrumented site and the material in Unit 2 (Figure 4.8) would be part of a very large outwash delta created by release of material from this ice lobe into the existing lake. This is a possible alternative which may be of interest to future more detailed studies in the area. But at least as a first approximation, it is believed that the soil properties would not be substantially different for any of the hypotheses:

4.2.6 Site Investigation at West Portal

Geological and geotechnical investigation was initially reported by Thurber Consultants Ltd. (1981). This study included geological mapping, diamond drill holes and field rock testing (Schmidt Hammer, Point Load Tests and RQD determinations). Two 5m deep test pits were later excavated in the proximity of the West Portal in an attempt to better characterize the ground. The test pits were inconclusive, as "the material encountered could be either blocky weathered bedrock or very large boulders".

Further investigation by Piteau and Associates (1982), which included field inspection, extra boreholes, seismic refraction surveys and piezometer falling head tests, led to the characterization of the material as unconsolidated

alluvial and colluvial deposits, with numerous cobbles and boulders up to about 60cm in diameter, in a silty sand and gravel matrix. Groundwater was not found above the tunnel invert level. This information led to classifying the portal section as soft ground requiring heavy support.

This interpretation of the characteristics of the soil deposits was, in principle, supported by inspection of the tunnel face carried out at various stages of tunnel construction. At the instrumented section, the dominant unit consisted of a weakly stratified diamicton, where boulders ($\phi > 20\text{cm}$) constituted 40 to 80% of the deposit (Plate 4.2). The matrix material was predominantly sand. The boulders were sub-angular to rounded (scale is that of Dackombe and Gardiner, 1983), up to 100cm in diameter and were composed of quartzite, garnet schist and quartzitic phillite (Piteau and Associates, 1982). This composition reflects the local bedrock.

A secondary unit consisted of well sorted, well rounded gravels and cobbles. These relatively thinner layers appeared to dip gently downslope, were cemented by carbonate, and occurred in beds within the bouldery soils. It should be added that the boulders in the main unit were, as a rule, tightly packed. This, in association with the cemented gravels and cobbles, required the use of some mild blasting during construction.

The information collected during these investigations is summarized in Figure 4.4. Due to the limited exposures

provided during tunnel excavation, any conclusion regarding the origin of the Unit 2 in Figure 4.3, based solely on these inspections, is speculative. It appears possible, however, that these soils were deposited during alternate periods of mass wasting of the valley slopes and periods of predominantly fluvial or glaciofluvial activity, responsible for the well sorted and rounded gravels and cobbles referred to above. This concept would be in agreement with an association of geomorphic processes 1 and 2 referred to in Section 4.2.4.1.

On the other hand, there is topographic evidence which suggests that at least a portion of this material may have come from the Connaught Creek Valley, possibly through processes such as those described in Item 3, Section 4.2.4.1. The fact that the area is still affected by avalanches and mudflows favours this hypothesis, since these activities were probably more intense in immediate postglacial times. This could account for the large amount of sediment deposited at the possible fan.

Another possibility is that the soils in Unit 2 were deposited by any of the processes discussed above and were later reworked by water; this would account for the low silt-clay content which appears to distinguish Unit 2 from Unit 1. This possibility appears to be favoured by Piteau and Associates (1982).

4.2.7 Soil Properties

Due to the nature of the bouldery soil at the tunnel site, very little testing which could yield deformation and strength parameters of interest to the present study, was carried out. However, extensive characterization testing of the materials in the area is reported by Thurber Consultants Ltd. (1983b) and will be summarized herein. The majority of these properties were obtained at nearby sites along the railway construction route rather than at the West Portal¹. Hence, conditions may depart from those at the instrumented section. Nevertheless, it is believed that these results, when interpreted within the geological framework, allow estimates of the parameters of interest to be made with some confidence.

In the following, reference will be made to 'kame-moraine' and 'delta' units, which are terms adopted by Thurber Consultants Ltd. (1983a) and correspond broadly to Units 1 and 2 in Figure 4.3. The sampling program, reported by Thurber Consultants Ltd. (1983b), consisted mainly of extracting disturbed samples from surface exposures, subsurface drilling and test pit excavation from an access road located at the proposed new track. In addition, insitu density tests using a nuclear densometer were conducted on shallow pits in the bouldery soil.

¹ The majority of the data reported herein is from the area west of Stoney Creek (Figure 4.3), which is thought to be geotechnically similar to the study site.

4.2.7.1 Characterization Properties

Natural Moisture Contents

A summary of natural moisture contents is shown in Figure 4.5. The deposits range in moisture content from 4.2 to 29.4% with a mean value of 10.1%. The higher (>15%) values were, however, obtained in soils with a silt-clay content typically above 30% and are not considered representative of the West Portal site. Values close to the mean or slightly lower would be more characteristic of the West Portal deposits, which clearly lack a significant fines content.

The trend in Figure 4.6 indicates the dependency of the moisture content on the silt-clay content for the local soils. The predominantly lower silt-clay contents available at the tunnel site allows one to speculate that natural water content is probably low at this area, which is consistent with a single moisture content (average of three determinations), obtained by the writer at the tunnel face, in one of the instrumented sections (m.c.=7.3%).

Atterberg Limits

Atterberg Limits were determined for the minus #40 sieve fraction ($\approx 0.4\text{mm}$) for selected samples containing a large percentage of fines. Although the soils at the West Portal are more sandy and therefore less plastic, it is observed that, when placed on the plasticity chart (Figure 4.7), the soils tested fall among the points attributed to coarse-grained supraglacial diamictons by Sladen and Wrigley (1983). Results for other tills such as those found in Edmonton

normally fall close to the T-line, introduced by Boulton and Paul (1976). Casagrande's A-Line is also shown and it is interesting to observe that, according to his original classification chart (e.g., Terzaghi and Peck, 1948:35), the coarse-grained supraglacial diamictos could be classified as cohesionless, of low plasticity and possibly of low compressibility. These are features which may characterize these deposits, which enhances the usefulness of Atterberg Limits for preliminary estimates of properties of these soils.

Grain Size Distribution

Grain size characteristics may be evaluated by means of a textural chart presented in Figure 4.8a. Most of the samples are characteristic of the coarse-grained diamictos that dominate the kame-moraine deposits (Unit 1 in Figure 4.3) but some finer soils, possibly of glacio-lacustrine origin, are also depicted. Points representing 'delta' deposits are believed to better represent the soils in the West Portal (Unit 2 in Figure 4.3). Material designated as 'landslide' in Figure 4.8a includes colluvium, debris flow and slumped material and can hardly be differentiated from the kame moraine unit in terms of grain size. This suggests that these are, in fact, kame moraine soils which were re-sedimented by post-glacial mass wasting processes.

Figure 4.8b shows textural characteristics of soils typical of glacial valleys (Derbyshire and Love, 1986) and it is apparent that the soils displayed in Figure 4.8a show

similar characteristics. By comparing the two figures, one could tentatively establish that at least some of the 'kame-moraine' soils (though not at the West Portal) could be of subglacial origin. This would support the occurrence of a 'basal till', mentioned by Thurber Consultants Ltd. (1983a)¹. However, it was not possible to establish the specific origin of the samples from any of these figures due to insufficient published data. Further studies, specifically aimed at establishing geotechnical facies, could clarify this tendency and make textural diagrams such as those in Figure 4.8 useful for geotechnical classification purposes.

Densities

Dry densities were determined in fourteen shallow test pits close to the future railway track by means of nuclear densometers. The average of 108 determinations was found to be $\bar{\gamma}_d=20.1\text{kN/m}^3$, with a standard deviation $s=1.22\text{kN/m}^3$. Standard Proctor maximum densities obtained for samples in the same test pits yielded values which were slightly higher. ($\bar{\gamma}_d=20.9\text{kN/m}^3; s=4.47$), as shown in Table 4.4.

Using the average water content reported above (10.1%) and a specific gravity value $G=2.7$ (consistent with TCL's data) and applying fundamental weight/volume relationships,

¹ Fulton (1987, personal written communication) points out that moraine-like landforms sometimes contain till-like diamictos, which might have originated as colluvium and were later overridden, but not completely reworked by the glaciers. This would be another possibility for explaining the origin of this material.

average values for the bulk density and void ratio are found to be $\gamma = 22.1 \text{ kN/m}^3$ and $e = 0.32$ respectively.

Permeability

Falling head piezometer tests were performed by Piteau and Associates (1982) at the West Portal. The values obtained range from $k = 10^{-6} \text{ m/s}$ to $k = 10^{-3} \text{ m/s}$. Due to the coarse grained nature of the deposit at the instrumented sections, it is believed that the actual permeabilities are close to the upper portion of this range.

Overconsolidation Ratio

Although this type of deposit is thought to be normally consolidated at the time of deposition (see Table 4.2), a variety of processes acting during and after glaciation may have caused the deposits to be overconsolidated. In the West Portal area, for instance, landslide activities could have removed part of the overburden, leaving the tunnel section overconsolidated. Also, post-depositional chemical alterations due to cementing agents may also provoke overconsolidation (e.g., Holtz and Kovacs, 1981:294). No attempt has been made to quantify the OCR value, but evidence from back analysis of field instrumentation, presented in the following, suggests K_0 values slightly higher than normally consolidated values.

4.2.7.2 Shear Strength

Shear Strength from Triaxial Tests

The strength properties were determined from five multi-stage consolidated undrained triaxial tests with pore pressure measurement on 4 inch diameter compacted samples. Results presented by Kenney and Watson (1961) suggest that these yield test strengths comparable to tests carried out in distinct samples at different confining stresses. Moreover, since a range of confining pressures is applied to the same sample, minimization of problems due to singularities in different samples is attained. The triaxial test specimens were prepared to initial dry densities of 21.1 to 21.7 kN/m³, which are comparable to the values obtained from the nuclear densometer tests (Table 4.4).

Results from all five tests reported by Thurber Consultants Ltd. (1983b) were collected and replotted in Figure 4.9. Since these tests were conducted on the minus 3/4" fraction and a tendency for a reduction in the friction angle with increasing particle size is known to exist in similar soils, a reduction of 2° may be applied (Marachi et al., 1972:Figure 10). The value of $\phi' = 40^\circ$ appears to be a reasonable approximation for the triaxial friction angle of the material insitu. The cohesion value, however, is probably underestimated, since the eventual cementation which could be present would have been eliminated during sampling and recompaction. Based on studies on natural cemented sands with comparable friction angles carried out by Clough et al. (1981), one could estimate the insitu cohesion due to

cementation varying from 12kPa (weakly cemented) to 175kPa (moderately cemented).

Shear Strength from Semi-Empirical Methods

Since the number of triaxial tests was fairly small and these were conducted on relatively small samples, the question of representativeness of the results in Figure 4.9 may arise. A number of indirect procedures were surveyed which could provide an insight into the problem and are summarized in Table 4.5. It is apparent that the $\phi' = 40^\circ$ is a reasonable estimate, in the sense that when compared to the values, it is neither too conservative nor too optimistic. However, many of the estimates on Table 4.5 are based primarily on an estimated relative density and should, therefore, be viewed with caution.

A more elaborate procedure, which includes some empirical input but is based on a behavioural model is that by Barton and Kjaernsli (1981). It is perhaps more appropriate since it allows inclusion of several influencing parameters, including the geomorphic origin. Based on an analogy with the shear strength of rock joints Barton and Kjaernsli suggest that the following equation may be used for estimating ϕ in rockfill materials:

$$\phi = R \cdot \log\left(\frac{S}{\sigma'_n}\right) + \phi_b \quad [4.1]$$

where:

1) S is an equivalent, size dependent strength of the rockfill particles, function of the uniaxial compressive strength of the rock particles and of the d_{50} particle size, determinable from Figure 4.10 (obtained by Barton and Kjaernsli by trial and error fitting of numerous tests with equation 4.1).

2) R is an equivalent roughness of the rockfill, which allows the effect of particle roundedness and smoothness of particles to be included. It may be obtained from Figure 4.11, which was constructed in a similar fashion as Figure 4.10 (Barton and Kjaernsli, op.cit.). It is observed in this figure that the R value may also be related to the genetic origin of the materials.

3) σ'_n is the effective normal stress acting on the sheared surface.

4) ϕ_b is the basic friction angle of smooth, planar, unweathered rock surfaces, which according to Barton and Kjaernsli varies between 25 and 35°, with an average 27.5° derived from Norwegian experience. For unweathered rocks, ϕ_b equals the residual friction angle ϕ_r , which, as a first approximation, may be related to the natural slope angle (Chandler, 1973; Dusseault, 1977). For the study area, $\phi_b=27.5^\circ$ is probably a close approximation of the natural slope angle of the soil material along the tunnel alignment.

Using an S/σ_c value of 0.3, corresponding to a d_{50} value of about 30, (compatible with Thurber's data), a σ_c of 80Mpa

(approximate average for the quartzitic phyllites at the site, determined by Piteau and Associates, 1982), $\phi_b = 27.5^\circ$ and R values for different void ratios, Figures 4.12 and 4.13 are obtained for "glaciofluvial" and "moraine" materials.

These figures illustrate the dependency of the friction angle on the confining stresses, and it is seen that for $\sigma'_n = 250 \text{ kPa}$ which is believed to approximate the insitu mean confining stress at the tunnel crown level, values of ϕ' ranging from about 38° to 48° are found for $0.2 < e < 0.4$, a range believed to encompass the actual natural void ratio. The average between these two values is $\phi' = 43^\circ$, which would correspond to an e of about 0.3, both these values being fairly close to those reported by Thurber Consultants Ltd. (1983b) for their triaxial samples. This void ratio is also believed to be close to the existing value.

4.2.7.3. Deformation Properties

Deformation Properties from Triaxial Tests

The following moduli were determined from the same multistage triaxial tests of the preceding item. Table 4.6 summarizes this data. Because the moduli are known to depend on the confining stress, it is convenient to express them according to the following expression, which is attributed to Janbu (1963):

$$E = K_E p_a \left(\frac{\sigma_3}{p_a} \right)^n \quad [4.2]$$

in which E is the modulus (e.g., the initial tangent modulus E_1), K_E is the Young's 'modulus number', p_a is the atmospheric pressure, σ_3 is the confining stress, and n is the modulus exponent. The moduli were obtained from the second and third cycles in the stress-strain curves reported by Thurber Consultants Ltd. (1983b), normalized by the atmospheric pressure (p_a) and plotted against the normalized confining pressure (σ_3/p_a) in a log-log plot. These procedures are well known in geotechnical engineering (e.g., Duncan and Chang, 1970; Duncan et al., 1980) and are illustrated in Figure 4.14, where K_E is the intercept at $\sigma_3/p_a=1$ and n is the slope of the line. The parameters obtained ($K_E=500$ and $n=0.5$) are reasonable when compared with the values recommended by Duncan et al. (op.cit.) for compacted granular materials such as that being dealt with ($200 < K_E < 600$ and $n=0.4$).

It should be noted that using the parameters obtained from Equation 4.2 with:

$$\sigma_3 = K_0 \sigma_1 = (1 - \sin \phi') \sigma_1 \quad [4.3]$$

with $\phi'=40^\circ$ and $\sigma_1'=409\text{kPa}$ ($\cong \sigma_1'$ at tunnel axis) will yield an $E \cong 61\text{MPa}$. This is thought to be an underestimate of the insitu modulus, as will be discussed elsewhere in this chapter. There are several reasons for this:

- 1) Although the samples were compacted to densities comparable to the field conditions, the natural matrix

could hardly be reproduced. The cementation of the grains, for instance, has been found to have a very significant effect on the stiffness of these soils, although the friction angle is not significantly affected (Clough et al., 1981; Skempton, 1986). For naturally cemented sands, Clough et al. (op.cit.) found modulus numbers varying from $K_E=700$ (uncemented specimens) to $K_E=2700$ (strongly cemented specimens), representing a fourfold variation in the modulus.

2) The natural soil is thought to be overconsolidated (see section on back-analysis of instrumentation). Analysis of tests on many soils by Mayne and Kulhawy (1982) suggests that the following formulae may be used as a first approximation:

$$K_{0-NC} = 1 - \sin \phi' \quad [4.4]$$

$$K_{0-OC} = K_{0-NC} (\text{OCR})^{\sin \phi'} \quad [4.5]$$

where K_{0-NC} represents K_0 of normally consolidated soils and OCR is the overconsolidation ratio. It is clear that the use of results from Equation 4.5 instead of from Equation 4.4 in Equation 4.3 would result in a higher K_0 and consequently a higher modulus.

3) Relatively recent studies which have been carried out at the Imperial College of Science and Technology (U.K.) have shown that moduli from conventional triaxial stress-strain curves such as those reported by Thurber

Consultants Ltd. (1983b) tend to be underestimates. This is discussed in more detail in the following section which deals with the dynamic E' values.

Deformation Properties from Empirical Correlation

In view of the numerous difficulties in estimating the deformability of natural deposits, several authors have attempted to obtain moduli from empirical correlations. One of the first attempts was given by Janbu (1963), who plotted K_M values¹ against the soil porosity for a wide range of geotechnical materials (Janbu, 1963: Figure 4). Correlations between the porosity (or the void ratio) and the stiffness have also been traditionally used in the field of soil dynamics (e.g., Hardin, 1978).

An attempt has been made, in the present work, to establish a correlation between the void ratio of natural soils and the modulus number K_E . Data were selected from published case studies where the soil presented characteristics similar to those of the supraglacial diamictons described earlier in this chapter. A summary of this data is given in Table 4.7.

Figure 4.15 shows the data from Table 4.7 and values obtained by Duncan et al. (1980:53) for rockfills thought to be geotechnically similar to the materials in the present

¹ K_M are modulus numbers determined from oedometer tests, as opposed to K_E , which are determined from conventional triaxial tests.

study (only GW and GP, predominantly sandy rockfills). The bounds proposed by Janbu (op.cit.) are also shown and were obtained using the following relationship, with an assumed Poisson's ratio (ν) of 0.25:

$$K_M = K_E \frac{(1 - \nu)}{(1 + \nu)(1 - 2\nu)} \quad [4.6]$$

These bounds have been shown to encompass a wide range of soils by Janbu (1963 and 1985) and it is observed that this holds true for a great number of the natural soils surveyed. It is clear, however, that the rockfill cases reported by Duncan et al. (op.cit.) will yield a considerably lower K_E for a given void ratio e , which can probably be ascribed to the same factors discussed above, in association with the results of triaxial tests.

In Figure 4.16, only the points corresponding to the natural soils in Figure 4.15 are replotted. Furthermore, points lying outside Janbu's bounds are rejected, as a criterion to eliminate possible inconsistencies. An exponential curve fitting procedure through the remaining points results in the equation shown in Figure 4.15. For a range of void ratios $0.2 < e < 0.6$, which encompasses all cases, K_E 's varying from 572 to 2598 are found. Estimating σ_3' from Equation 4.3, this will result in a range of $E=70-316$ MPa for the deformability at the tunnel axis level. The upper value approximates the moduli obtained by back analysis of the

tunnel instrumentation, presented elsewhere in this chapter. But if one considers a higher K_0 value such as 0.7, corresponding to a lightly overconsolidated soil; the range of moduli estimated is $E=97$ to 441 MPa. This illustrates the importance of the correct evaluation of the overconsolidation ratio of the deposits.

Moduli from dynamic tests

Traditionally, mechanical properties of soils for use in deformation analyses have been measured by conventional insitu or laboratory tests. In recent years, due to the usually high costs associated with such tests, attention has been given to the possibility of using the results of seismic methods for such purposes. For instance Morris and Abbiss (1979) and Abbiss (1981) reported results from extensive testing carried out at the Building Research Station (U.K.), which show that moduli obtained in seismic wave propagation tests are comparable to those obtained through more conventional techniques such as the self-boring pressuremeter test, provided a strain correction is applied. This strain correction is required due to the typical non-linear behaviour of soils: dynamic measurements are carried out at very low strain levels (generally $\epsilon < 10^{-4}\%$) and tend to approximate the actual initial tangent modulus of a stress-strain curve, whereas in conventional static tests the modulus is measured at much higher strains (typically $\epsilon > 0.1\%$) and is therefore much lower.

More recently Jardine et al. (1985) reported laboratory investigations on the behaviour of London clay at very small strains, using a newly developed technique (Costa Filho, 1980; Jardine et al., 1984). They noted with considerable interest that "the dynamic values of the shear modulus obtained by Abbiss (1981) using geophysical methods give values of E_u ($\approx 3G$) which are approximately 30% greater than the values of $E_u(0.01)$ [i.e., the undrained modulus at 0.01% strain] found in UU tests". It has been recently shown that this low strain modulus is of great importance in geotechnical numerical analyses of excavations (Fourie et al., 1986).

Also, for the case of deeply buried sediments or for soils where no traditional sampling techniques are applicable, geophysical methods may be the only reliable way of estimating these mechanical properties (e.g., Azimi et al., 1983; Dusseault, 1986).

Seismic techniques available for measuring dynamic soil properties are described in detail by Woods (1978). In essence, most techniques involve the measurement of sonic wave propagation velocities through generation and registration of seismic pulses. Two types of waves are usually measured in engineering studies:

- 1) Compressional or longitudinal waves (V_L) are those in which the particle motions are in the direction of propagation. The determination of the modulus of elasticity from the compressional wave is as follows:

$$E = V_L^2 \rho \frac{(1 + \nu)(1 - 2\nu)}{(1 - \nu)} \quad [4.7]$$

$$G = V_L^2 \rho \frac{(1 - 2\nu)}{(2 - 2\nu)} \quad [4.8]$$

where E is the Young's modulus, G is the shear modulus ($G = E/(2+2\nu)$), ρ is the mass density and ν is the Poisson's ratio. These equations are valid for an elastic, isotropic material and are derived in Jaeger and Cook (1979).

2) Transverse or shear waves (V_S) are those in which the particle motions are perpendicular to the direction of propagation. Moduli calculation is as follows:

$$E = 2 V_S^2 \rho (1 + \nu) \quad [4.9]$$

$$G = V_S^2 \rho \quad [4.10]$$

One should also note that the Poisson's ratio of the material can be calculated if one knows the values of V_L and V_S :

$$\nu = \frac{1}{2} \frac{2 \left(\frac{V_L}{V_S} \right)^2 - 1}{\left(\frac{V_L}{V_S} \right)^2 - 1} \quad [4.11]$$

Compressional waves are the first to arrive at detecting instruments and are the most easily measured. Shear waves are slower than the compressional waves and their velocities are usually more difficult to measure, with conventional equipment, since the first shear wave arrivals from small explosive charges are indistinguishable from later arriving compressive waves which have taken longer paths. In practice, the problem is usually treated by using shear wave rich energy sources and the so called "direct methods", where there is a direct propagation between the source and the detector (e.g., Woods, 1978; Fialho Rodrigues, 1979). Also, it is easily verified through Equation 4.7, above that the modulus determined from the compressional wave velocity (V_L) alone is particularly sensitive to the choice of the Poisson's ratio and, therefore, a method which yields both V_L and V_S is ideally desired.

The moduli presented in Table 4.8 were estimated from seismic refraction tests the West Portal area. In addition to difficulties associated with application of this specific method (e.g., Fialho Rodrigues, 1979), only the longitudinal waves were determined and a Poisson's ratio of 0.12 was assumed¹. On the other hand, it should be considered that the tests were conducted by an experienced geophysical team (Piteau and Associates, 1982) and that any other tests would

¹ The value of the Poisson's ratio is known to depend on the strain level (e.g., Krizek, 1977). The dynamic (i.e., low strain) value of ν is usually chosen between 0 and 0.2 and a value of 0.12 is suggested by Hardin (1978).

also present limitations, for instance related to the occurrence of extreme values.

In order to convert the dynamic modulus to the static modulus, a correction must be applied. Choosing a correction factor is not an easy task, since the value $E_{\text{static}}/E_{\text{dynamic}}$ will be highly dependent on the strain level, void ratio and confining stress. The correction factor range estimated for the local soils is $0.05 < E_{\text{static}}/E_{\text{dynamic}} < 0.15$, which is based on a semi-empirical procedure outlined by Seed and Idriss (1970) for sands and adapted for coarser soils based on empirical equations published by Kokusho and Esashi (1981). The calculations are presented in detail by Seed and Idriss (op. cit.) and are briefly summarized in Figure 4.17.

Figure 4.17 also shows values actually measured by Ortigosa et al. (1981) for a gravelly soil comparable to the that of the present study. The prediction is not perfect, which could be attributed to the fact that the equations by Kokusho and Esashi (op.cit.) were derived from large scale triaxial tests on remoulded samples, while the experimental points are for field tests on natural soils. On the other hand in the laboratory tests a better control of test conditions was probably achieved. It is also noteworthy that the correction estimated is in close agreement with existing empirical recommendations (e.g., Hansbo, 1977; Massarch, 1981).

It will be seen further in this chapter, that the range estimated for E_{static} is reasonable when compared with values

obtained through back analysis of the field instrumentation. It may be suggested, therefore, that the use of geophysical methods is a possible way of assessing the deformability of deposits in which representative sampling and testing poses a problem. However, due to the well known imprecisions associated with seismic refraction techniques, it is believed that future attempts should employ direct methods such as the cross-hole and down-hole techniques, described by Woods (1978), which eliminate most of the problems associated with the seismic refraction approach¹.

4.2.7.4 Comments

Due to the complexity of the deposits, the properties discussed above should only be viewed as guidelines and may not account for local variations. For instance the manner of bedding, which in the deposits is neither uniform nor continuous, and the possible complex loading history, are known to have a marked influence on the deformability (Lambrecht and Leonards, 1978). Also, it is possible that stiffness anisotropy may occur in places.

Nevertheless, it should also be remembered that the soil in question does not allow conventional sampling and testing so it seems reasonable that, for a practical application, the properties should be cross-checked by all available methods. Table 4.9 summarizes the information reported above. The

¹ The cross-hole method is quoted by Wroth in his Rankine Lecture as being a reliable way to estimate the modulus of soils (Wroth, 1984).

properties derived from the studies by Piteau and Associates (1982) and by Thurber Consultants Ltd. (1983b) are also shown and it is to be noted that most property values fall within the ranges estimated through the correlations with similar deposits.

4.2.8 Construction Details

Excavation was carried out using a heading and bench procedure, the top heading being about 4.5m high to the full width of the tunnel. The heading was driven from the West Portal and stopped when hard rock was encountered at about 200m from the portal. Benching started about two months after excavation of the heading. Excavation was carried out with a CAT931 backhoe and two Wagner LHD ST muckers were used to remove the spoil. Despite the 'soft ground' classification, a certain amount of mild blasting was required for the excavation of each round. Excavation rounds in the instrumented section averaged 0.9m for the heading and 2.4m for the bench (Figure 4.18). In the instrumented area, overbreaks of 30-50cm were measured on each side and were estimated at 40-70cm at the crown.

A typical cross section of the tunnel is shown in Figure 4.19. The initial support was provided by steel sets (W8x48 at 90cm intervals), with the aid at steel spiles at the crown (shown on Figure 4.18). These spiles consisted of $\varnothing=1$ " rebars placed into pre-drilled holes about 3m long and spaced about 30cm (total of 16-18 spiles). These ungrouted spiles were

restricted to the crown area and worked more as a precaution against boulder falls than as a proper support. Occasionally, during construction, one of the spiles would get loose and fall from the roof of the tunnel.

Dry mix shotcrete was sprayed immediately after excavation of each round and after the steel members were placed and blocked against the ground. The total shotcrete thickness was on average about five centimeters. In the area beneath the highway longitudinal concrete wall beams were placed at the base of the ribs, along the top heading. These were about 120cm high and confined between the excavated walls and corrugated steel sheets (not shown in Figure 4.19).

To avoid excessive deformation of the highway the whole area below it was subject to a grouting program. Cement grout was injected from the surface, aimed at forming a protective arch around the upper portion of the tunnel. It was not possible to make a proper evaluation of the extent and efficiency of this treatment. However during excavation, some evidence was found that the grout was unable to penetrate the dense soil and remained within the borehole limits.

4.3 Monitoring Program

The main purpose of the instrumentation reported herein was to assess the effects of portal and tunnel excavation on the overlying highway, located about 14.0m above the tunnel crown. Within the context of this thesis, results of this monitoring program are used for evaluation of the ground

properties, thus complementing the studies reported in preceding items. Also, it is considered that interpretation of the instrumentation results provides insights into the behaviour of this large cross section soft ground tunnel which might be useful for other similar projects.

The West Portal area (Figure 4.3) was instrumented and monitored continuously during the periods of crossing (i.e., heading portion and bench portion). The readings were evaluated as soon as they were taken with the provision that corrective measures would be taken should the results indicate excessive movement. An extensive amount of data was collected and interpreted, but only selected portions, characteristic of the tunnel behaviour, are presented herein. The complete set of field data is summarized in Eisenstein and Heinz (1986). The schedule of readings is shown on Table 4.10.

The instruments were arranged according to the plan provided in Figure 4.20. The layout of the settlement points' location was intended to cover the largest possible area and, at the same time, avoid interference with construction equipment and traffic, active on the location at the time when the points were placed. The location of some of the instruments were tied to a more general survey program, carried out by Nortech Surveys, enabling an exact calculation of the distance of their location at the surface to the face of the tunnel. A typical instrumented section is shown on Figure 4.21.

4.3.1 Types of Instruments

The number of instruments installed was as follows:

- 24 settlement points
- 5 slope indicators
- 5 multipoint extensometers (total of 32 magnets)
- 2 bench marks
- 12 vibrating wire strain gages (attached to the steel ribs inside the tunnel).

Similar instrumentation programs were used extensively in other projects carried out in the past at the University of Alberta (e.g., Eisenstein et al., 1981a; 1981b). The types of instruments which were used in the present study are described in these papers and on the comprehensive work by El-Nahhas (1980). Measuring procedures generally followed recommendations by Cording et al. (1975). Due to these considerations, it is thought that a brief description of the instruments will suffice.

Settlement Points

These instruments are used to measure the vertical displacement of soil near the ground surface. The settlement is measured by surveying the level change of the top of a steel rod inserted in a 4" diameter borehole to a shallow depth (about 1.6m), to avoid disturbance due to frost action or other surface effects. A PVC pipe is placed around the upper part of the rod, in order to eliminate the friction

between the rod and the subsequently placed backfill material.

Optical levelling was carried out using a Geotec AL-23 instrument. A special surveying rod which is provided with a vertical level bubble and which can be read to the nearest 0.5mm was used. The sight distance was limited to 10m or less, following recommendations by Cording et al. (op.cit.). Surveying closing errors were generally kept within $\pm 0.5\text{mm}$.

Multipoint Extensometer

These instruments are used to measure vertical displacements at points in depth below the surface. Magnetic multipoint extensometers have two basic components, i.e., magnets anchored permanently on the ground and an access tube. Axially magnetized circular magnets are placed inside a PVC housing. These magnet assemblies are inserted and attached to the borehole walls and hence move together with the soil. Measurements are carried out by lowering a probe down the access tube which is installed at the center of the borehole and serves as a guide for the movement of the magnet assemblies. As the probe reaches the magnetic field, it activates a buzzer at the surface.

Distances from the top of the access tube to the magnets are measured with a tape which is lowered with the probe. After optical surveying of the access tube, the total movements are calculated from the relative displacements measured. Reproducibility of 1mm is normally achieved with

this instrument at depths such as those encountered in this project, except in the case of extensometers which are not placed vertically, where performance is poorer due to increase in friction between the probe and the access tube. The calculation procedure for the displacements measured with these inclined extensometers is somewhat unconventional and is therefore illustrated in Figure 4.22

Slope Indicators

These instruments are used to measure the profile of horizontal displacement along a borehole. A slope indicator comprises three components: casing, probe and readout unit.

The casing consist of 3m sections of plastic tubing, provided with four longitudinal grooves equally spaced around the inside circumference. It is placed and grouted in a predrilled borehole ($\text{Ø}=4\frac{1}{2}$ ") and is flexible enough to move with the soil when it deforms laterally. The deformation of the casing (and hence of the surrounding soil) is measured by determining the inclination of the casing at various depths with the probe.

The probe is lowered into the casing and read at specific intervals in order to determine the inclination of the casing. Lateral displacements of the casing at successive times are determined from the changes in inclination occurring since the initial measurements. The total lateral profile of the fixed casing is found by summing the

individual lateral displacements from the bottom of the casing to the top.

The lateral profile of the casing is usually determined in two mutually perpendicular vertical planes (directions A and B). In the present case, direction A in all instruments was chosen to give the direction of movements approximately perpendicular to the Trans-Canada Highway, whereas direction B gives the movements towards the tunnel axis.

Vibrating Wire Strain Gauges

Strain gauges are usually installed inside the tunnel in the lining, to measure strains in the support members. Although several types are available, it appears that in tunnel instrumentation programs, preference is normally given to the vibrating wire type due to its resistance to dusty, humid environments and to the added advantage of independence of the length of the leads and long term reliability (El-Nahas, 1980). In the present study, the strain gauges were installed in the steel ribs, as illustrated in Figure 4.23.

It should be noted that all gauges were installed in the lower portion of the tunnel (i.e., during the excavation of the bench). Ideally, the crown area should have been instrumented, but this was not possible due to an unavoidable delay in the ordering of the units. The gauges used were manufactured by Irad Gage (Model SM-SW) and a portable readout unit (Irad Gage MB-6LU) was used, which

displays strains directly. Readings of temperature in the member were also obtained through an ancillary readout.

In order to protect the gauges from the shotcrete impact, the assemblage provided by the manufacturer was embedded in silicone and further covered by a steel plate. The leads were protected by an aluminium flexible tube, with each end housed in a steel box which was covered after each reading.

4.3.2 Results and Interpretation of Instrumentation

For a proper analysis of the results of tunnel instrumentation, it is often appropriate to subdivide the length of the tunnel into zones with similar construction and/or geotechnical characteristics. For this instrumented portion of the Mount Shaughnessy tunnel, it was felt appropriate to take three different zones, as depicted in Figure 4.24:

- 1) In Zone I, the proximity to the portal, where the slope was cut prior to tunnel excavation and the occurrence of a looser surficial material are believed to have affected the displacement behaviour, which show magnitudes about 50% higher than in the other sections.
- 2) Most of the instruments are concentrated in Zone II. In addition to being away from the slope and in a different, denser material, this zone was grouted and this could be claimed to justify the better behaviour. However, evidence was found, during construction, that

the grout (injected from the surface) was unable to penetrate the dense soil. It seems therefore possible that the smaller settlements were mainly due to the better ground properties found in this area and to the greater distance from the slope.

3) Zone III comprises the instruments placed across the highway (i.e., farthest from the portal). Although the geotechnical characteristics are probably identical to those of Zone II, it is believed that the behaviour of the instruments in this zone was affected by the traffic on the surface (there was an adjacent parking area, as well as the entrance of an access road).

4.3.2.1 Surface Settlements

Figure 4.25 shows the final surface settlements occurring in planes perpendicular to the tunnel axis, representative of zones I, II and III. It is seen that on average the settlements for the four points in Zone I are considerably higher than in Zones II and III. The maximum settlement recorded was at SP1 ($\approx 11.5\text{mm}$), which is located close to the portal and in sloping ground (see Figure 4.20). This settlement is not representative of Zone II, close to the highway, where the maximum settlement was slightly less than 3mm. The settlements in Zone III are also very small, on average below 2mm. The asymmetry in the settlement trough in this zone is believed to have been caused by surface traffic, since SP21 (with settlement $> 2\text{mm}$) was located close to the

entrance of the access road. The surface distortions (the slope of the settlement trough) in Zones II and III are also small.

All readings taken at the surface settlement points (SP's) were plotted against time and are presented in Appendix B. It is apparent that the movements which took place in all points were largely due to tunnel excavation. Some of the settlement points, notably SP1 and SP3, located in Zone I, show a pronounced increase in displacement in the "long term" reading (April, 1986). Due to the proximity of the slope, it may be speculated that this increase is associated with small slope movements rather than with the tunnel activities.

4.3.2.2. Subsurface Settlements

The evolution of subsurface settlement, given by the readings of multipoint extensometers (ME's) are plotted versus the distance to the excavation face and the full data are presented in Appendix C. The pattern of displacement evolution seems to be typical of mined shallow tunnels (Heinz, 1984:254), with about 30 to 40% of vertical displacements occurring ahead of the tunnel face. A stabilizing trend is observed as soon as the face is about 12m from the instrument, i.e. about two excavated diameters for the heading portion. Figures 4.26a and 4.26b represent the typical behaviour near the crown and the results for all other points are presented in Appendix C. It is noticed that

the majority of the displacements were caused by excavation of the top heading.

Figures 4.27 to 4.29 depict the subsurface settlement behaviour with depth for each of the vertical extensometers. This type of plot is useful for examining the amount of deformation of the ground above the tunnel and to evaluate the loss of ground caused by excavation. The pattern shown in the curves for ME-2 and ME-3 seems to be typical of tunnels constructed in urban areas under good ground control conditions (see, for instance, the cases analyzed by Negro, 1988). However, the abrupt increase of displacement in ME-1, close to the tunnel crown, may be interpreted as a zone of localized failure or "loosening" above the crown. It should be noted that this instrument is located in Zone I and the readings were likely subject to effects such as stress relief due to the proximity of the excavated slope and the existence of a looser soil.

Finally, it is observed that the the sub-surface displacements measured in Zones II and III are fairly small for the size of the tunnel and the construction technique used. This is also confirmed by the readings in ME-4 and ME-5 (inclined extensometers under the highway), which are included in Appendix C. This fact is discussed in the analysis of loss of ground, presented in the following paragraphs.

4.3.2.3. Horizontal Displacements

Horizontal displacements were measured by slope indicators which were installed primarily with the intent of monitoring the movements due to the cutting of the slope for portal construction. The only instrument that yielded useful information for the present study was SI-3 (Figure 4.20), which was located at about 3.0m from the tunnel wall. Unfortunately, grouting around the casing of this instrument, especially in the portion above the tunnel, was not fully successful. This fact was noted during the readings, which took a long time to stabilize and were not always consistent. Also, it appeared that this same problem occurred at the bottom of the casing.

The solution adopted was to disregard the results in the upper portion (approximately above the tunnel crown) and to adopt a new zero at about 3.0m above the bottom of the borehole. The results obtained are plotted in Figure 4.30 and although the trends appear to be consistent with observations in other projects (e.g., El-Nahhas, 1980), these results should be viewed with caution. They will be discussed, in conjunction with the numerical analysis.

4.3.2.4. Loads on the Support

Ideally, the strains measured in the support members could be used to evaluate the loads which are acting on the support system. In the present case, interpreting the readings proved to be a difficult task, due mainly to the irregular nature of the wood blocking between the ribs and

the soil and the consequent erratic load transfer from the ground to the support.

The strains measured in the 12 gauges are plotted against the distance to the bench in Figure 4.31, for the two instrumented sections (I and II, shown in Figure 4.24). The strain history shown begins after the ribs were erected and blocked and it is worth noticing the wide variations displayed by the readings in the bottom strut. This variation is attributed to traffic inside the tunnel. Rib temperatures were measured together with all readings and were found to vary little during the period represented in Figure 4.31 (oscillations were within $\pm 0.3^{\circ}\text{C}$ for all instruments). Therefore, errors introduced by temperature variations such as those discussed by Brierley (1975) are believed to be minimal¹.

The average strains calculated for the mid-section of the steel members assuming Hooke's law and a linear distribution of strain were mostly tensile strains. For the last reading, taken when the excavation of the bench had passed the test sections by about 100m, average thrusts were +9.98kN (Section A) and +11.69kN (Section B). The magnitude of these tensile forces is fairly small when compared to the overburden load at the measurement level ($T = \gamma \cdot z \cdot \text{radius}$)

¹ Although the gauges are theoretically compensated for changes temperature when connected to a steel member, practice shows that small differences in the coefficients of thermal expansion of the two steels may yield changes in reading which are unrelated to changes in the rib stress. Also, temperature has been found to affect the rate of internal gauge creep (zero drift), as reported by Brierley (1975).

-1431kN). These tensile forces may indicate that the loads acting on the ribs were small, but any conclusion will be speculative, due to the uncertain boundary conditions discussed previously. It should be noted that the protective (5cm) layer of shotcrete did not exhibit any signs of distress at the instrumented sections during the period of readings. This could be interpreted as an indication of small loads.

4.4 Analysis of Field Results

In the following sections, results mainly from Zone II will be analyzed. This data was considered to represent average conditions for this case history, which can therefore be compared to other cases.

4.4.1 Loss of Ground

Excavation of a tunnel generally causes the soil to displace inwards around the tunnel perimeter. The volume of soil so displaced is termed the loss of ground (V_1) and is expressed as a volume per unit length of the tunnel. The loss ground may also be expressed as a percentage of the total tunnel volume, $V_1(\%) = V_1/V_t$. A simplified empirical procedure which was presented and checked against field measurements by Cording and Hansmire (1975) may be used for estimating the loss of ground. These authors verified that the volume lost into tunnels could be estimated from deep vertical displacement measurements by an expression of the form:

$$V_1 = 2 \delta (a + y) \quad [4.13]$$

where V_1 is the volume lost into the tunnel (m^3/m) and δ is the deep vertical displacement measured at a distance y above the crown. According to Cording and Hansmire (1975), the distance y has to be small with respect to the tunnel radius a , otherwise the equation will not estimate the loss of ground correctly.

An analysis of the results of a typical vertical displacement close to the tunnel crown given by extensometer ME-2 (Figure 4.28), allows an estimation of the loss of ground at several construction stages. (Figure 4.32). It is observed that excavation of the top heading was responsible for the largest portion of the loss of ground (about 75% of the total V_1), whereas bench excavation accounted for the remaining displacement. This same apportioning of the loss of ground is a feature already observed in other large cross-section projects (e.g., Eisenstein et al., 1986). Of interest is also the loss of ground at the heading face, which represents about 27% of the total. This amount compares well with values calculated for tunnels excavated using the New Austrian Tunnelling Method (NATM), as shown in Table 11. Also, it may be noted that the total loss of ground, expressed as a percentage of the tunnel volume, is less than that of the NATM tunnels. One of the characteristics of the NATM is good ground control, by

accomplished by immediate application of the shotcrete support as a full circle and as close as possible to the tunnel face. This was not the case at the Mount Shaughnessy Tunnel, where the shotcrete support action was limited due to an irregular excavation profile and invert closure was accomplished only at some distance behind the face. Considering this relatively relaxed construction sequence, the remarkably low loss of ground could be attributed to the good quality of the soil mass.

4.4.2 Back Analysis of Displacements

4.4.2.1 Proposed Method

As discussed previously, the properties of bouldery deposits such as those encountered on this project are difficult to assess. One alternative for evaluation of soil properties is the back analysis of field instrumentation through numerical techniques such as the Boundary Element Method (BEM). For the purpose of evaluating the deformability parameters of the ground, some simple, two-dimensional analyses by the BEM were carried out. A version of the program, published by Hoek and Brown (1980) and implemented at the University of Alberta by the writer, was used. The ground was modelled by a linearly elastic, homogeneous, isotropic model. The output stresses and displacements represented a one-step unloading of the unlined tunnel boundary, from the original insitu stress state. Provision was made for gravity loading and for implementation of insitu

stress ratios (" K_0 ") values independent of Poisson's ratio. These simplifying hypotheses are considered reasonable in the present case, since the soil is fairly stiff and loads on the support are presumably small.

Based on these hypotheses an extension of the method proposed by Negro and Kuwajima (1985) for a quick estimate of the ground deformability and of the insitu stress ratio is proposed. This new method uses the dimensionless displacement introduced by those authors:-

$$\Delta_i = \frac{u_i E}{2 R_{eq} p} \quad [4.14]$$

where u_i is the radial displacement of a point near the tunnel (not necessarily on the perimeter), E is the ground modulus, p is the radial stress at the point where the displacement is measured and R_{eq} is the radius of a circle with the same area as the tunnel cross section (A_t):

$$R_{eq} = \sqrt{\frac{A_t}{\pi}} \quad [4.15]$$

One should note that, as opposed to the method by Negro and Kuwajima (op.cit.), the gravity effect is included. In other words, the analyses represent more appropriately the case of a shallow tunnel, where the increase of the vertical stress with depth, in the region about the tunnel, is

significant. The method proposed is illustrated in Figure 4.33 and the sequence of calculations is as follows:

a) Estimate a possible range of variation for E and K_0 (e.g., Section 4.2).

b) Run BEM program for combinations of E and K_0 . The extreme values should be included.

c) These analyses will yield the radial displacements above the crown (u_{crown}) and near the tunnel wall (u_{wall}) for pre-determined points, which are a function of the field position of the instruments. The behaviour observed is illustrated in Figure 4.33b.

d) For each of these points (i.e., crown and wall), and using the dimensionless displacements given by equation 4.14, one may obtain equations 4.16 and 4.17 below. One should note that the variation with the displacements with K_0 is essentially linear and hence it suffices to run the program for one value of E and two values of K_0 .

$$\Delta_{\text{crown}} = a + b K_0 \quad [4.16]$$

$$\Delta_{\text{wall}} = c + d K_0 \quad [4.17]$$

e) Substitute the field readings in equations 4.16 and 4.17, with the Δ_i values expressed by equation 4.14.

f) Rearrange equations 4.16 and 4.17, so that a system of two equations and two unknowns (E and K_0) is

obtained. This system is, in general, linearly independent:

$$E = e + f K_0 \quad [4.18]$$

$$E = g + h K_0 \quad [4.19]$$

(Note: a, b, c, d, e, f, g and h are constants, which are a function of the characteristics of the problem).

g) Solve the system of equations 4.18 and 4.19, as illustrated graphically in Figure 4.33e.

4.4.2.2 Application of the Proposed Method

The above procedure was applied to the case of the Mount Shaughnessy Tunnel. Ranges of K_0 and E were estimated to be $K_0=0.3$ to 0.8 and $E=100\text{MPa}$ (minimum from correlations with similar deposits: Table 4.9) to $E=750\text{MPa}$ (average from seismic tests: Table 4.9). The sequence of calculation and the results are illustrated in Figure 4.34, for the case of the full cross section. The values obtained ($K_0=0.697$ and $E=386\text{kPa}$) are fairly close to those estimated by Heinz et al. (1987) using the same numerical technique but with a trial and error approach (Figure 4.35)

The same method was applied to the case of the excavation of the heading only, yielding $K_0=0.714$ and $E=680\text{MPa}$. This higher E modulus could be attributed to

imprecisions in the measurements but may also represent a certain amount of "softening" (i.e., mobilization of strength implying in a decrease of the soil modulus). It is observed, however, that both values of E are reasonable when compared to those estimated previously (Table 4.9).

It should also be noted (Figure 4.35) that the agreement with the slope indicator readings is only approximate, which can be attributed to the simplicity of the model used and to the fact that the excavation in stages was not taken into account. Nevertheless, the method proposed, which requires the use of the widely known boundary element program by Hoek and Brown (1980), is very simple and several alternatives may be readily investigated. It is suggested that moduli determined in this manner may be used for initial estimates in more refined analyses through methods such as the Finite Element Method.

4.4.3 Estimate of Loads from Displacements

Having estimated the E modulus of the soil mass using the preceding procedures, the dimensionless displacement U, for the full cross section, given by equation 3.7 (Chapter 3) may be calculated. In order to obtain the displacement at the tunnel perimeter, those given by extensometers ME-2 and ME-3 (Figures 4.28 and 4.29) were extrapolated to the crown level using results of parametric non-linear finite element analyses (Eisenstein and Negro, 1985). An average of $u_{\text{crown}}=9.7\text{mm}$ for the two sections is obtained.

Using equation 3.7 with an E modulus of 530MPa (average from back analysis) one obtains an "average" U value of 1.8, for an equivalent diameter of 9.55m (correction for overbreak included). With this value, the load factors, estimated through the use of Negro's (1988) Figure 2.8 (also Figure 3.9, Chapter 3), are found in the range 0.54-0.94.

One may now attempt to estimate the average load on the support, through use of Equation 3.8 (Chapter 3). The value of σ_{tc} , however, cannot be estimated using the solutions given in Chapter 3, since these do not apply when L/D tends to infinity such as in the present case. Alternatively, the solution by D'Escatha and Mandel (1974), for L/D= ∞ given by Negro (1988) may be used. Applying H/D=1.56 into Negro's Figure 6.126, one obtains $\sigma_{tc}=0.164\gamma D$ (for c=0) and $\sigma_{tc}=0$ (for c=28kPa), which are the extremes shown by Negro. The latter value is adopted herein, since the soil in question is considered at least moderately cemented. The range of σ_t/σ_v which is obtained is 0.06 (for LF=0.94) to 0.46 (for LF=0.54). These relatively low stresses seem to be consistent with the possibility of no significant stresses being transferred to the support, discussed in Section 4.3.2.4 above.

4.5 Design Considerations

As noted previously, the Mount Shaughnessy Tunnel has characteristics which depart somewhat from those of the tunnels reviewed in Chapter 2. Nevertheless, it does have

features which enable its classification as Type T1a (Figure 2:3, Chapter 2) and an attempt to apply some of the empirical recommendations developed in Chapter 2 is considered worthwhile.

4.5.1 Prediction of Surface Settlements

Given the ground properties reviewed in this chapter, this case history fits the soft ground class designated as Class III (Coarse Grained Coherent), described in Chapter 2. For the present site conditions, which involved excavation under an important highway, it seems reasonable to adopt the parameters suggested in Chapter 2 for "urban" conditions, i.e., $V_s/V_{tn}=0.3$ and $S=1.0$.

Assuming initially that the ground deformability was unknown and using an excavated area of $64m^2$ (i.e., assuming that the amount of overbreak was not known at the time of the prediction), one obtains a volume of the settlement trough $V_s=0.192m^3/m$. With this value, adopting an equivalent tunnel radius of $a=4.5m$ and using the properties of the trough outlined in Figures 2.21 and 2.22 (Chapter 2), a settlement $S_s=9.6mm$ is predicted at the tunnel axis. Assuming the surface settlement trough to follow the error function (Figure 2.21), Curve I in Figure 4.36 is obtained. It is observed that, in this case, the adoption of the empirical recommendation $V_s/V_{tn}=0.3\%$ led, to an overprediction of the surface settlements and of the slope of the trough.

Alternatively, the maximum settlement may be calculated using the parameter \bar{S} which is, as discussed in Chapter 2, a dimensionless settlement:

$$\bar{S} = \frac{E S_s}{\gamma D^2} \quad [2.1]$$

Applying the expression to the case of the Mount Shaughnessy Tunnel with an $E=530\text{MPa}$ (average from back analyses in Section 4.4.2.1) one obtains a maximum settlement $S_s=3.4\text{mm}$ and Curve II in Figure 4.36. When compared to the field readings, this second curve represents a dramatic improvement in the estimate. However, it is easily verifiable that this second method will produce good results only if the insitu E modulus is known accurately. For instance, for an E ranging from 100-750MPa, estimated before the back analyses were carried out (Section 4.4.2.1 above), maximum settlements range from 2.4 to 17.9mm, which is a rather large interval. Nevertheless, this finding reinforces the necessity of precise determinations of the ground deformability for attaining accurate predictions.

4.5.2 Construction Procedure

The construction procedure adopted for the case of the Mount Shaughnessy tunnel departs from those normally employed in Class III in urban areas (cases 9, 23 and 24, Appendix A). The most salient difference is that the top heading was

excavated fully, without a temporary invert closure, before bench excavation started. This procedure is, however, usual in the case of non urban tunnels, as discussed in Chapter 2.

In order to compare the construction parameters in the instrumented area with values used in practice, Table 4.12 is presented. Since the Mount Shaughnessy Tunnel is non urban, but the section in question underlies a sensitive highway, values for both the urban and non-urban case are included. It is observed that the values actually used in the Mount Shaughnessy Tunnel are close to those used in non-urban tunnels. However, the larger surface settlements in non-urban areas, which normally result from these more relaxed procedures, were not verified. It is believed that this was due to the ground in the Mount Shaughnessy Tunnel case having more favourable properties than those of the base cases surveyed. Nevertheless, it is observed that following the empirical recommendations for Class III - Non Urban (Figure 2.27, Chapter 2) would result in construction parameters comparable to those actually used, which suggests that the recommendations are reasonable.

4.5.3 Initial Support

The initial support adopted in the Mount Shaughnessy Tunnel was different from that usually used in the large cross section tunnels reported in Chapter 2. The thin layer of shotcrete employed ($\approx 5\text{cm}$) did have a stabilizing purpose and not a structural function.

In order to evaluate the adequacy of the empirical recommendations, design quantities for a hypothetical shotcrete lining were obtained through a two-dimensional, plane strain analysis of the Mount Shaughnessy Tunnel case history. The ground was discretized using 8 node isoparametric elements and the lining was represented by 3 node isoparametric beam elements. Both materials were assumed to behave linearly elastically.

The program ADINA (Automatic Dynamic Incremental Nonlinear Analysis) was used, which is described in detail by Bathe (1982) and ADINA Engineering (1984). The procedures for simulating the excavation and support of shallow tunnels using this program were described extensively by Heinz (1984). The lining elements (thickness $t=30\text{cm}$) were installed immediately upon excavation and no stress relief was allowed, an approach considered conservative and which is comparable to currently available closed form solutions (e.g., Ranken, 1978; Hartmann, 1985). Regarding the linear elastic behaviour, it has been shown that reasonable results may be obtained, provided convenient moduli are adopted for the soil and for the lining (e.g., Negro, 1988).

The finite element mesh and all relevant properties are summarized in Figure 4.37. It should be noted that the soil modulus shown ($E=300\text{MPa}$) was for the tunnel axis and was varied with the depth according to Equation 4.2 with an exponent $n=0.5$. This 300MPa value represents about 50% of the maximum initial tangent modulus given by the back analyses in

Section 4.4.2, which seems to be a conservative approach in the present case. The 50% value is also suggested as a rule of thumb for use in elastic analyses by Negro (1988). The shotcrete modulus adopted ($E=15\text{GPa}$) has been proposed by Duddeck and his co-workers as an acceptable design value, which would include the effects of gradual hardening, creep and shrinkage. The K_0 value chosen (0.8) is believed to represent an upper limit for the soil deposit and is more critical for this type of tunnel cross section than lower values of K_0 (Diniz, 1978).

Figure 4.38 summarizes the results of this analysis. A simple analysis of the stresses at five selected sections showed that only the minimum reinforcement is required. This minimum reinforcement could be taken as two Q188 (1.88cm²/m) welded wire meshes, as discussed in Section 2.5.4, or 0.15% on each side, as in the Butterberg case, Figure 2.27. This will likely depend on factors such as existence of local codes, etc. Adopting the latter value for a preliminary estimate (e.g., for cost estimates) of the reinforcement may be an acceptable option.

4.6 Summary

In this chapter, several aspects related to the geotechnical behaviour of the Mount Shaughnessy Tunnel were examined. The points considered most relevant are discussed in the following sections.

4.6.1 Geological and Geotechnical Characterization

The tunnel was excavated in a bouldery soil which allowed very limited sampling and testing by conventional means. Interpreting the site with the aid of existing geological models allowed the establishment of correlations with similar deposits and therefore an estimate of the properties. Ancillary empirical methods were also examined and adapted to the present case. A summary of the soil properties estimated is given in Table 4.9. This geological/geotechnical study is believed to be of value for future projects in similar mountainous environments.

4.6.2 Instrumentation

Results of the field instrumentation program at the West Portal were evaluated in terms of the geotechnical performance of the tunnel. The loss of ground associated with different stages of the tunnel construction was very small and comparable to that of tunnels where technologies such as the NATM were used. Although several precautionary measures were taken in order to reduce ground movements due to tunnel excavation, it is believed that the good performance is largely attributable to the favourable properties of the ground.

A simple procedure using elastic analyses by the Boundary Element Method and displacement measurements was used to verify the estimates made of the soil properties. The results of this analysis confirm the hypothesis made

regarding the favourable conditions encountered during excavation.

4.6.3 Design Considerations

Some of the empirical recommendations developed in Chapter 2 were applied to the case of the Mount Shaughnessy Tunnel. The actual excavation procedure does not show significant departures from those which have been employed in similar non-urban large cross-section tunnels. The surface settlements were, however, smaller than those expected for similar tunnels in urban areas which, given the somewhat relaxed excavation procedures employed, must be attributed to good ground quality.

Results of simple finite element elastic analyses suggest that an initial shotcrete support such as that which has been used in similar large cross section tunnels could be employed in the present case. However, the decision concerning this alternative will probably depend on other factors of non geotechnical nature.

Table 4.1 Subdivisions of late Quaternary events and deposits in British Columbia Southern Interior (based on Fulton, 1984)

Geologic-climate Units	Stratigraphic Unit	Recognized Soil Deposits	Remarks
Postglacial	Postglacial Sediments	Fluvial sediments, eolian & lacustrine deposits. Colluvial talus, slopewash and landslide material	Source: Clague (1981)
Fraser Glaciation	Kamloops Lake Drift	Till, glaciofluvial and glaciolacustrine sediments (evidence for three stades and two interstades).	Approx. time interval of glaciation according to Fulton & Smith (1978).
Olympia Nonglacial Interval	Bessete Sediments	Predominantly sand and gravel; locally fine grained sediments and peat.	
Okanagan Centre Glaciation	Okanagan Centre Drift	Till; glaciofluvial sands and gravels and lacustrine sediments.	
Westwold Interglaciation	Westwold Sediments	Fluvial sands and gravels including minor lacustrine material.	

Years B.P. x 10³
0 10 20 30 40

Table 4.2 Some typical properties of soils in glaciated upland valleys

	Boulton et al. (1976-1981)*	Eyles (1983)	Fookes et al. (1975a,b)	Whalley (1975)	Pellegrino (1965) Croce et al. (1963)
Geological charact.	Supraglacial diamictons	Supraglacial diamictons	Kame Terrace	Lateral Moraine	Fan Deposits
Grain size:					
% >2mm	-	high	60	20-80 (**)	70-85
% sand (0.06-2mm)	-	-	24	20-50	-
% silt+clay (<0.06)	<15	<15	16	<25	<15
Bulk density (kN/m ³)	"low"	11.8-21.6	17.7-20.6	21.7-24.2	17.7-19.6
Void ratio	-	0.25-1.00	-	-	0.15-0.54
Nat. moist. cont. (%)	-	6.0-14.0	13.5	8.0-12.0	-
Atterberg Limits:					
wl (%)	-	10.0-22.0	22	23	-
PI (%)	-	0.0-8.0	7	0	-
Drained strength:					
c' (kPa)	-	12 (?)	0	0-10	10.0-40.0
φ' (°)	"high"	-	36.6	>40 (***)	36.9
Deformability:					
E (MPa)	-	"variable"	-	-	370.0-1700.0
OCR	NC	NC	-	-	30-160 (****)

Notes:
 (*) Includes: Boulton and Paul (1976); Boulton and Eyles (1979) and Boulton and Deynoux (1981)
 (**) On minus 3" samples
 (***) On compacted samples
 (****) Unload-reload moduli are probably higher

Table 4.3 Properties of natural soils from major dam projects in British Columbia

Characterization of deposit	Portage Mountain Dam (1)		Duncan Dam		Mica Dam	
	Morgan and Harris (1967)	Gordon and Duguid (1970)	Webster (1970)			
Soil type	"Moraine of glaciofluvial origin"					
	Silty sand Grav. sand Sandy grav. Sandy grav. to gravel					
USC	SM	GW	GW-GP	GP		
Field dry dens. (kN/m ³)	20.1	20.9	21.4	17.3-17.9	21.1 (4)	21.1 (4)
Field moist. cont. (%)	6.9	6.1	4.0	1.6-2.0	10.8	9.0-12.0
Field bulk dens. (kN/m ³)	21.5	22.2	22.3	17.6-18.2	23.4	23.0-23.6
Field void ratio (C=2.7)	0.32	0.27	0.24	0.48-0.53	0.26	0.16-0.19 (5)
Max. lab. dry dens. (kN/m ³)	20.4 (2)	21.7 (2)	21.5-22.0	18.1	20.1	21.6-22.2
Estimated permeab. (cm/s)	0.00002	0.0001	E-03/2E-05	10		
Drained strength:						
c' (kPa)	0 (3)	0 (3)	0 (3)	0 (3)		
φ' (°)	37.0	38.0	38.0	36.0		
Atterberg Limits:						
wl (%)	-	-	-	-	17.6	-
PI (%)	-	-	-	-	4.3	-

- Notes:
- (1) Renamed W.C. Bennet Dam
 - (2) ASTM D698 - 6" mould
 - (3) Apparent cohesion neglected
 - (4) Probably estimated
 - (5) G=2.78 (Skermmer/Hillis, 1970)

Table 4.4. Field dry densities from Thurber Consultants Ltd.
(1983b)

NUCLEAR DENSOMETER			STANDARD PROCTOR (1)	
Test Pit #	No. Tests	Av. Bulk Dens. (kN/m ³)	Av. Bulk Dens. (kN/m ³)	
252	7	20.34	22.15	
253	8	19.29	-	
254	7	19.61	21.68	
255	9	21.52	22.78	
256	8	21.52	22.15	
257	8	19.65	21.99	
258	7	19.24	-	
259	8	21.02	22.31	
260	8	21.33	-	
261	7	19.86	-	
262	7	19.15	21.84	
263	8	21.37	21.68	
264	8	20.82	21.68	
265	8	17.25	20.11	
Average:		20.14	21.84	
Stand. Dev		1.22	0.7	

Notes:

(1) Correction for grain size applied

Table 4.5 Some procedures for empirical determination of drained friction angle of coarse grained soils

Reference	Estimated ϕ' (°)	Brief description of procedure/assumptions
Kjaernsli (1968)	44.3-47.5	W. porosity $n=0.24$ estimated fr. γ and m.c. by Thurber (1983b), enter Kjaernli's Fig. 9 (values fluvial gravels; Norwegian experience with rockfills - n vs. ϕ chart)
Leps (1970)	38.0-48.0	W. $\gamma=22.1 \text{ kN/m}^3$, calc. σ_v' at tunnel axis ($\approx 18.5 \text{ m}$) and enter Leps σ vs. ϕ chart for rockfills)
NAVFAC (1971)	33.7-38.7	W. void ratio=0.32, enter NAVFAC's Fig. 3.7 (density vs. frict. angle), assuming materials are GP-GW. Values are thought to be conservative due to the nature of the manual.
Schmertmann (1978)	43	W. void ratio=0.32, compute relative density $R_e=0.68$ using $e_{\min}=0.26$ and $e_{\max}=0.45$ suggested by Wilson and Marsal (1979) for well graded rockfills. Enter Schmertmann's R_e vs. ϕ chart, derived from earlier studies by Burmister (1948).

Table 4.6 Deformability parameters from multistage triaxial tests by Thurber Consultants Ltd. (1983b).

Test #	σ_3 (kPa)	E (MPa) ¹	σ_3/p_a	E/ p_a
R1	306.8	184.687	3.028	1822.7
	460.6	268.139	4.546	2646.3
R2	262.0	125.966	2.586	1243.2
R3	289.6	172.375	2.858	1701.2
	510.2	275.800	5.035	2721.9
R4	386.1	206.855	3.810	2041.5
	551.6	413.700	5.440	4082.9
R5	265.5	120.662	2.620	1190.8
	427.5	246.250	4.219	2430.3

Notes:

- (1) E values correspond to unload-reload in 2nd and 3rd cycles
- (2) Carried out on "Delta" material, believed to represent West Portal soils

Table 4.7 Summary of data collected for void ratio versus modulus number correlation

Type of Deposit	Reference	Void-ratio	KE	Remarks
Moraine	Janbu (1963)	0.28	1583	KE derived from KM assuming
Moraine	Janbu (1963)	0.42	833	Poisson's ratio (PR) = 0.25
Moraine	Janbu (1963)	0.52	533	
Fluvioglacial	Croce et al. (1963)	0.1	75	E values from text (p. 336)
Fan Outwash	Croce et al. (1963)	0.35		(*)
Fan Outwash	Croce et al. (1963)	0.35		(*)
Fan Outwash	Pellegrino (1965)	0.14	1549	(*)
Fan Outwash	Pellegrino (1965)	0.39	1959	(*)
Moraine	Pellegrino (1965)	0.54	846	(*)
Bouldery Alluvium	Bhide (1981)	0.35	1325	KE from KM w. PR=0.25 - n=0 (*)
Bouldery Alluvium	Prakash/Ranjan (1981)	0.61	763	e from Prakash (1981) - n=0.5 (**)
Rock Debris	Yoshimoto/Doi (1981)	0.32	1155	KE from KM (*)
Glacial Gravels	Duddeck et al. (1981)	0.35	1461	KE from unl./rel. KM fr. plate load test
Fluvial Gravel	Ortigosa et al. (1981)	0.28	2462	KE from KM fr. plate load test

Notes:

- (*) Correction factor for unload-reload applied according to Duncan et al. (1980:13) with e_{max}/e_{min} from Wilson & Marsal (1979)
- (**) KE from subgrade reaction using Bowles (1982:Eqn. 9-6a)

Table 4.8 Summary of data from seismic velocity lines at West Portal (data from Piteau and associates, 1982: Figures 7, 8 and 9)

Line	V_L (m/s)			Remarks
	Top Layer ¹	Interm. Layer ²	Bottom Layer ³	
7	716.3	1691.6 2276.9	3810.0 4946.9	-
11	784.9	1200.9	3011.4	Distegarded ⁴
12	304.8	1603.2	4328.2	-
13	234.7	1950.7	4077.3	-

Notes:

- (1) Top Layer = 5 m
- (2) Material through which tunnel was excavated
- (3) Bedrock
- (4) Considered innacurate due to vibrations of waterfall (Piteau & Ass., 1982:12)

\bar{V}_L = Average for interm. layer (except Line 11) = 1880.6 m/s

$$E_{dyn} = V_L^2 \rho \frac{(1 + \nu)(1 - 2\nu)}{(1 - \nu)}$$

$$\rho = 2242.6 \text{ kg/m}^3$$

$$E_{dyn} = 7672 \text{ MPa (for } \nu = 0.12 \text{ suggested by Hardin, 1978)}$$

$$E_{static} = 384 \text{ to } 1151 \text{ MPa (for correction factors } 0.05 - 0.15 - \text{ see text)}$$

Table 4.9 Comparison between estimated and measured soil properties (values shown are average for Units 1 and 2 in Figure 4.3)

Soil Property	From Correlations with Similar Deposits		From Field and Laboratory Tests (1)	
	Range	Remarks	Values	Remarks
Unified Soil Classification	GM-GP-GW		GM-GW	
Grain Size: % $\phi > 2$ mm % sand % silt ⁽³⁾ + clay	20-80 20-50 <15%	Mainly analyses on minus 3" samples	40 45 15	Average from surface exposures; tests on minus 3" samples. Silt-clay content at West Portal is lower.
Atterberg Limits: LL (%) IP (%)	10-23 0-8		19.9 3.5	Average from surface exposures.
Natural Moisture Content (%)	<15		10.1	Average from surface exposures/test pits.
Bulk Density (kN/m ³)	17.5-23.5		22.1	Derived from nuclear densometer tests in shallow test pits.
Void Ratio	0.20-0.60		0.32	
Deformability E (MPa)	97-441	Estimated at tunnel axis depth	61 380-1150	Estimated from triaxial tests (2) Estimated from seismic tests (3).
Drained Strength c' ϕ' (°)	0-40 36-(>40)		0 40°	Average from triaxial tests (2,4)

- Notes: (1) Thurber Consultants (1983) and Piteau and Associates (1982).
 (2) Multi-stage CU tests with pore pressure measurements; 8" long/4" diameter samples of $<3/4$ " material compacted to approximately 100% of Standard Proctor maximum density.
 (3) Correction applied for strain level.
 (4) Correction applied for max. grain size.

Table 4.10 Schedule of readings for ground instruments

Date	Face Station	Instruments	Remarks
29 Apr 85		SI	Before excavation of slope
07 May 85		SI	Excavation at elevation 3190
28 May 85		SI	Excavation at elevation 3157
04 Jun 85		SI	Excavation at elevation 3147
05 Jul 85	752+62	SI, SP, ME	Excavation of tunnel started 14 Jun
09 Jul 85	752+47	SI, SP, ME	
10 Jul 85	752+38	SP, ME	
11 Jul 85	752+28	SI, SP, ME	
12 Jul 85	752+18	SI, SP, ME	
13 Jul 85	752+11	SP, ME	
14 Jul 85	751+96	SI, SP, ME	
15 Jul 85	751+84	SP, ME	
16 Jul 85	751+75	SP, ME	
17 Jul 85	751+67	SI, SP, ME	
18 Jul 85	751+58	SI, SP, ME	
19 Jul 85	751+49	SP, ME	
20 Jul 85	751+34	SI, SP, ME	
21 Jul 85	751+22	SI, SP, ME	
22 Jul 85	751+10	SI, SP, ME	
23 Jul 85	751+01	SI, SP, ME	
24 Jul 85	750+92	SP, ME	Heading crossing complete
29 Aug 85	748+11	SP, ME	
03 Oct 85	752+47.5	SP, ME	
07 Oct 85	752+26.5	SP, ME	
08 Oct 85	752+5.5	SP, ME	
09 Oct 85	751+87.5	SP, ME	
10 Oct 85	751+70.5	SP, ME	
11 Oct 85	751+52.5	SP, ME	
25 Oct 85	749+83	SI, SP, ME	Bench crossing complete
17 Apr 86	-	SI, SP, ME	After winter season

Table 4.11 Loss of ground expressed as a percentage of tunnel volume - comparison with NATM case histories (data from Heinz, 1984)

Tunnel	Soil	$\% V_g$ @ face	$\% V_g$ (total short term)
Mt. Shaughnessy	sandy		
	gravel	0.03	0.11
Frankfurt L.25/III	marl	0.28	0.74
Frankfurt L.17/V	marl	0.09	0.48
Munich L.8.1/18.2	marl	0.09	0.23
Frankfurt L.6/W.2	gravel	-	0.17
Frankfurt ABV/G	clayey		
	sand	0.06	0.16
Butterberg	gravel		
	sandy		
	silty	-	0.36

Table 4.12 Comparison between the construction parameters from empirical recommendations with those actually used at the Mount Shaughnessy tunnel

Parameter	Non Urban	Urban	Mount Shaughnessy
Ah (m ²)	19 - 26	16	= 28
L (m) ^{1,2}	10.5-16.5	2.7	>>16.5
La = s (m)	1.2	1.0	0.9

Notes:

- 1) Invert closure distance in the top heading
- 2) $D_m \approx 3$ m

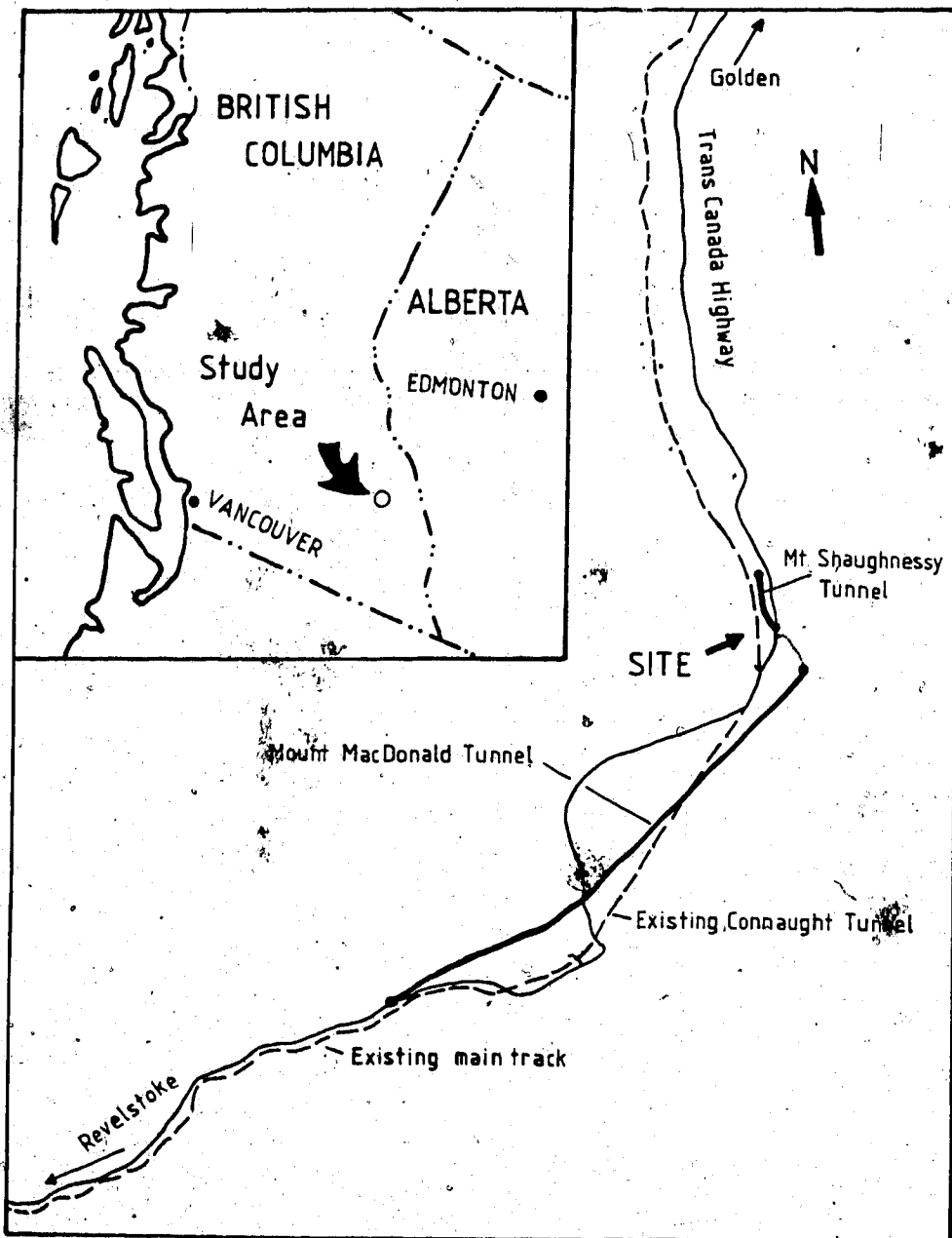
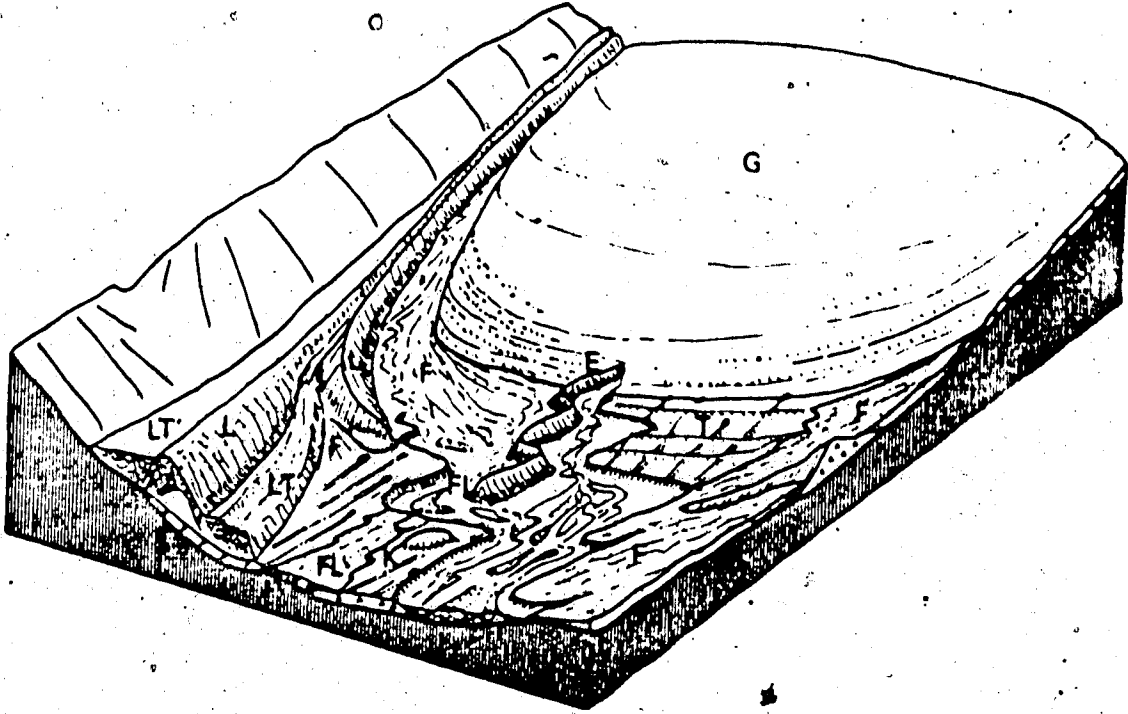


Figure 4.1 Location of Rogers Pass Project



Key:

- (G) Glacier
- (L) Lateral Ice-Cored Moraine
- (LT) Lateral Ice-Contact Terrace (Kame Terrace)
- (F) Alluvial Fan
- (E) Esker
- (K) Kame
- (T) Turbidity Flow
- (FL) Fluvioglacial Surface

Figure 4.2 Model for interpretation of upland valleys which have been subject to glaciation (modified after Boulton and Deynoux, 1981)

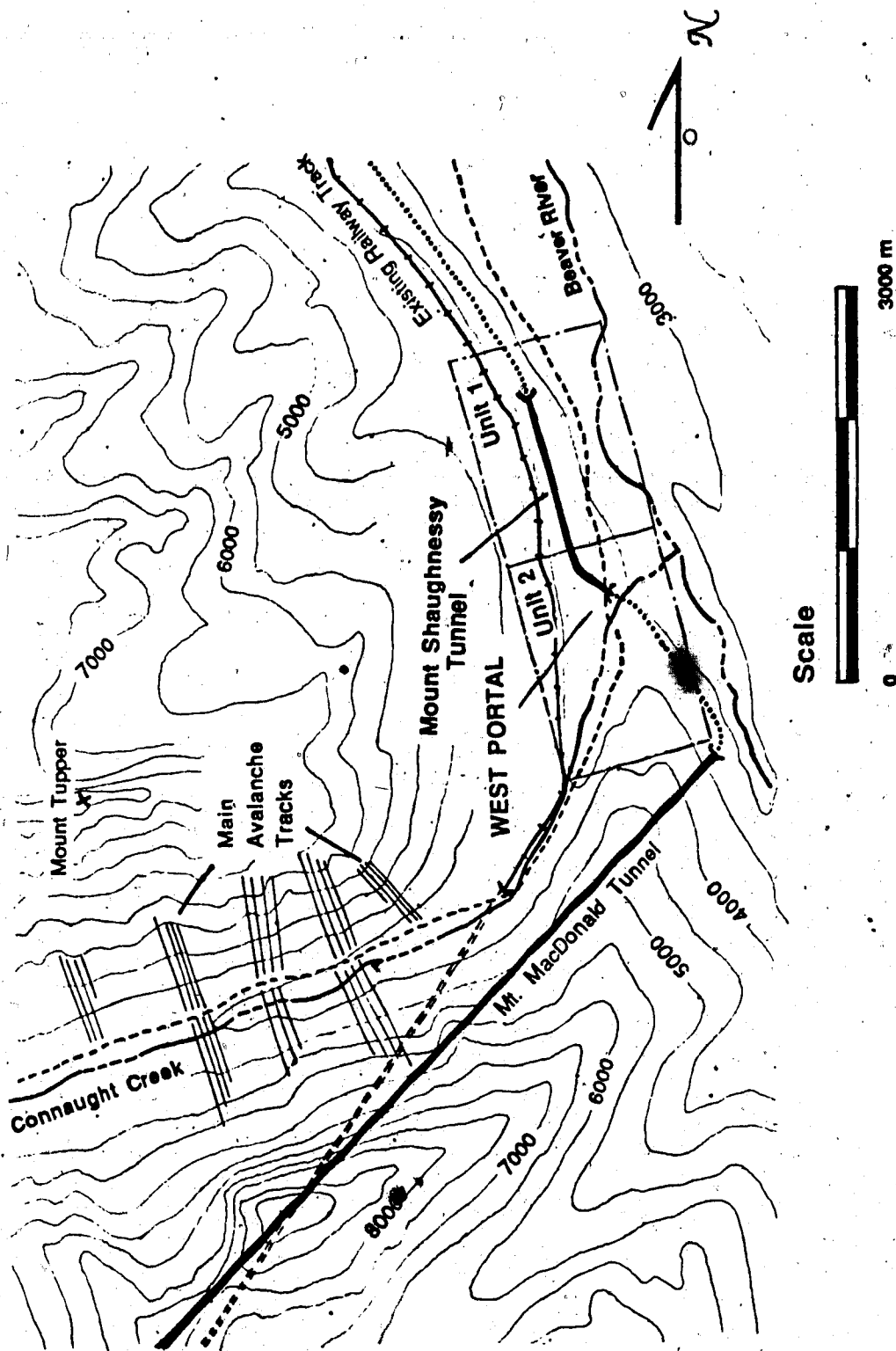


Figure 4.3 Main physiographic features of the study area (based on BC 82N/6 Map - Blaeberry Scale 1:50000 - Dept. of Energy, Mines and Resources - Surveys and Mapping Branch)

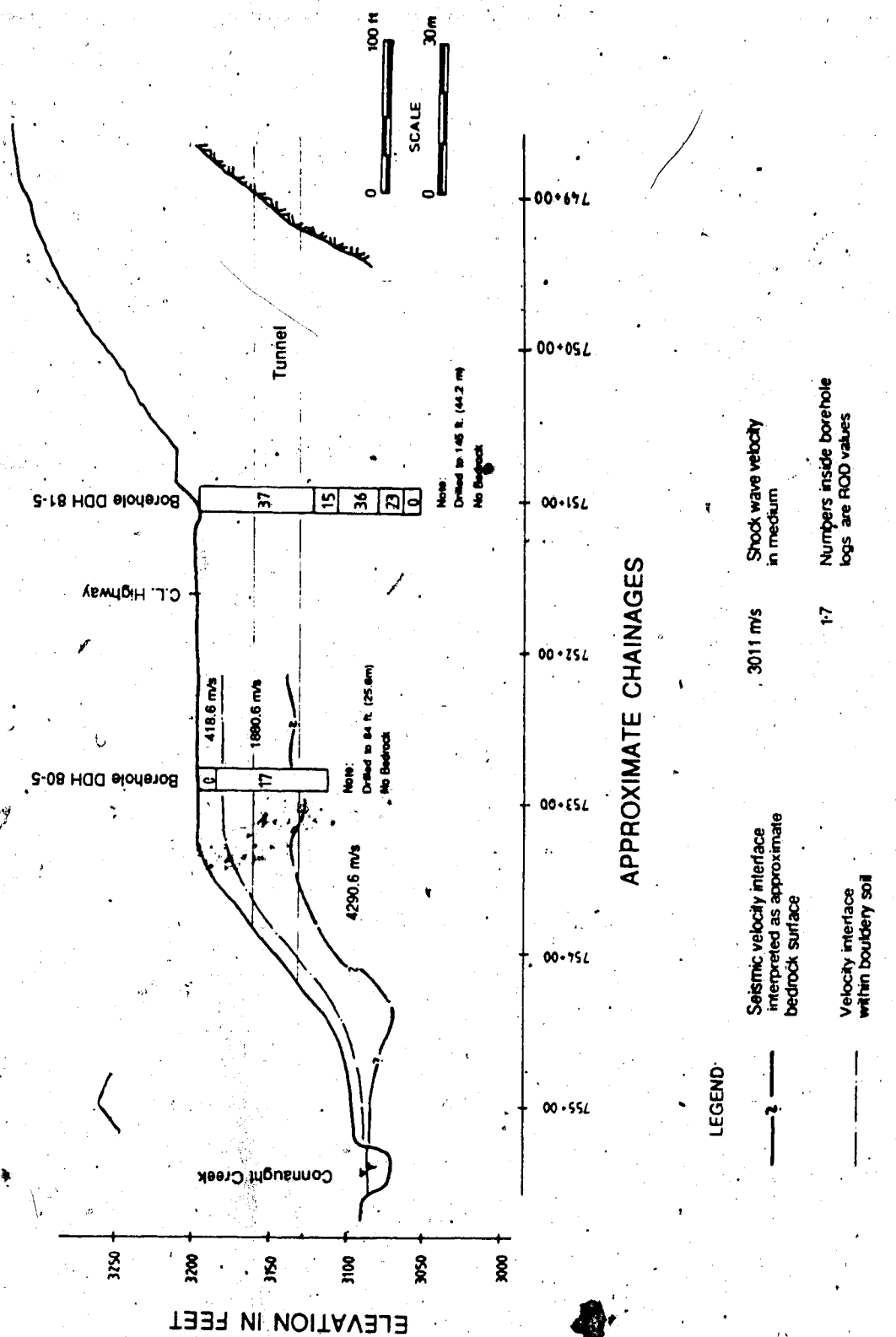


Figure 4.4 Longitudinal profile under Trans-Canada Highway (modified after Piteau and Associates, 1982)

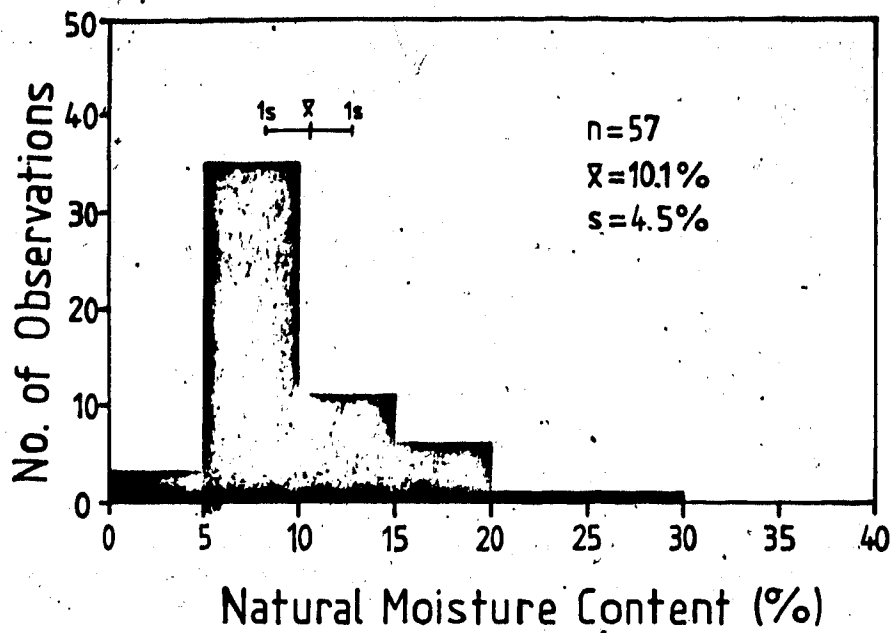


Figure 4.5 Histogram for natural moisture contents at the study area

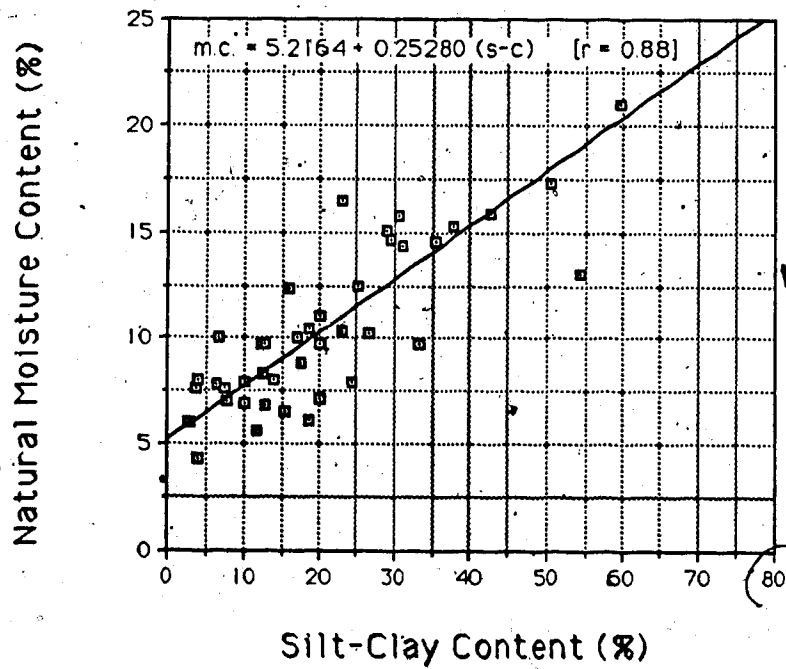


Figure 4.6 Dependency of moisture content on silt-clay content for soils at the study area

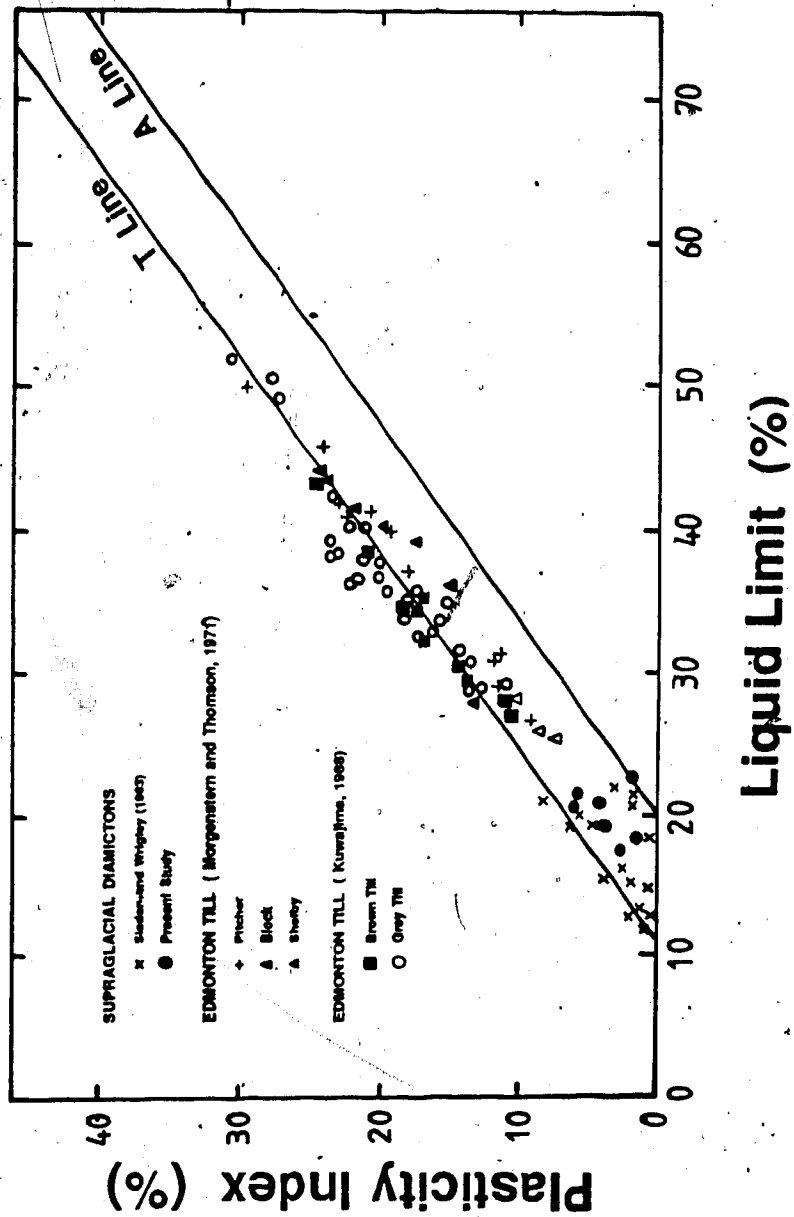


Figure 4.7 Plasticity chart showing coarse grained supraglacial diamictions, Edmonton tills and soils at the study area (adapted from Sladen and Wrigley, 1983)

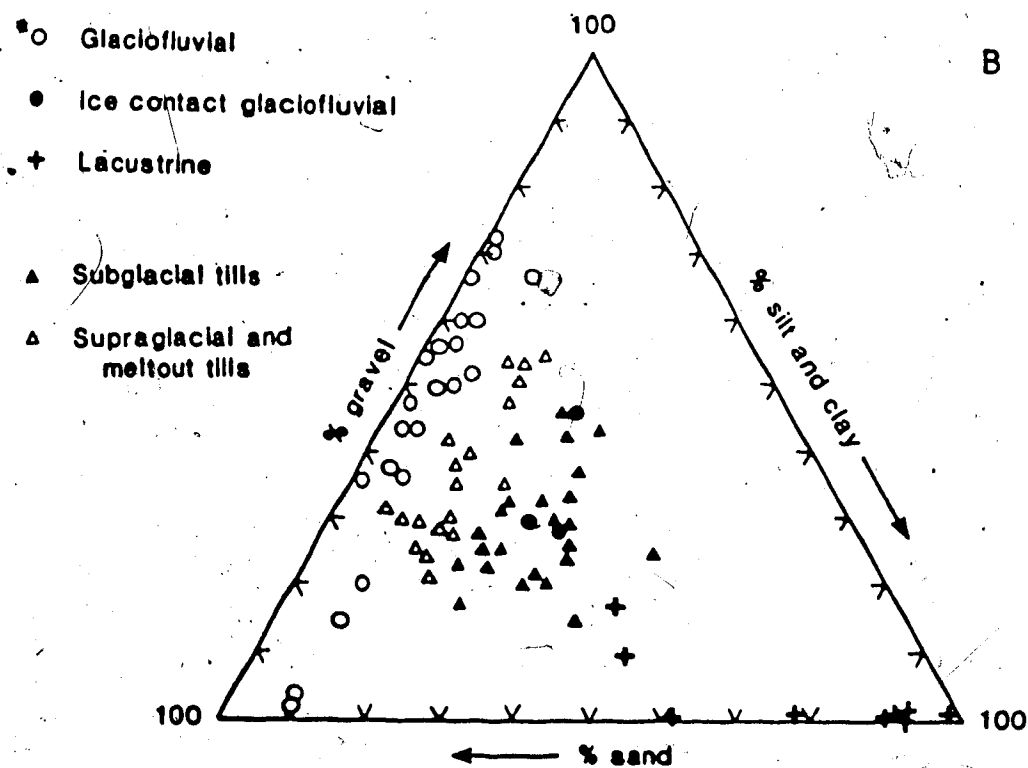
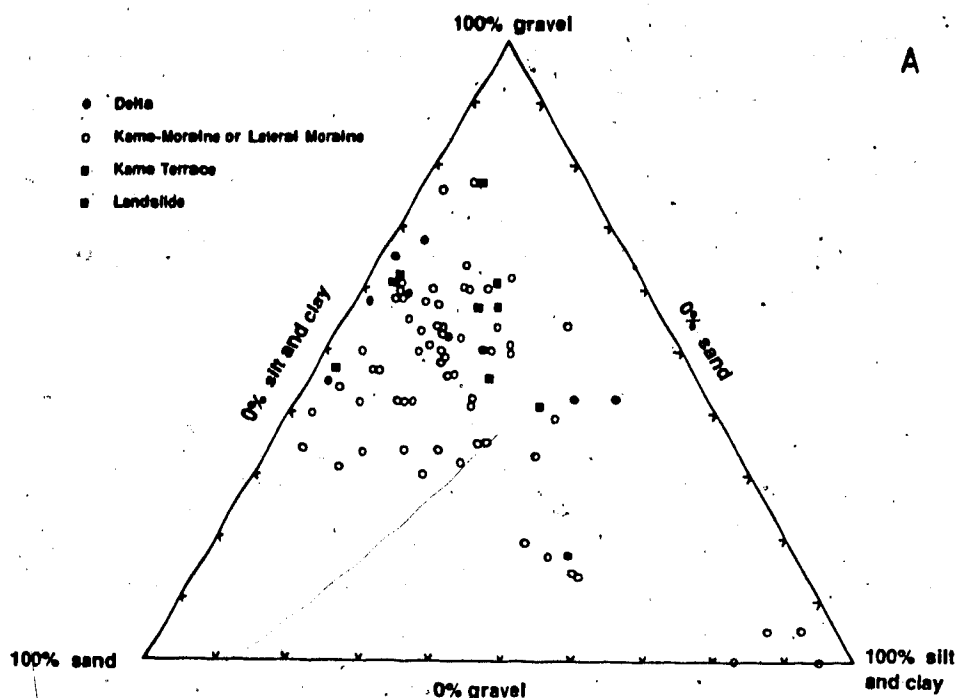


Figure 4.8 Textural diagrams showing differentiation between various types of glacial sediments (a:study area; b:modified after Derbyshire and Love, 1986)

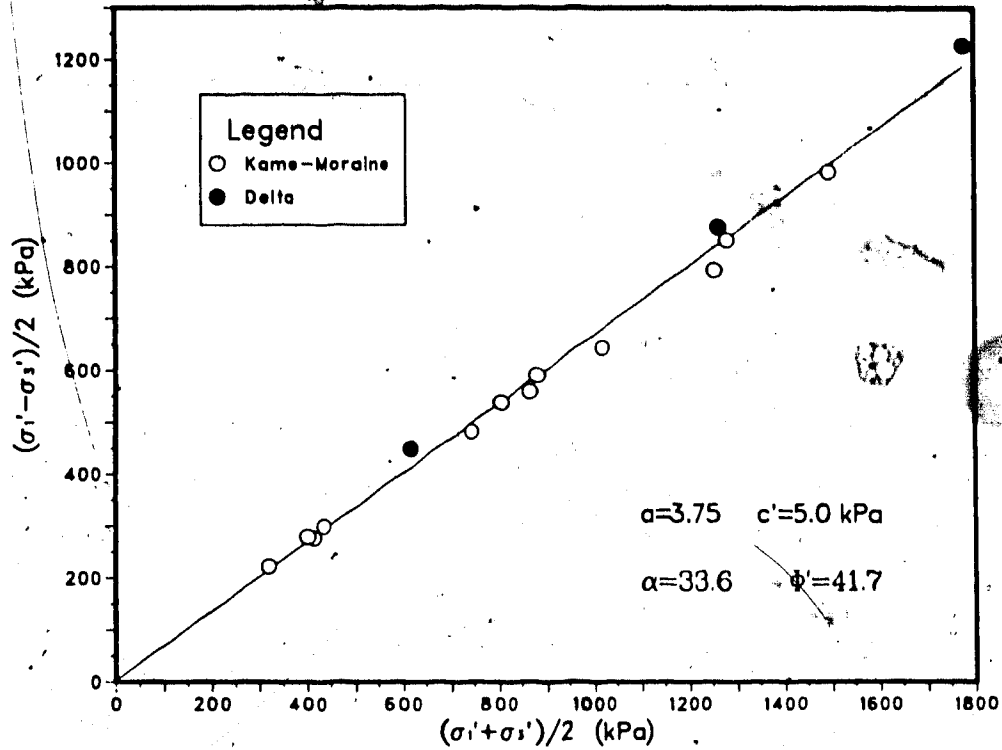


Figure 4.9 Shear strength from recompacted samples of soils at the study area (tests by Thurber Consultants Ltd., 1983b)

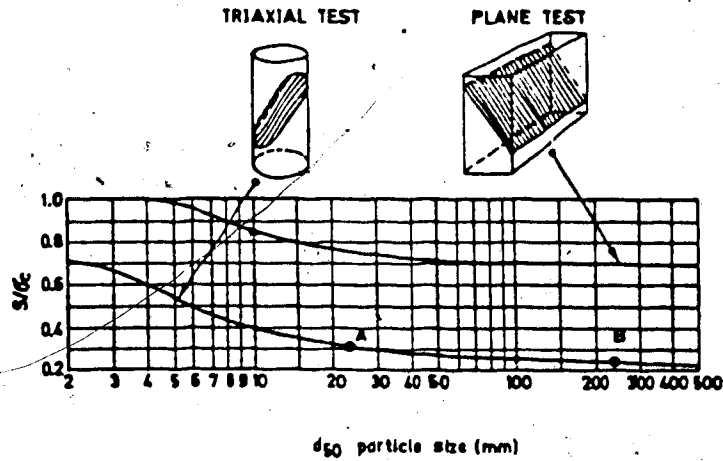
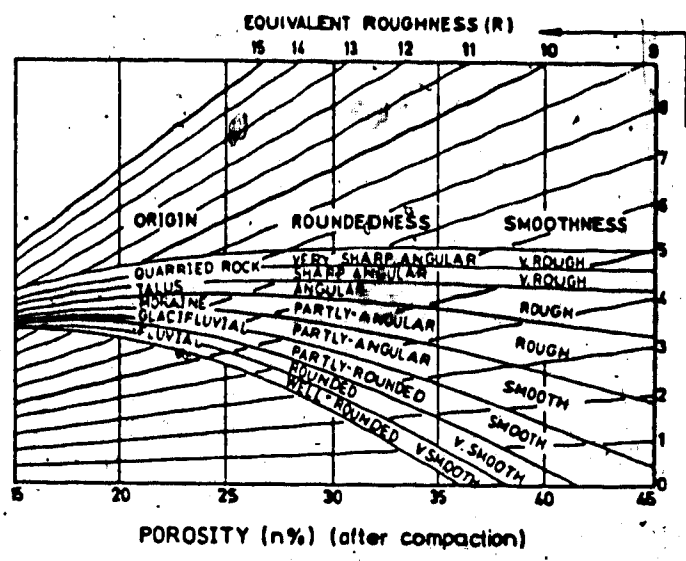


Figure 4.10 Chart for estimating Equivalent Strength of rock-fills (S) based on uniaxial compressive strength and particle size (modified after Barton and Kjaernsli, 1981)



EXAMPLES SHOWING DEGREE OF ROUNDEDNESS

QUARRIED ROCK	TALUS	MORaine	GLACIFLUVIAL MATERIAL	FLUVIAL MATERIAL

Figure 4.11 Chart for estimating Equivalent Roughness (R) of rockfills based on porosity, origin of the materials and degree of roundedness and smoothness of particles (modified after Barton and Kjaernsli, 1981)

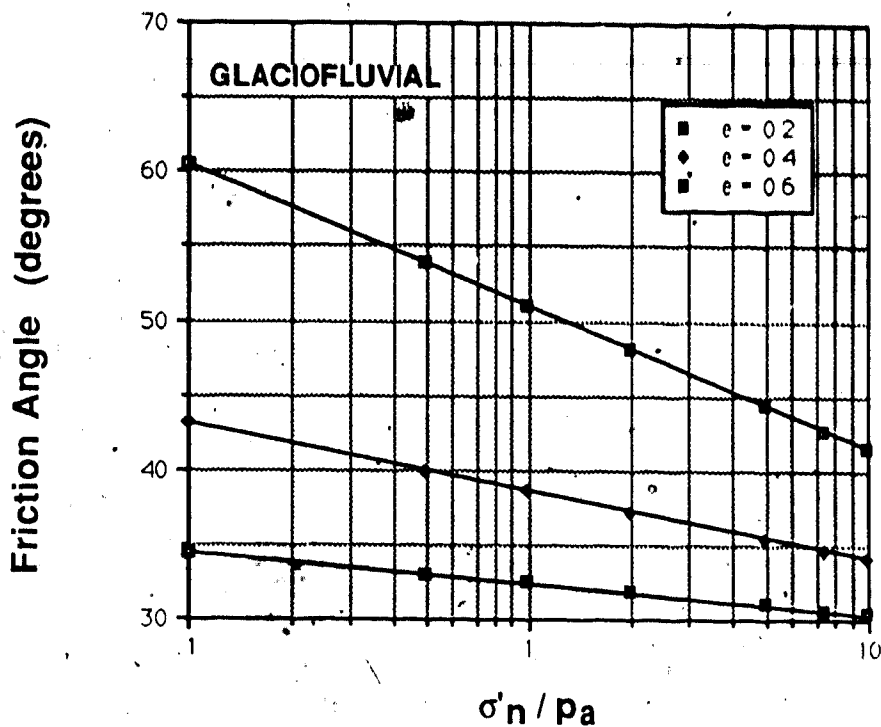


Figure 4.12 Chart for estimating friction angle of materials of glaciofluvial origin (compr. strength of rock = 80MPa)

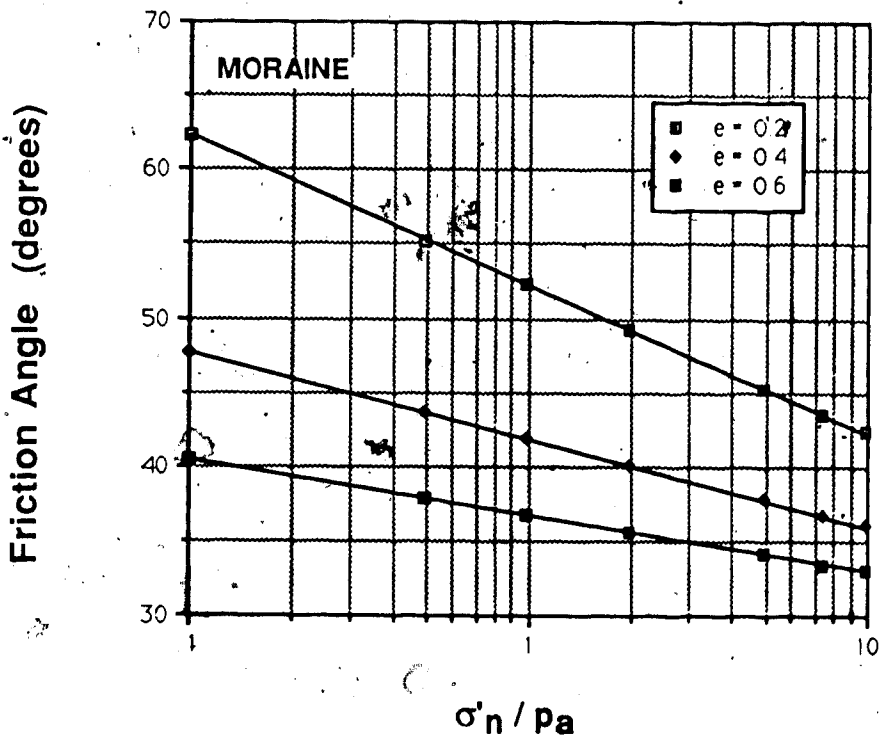


Figure 4.13 Chart for estimating friction angle of materials of morainic origin (compr. strength of rock = 80MPa).

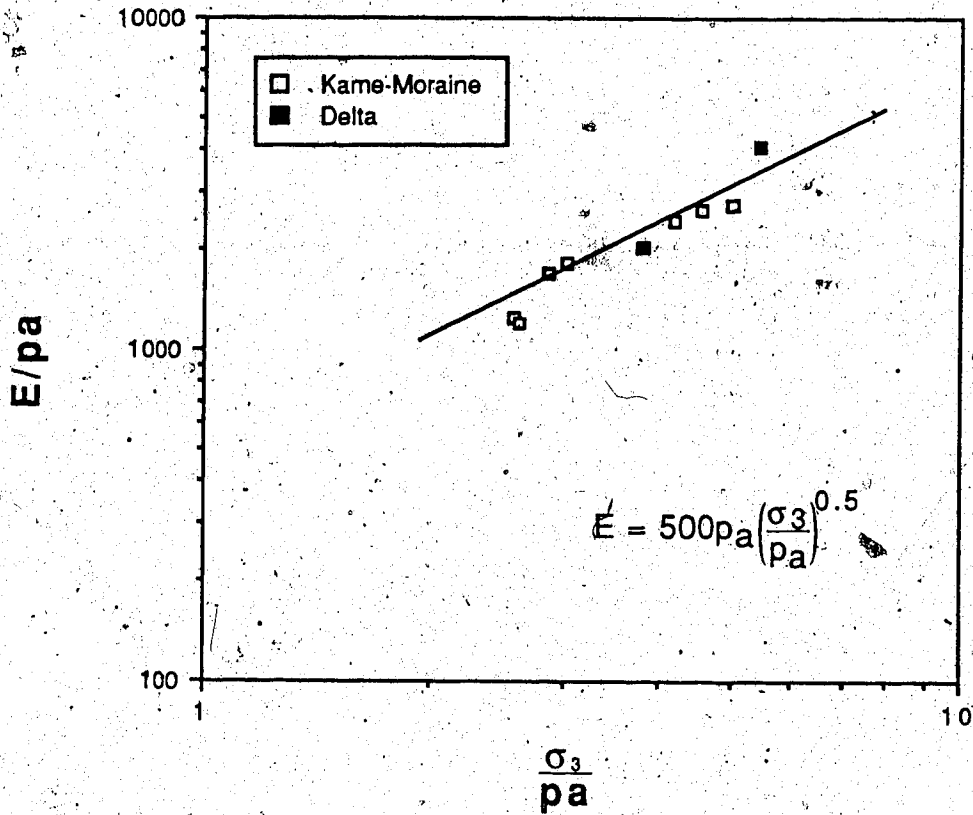


Figure 4.14 Variation of normalized modulus with normalized confining pressure (data from triaxial tests by Thurber Consultants Ltd., 1983b)

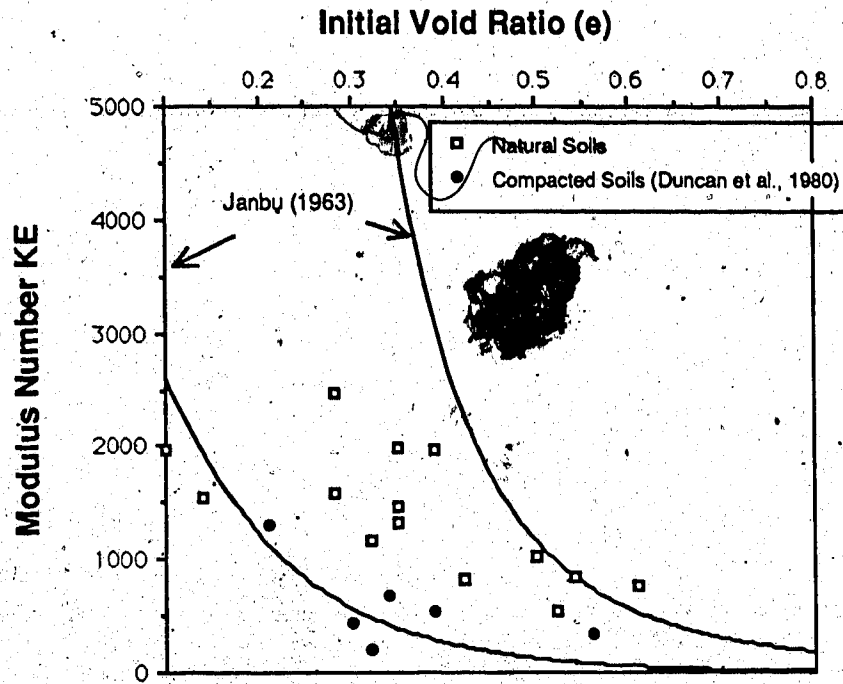


Figure 4.15 Void ratio versus modulus number for natural and compacted coarse grained soils (data from Table 4.7)

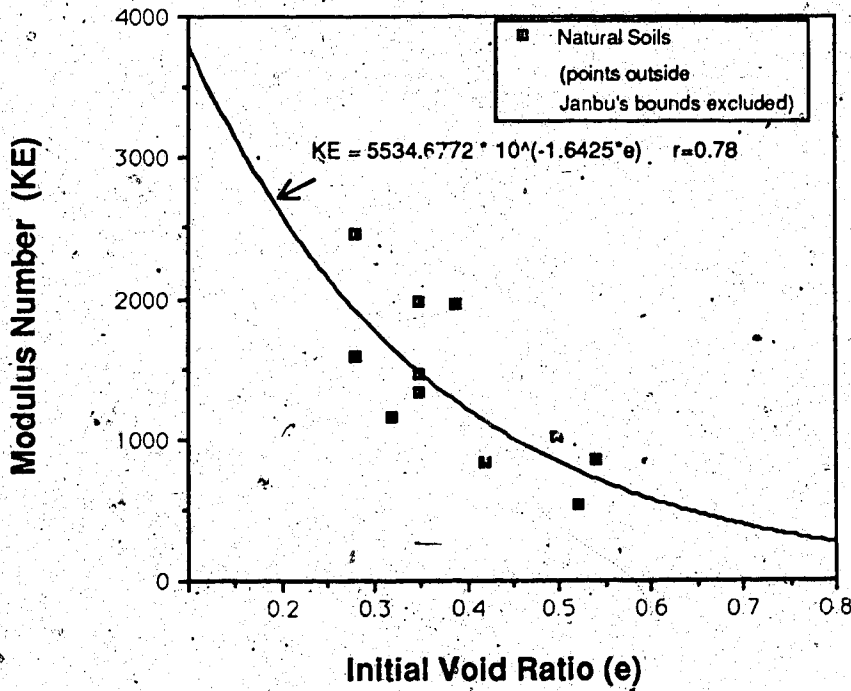
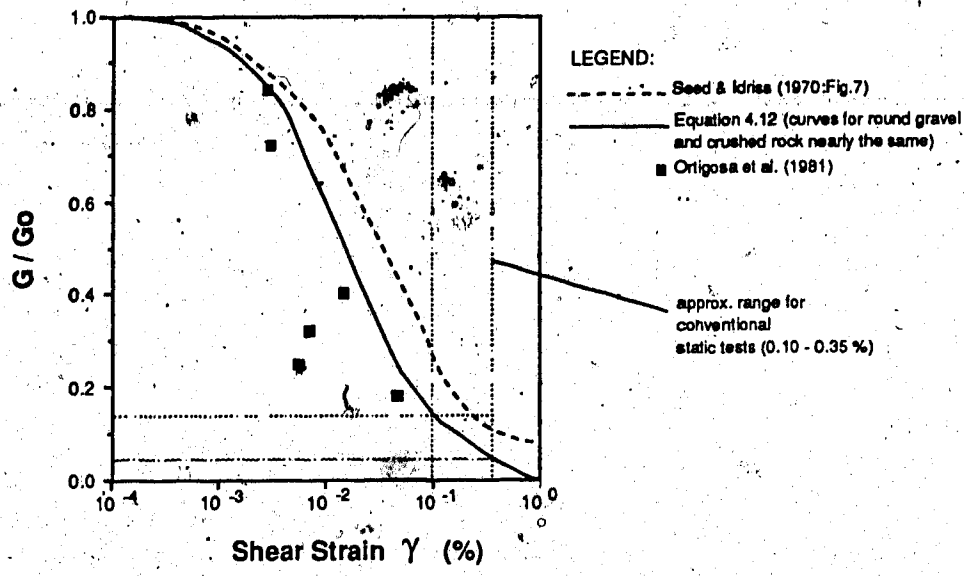


Figure 4.16 Correlation between void ratio and modulus number for natural coarse grained soils (data from Table 4.7)



$$\frac{G}{G_0} = \frac{1}{1 + \frac{\gamma}{\gamma_r}} \quad [4.12]$$

where:

$$G_0 = a \cdot \frac{(b - e)^2}{1 + e} (\text{OCR})^c \cdot (\sigma_n)^d$$

$$\gamma_r = \frac{\tau_0}{G_0} \quad \text{and:}$$

$$\tau_0 = \left(\left(\frac{1 + K_0}{2} \sigma_v \sin \phi + c \cos \phi \right)^2 - \left(\frac{1 - K_0}{2} \sigma_v \right)^2 \right)^{0.5}$$

a, b, c and d are empirical constants (Kokusho/Esashi, 1981)

ROUND GRAVEL: a=8400, b=2.17, c=0 and d=0.60

CRUSHED ROCK: a=13000, b=2.17, c=0 and d=0.55 (e=void ratio)

(moduli are in kPa)

Figure 4.17 Illustration of procedure for correcting the dynamic moduli to static values

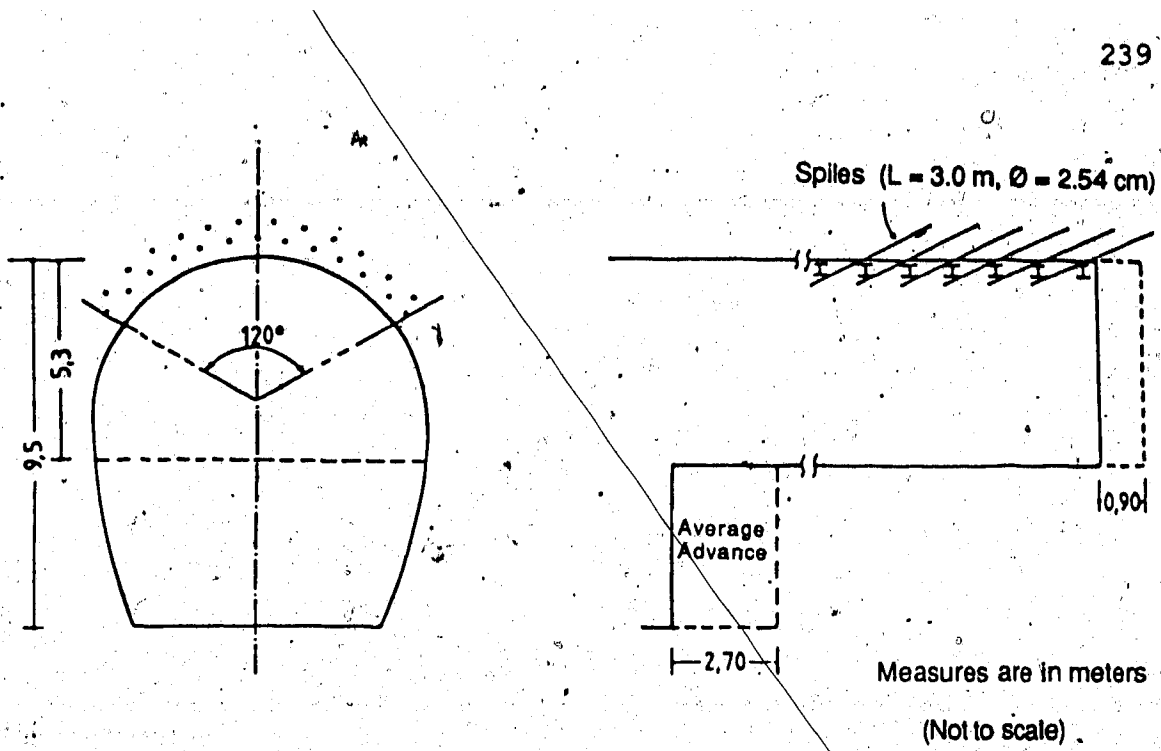


Figure 4.18 Typical excavation sequence

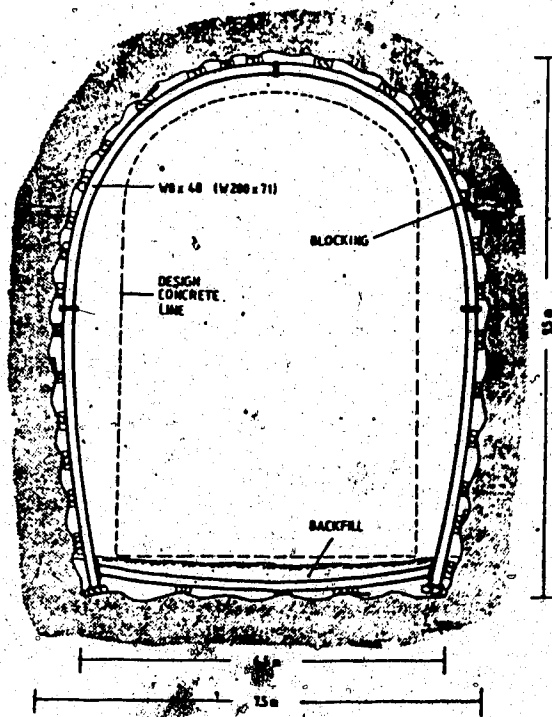
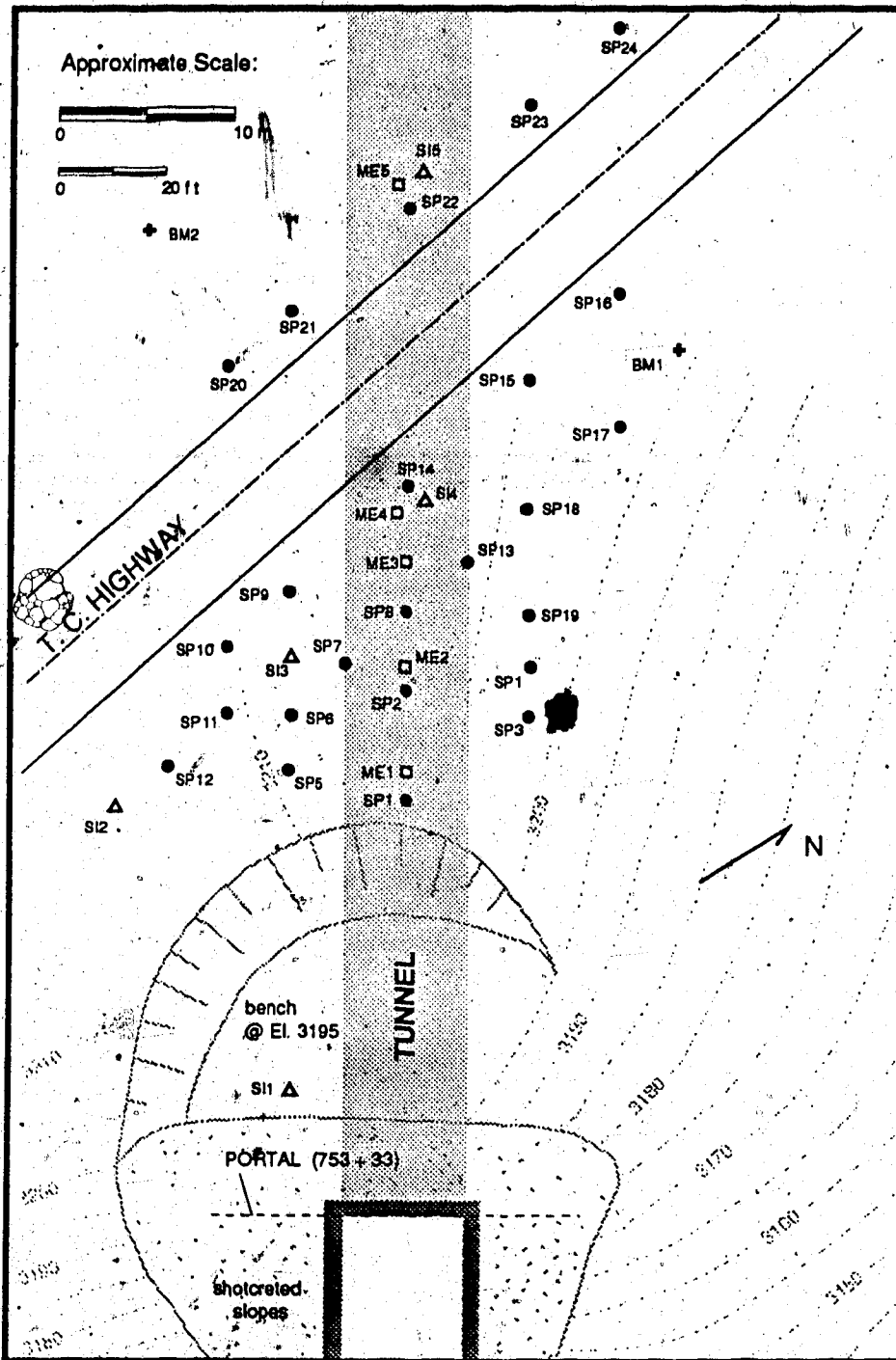


Figure 4.19 Tunnel cross section with lining detail



LEGEND:

- + Bench Mark
- Settlement Point
- Multipoint Extensometer
- △ Slope Indicator

Note: Location of settlement points is approximate (see App. B for exact locations)

Figure 4.20 Location of all instruments in plan

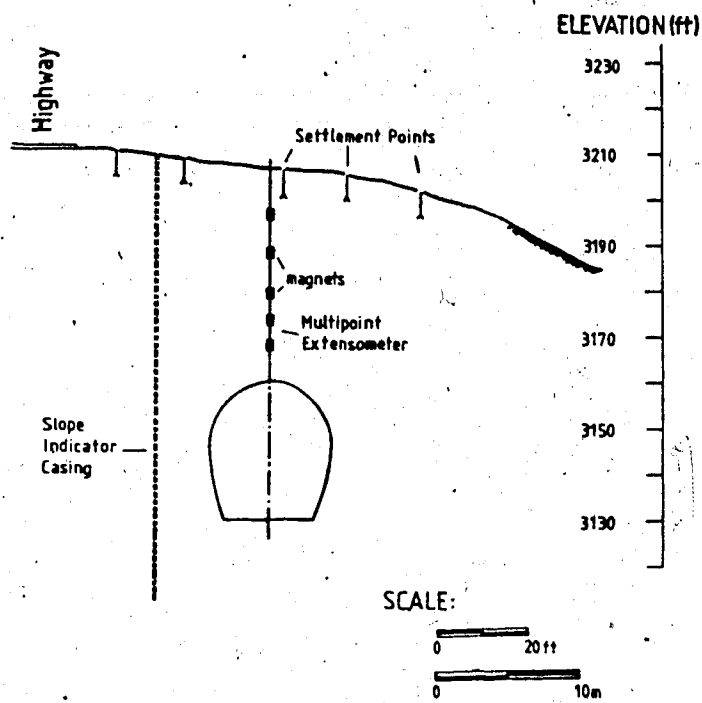


Figure 4.21 Typical instrumented section

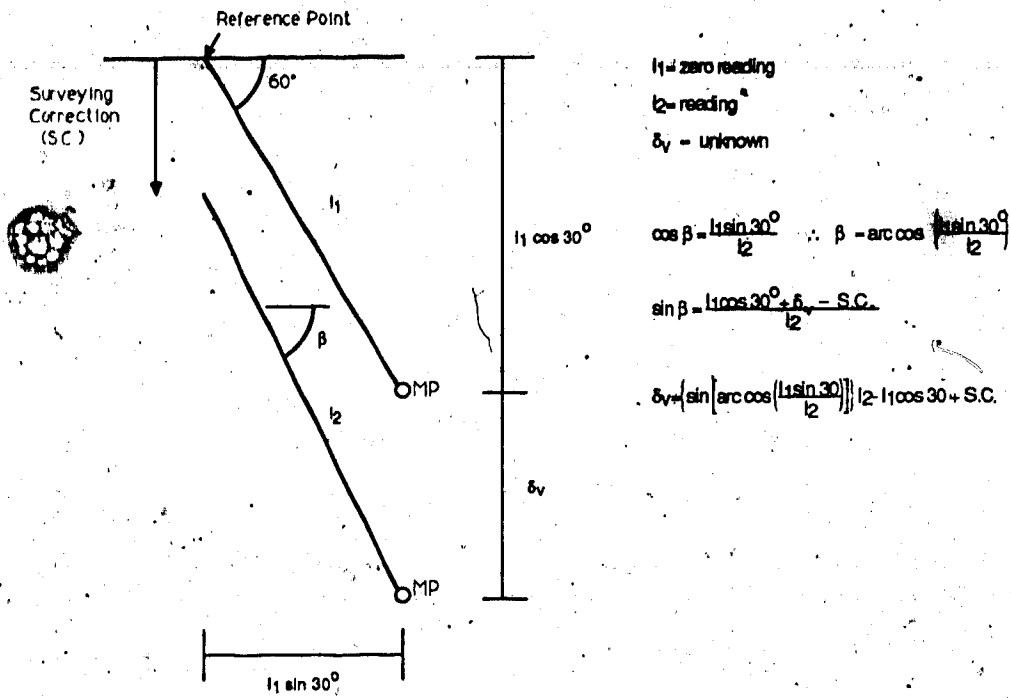


Figure 4.22 Calculation procedure for inclined extensometers

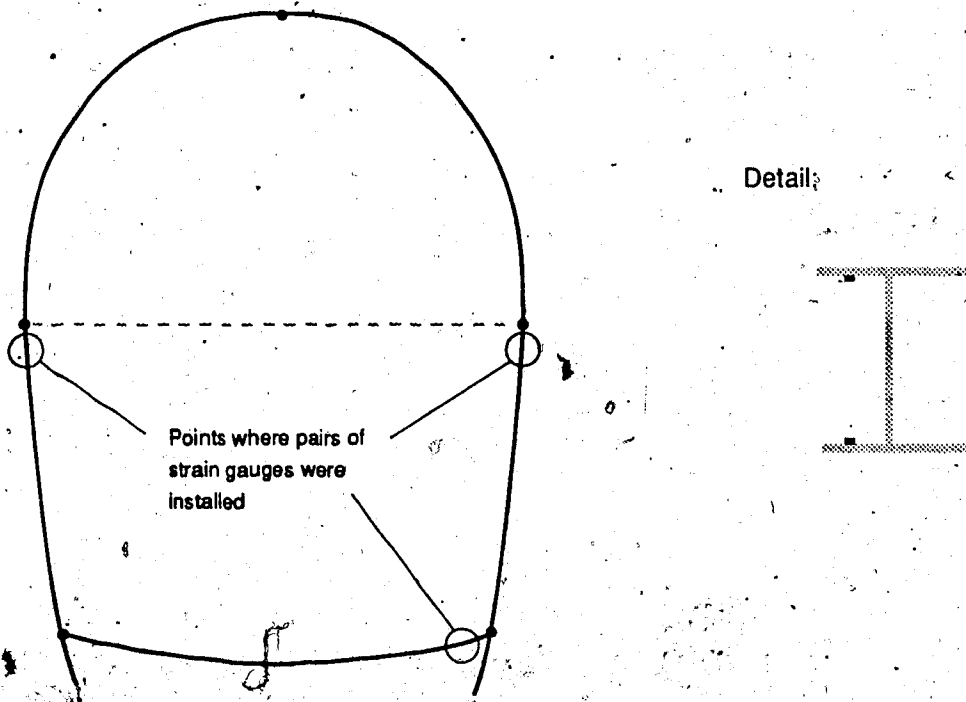


Figure 4.23 Illustration of placement of strain gauge

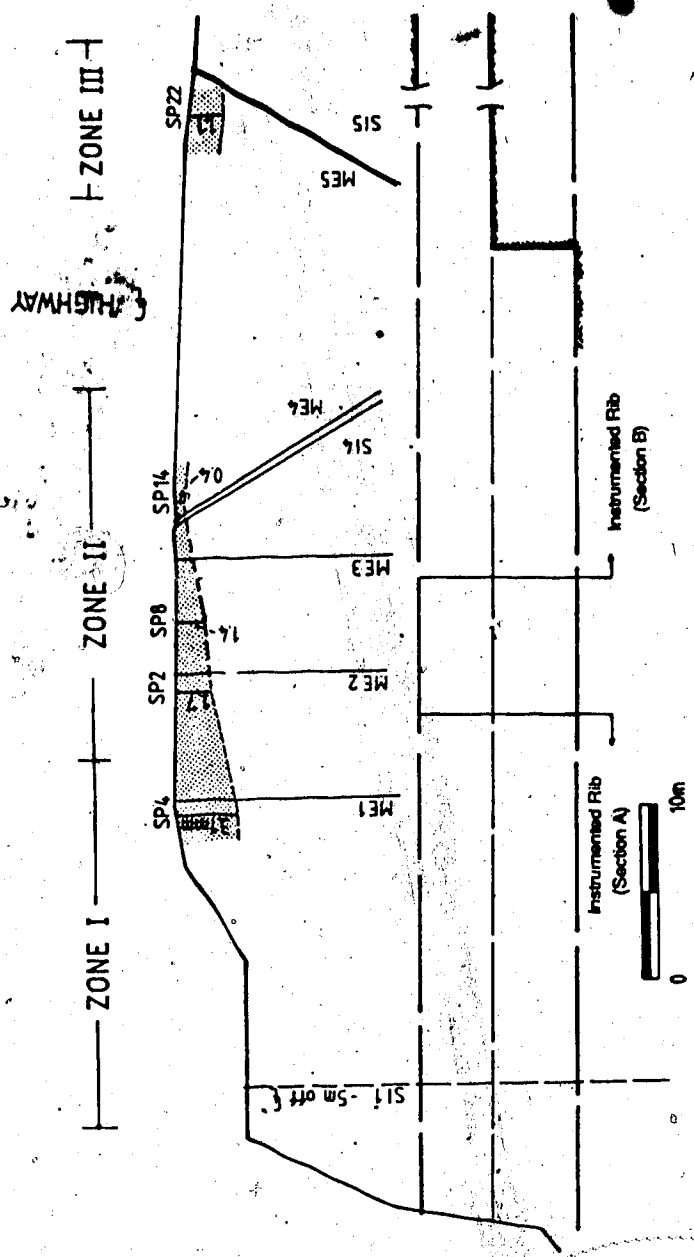
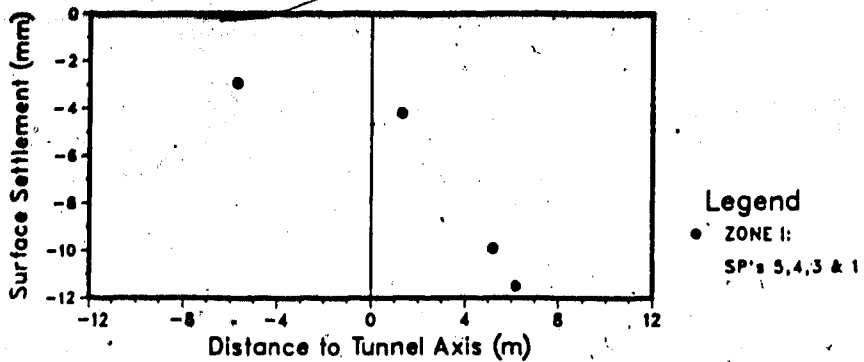
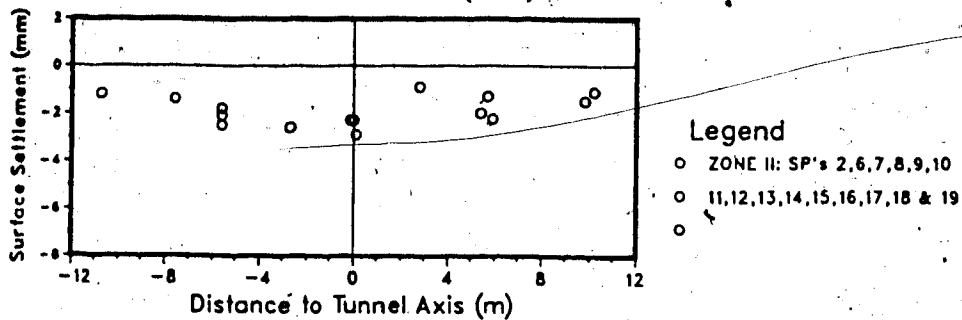


Figure 4.24 Zoning of instrumented area according to magnitude of surface settlements after bench excavation

SURFACE SETTLEMENTS - ZONE I (Slope effect) - 17.APR.86



SURFACE SETTLEMENTS - ZONE II (Main) - 17.APR.86



SURFACE SETTLEMENTS - ZONE III (Across TCH) - 25.OCT.85

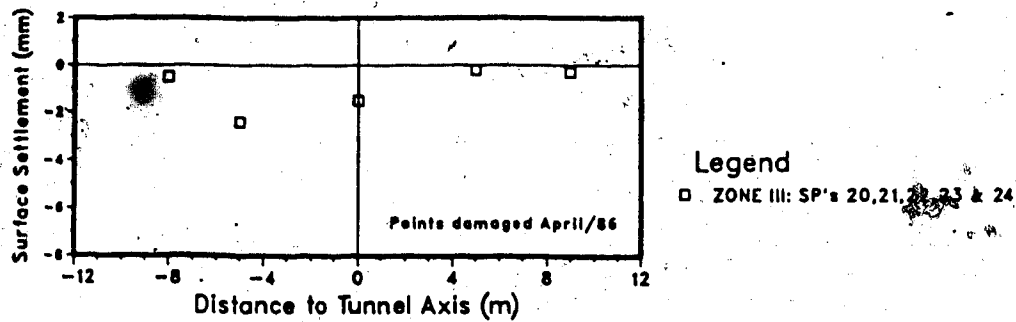


Figure 4.25 Final surface settlements in Zones I, II and III

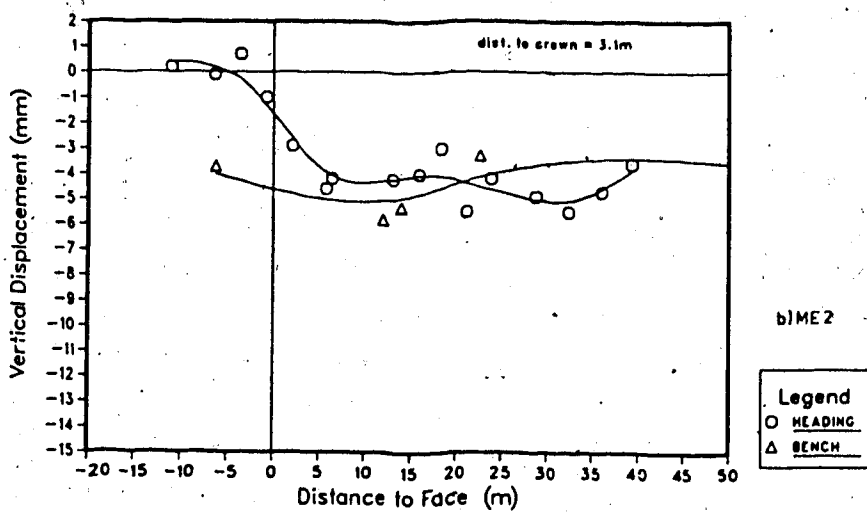
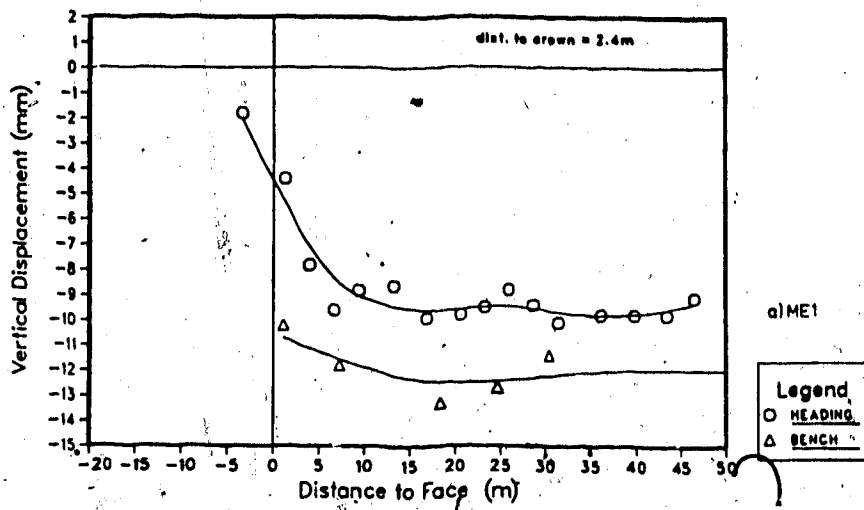


Figure 4.26 Typical subsurface settlement behaviour close to the tunnel crown (Zones I and II)

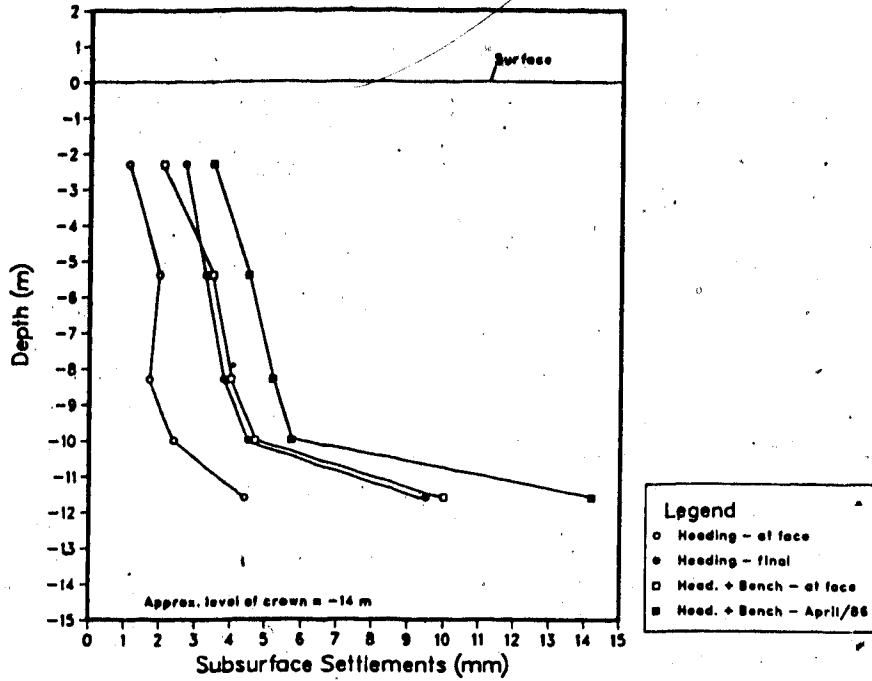


Figure 4.27 Subsurface settlement profile: ME1

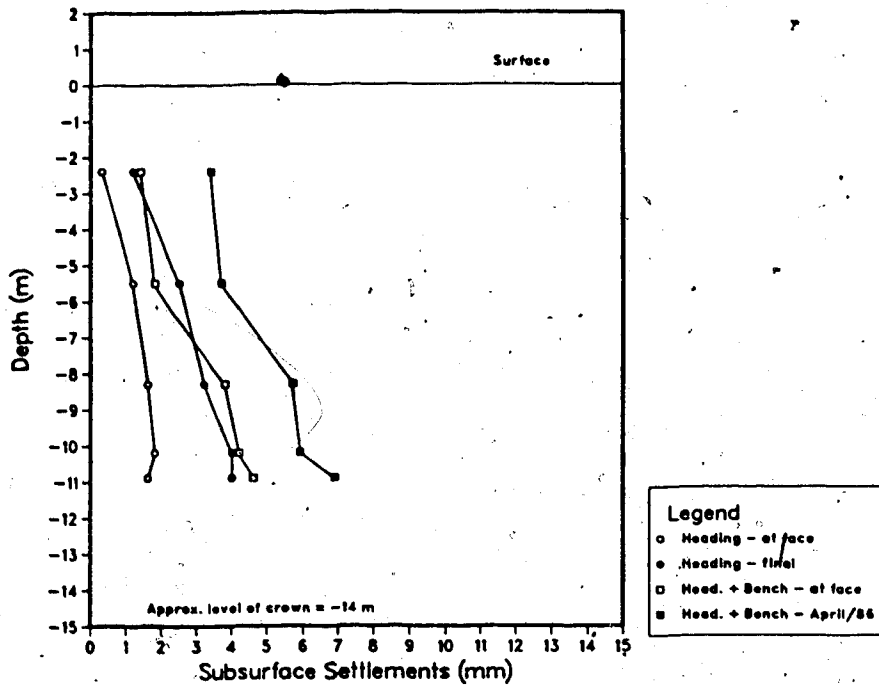


Figure 4.28 Subsurface settlement profile: ME2

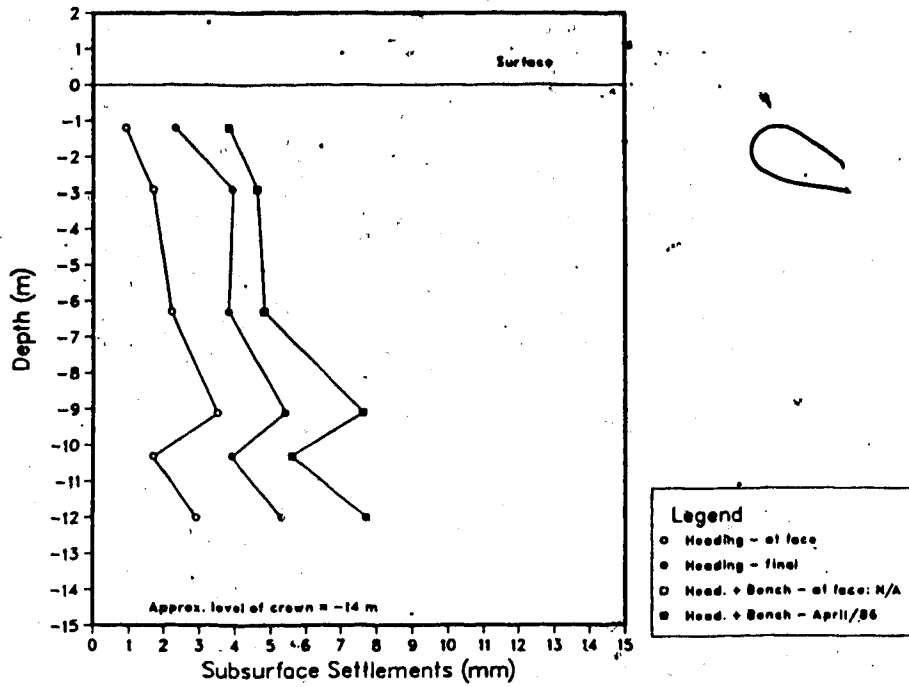


Figure 4.29 Subsurface settlement profile: ME3

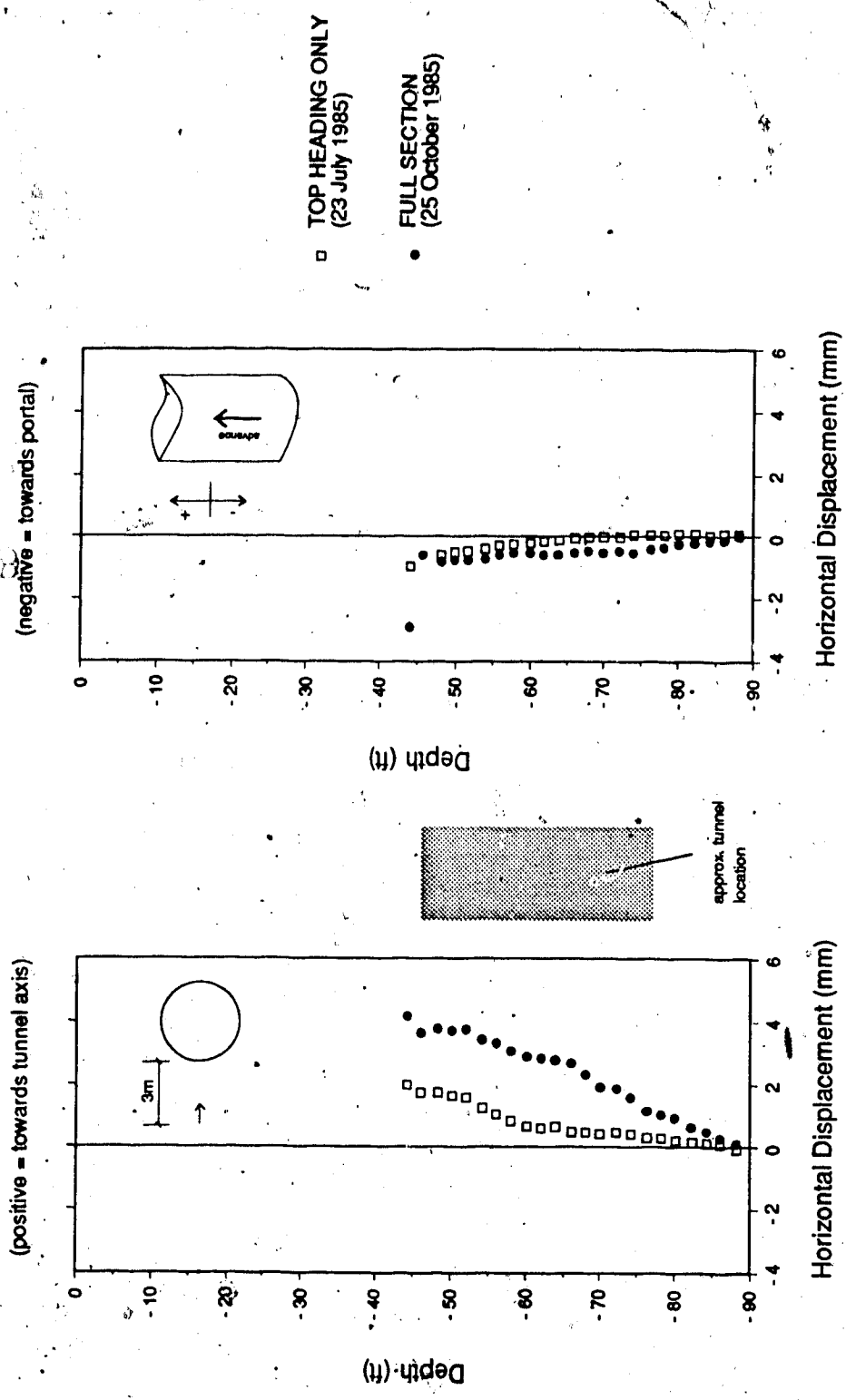


Figure 4.30 Horizontal displacements measured at Slope Indicator SI-3

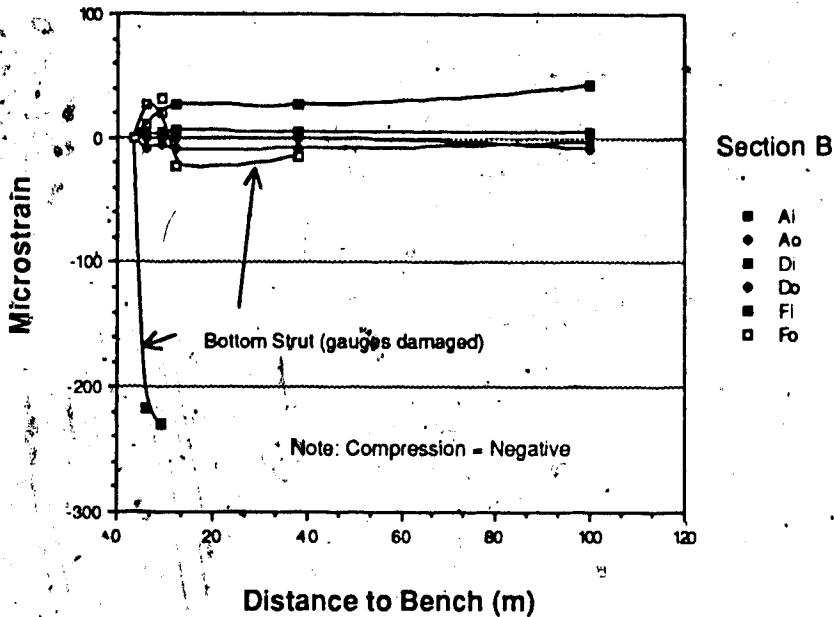
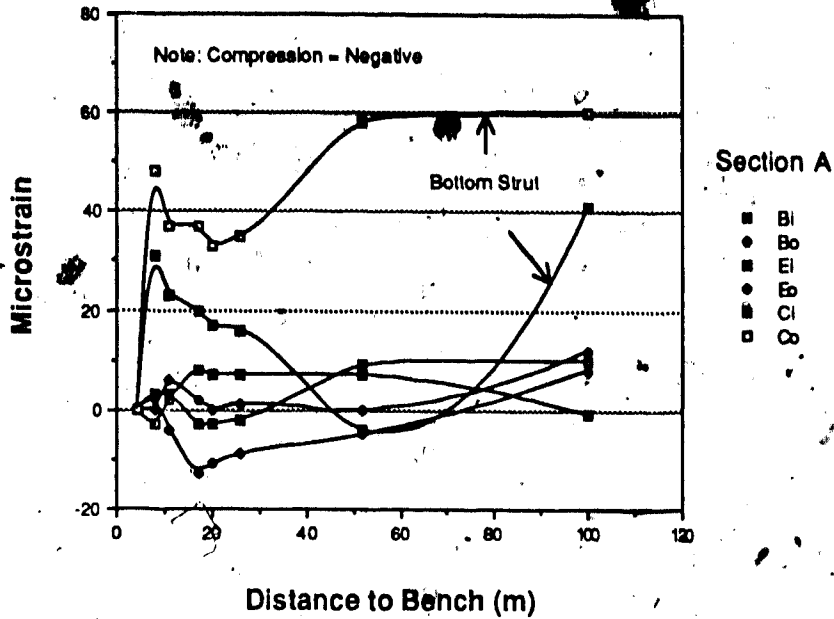


Figure 4.31 Strains in the steel ribs vs. distance to excavation bench

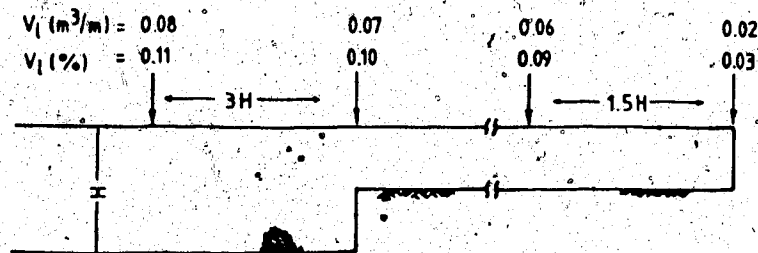
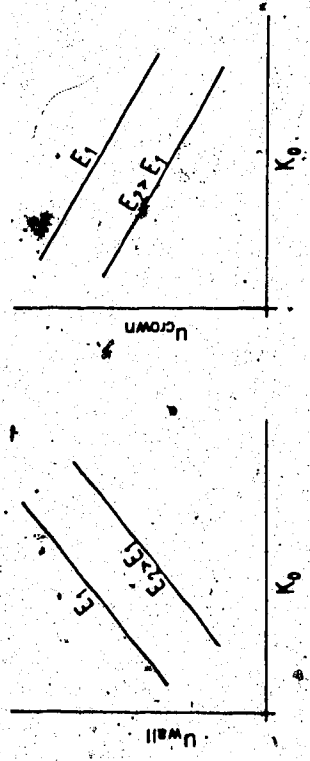


Figure 4.32 Loss of ground versus position of excavation face

a) Displacements calculated numerically:



b) Observed behaviour:



c) Displacements are made dimensionless:

$$\Delta_i = \frac{u_i \cdot E}{2 \cdot \text{Req} \cdot p} = f(K_0) = \begin{cases} a + b \cdot K_0 & \text{(crown)} \quad [4.16] \\ c + d \cdot K_0 & \text{(wall)} \quad [4.17] \end{cases}$$

d) Substitute the u_i values (measured) into Equations 4.16 and 4.17, yielding:

$$[4.16] \rightarrow E = e + f K_0 \quad [4.18]$$

$$[4.17] \rightarrow E = g + h K_0 \quad [4.19]$$

e) Solve the above system of equations:

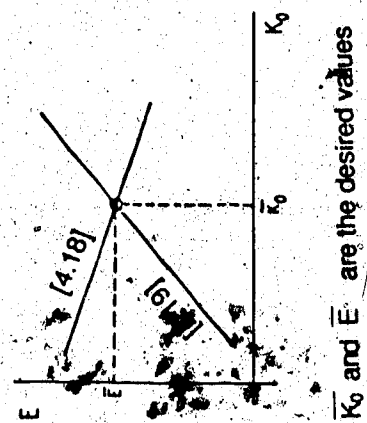


Figure 4.33 Sequence of calculations on proposed method for estimating E and K₀

From the Boundary Element analyses:

$$\Delta_{\text{crown}} = 1.013 - 0.384 K_0 \quad [4.16]$$

$$\Delta_{\text{wall}} = -0.275 + 939.583 K_0 \quad [4.17]$$

Measurements:

crown: 5.5 mm (@ 3m from tunnel)

wall: 3.0 mm (@ 3m from tunnel)

Substituting into [4.16] and [4.17] above:

$$E = 522.076 - 197.929 K_0 \quad [4.18]$$

$$E = -259.416 + 939.583 K_0 \quad [4.19]$$

Solution:

$$K_0 = 0.687 \quad \text{and} \quad E = 386 \text{ MPa}$$

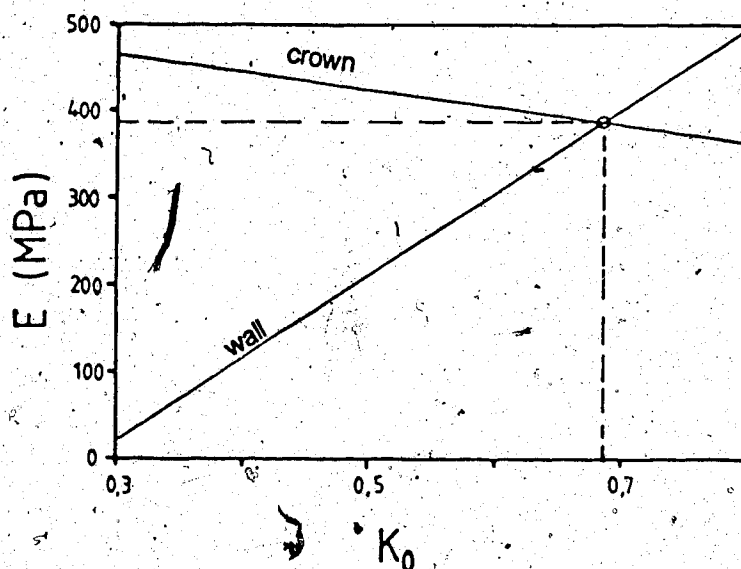


Figure 4.34 Application of proposed method for estimating E and K_0 to the case of the Mount Shaughnessy tunnel.

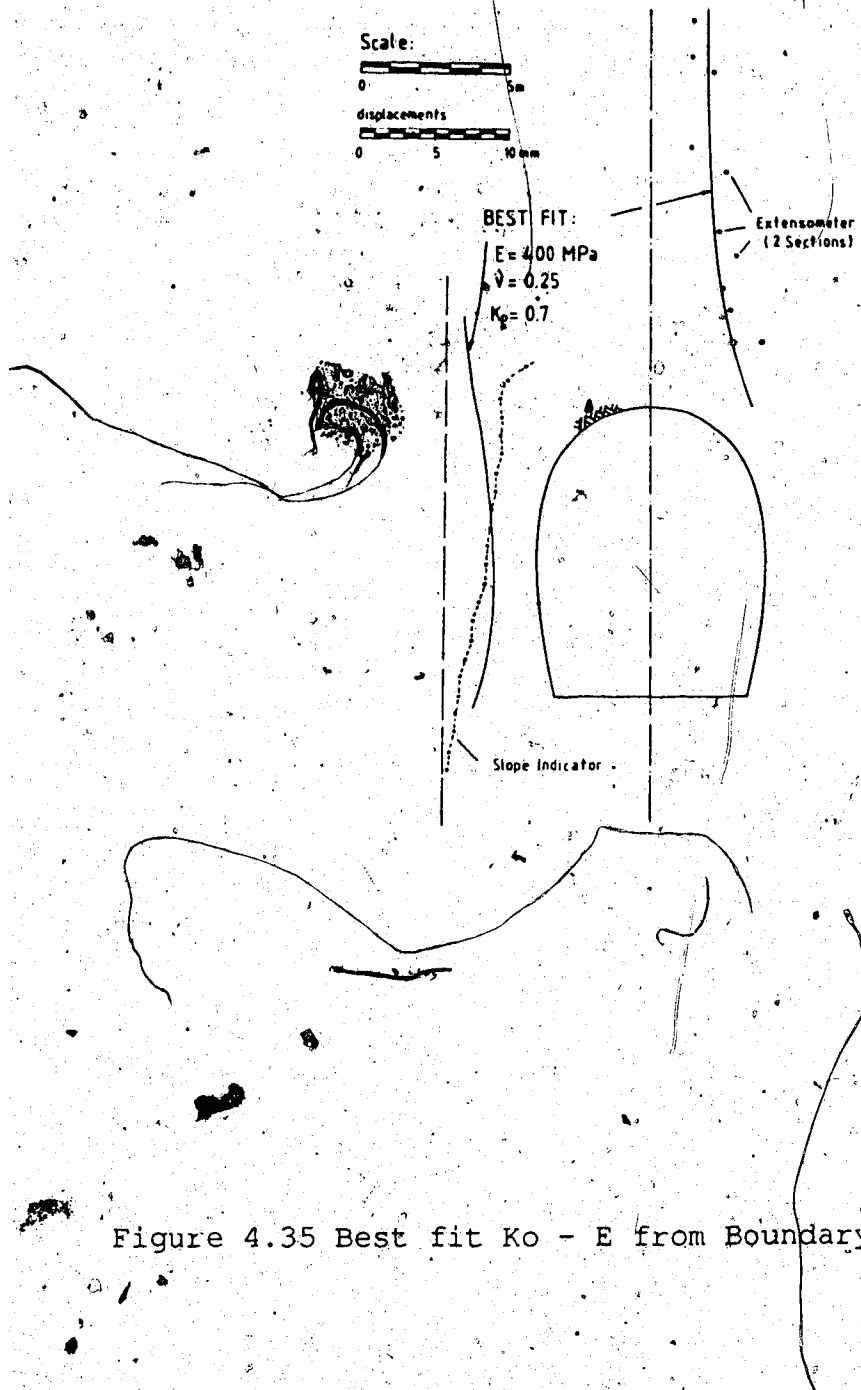


Figure 4.35 Best fit $K_0 - E$ from Boundary Element Analyses

B

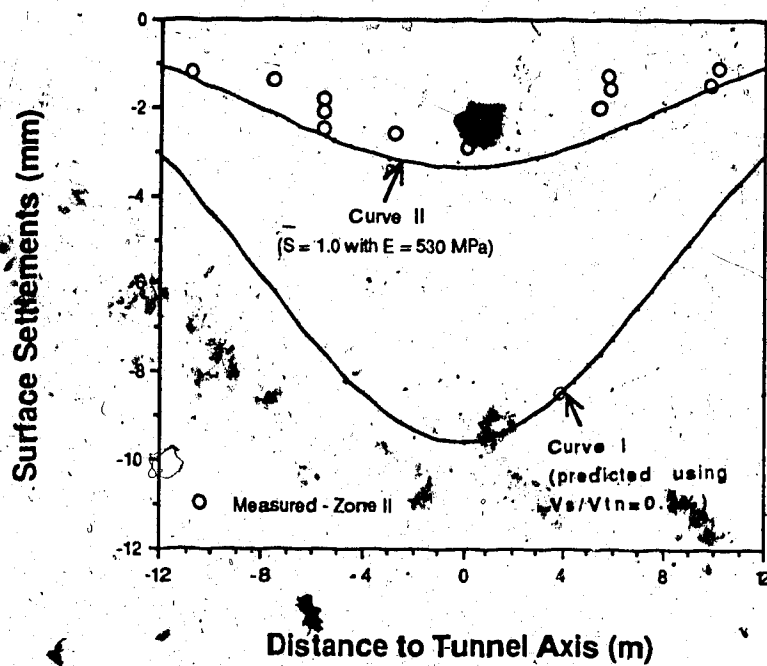
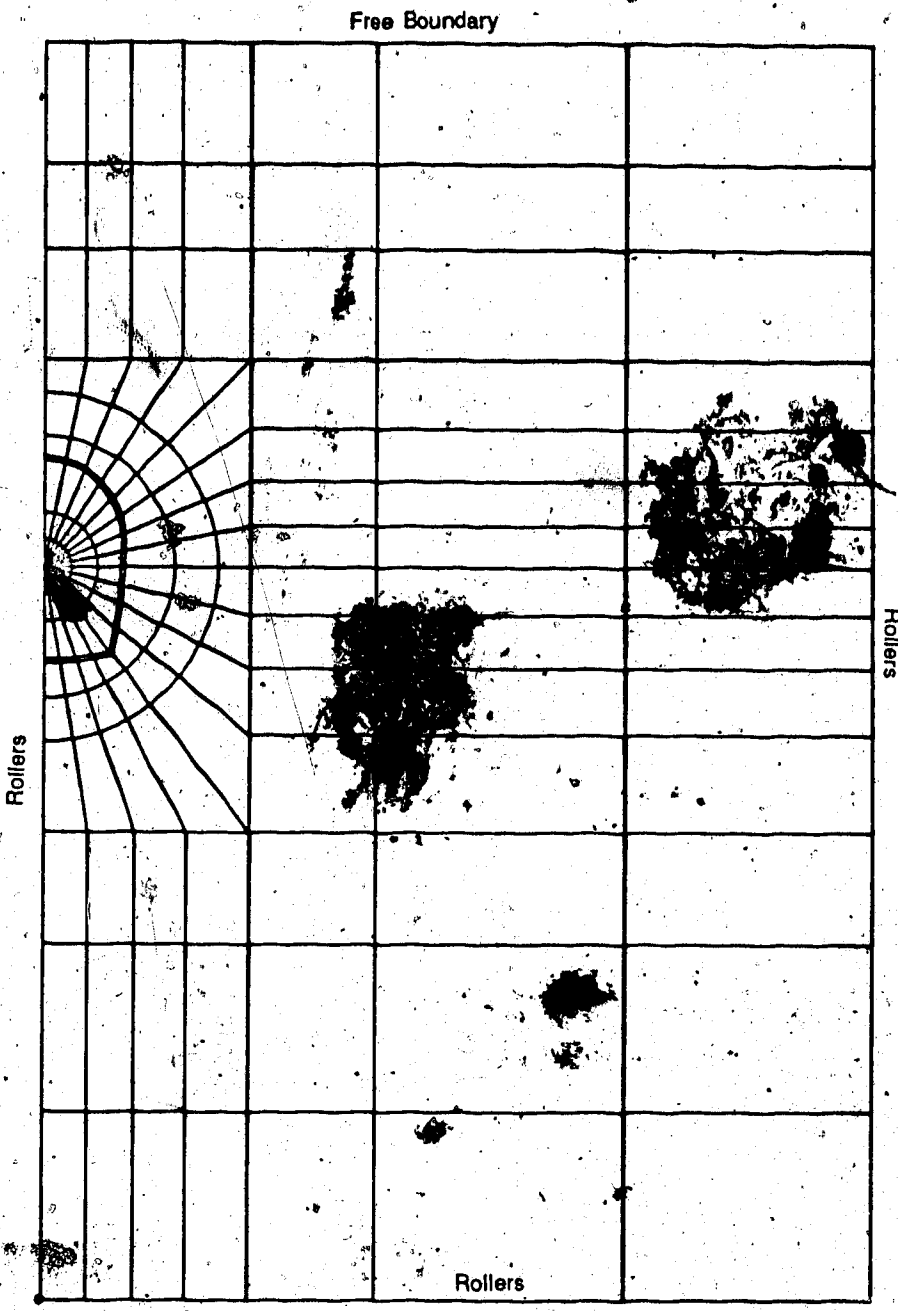


Figure 4.36 Surface settlements predicted using empirical recommendations versus actual readings



Fixed

Properties:

Soil: $E = 300 \text{ MPa}$ (@ tunnel axis)

$$K_0 = 0.8 = \frac{\nu}{1 - \nu}$$

Shotcrete: $E = 15 \text{ GPa}$

$$\nu = 0.2$$

Figure 4.37 Finite Element mesh for lining analyses

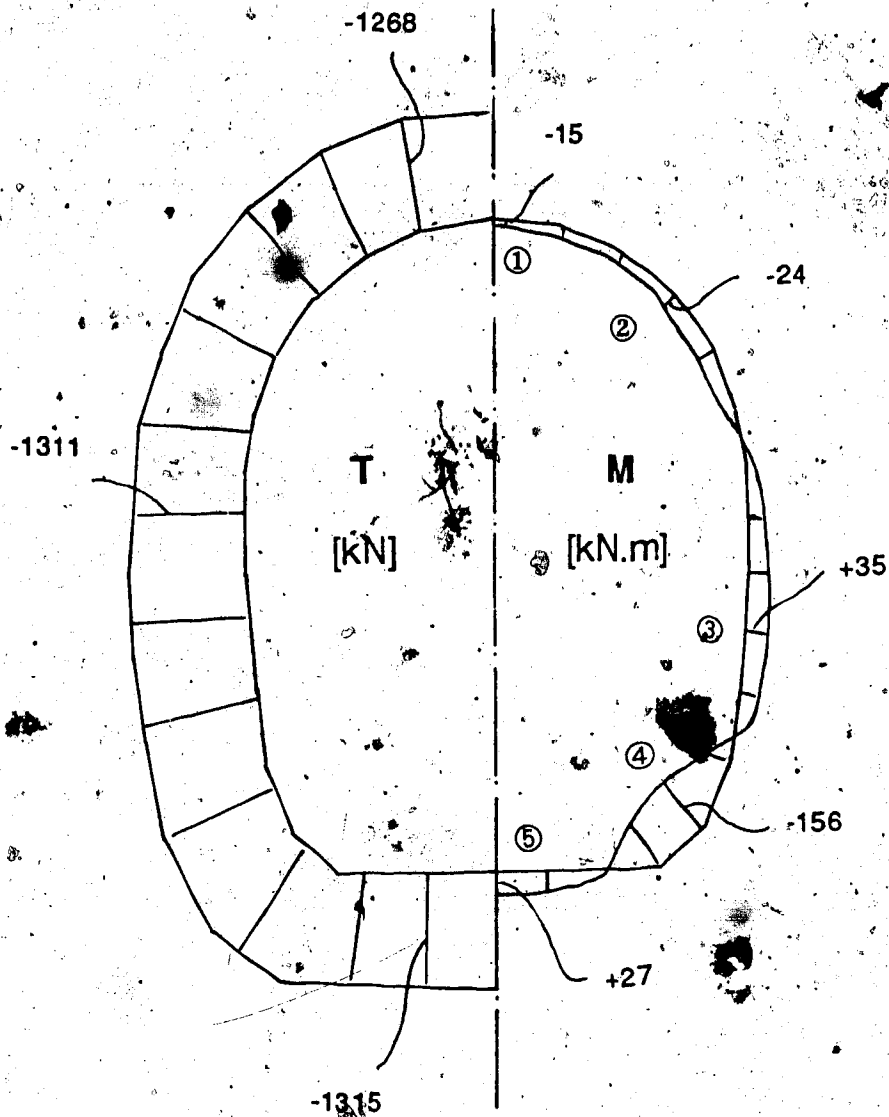


Figure 4.38 Results of plane strain, elastic finite element analysis - lining is represented by isoparametric beam elements.



Plate 4.1 Study area, looking northward along Mount Shaughnessy Tunnel alignment



Plate 5.2 Aspect of excavation of West Portal

5. SUMMARY AND CONCLUSIONS

5.1 Introduction

In the last two decades, the increasingly high costs associated with open excavations in urban areas has instigated several major developments in the art of tunnelling in soft ground. Large cross section tunnels have been shown to be a viable solution for certain situations not adaptable to conventional shield tunnelling, such as junctions of rapid transit lines or subway stations. It is noteworthy that the necessity for alternatives to shield tunnelling was pointed out by Peck et al. (1972:260), although no formal option was specified at that time.

This thesis has examined some geotechnical aspects related to design and behaviour of large cross section tunnels in soft ground. Within the scope of this work, large cross sections have been defined as those whose continuous (i.e., without intermediate pillar support) cross sectional excavated area exceeds 60m^2 . This definition was found to encompass most double track highway, railway and subway tunnels, subway stations and some single track railway tunnels. Furthermore, the research has concentrated on tunnels using shotcrete as initial support.

The purpose of this thesis has been to review current practice of construction and design of large cross section tunnels in soft ground and formulate preliminary design concepts. This framework was chosen due to the fact that the design of such underground structures is a relatively new

subject, which has evolved mainly in areas outside North America.

The work consisted mainly of three essentially independent studies, namely an overview of current practice, the development of simple solutions for verification of tunnel stability and the documentation of an actual case history. An attempt was made to present both empirical and analytical findings in ways considered useable by the engineer engaged in day-to-day design.

5.2 Overview of Current Practice

As a result of collecting and summarizing data from case histories described in the literature, augmented by personal correspondence with authors and companies, a catalogue of 25 large cross section tunnels was established. This catalogue is at Appendix A. Based on this review, supplemented by a few explanatory additional key papers, some important points emerged and are listed below:

1. Large cross section tunnels with up to 150m^2 of excavated cross section and no intermediate pillars for permanent support have been constructed in various ground conditions. No cases were found of such tunnels in soft clays, which confirms an earlier assessment by Heinz (1984), that the NATM may not be an appropriate tunnelling method in these soils.

It was suggested (Heinz, 1984) that this method is not appropriate in situations where significant face displacements are anticipated, unless ground improvement techniques are used.

2. Examination of some of these case histories suggests that completing the invert as close as possible to the tunnel face is a major concern. In several cases, a temporary invert closure within an individual heading was used. In non-urban areas a more relaxed excavation sequence, with larger invert closure distances, appears to be a frequent choice, but probably results in larger surface settlement.

3. Some fairly recent Japanese cases (urban and non-urban) were excavated in sands described as essentially cohesionless. Extra precautions taken during the excavation of these tunnels (e.g., the spraying of a resin coating on the exposed soil before shotcreting) are believed worthy of future investigation. Also, it should be noted that Japanese practice, as shown by the cases reviewed, appears to make use of ground anchors, a technique which has been dismissed in recent German soft ground applications of the NATM. No details were found of these anchors and the assessment of their effectiveness is a subject which deserves further attention.

4. In order to control ground deformation and maintain face stability in large cross section soft ground tunnels, use is made of 'staged excavation'. This consists in avoiding full face advance by sequentially driving smaller, specially arranged, individual headings. Although an unlimited number of excavation

stages may be envisaged, there appears to be a tendency to rely on some typical layouts which were reviewed and classified (Figure 2.3).

5. Selection criteria for the excavation scheme were examined but no rigid rules could be established since the choice of a scheme appears to depend on several factors, not exclusively of geotechnical nature. For tunnels with more than about 90m^2 , constructed in geotechnically unfavourable ground, preference appears to be given to the scheme termed T3, where initial advance makes use of side galleries (Figure 5.1). An alternative scheme, termed T2b, is apparently preferred for smaller cross sections under the same circumstances (Figure 5.2).

6. Two-dimensional finite element analyses were carried out to compare the relative performance of three excavation schemes (T1b, T2a and T3). Through these numerical studies it was shown that the T3 scheme (with side galleries) is superior to heading and bench schemes (T1b and T2a) in terms of maximum settlement generated and a flatter slope of the surface settlement trough.

7. The results of these numerical analyses were compared with field measurements from an actual case history. It was seen, that, despite several simplifications introduced in the simulation, aspects of field behaviour could be reproduced hence reinforcing the validity of these studies.

8. It was also verified in these numerical studies that excavation of the top heading is responsible for a significant amount of the total settlement. Indication from some case histories exists that excavation of this portion requires special attention and appears to consume more time than other operations.

9. Construction parameters believed significant for design were selected and recorded for all cases examined. In order to make this information readily accessible, all cases studied were classified into four ground classes and empirical recommendations, based on the values surveyed, were proposed for each ground class (Figures 2.25 to 2.28). These summary figures are expected to enable at least a preliminary establishment of construction procedures and support quantities. It should be pointed out, however, that the information collected was limited mostly to published material and, as such, care should be exercised in the application of the recommendations outlined. It is believed that as more information becomes available, the figures presented could be improved.

10. The average support quantities were not found to vary significantly between the proposed ground classes. However, a noticeable variation was found in the construction parameters, depending on the environment in which the tunnel was built (i.e., urban, non urban or sensitive urban).

5.3. Tunnel Stability

Simple solutions, based on the bound theorems of the theory of plasticity, were applied to the problem of assessing the three dimensional stability of the tunnel heading. The work presented consisted of a summary of the theoretical framework, extension of an existing lower bound solution (Mühlhaus, 1985) and its validation using results of tunnel model tests and actual case histories.

It was shown how these lower bound solutions could be applied to the problems of evaluating critical values of the unsupported length close to the tunnel face and of the critical diameter of an opening, beyond which instability could occur. Despite the theoretical nature of these studies, it is believed that their simplicity may allow practitioners to carry out sensitivity studies, perhaps in association with empirical data such as that presented in Chapter 2. A few additional findings which emerged from this study are:

1. Although the lower bound solutions were expected to provide safe estimates of the various parameters in question, the theoretical results, when compared to findings from model experiments, were found to be reasonably close to the collapse values of these parameters. It appears, therefore, that the lower bounds obtained could be close to the exact theoretical solution, for the range of parameters investigated.

2. The results obtained from the theory were comparable to those from model experiments, but application to a few actual tunnels indicates that use of these solutions in practice will require considerable judgement in the selection of strength parameters. Use of partial factors of safety to be applied to these parameters may be a solution, as has already been suggested by several authors (e.g., Gudehus and Melix, 1986).

3. The solutions derived were shown to be very sensitive to the choice of strength parameters. The drained lower bound is particularly sensitive to the value of the cohesion of the soil mass, which is rarely known with accuracy. It appears therefore that future site investigation and testing programs should pay close attention to the determination of this strength parameter and its natural variation.

4. The concept of load factor (Section 3.3.2) was examined with respect to its relationship with settlement. It appears that there is, as suggested by Mair et al. (1981), a promising relationship between load factor and settlement. Application of relationships between the load factor and dimensionless displacements proposed by Negro (1988), in association with the derived lower bound solution, seem to provide a quick method for evaluating loads from measured displacements.

5. An assessment of tunnel stability using these simple solutions is attractive, but may not be appropriate in

every case. In many instances, stability problems in the field have been shown to be associated with minor geological details (e.g., Matheson, 1970). Given the likely catastrophic consequences associated with tunnel heading failures, it is believed that a thorough site investigation will always be required for projects such as those approached in the present work.

5.4 Mount Shaughnessy Tunnel

The geometry and construction characteristics of this tunnel depart somewhat from other large cross section tunnels reviewed in the thesis. It is believed, however, that lessons from this field case may be applicable to large cross section tunnels in general, particularly to those constructed in similar ground (Class III -- Coarse grained coherent, as defined in Chapter 2).

5.4.1 Geological and Geotechnical Characterization

Considerable attention was paid to the geological and geotechnical characterization of the site, where the existing bouldery soil allowed very limited soil testing. Interpreting the site with the aid of geological models provided a starting point for estimates of the soil properties through correlations with similar deposits for which properties were known. Several ancillary procedures for estimating the soil properties were investigated. It is believed that a close examination of the topics presented in Chapter 4 will be of

value for future projects in similar mountainous environments.

For most soil properties, it is believed that reasonable estimates were derived. A major uncertainty, however, regards the insitu cohesion due to cementation. Although large scale tests could be envisaged, a more practical alternative would be perhaps to attempt to classify natural deposits as weakly cemented, moderately cemented and strongly cemented, based on simple field tests and simultaneous laboratory investigations. This terminology has already been used by Clough et al. (1981) for description of the cementation in sands and that work could be used as a starting point for such research. The use of large diameter auger holes may be an appropriate tool for inspection of the cementation condition of the ground insitu.

Use of dynamic measurements appears to be a promising way to estimate the insitu ground modulus in bouldery deposits such as that in question. The moduli obtained in the present study should be viewed only as rough estimates due to the numerous assumptions involved in the calculations. It is believed that further studies should employ direct shear wave measuring methods, which have been reported as a reliable way to estimate the soil modulus. Also, it seems worth noting that static moduli derived from dynamic measurements have been shown to approximate the 'low-strain' soil modulus, which appears to be an important parameter for geotechnical analyses (e.g., Fourie et al., 1986).

5.4.2 Monitoring Program

Results of the field instrumentation program at the West Portal of the Mount Shaughnessy Tunnel were evaluated in terms of the geotechnical performance of the tunnel. The loss of ground associated with different stages of the tunnel construction was very small and comparable to that observed in tunnels where technologies such as the NATM were used. Although several precautionary measures were taken in order to reduce ground movements due to tunnel excavation, it is believed that the good performance was mostly attributable to the favourable properties of the ground.

A simple back analysis procedure was developed for estimating E and K_0 from measurements of displacement. It is believed that this procedure can be applied in tunnels in fairly stiff soils where no significant departure from elastic conditions is expected away from the tunnel perimeter.

5.4.3 Design

According to the classification outlined in Chapter 2, the soil in question would be characterized as Class III (Coarse grained coherent). The excavation procedure employed did not show significant departures from that which has been employed in similar large cross section tunnels in non-urban areas. The measured surface settlements were, however, smaller than those expected for similar tunnels in urban

areas which, given the somewhat relaxed excavation procedures employed, must be attributed to the good ground quality.

Results of a simplified numerical analysis suggests that an initial shotcrete support such as that used in similar situations could be employed in the present case. It is recognized, however, that the decision concerning this alternative will probably depend on factors of non-geotechnical nature (e.g., contractual aspects).

5.5 Suggestions for Further Studies

The investigations reported in this thesis provide only a brief insight into what appears to be a promising area for soft ground tunnelling research. Improving the empirical recommendations by adding data from new case histories would be of practical interest. It should be stressed, however, that published studies offer only limited insight into the actual tunnel behaviour. It is believed, therefore, that future research on large cross section tunnels in soft ground should concentrate on detailed instrumentation of actual case histories and perhaps on numerical modelling. Given the complex sequences of excavation used in these tunnels, meaningful numerical modelling will likely require a three dimensional approach and the work by Heinz (1984) may be useful as a starting point for further research. It is suggested that in these studies, attention should also be given to design assumptions for the final lining.

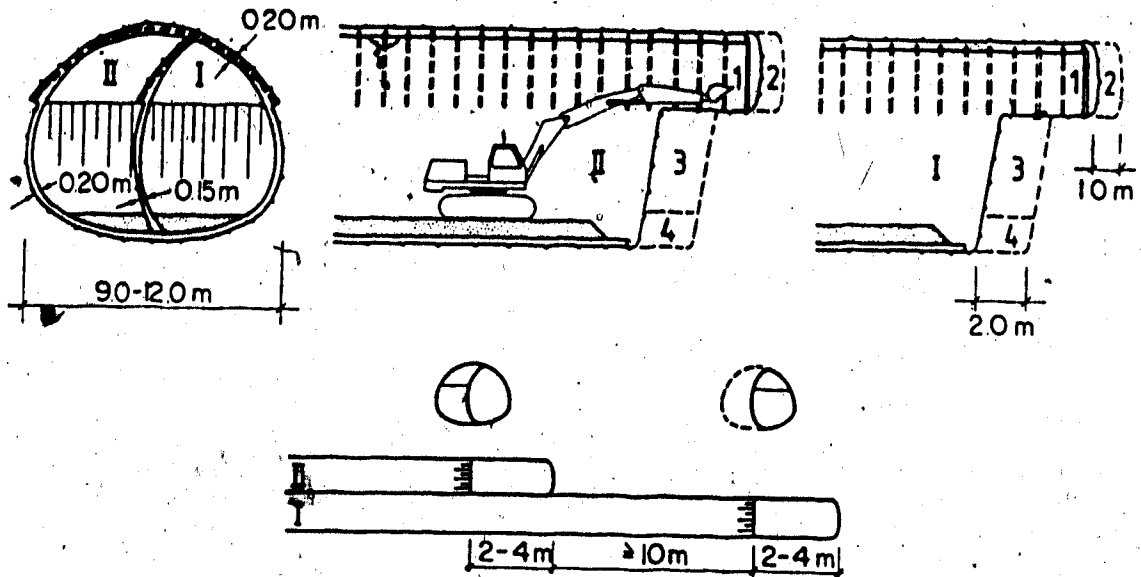


Figure 5.1 Illustration of T2b scheme of staged excavation (modified after Hochmut et al., 1987)

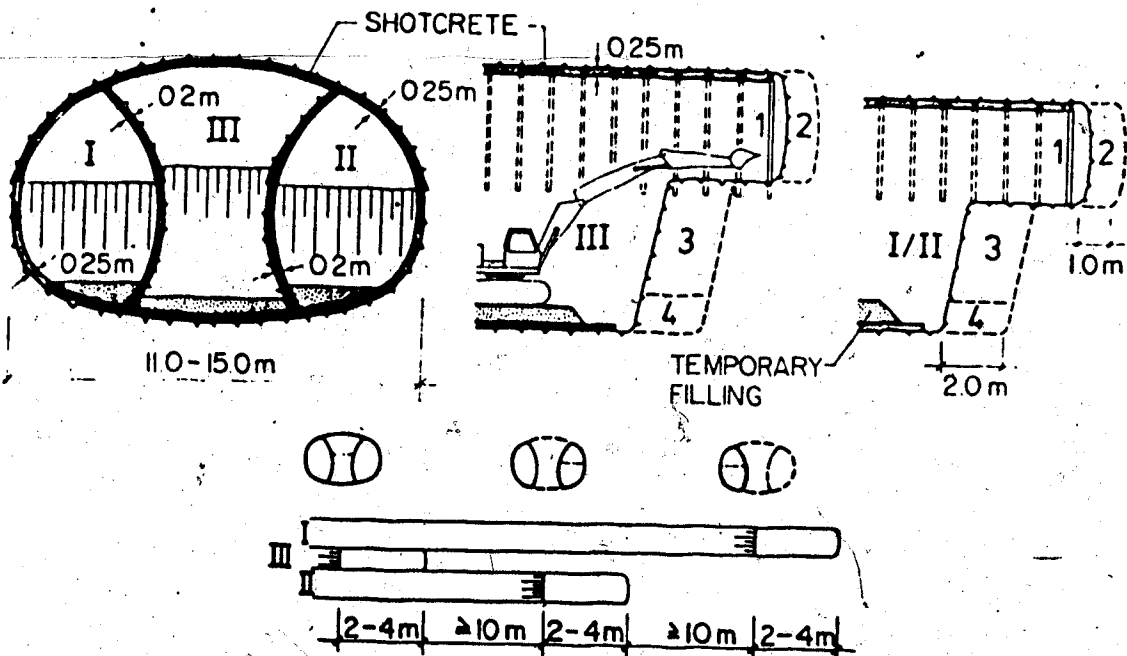


Figure 5.2 Illustration of T3 scheme of staged excavation (modified after Hochmut et al., 1987)

BIBLIOGRAPHY

- Abbiss, C.P., 1981. Shear wave measurement of the elasticity of the ground. *Geotechnique* 31, 1, pp.91-104.
- Achuff, P.L., Holland, W.D., Coen, G.M. and van Tighem, K., 1984. Ecological land classification of Mount Revelstoke and Glacier National Parks, British Columbia. Publication No. M-84-11, Alberta Institute of Pedology, Volumes 1 and 2.
- ADINA Engineering, 1984. ADINA - A Program for Automatic Dynamic Incremental Nonlinear Analyses. User's Manual (Report AE 84-1).
- Atkinson, J.H., 1981. Foundations and slopes: An introduction to applications of critical state soil mechanics. Halsted Press - John Wiley and Sons, New York, 382p.
- Atkinson, J.H. and Cairncross, A.M., 1973. Collapse of a shallow tunnel in a Mohr-Coulomb material. Proceedings of the Symposium on the role of plasticity in soil mechanics, Cambridge, pp.202-206.
- Atkinson, J.H. and Mair, R.J., 1981. Soil mechanics aspects of soft ground tunnelling. *Ground Engineering* (July), pp.20-26 and 38.
- Atkinson, J.H. and Potts, D.M. 1977(a). Subsidence above shallow tunnels in soft ground. *Journal of the Geotechnical Engineering Division - ASCE*, Vol. 103, pp.307-325.
- Attewell, P. 1978. Ground movements caused by tunnelling in soil. In: *Large Ground Movements and Structures* (edited by J.D. Geddes), Pentech, London, pp. 812-948.
- Azimi, C., Desvarreux, P., Guerpillon, Y., and Keime, F., 1983. Reconnaissance des sols non carottables a gros elements. *Bulletin IAEG* No. 26-27, pp.143-151.
- Babendererde, S., 1985. Tunnel linings. *Tunnel*, 2, pp. 61-71.
- Barton, N. and Kjaernsli, B., 1981. Shear strength of rockfill. *Journal of the Geotechnical Engineering Division, ASCE*, Vol. 107, pp.873-891.

- Baudendistel, M., 1979. Zum Entwurf von Tunneln mit grossem Ausherscherschnitt. Rock Mechanics, Suppl. 8, pp.75-100.
- Bauernfeind, P., 1984. Weiterentwicklung der "Neuen österreichischen Tunnelbauweise" im Zuge des U-Bahnbaues in Nürnberg. Forschung+Praxis, 29 (Alba, Düsseldorf), pp.180-189.
- Bauernfeind, P., Gartung, E. and Adams, F.J., 1986. Large subway tunnel cross sections at Nuremberg. Proceedings, ITA International Congress on Large Underground Openings, Firenze, Vol. I, pp.634-643.
- Bauernfeind, P., Müller, F. and Müller, L. 1978. Tunnelbau unter historischen Gebäuden in Nürnberg. Rock Mechanics, Suppl. 6, pp.161-192.
- Bathe, K.J., 1978. ADINA: A finite element program for automatic dynamic incremental nonlinear analysis. Report 82448-1, MIT.
- Bathe, K.J., 1982. Finite element procedures in engineering analysis. Prentice-Hall, New Jersey, 735p.
- Bell, F.G. 1983. Engineering properties of soil and rocks, 2nd Edition. Butterworth, London, 149p.
- Benson, R.P., Hostland, L.O. and Charlwood, R.G., 1985. the Canadian Railway tunnels in British Columbia. In: Canadian Tunnelling 1985 (Tunnelling Association of Canada), pp. 23-36.
- Beton Kalender, 1981. Verlag von Wilhelm Ernst & Sohn, Berlin.
- Bhide, S.B. 1981. Field and laboratory tests on bouldery soils. Proceedings, Geomech-81: Symposium on Engineering Behaviour of Coarse Grained Soils, Boulders and Rocks, Hyderabad (Indian Geotechnical Society), Vol. 1, pp.111-117.
- Bjerrum, L. and Eide, O., 1956. Stability of strutted excavations in clay. Geotechnique, Vol. 6, No. 1, pp.32-47.
- Bolton, M., 1979. A guide to soil mechanics. The MacMillan Press Ltd., London. 439p.

- Bolton, M., 1981. Limit state design in geotechnical engineering. *Ground Engineering* (September), pp. 39-46.
- Boulton, G.S. and Deynoux, M. 1981. Sedimentation in glacial environments and the identifications of tills and tillites in ancient sedimentary sequences. *Precambrian Research* 15, pp.397-422.
- Boulton, G.S. and Eyles, N. 1979. Sedimentation by valley glaciers; a model and genetic classification. In: *Moraines and Varves* (edited by C. Schluchter), Balkema, Rotterdam, pp.11-23.
- Boulton, G.S. and Paul, M.A. 1976. The influence of genetic processes on some geotechnical properties of glacial tills. *Quarterly Journal of Engng. Geology*, 9, pp. 159-194.
- Bowles, J., 1982. *Foundation analysis and design*, 3rd edition. McGraw-Hill, New York, 816p.
- Brady, B.H.G. and Brown, E.T. 1985. *Rock mechanics for underground mining*, George Allen & Unwin, London, 527p.
- Brierley, G.S., 1975. The performance during construction of the liner for a large, shallow underground opening in rock. Ph.D. Thesis, University of Illinois at Urbana-Champaign.
- Broms, B.B. and Bennermark, H., 1967. Stability of clay at vertical openings. *Journal of the Soil Mechanics and Foundations Division, ASCE*, Vol. 93, pp.71-94.
- Brown, E.T., 1981. Putting the NATM into perspective. *Tunnels and Tunnelling*, November, pp.13-17.
- Burmister, D., 1948. The importance and practical use of relative density in soil mechanics. *Proceedings, ASTM*, Vol. 48, pp. 1249-1268.
- C.P. Rail, 1985. The Rogers Pass Tunnels. In *Canadian Tunnelling 1985* (Tunnelling Association of Canada), pp.13-22.
- Calladine, C.R. 1969. *Engineering Plasticity*. Pergamon Press, Oxford, 318p.
- Camsell, C. 1914. *Guide to the geology of the Canadian National Parks: Canadian Pacific Railways between*

- Calgary and Revelstoke. Department of the Interior, Ottawa.
- Casagrande, A., 1948. Classification and identification of soils. *Trans. ASCE*, Vol. 113, pp.901-930.
- Casarin, C., 1977. Soil deformations around tunnel headings in clay. M.Sc. Thesis, University of Cambridge.
- Casarin, C. and Mair, R.J., 1981. The assessment of tunnel stability in clay by model tests. In: *Soft-Ground Tunneling, Failures and Displacements* (edited by D. Resendiz and M.P. Romo), Balkema, Rotterdam, pp.33-44.
- Celestino, T.B., Domingues, L.C.S., Mitsuse, C.T., Hori, K. and Ferrari, O.A., 1985. Recalques decorrentes da construção por NATM de um túnel urbano de grandes dimensões e pequena cobertura. *Proceedings, 2nd Symposium on Underground Excavations, Rio de Janeiro (ABGE - Brazilian Association of Engineering Geology)*, Vol. 1, pp. 325-347.
- CGS, 1985. *Canadian Engineering Foundation Manual*. Canadian Geotechnical Society.
- Chambosse, G., 1972. Das Verformungsverhalten des Frankfurter Tons beim Tunnelvortrieb - Berichte über Messungen in der Frankfurter Innenstadt. *Mitteilungen der Versuchsanstalt für Bodenmechanik und Grundbau der Technischen Hochschule Darmstadt*, Heft 10.
- Chandler, R.J., 1973. The inclination of talus, arctic talus terraces and other slopes composed of granular materials. *Journal of Geology*, Vol. 81, pp.1-14.
- Chen, W.F. 1975. *Limit analysis and soil plasticity*. Elsevier, Amsterdam, 638p.
- Chinn, T.J.H., 1979. Moraine forms and their recognition on steep mountain slopes. In: *Moraines and Varves* (edited by C. Schluchter), Balkema, Rotterdam, pp.51-57.
- Church, M. and Ryder, J.M. 1972. Paraglacial sedimentation: a consideration of fluvial processes conditioned by glaciation. *Geological Society of America Bulletin*, Vol. 83, pp. 3059-3072.
- Clague, J.J., 1981. Late Quaternary geology and geochronology of British Columbia - Part 2: Summary and discussion of

- radiocarbon-dated Quaternary history, Proc. Geol. Survey of Canada, Paper 80-35.
- Clough, G.W. and Schmidt, B., 1981. Design and performance of excavations and tunnels in soft clay. In: *Soft Clay Engineering* (edited by E.W. Brand and R.P. Brenner), Elsevier, pp.569-634.
- Clough, G.W., Sitar, N., Bachus, R.C. and Shafii Rad, N., 1981. Behaviour of cemented sands under static loading. *Journal of Geotechnical Engineering, ASCE*, Vol. 107, pp.799-817.
- Cording, E.J. and Hansmire, W.J., 1975. Displacements around soft ground tunnels. *Proceedings, 5th Pan-American Conference of Soil Mechanics and Foundation Engineering, Buenos Aires, Vol. 4*, pp.571-633.
- Cording, E.J., Hendron, A.J., Hansmire, W.H., Mahar, J.W., MacPherson, H.H., Jones, R.A. and O'Rourke, T.D., 1975. Methods for geotechnical observations and instrumentation in tunneling. NTIS PB-252585 and PB-252586.
- Costa Filho, L.M., 1980. A laboratory investigation of the small strain behaviour of London Clay. Ph.D. Thesis, University of London.
- Croce, A., Dolcetta, M., Finzi, D. and Martinelli, D., 1963. Compressibility of soils of glacial origin. *Proceedings, 3rd ECSMFE, Wiesbaden, Vol. 1*, pp.327-336.
- Cruz, H.J.V., Couto, J.V.S., Hori, K., Salvoni, J.L. and Ferrari, O.A., 1982. Os túneis do prolongamento norte - uma primeira avaliação do NATM em área urbana. *Proceedings, 1st Symposium on Underground Excavations, Rio de Janeiro (ABGE - Brazilian Association of Engineering Geology)*, pp.297-316.
- Cruz, H.J.V., Hori, K., Ferrari, O.A. and Ferreira, A.A., 1985. A construção, em NATM e em área urbana, de um túnel de grande seção - O túnel de via dupla do Prolongamento Norte. *Proceedings, 2nd Symposium on Underground Excavations, Rio de Janeiro (ABGE - Brazilian Association of Engineering Geology)*, Vol. 1, pp.391-411.
- Dackombe, R.V. and Gardiner, V., 1983. *Geomorphological Field Manual*. George Allen & Unwin, London, 254p.

- Daly, R.A., 1915. A geological reconnaissance between Golden and Kamloops, B.C. along the Canadian Pacific Railway. Geological Survey of Canada, Memoir 68.
- Davis, E.H., 1968. Theories of soil plasticity and the failure of soil masses. In: Soil mechanics-selected topics (edited by I.K. Lee); Butterworth, London, pp.341-380.
- Davis, E.H., Gunn, M.J., Mair, R.J. and Seneviratne, H.N., 1980. The stability of shallow tunnels and underground openings in cohesive material. *Geotechnique* 30, No. 4, pp.397-416.
- Deere, D., Peck, R.B., Monsees, J.E. and Schmidt, B., 1969. Design of tunnel liners and support systems, NTIS PB-183799.
- Deix, F. and Gebeshuber, J. 1987. Erfahrungen mit der NÖT beim U-Bahn-Bau in Wien. *Felsbau* 5, No. 3, pp.115-124.
- Derbyshire, E. and Love, M.A., 1986: Glacial Environments. In: A Handbook of Engineering Geomorphology (edited by P.G. Fookes and P.R. Vaughan), Chapman and Hall, New York, pp.66-81.
- D'Escatha, Y. and Mandel, J., 1974. Stabilité d'une galerie peu profonde en terrain meuble. *Revue de L'Industrie Minerale* (Special Issue), Avril, pp.45-53.
- DGEG, 1979. Bodenmechanische Untersuchungen - Teil 1: Einteilung der Böden - Bodenklassifizierung. In: Taschenbuch für den Tunnelbau; Deutsche Gesellschaft für Erd- und Grundbau e.V., Glückauf, Essen.
- Diniz, R.A.D.C., 1978. Schnittgrößen in kreisförmigen und elliptischen Tunnelwandungen aus Beton. Doctoral Dissertation, Technische Universität München.
- Distelmeier, H., 1980. Aufgaben des Bauleiters bei der Abwicklung eines Bauvorhabens am Beispiel eines Schildvortriebes. Gastvorlesung, Ruhr-Universität Bochum.
- Döllnerl, A., Hondl, A. and Proksch, E., 1976. der U-Bahnbau und die Massnahmen zum Schutz des Stephandomes. Proceedings, 6th ECSMFE, Vienna, Vol. 1.1, pp. 119-126.

- Drinker, H.S., 1878. Tunnelling, explosive compounds and rock drills. John Wiley & Sons, New York.
- Duddeck, H. and Erdmann, J., 1985. On structural design models for tunnels in soft soil. *Underground Space*, Vol. 9, pp.246-259.
- Duddeck, H., Meister, D., Werner, E., Schlegel, R. and Theurer, M., 1979. Road tunnel in very soft soil in terrace deposits in the Harz Mountains, Germany. *Tunnelling '79*, pp.205-215.
- Duddeck, H., Meister, D., Werner, E., Schlegel, R. and Theurer, M., 1981. Strassen-Tunnel Butterberg in Osterode/Harz. *Bauingenieur*, 56, pp.175-185.
- Duddeck, H., Städing, A. and Schrewe, F., 1984. Zu den Standsicherheits-untersuchungen für die Tunnel der Neubaustrecke der Deutsche Bundesbahn. *Felsbau*, 2, No. 3, pp. 143-151.
- Duncan, J.M., Byrne, P., Wong, K.S. and Mabry, P., 1980. Strength, stress-strain and bulk modulus parameters for finite element analysis of stresses and movements in soil masses. Report UCB/GT/80-01, University of California, Berkeley, 77p.
- Duncan, J.M. and Chang, C.V., 1970. Nonlinear analysis of stress and strain in soils. *Journal of the Soil Mechanics and Foundations Division. ASCE*, Vol. 96, pp.1629-1653.
- Dusseault, M.B., 1977. Geotechnical characteristics of the Athabasca oil sands. Ph.D. Thesis, Dept. of Civil Engineering, University of Alberta.
- Dusseault, M.B., 1986. The use of geophysical logs in geotechnical engineering. Proc. 39th Canadian Geotechnical Conference, Ottawa, pp.29-41.
- Dysli, M. and Fontana, A., 1982. Deformations around the excavations in clayey soil. *Proceedings International Symposium on Numerical Methods in Geomechanics*, Zürich, September, pp.634-642.
- Egger, P., 1975. Erfahrungen beim Bau eines seichtliegenden Tunnels in tertiären Mergeln. *Rock Mechanics*, Suppl. 4, pp.41-54.

- Eisenstein, Z. and Branco, P., 1985a. Observational method applied to ground control at the Edmonton LRT Tunnel. Canadian Tunnelling (Tunnelling Association of Canada), pp.51-65.
- Eisenstein, Z. and Branco, P., 1985b. Convergence-confinement method in shallow tunnels. Proceedings, 11th ICSMFE, San Francisco, Vol. 4, pp. 2067-2071.
- Eisenstein, Z., El-Nahhas, F. and Thomson, S., 1981a. Pressure-displacement relations in two systems of tunnel lining. In: Soft Ground Tunnelling, Failures and Displacements (edited by D. Resendiz and M.P. Romo); Balkema, Rotterdam, pp.85-94.
- Eisenstein, Z., El-Nahhas, F. and Thomson, S., 1981b. Strain field around a tunnel in stiff soil. Proceedings, 10th ICSMFE, Stockholm, Vol. 1, pp.283-288.
- Eisenstein, Z., Heinz, H. and Negro, A., 1984. On three-dimensional ground response to tunnelling. Proceedings, ASCE Geotech' 84, Atlanta, (edited by K.Y. Lo), pp.107-127.
- Eisenstein, Z., Heinz, H. and Negro, A., 1986. Multiple stage excavation schemes for large openings in soft ground. Proceedings, ITA International Congress on Large Underground Openings, Firenze, Vol. 1, pp.710-719.
- Eisenstein, Z. and Heinz, H., 1986. Ground displacements at the West Portal and at the crossing of the Trans-Canada Highway of the CP Rail Shaughnessy tunnel for the period April 1985 - April 1986. Unpublished Report to CP Rail, Dept. of Civil Engineering, University of Alberta.
- Eisenstein, Z. and Negro, A., 1985. Comprehensive design method for shallow tunnels. Proceedings, ITA International Conference on Underground Structures in Urban Areas, Prague, pp.7-20.
- Eisenstein, Z. and Sorensen, K.L., 1986. Tunnelling for the South LRT extension in Edmonton, Alberta. In: Canadian Tunnelling 1986 (Tunnelling Association of Canada), pp. 19-30.
- Eisenstein, Z. and Sorensen, K.L., 1987. Metro extension in Edmonton - complex geology accomodated en route. Tunnels and Tunnelling, November, pp. 45-50.

- Eisenstein, Z. and Thomson, S., 1978. Geotechnical performance of a tunnel in till. *Canadian Geotechnical Journal*, Vol. 15, pp.332-345.
- El-Nahas, F., 1980. The behaviour of tunnels in stiff soils. Ph.D. Thesis, Department of Civil Engineering, University of Alberta.
- Eyles, N. 1983. The glaciated valley landsystem. In: *Glacial geology, an introduction for engineers and earth scientists* (edited by N. Eyles), Pergamon Press, Oxford, pp. 91-110..
- Fialho Rodrigues, L., 1979. Método de prospecção sísmica em geologia de engenharia: a importância da onda de corte. Thesis, Laboratório Nacional de Engenharia Civil, Lisboa, Portugal.
- Fookes, P.G., Gordon, D.L. and Higginbottom, I.E., 1975. Glacial landforms, their deposits and engineering characteristics. Proceedings, Symposium on the Engineering Behaviour of Glacial Materials, University of Birmingham. The Midland Soil Mechs. and Fdn. Engng. Society, pp. 18-51.
- Fookes, P.G., Hinch, L.W., Huxley, M.A. and Simons, N.E., 1975. Some soil properties in glacial terrain - the Taff Valley, South Wales. Proceedings, Symposium on the Engineering Behaviour of Glacial Materials, University of Birmingham. The Midland Soil Mechs. and Fdn. Engng. Society, pp. 100-123.
- Fourie, A.B., Potts, D.M. and Jardine, R.J., 1986. The determination of appropriate soil stiffness parameters for use in finite element analyses of geotechnical problems. Proceedings, 2nd International Symposium on Numerical Models in Geomechanics, Ghent, pp.227-235.
- Fujimori, T., Uchiyama, C., Kunimi, H. and Takasaki, H., 1985. Use of NATM in soft ground near Tokyo, Japan. Proceedings, Tunnelling'85, Brighton, pp.93-102.
- Fulton, R.J., 1968. Olympia Interglaciation, Purcell Trench, British Columbia, Geological Society of America Bulletin, Vol. 79, pp.1075-1080.
- Fulton, R.J., 1984. Quaternary glaciation, Canadian Cordillera, Proc. Geol. Survey of Canada, Paper 84-10.

- Fulton, R.J. and Smith, G.W., 1978. Late Pleistocene stratigraphy of south-central British Columbia, Canadian Journal of Earth Sciences, Vol. 15, pp.971-980.
- Gais, W.H., Harpf, R. and Herg, M., 1985. Hohlräumeicherung beim Nürnberger U-Bahnbau - Messergebnisse zum Tragverhalten, Forschung + Praxis, 29 (Alba, Düsseldorf), pp.196-201.
- Gomi, M. and Higo, M. 1984. Control methods for weak rock with the NATM. Proceedings, 1st Latin-American Congress of Underground Constructions, Caracas, ITA, pp.485-492.
- Golser, J. 1981. Tunnel design and construction with NATM in weak rock. Proceedings of the International Symposium on Weak Rock, Tokyo, Vol. 1, pp. 933-938.
- Gordon, J.L. and Duguid, D.R., 1970. Experiences with cracking at Duncan dam. Transactions, 10th ICOLD, Montreal, Vol. 1, pp.469-485.
- Gudehus, G. and Mélix, P., 1986. Standsicherheitsnachweise für Bauzustände von Tunneln in Schwach Kohäsivem Gebirge. Forschung + Praxis, 29 (Alba - Düsseldorf), pp.145-152.
- Gunn, M.J., 1984. The deformation of ground near tunnels and trenches. Cambridge University Engineering Department Research Report to the Director of the Transport and Road Research Laboratory.
- Hammer, W., 1978. Geräteauswahl und Erprobung für die Arbeiten am Sendlinger-Tor-Platz. In: Moderner Tunnelbau bei der Münchener U-Bahn (edited by H. Lessmann). Springer, pp. 127-140.
- Hansbo, S., 1977. Dynamic consolidation of rockfill at Uddevalla shipyard. Proceedings, 9th ICSMFE, Tokyo, Vol. 2, pp.241-246.
- Hardin, B.O., 1978. The nature of stress-strain behaviour for soils. Proc. ASCE Geot. Engng. Div. Specialty Conf. on Earthquake Engng. and Soil Dynamics, Pasadena, Vol. 1, pp.3-90.
- Harpf, R. and Gais, W.H., 1983. Vortrieb im Lockermaterial und im aufgelockerten Gebirge. Felsbau, 1, No. 1/2, pp. 49-53.

- Hartmann, F., 1985. Einfache Berechnung überschütteter, kreisförmiger Rohre von beliebiger Steifigkeit: Elastizitätstheorie des überschütteten Rohres. Bautechnik, 62, Heft 7, pp.224-235.
- Heinz, H., 1984. Applications of the New Austrian Tunnelling Method in urban areas. M.Sc. Thesis, Department of Civil Engineering, University of Alberta.
- Heinz, H., Eisenstein, Z. and Thomson, S., 1987. Monitoring of a railway tunnel excavated through bouldery soil. Proceedings, VI Australian Tunnelling Conference, Melbourne (Australasian Institute of Mining and Metallurgy), Vol. 2, pp.183-189.
- Heuer, R.E., 1985. Discussion on 'State-of-the-Art: Soft Ground Tunneling', by R.B. Peck. Journal of Geotechnical Engineering, ASCE, Vol. 111, pp. 669-671.
- Hochmut, W., Krischke, A. and Weber, J., 1987. Subway construction in Munich; developments in tunnelling with shotcrete support. Rock Mechanics and Rock Engineering 20, pp. 1-38.
- Hoek, E. and Brown, E.T., 1980. Underground excavations in rock. 1st ed., The Institution of Mining and Metallurgy, London, 527p.
- Hofmann, H., 1976. Prognose und Kontrolle der Verformungen und Spannungen in Tunnelbau. In: Forschung + Praxis (Alba, Düsseldorf), 19, pp.94-100.
- Holland, S., 1964. Landforms of British Columbia.
- Holtz, R.D. and Kovacs, W.D., 1981. An introduction to geotechnical engineering. Prentice Hall, New Jersey, 733p.
- Horiuchi, Y., Kudo, T., Tashiro, M. and Kimura, K., 1986. A shallow tunnel enlarged in diluvial sand. Proceedings of the ITA International Congress on Large Underground Openings, Firenze, Vol. 1, pp.752-760.
- Hunt, R.E., 1984. Geotechnical engineering investigation manual. McGraw-Hill, 983p.
- Imaki, J., Masumoto, H., Ueda, S., Amano, M. and Kurihara, H., 1984. Execution of large cross section tunnel by New

- Austrian Tunnelling Method in sandy soil with small cover. Proceedings, 1st Latin-american Congress of Underground Constructions, Caracas, ITA, pp.503-508.
- ITA, 1986. International Congress on Large Underground Openings, International Tunnelling Association, Firenze, Italy.
- Jaeger, J.C., and Cook, N.G.W., 1979. Fundamentals of rock mechanics, 3rd. Ed., Chapman and Hall, London.
- Jagsch, D., Müller, L. and Hereth, A., 1974. Bericht über die Messungen und Messergebnisse beim Bau der Stadtbahn Bochum Los A2. Interfels Messtechnik Information, pp. 11-13.
- Janbu, N., 1963. Soil compressibility as determined by oedometer and triaxial tests. European Conference on Soil Mechanics and Foundation Engineering, Wiesbaden, Germany, Vol. 1, pp.19-25.
- Janbu, N., 1985. Soil models in offshore engineering. 25th Rankine Lecture, Geotechnique 35, No. 3, pp. 241-281.
- Jardine, R.J., Fourie, A., Maswoswe, J. and Burland, J.B., 1985. Field and laboratory measurements of soil stiffness. Proceedings, 11th ICSMFE, San Francisco, Vol. 2, pp.511-514.
- Jardine, R.J., Symes, N.J. and Burland, J.B., 1984. The measurement of soil stiffness in the triaxial apparatus. Geotechnique, Vol. 34, No. 3, pp.323-340.
- Kaiser, P.K., 1981. A new concept to evaluate tunnel performance: influence of excavation procedure. Proceedings, 22nd U.S. Rock Mechanics Symposium, Boston, pp. 264-271.
- Katzenbach, R., 1981. Entwicklungstendenzen beim Bau und der Berechnung oberflächennaher Tunnel in bebautem Stadtgebiet. Mitteilungen der Versuchsanstalt für Bodenmechanik und Grundbau der Technischen Hochschule Darmstadt, Heft 24.
- Kenney, T.C. and Watson, G.H., 1961. Multiple-stage triaxial test for determining c' and ϕ' of saturated soils. Proc. 5th ICSMFE, Paris, Vol 1, pp.191-195.

- Kerschner, H., 1981. The formation of lateral moraines: a comment on 'Drumlins and large scale flutings related to glacier folds' (by J. Shaw). Arctic and Alpine Research, Vol. 13, No. 4, pp. 439-441.
- Kimura, T., and Mair, R.J., 1981. Centrifugal testing of model tunnels in soft clay. Proceedings, 10th ICSMFE, Stockholm, Vol. 1, pp.319-322.
- Kjaernsli, B., 1968. General procedure in investigation, design and control during construction of earth and rockfill dams in Norway. In: NGI Publication No. 80, pp. 1-20.
- Klawa, N. and Schreyer, J., 1979. Tunnelling costs and their most important relationships. Forschung + Praxis, 22 (Alba, Düsseldorf), 146p.
- Kochen, R., Negro, A., Heinz, H. and Rottmann, E., 1985. Simulação de escavações subterrâneas por elementos finitos. Proceedings, 2nd Symposium on Underground Excavations, Rio de Janeiro (ABGE - Brazilian Association of Engineering Geology), Vol. 1, pp.195-217.
- Kokusho, T. and Esashi, Y., 1981. Cyclic triaxial tests on sands and coarse materials. Proceedings, 10th ICSMFE, Stockholm, Vol. 1, pp.673-676.
- Krischke, A. and Weber, J., 1981. Erfahrungen bei der Erstellung grosser Tunnelquerschnitte in Teilvorrieben beim Münchener U-Bahn-Bau. Rock Mechanics, Suppl. 11, pp.107-126.
- Krischke, A., 1987. Shotcreting methods with compressed air. Proceedings, VI. Australian Tunnelling Conference, Melbourne (Australasian Institute of Mining and Metallurgy), Vol. 2, pp.161-168.
- Krizek, R.J., 1977. Fabric effects on strength and deformation of kaolin clay. Proc. 9th ICSMFE, Tokyo, Vol. 1, pp.169-176.
- Kuwajima, F.M., 1988. Ph.D. Thesis in preparation. Dept. of Civil Engineering, University of Alberta.
- Laabmayr, F. and Pacher, F., 1978. Projekt Sondervorschlag U-Bahn Linie 8/1 Los 9/18.2. In: Moderner Tunnelbau bei der Münchner U-Bahn, Springer (edited by H. Lessmann), pp. 29-53.

- Laabmayr, F., and Weber, J., 1978. Messungen, Auswertung und ihre Bedeutung. In: Moderner Tunnelbau bei der Münchener U-Bahn, Springer, (edited by H. Lessmann), pp.73-96.
- Laabmayr, F., and Swoboda, G. 1986. Grundlagen und Entwicklung bei Entwurf und Berechnung im seichtliegenden Tunnel - Teil 1. Felsbau 4, No. 3, pp.138-143.
- Lambrechts, J.R. and Leonards, G.A., 1978. Effects of stress history on the deformation of sand. Journal of the Geotechnical Engineering Division, ASCE, Vol. 104, pp.1371-1387.
- Laue, G. 1981. Offene- oder geschlossene Bauweise? Tunnel 1, pp.28-33.
- Leichnetz, W., and Kirschke, D. 1986. Bergmännische Tunnelbauverfahren bei den Neubaustrecken der DB Baugrundtagung Nürnberg (preprint obtained from the first author).
- Leps, T.M., 1970. Review of shearing strength of rockfill. Journal of the Soil Mechanics and Foundation Division, ASCE, Vol. 96, pp.1159-1170.
- Lessmann, H., 1980. Die Spritzbetonbauweise bei der U-Bahn-Linie 8/1 Los 9/18.2. - Erfahrungen und Erkenntnisse. In: U-Bahn Linie 8/1 (published by U-Bahn-Referat München), pp.217-228.
- Lessmann, H., 1986. Der Einfluss des Baubetriebes auf den Entwurf der Spritzbetonbauweise. Felsbau 4, No. 2, pp.79-84.
- Levson, V., 1986. Quaternary sedimentation and stratigraphy of montane glacial deposits in parts of Jasper National Park, Canada. M.Sc. Thesis, Department of Geology, University of Alberta.
- Lo, K.Y., 1970. The operational strength of stiff fissured clays. Geotechnique, 20, No. 1, pp.57-74.
- Maidl, B., 1984. Handbuch des Tunnel - und Stollenbaus. Band I: Konstruktionen und Verfahren. Glückauf, Essen, 423p.

- Mair, R.J., 1979. Centrifugal modelling of tunnel construction in soft clay. Ph.D. Thesis, University of Cambridge.
- Mair, R.J., Gunn, M.J. and O'Reilly, M.P., 1981. Ground movements around shallow tunnels in soft clay. Proceedings, 10th ICSMFE, Stockholm, Vol. 1, pp.323-328.
- Mair, R.J., Phillips, R. Schofield, A.N. and Taylor, R.N., 1985. Application of centrifuge modelling to the design of tunnels and excavations in soft clay. In: Application of Centrifuge Modelling to Geotechnical Design (edited by W.H. Craig), Balkema, Rotterdam, pp.357-380.
- Marachi, N.D., Chan, C.K. and Seed, M.B., 1972. Evaluation of properties of rockfill materials. Journal of Soil Mechanics and Foundation Division, ASCE, Vol. 98, pp.95-114.
- Massarch, K.R., 1981. Dynamic and static shear modulus. Proceedings, 10th ICSMFE, Stockholm, Vol. 4, pp.880-881.
- Matheson, D.S., 1970. A tunnel roof failure in till. Canadian Geotechnical Journal, 7, pp. 313-317.
- Mayne, P.W. and Kulhawy, F.H., 1982. K_0 -OCR relationships in soil. Journal of the Geotechnical Engineering Division, ASCE, Vol. 108, June, pp.851-872.
- Matsusita, Y. and Shimizu, R. 1986. Design and construction of the metro tunnel under Shinkansen station in an urban area. Proceedings, ITA International Congress on Large Underground Openings, Firenze, Vol. 1, pp.794-803.
- Meister, D. and Wallner, M. 1977. Instrumentation of a tunnel in extremely bad ground and interpretation of the measurements. Proc. Int. Symp. Field Measurements in Rock Mechanics (edited by K. Kovari), Zürich, pp.919-933.
- Mélix, P., 1987. Modellversuche und Berechnungen zur Standsicherheit oberflächennaher Tunnel. Publication of the 'Institut für Bodenmechanik und Felsmechanik der Universität Fridericiana in Karlsruhe', Heft 103.
- Miyazaki, T. 1982. Construction with NATM in volcanic ash (in Japanese). Doboku Gijutsu, Tokyo, Vol. 35, No. 7, pp. 50-60.

- Mollard, J.D. and Janes, J.R. 1984. Airphoto interpretation and the Canadian landscape. Energy, Mines and Resources Canada.
- Moreno, A. and Schmitter, J.J. 1981. Failures of shaft and tunnels in soft soils. In: Soft Ground Tunnelling: Failures and Displacements (edited by D. Resendiz & P.Romo), Balkema, Rotterdam, pp.23-32.
- Morgan, G.C. and Harris, M.C., 1967. Portage Mountain Dam: II. Materials. Canadian Geotechnical Journal, Vol. 4, No. 2, pp. 142-166.
- Morgenstern, N.R. and Cruden, D., 1979. Description and classification of geotechnical complexities. Proceedings of the Int. Symp. on the Geotechnics of Structurally Complex Formations, Capri, Associazione Geot. Italiana, Vol. 2, pp.195-203.
- Morgenstern, N.R. and Thomson, S., 1971. Comparative observations on the use of the Pitcher sampler in stiff clay. In: Sampling of Soil and Rock, ASTM STP 483, pp.180-191.
- Morris, D.V. and Abbiss, C.P. 1979. Static modulus of Gault clay predicted from seismic tests. Ground Engineering, 12, No. 8, pp.44-50.
- Mühlhaus, H.B., 1985. Lower Bound Solutions for Circular Tunnels in Two and Three Dimensions. Rock Mechanics and Rock Engineering, 18, pp.37-52.
- Müller, L., 1978. Removing misconceptions on the NATM. Tunnels and Tunnelling, October, pp.29-32.
- Müller, L., 1979. Die Bedeutung der Ringschlusslänge und der Ringschlusszeit im Tunnelbau. Proceedings of the 4th Congress of the ISRM, Montreux, Vol. 1, pp.511-519.
- Müller, L. and Bauernfeind, P., 1977. Bergmännische Auffahrung der U-Bahnstation Lorenzkirche unter historischen Gebäuden in Nürnberg (II). Tiefbau 5, pp. 349-359 and 6, pp. 452-463.
- Müller, L. and Spaun, G., 1977. Soft ground tunnelling under buildings in Germany. Proc. 9th ICSMFE, Tokyo, Vol. 1, pp.663-668.

- Mussger, K. 1981. Soft ground tunnelling under extreme shallow overburden. Proceedings, Conference on Shotcrete for Underground Support, Paipa, Colombia (Preprint, obtained from Geoconsult, Salzburg).
- NAVFAC, 1971. Design Manual DM-7: Soil Mechanics, Foundations and Earth Structures. U.S. Dept. of the Navy, Naval Facilities Engineering Command.
- Negro, A., 1988. Design of shallow tunnels in soft ground. Ph.D. Thesis, Department of Civil Engineering, University of Alberta.
- Negro, A., Heinz, H. and Eisenstein, Z., 1984. Análise de grande seção livre. Solos e Rochas (ABMS - Brazilian Society for Soil Mechanics), Vol. 7, pp.7-29.
- Negro, A. and Kuwajima, F.M., 1985. Deslocamentos ao redor de cavidades subterrâneas. Proceedings, 2nd Symposium on Underground Excavations, Rio de Janeiro (ABGE - Brazilian Association of Engineering Geology), Vol. 1, pp.234-249.
- OMTC, 1976. Tunnelling Technology: an appraisal of the State-of-the-Art for applications to transit systems. Published by Ontario Ministry of Transportation and Communications, Toronto, 166p.
- Ortigosa, P., Musante, H. and Kort, I., 1981. Mechanical properties of the gravel of Santiago. Proc. 10th ICSMFE, Stockholm, Vol. 2, pp.545-548.
- Oteo, C.S. and Sagaseta, C., 1982. Prediction of settlements due to underground openings. Proceedings, International Symposium on Numerical Models in Geomechanics, Zürich, September, pp.653-659.
- Ovesen, N.K., 1981. Towards a European code for foundation engineering. Ground Engineering (October), pp. 25-28.
- Peck, R.B., 1969. Deep excavations and tunneling in soft ground. Proceedings, 7th ICSMFE, Mexico, State-of-the-Art volume, pp.225-290.
- Peck, R.B., Hendron, A.J. and Mohraz, B., 1972. State-of-the-art of soft ground tunneling. Proceedings, 1st North American Rapid Excavation and Tunnelling Conference, Vol. 1, pp.259-286.

- Pellegrino, A., 1965. Geotechnical properties of coarse grained soils. Proc. 6th ICSMFE, Vol. 1, pp.87-91.
- Pelz, J. and Deix, F. 1985. Über den U-Bahn-Bau in Wien. Felsbau, 3, No. 4, pp. 198-211.
- Pierau, B., 1981. Tunnelbemessung unter Berücksichtigung der räumlichen Spannungs-Verformungszustände and der Ortsbrust. Publication of the 'Institut für Grundbau, Bodenmechanik, Felsmechanik und Verkehrswasserbau der R.W. Technische Hochschule Aachen, Heft 9, 182p.
- Piteau and Associates, 1982. Engineering geology and rock mechanics assessments for estimating support requirements for the proposed Rogers Pass Short Tunnel. Unpublished Report to CP Rail.
- Prakash, S. and Ranjan, G., 1982. In situ tests for measurement of soil properties in boulder deposit. Proceedings, IUTAM Conf. on Deformation and Failure of granular Materials, Delft. Balkema, Rotterdam.
- Prakash, S., 1981. Soil dynamics. McGraw-Hill.
- Rabcewicz, L.v., 1963. Bemessung von Hohlraumbauten, die 'Neue Österreichische Bauweise' und ihr Einfluss auf Gebirgsdruckwirkungen und Dimensionierung. Felsmechanik und Ingenieurgeologie, Vol. I/3-4, pp.224-244.
- Ranken, R.E., 1978. Analysis of ground-liner interaction for tunnels. Ph.D. Thesis, University of Illinois at Urbana-Champaign.
- Rziha, F., 1874. Lehrbuch der gesamten Tunnelbaukunst. Glückauf, Essen.
- Schmertmann, J.H. 1978. Guidelines for CPT performance and design. Publication No. FHWA-TS-78-209, Federal Highway Administration, Washington D.C. (quoted in Hunt, 1984:194).
- Schmidt, B., 1969. Settlements and ground movements associated with tunneling in soil. Ph.D. Thesis, University of Illinois at Urbana-Champaign.
- Schulz, W. and Edeling, H. 1972. Die Neue Österreichische Tunnelbauweise beim U-Bahnbau in Frankfurt am Main. Rock Mechanics, Suppl. 2, pp.243-256.

- Sëed, H.B. e Idriss, I.M., 1970. Soil moduli and damping factors for dynamic response analysis. Report EERC 70-10, University of California, Berkeley.
- Seneviratne, H.N., 1979. Deformations and pore-pressures around tunnels in soft clay. Ph.D. Thesis, University of Cambridge.
- Sherard, J.L., Woodward, R.J., Gisienski, S.F. and Clevenger, W.A. 1963. Earth and earth-rock dams: engineering problems of design and construction, Wiley, New York, 725p.
- Skempton, A.W., 1986. Standard penetration test procedures and the effects in sands of overburden pressure, relative density, particle size, ageing and consolidation. Geotechnique, 36, No. 3, pp.425-447.
- Sladen, J.A. and Wrigley, W. 1983. Geotechnical properties of lodgement till: a review. In: Glacial geology, an introduction for engineers and earth scientists (edited by N. Eyles), Pergamon Press, Oxford, pp. 184-212.
- Smirnoff, T.P. and Lundin, T.K., 1985. Design of initial and final support of pressure tunnels in the Phoenix SGC. Proceedings, RETC, New York, Vol. 1, pp.428-438.
- Stadt Essen, 1981. U-Stadtbahn Essen Baulos 18 (Unpublished note), 12p.
- Steiner, W. and Einstein, H.H., 1980. Improved design of tunnel supports: Volume 5 - Empirical methods in rock tunneling - review and recommendations. NTIS UMTA-MA-06-0100-80-8.
- Stroh, D. and Chambosse, G., 1973. Messungen und Setzungsursachen beim Tunnelvortrieb im Frankfurter Ton. Strassë Brücke Tunnel, Heft 2, pp.38-42.
- Széchy, K., 1973. The art of tunnelling. 2nd English Edition. Akadémiai Kiadó, Budapest, 1097p.
- Terzaghi, K., 1943. Theoretical Soil Mechanics. Wiley, New York.
- Terzaghi, K., 1950. Geologic aspects of soft-ground tunneling. In: Applied Sedimentation (edited by P.D. Trask). Wiley, New York, pp.193-209.

- Terzaghi, K. and Peck, R.B., 1948. Soil Mechanics in Engineering Practice. Wiley, New York.
- Theiner, J., 1983. Maschinen und Geräte. In: Taschenbuch für den Tunnelbau 1983 (Verlag Glückauf, Essen), pp.330-209.
- Thurber Consultants Ltd., 1981. Rogers Pass Tunnel - 1980 Geotechnical Investigation. Unpublished report to CP Rail.
- Thurber Consultants Ltd., 1983a/b. Rogers Pass Revision - Volumes 1 and 5. Unpublished reports to CP Rail.
- Timoshenko, S.P. and Goodier, J.N., 1970. Theory of elasticity, 3rd. edition. McGraw-Hill, New York.
- Tobishima Co., 1982. Tobishima Technical Report No. 9 - New Austrian tunnelling method, 10p.
- Wan, R., Chan, D. and Morgenstern, N.R., 1988. Modelling the development of rupture surfaces using displacement-type finite elements. Proceedings, 6th International Conference on Numerical Methods in Geomechanics, Innsbruck (edited by G. Swoboda), Vol. 1, pp. 373-378.
- Ward, W.H. and Pender, M.J., 1981. Tunnelling in Soft Ground. General Report, Session 2, 10th ICSMFE, Stockholm, Vol. 4, pp. 261-275.
- Webster, J.L., 1970. Mica dam designed with special attention to control of cracking. Transactions, 10th ICOLD, Montreal, pp. 487-510.
- Welzig, W. 1986. Vortriebs- und Gerätewahl in NÖT unter Berücksichtigung der geotechnischen Verhältnisse der Wiener U-Bahn-Baulose U6 and U3. Felsbau, 1, No. 1, pp. 6-10.
- Whalley, W.B. 1975. Abnormally steep slopes on moraines constructed by valley glaciers. Proceedings, Symposium on the Engineering Behaviour of Glacial Materials, University of Birmingham. The Midland Soil Mechs. and Fdn. Engng. Society, pp. 60-66.
- Wheeler, J.O., 1963. Rogers Pass map area, British Columbia and Alberta, Proc. Geol. Survey of Canada, Paper 62-32.

- Wilson, S.D. and Marsal, R.J., 1979. Current trends in design and construction of embankment dams. (Prepared for ICOLD and Geotechnical Engng. Division ASCE), 125p.
- Wittke, W. 1984. Felsmechanik. Springer Verlag.
- Woods, R.D. 1978. Measurement of dynamic soil properties. Proc. ASCE Geot. Engng. Div. Specialty Conf. on Earthquake Engng. and Soil Dynamics, Pasadena, Vol. 1, pp.91-178.
- Wong, C.K., 1986. Design and performance evaluation of tunnels and shafts. Ph.D. Thesis, Dept. of Civil Engineering, University of Alberta.
- Wroth, C.P., 1984. The interpretation of in situ soil tests (24th Rankine Lecture), Geotechnique, 34.
- Wroth, C.P. and Houlsby, G.T., 1985. Soil Mechanics - Property characterization and analysis procedures. Proceedings, 11th ICSMFE, San Francisco, Vol. 1, pp.1-55.
- Yoshimoto, K. and Doi, Y., 1981. Results of a tunnel excavation by means of NATM method. Proceedings International Symposium on Weak Rock, Tokyo, Vol. 1, pp.963-968.

Appendix A - Data from Case Histories

This Appendix contains information which is aimed at complementing the data on large cross section soft ground tunnels given in Chapter 2. Tables A.1 to A.25 contain a summary for each case and complement Tables 2.3 to 2.6 in Chapter 2. Tables A.26 and A.27 present complementary information on initial lining components used in some of the cases reviewed.

Table A.1 Data from case history No. 1

Case #1: Bochum Baulos A2 (Section #1)
<p>References:</p> <p>Jagsch et al (1974), Hoffman (1976), Müller and Spaun (1977) Heinz (1984), Maidl (1984), Negro (1988)</p>
<p>Location: Bochum, F.R.G. Year of Completion: 1973</p> <p>Environment: Urban</p> <p>Purpose: 2 track subway</p> <p>Excavation scheme: T1b</p> <p>Excavated Area (m²): 64 Width (m): 10.2 Height (m): 8.5</p> <p>Soil Cover (m): 5.5 - 13</p>
<p>Ground Type: Stiff coherent homogeneous</p> <p>Ground Description: clayey and sandy marls, sandstones - no significant groundwater</p> <p>Ground Properties: $c' = 32$ to 320 kPa, $\phi' = 25^\circ$, $E = 50-100$ MPa</p> <p>Tunnelman's Soft Ground Classification: Firm</p>
<p>Construction Procedure:</p> <p>Heading, bench and invert (closed 9 to 13m behind face)</p>
<p>Initial Support:</p> <p>25cm of shotcrete with 2(?) welded wire meshes TH 29/58 steel ribs spaced 0.8 - 1.2m</p>
Remarks:

Table A.2 Data from case history No. 2

Case #2: Bochum Baulos A2 (Section #2)	
References: Jagsch et al (1974), Hoffman (1976), Müller and Spaun (1977) Heinz (1984), Maidl (1984), Negro (1988)	
Location: Bochum, F.R.G.	Year of Completion: 1973
Environment: Urban sensitive	
Purpose: 2 track subway	
Excavation scheme: T1c	
Excavated Area (m ²): 64	Width (m): 10.2 Height (m): 8.5
Soil Cover (m): 12.5	
Ground Type: Stiff coherent heterogeneous	
Ground Description: clayey and sandy marls underlain by sandstones - no significant groundwater - very weak layer of sandy marl at tunnel axis level	
Ground Properties: c'=32 to 320 kPa, ϕ' =25°, E= 50-100MPa c'= 10 kPa, E=10MPa for weak sandy marl	
Tunnelman's Soft Ground Classification: Firm	
Construction Procedure: Heading, bench and invert (closed 4m behind face)	
Initial Support: 25cm of shotcrete with 2 welded wire meshes TH 29/58 steel ribs spaced 0.5 - 0.8m	
Remarks: This section was situated under important sensitive railway.	

Table A.3 Data from case history No. 3.

Case #3: Hasenbuck Tunnel	
References: Hoffman (1976), Müller and Bauernfeind (1977) Steiner and Einstein (1980), Bauernfeind (1984), Bauernfeind et al. (1986)	
Location: Nürnberg, F.R.G.	Year of Completion: 1973
Environment: Urban	
Purpose: 2 track subway	
Excavation scheme: T1a	
Excavated Area (m ²): 75	Width (m): 11.0 Height (m): 7.5
Soil Cover (m): H/D < 2.5	
Ground Type: Stiff coherent homogeneous	
Ground Description: soft rock (sandstone)	
Ground Properties: c' = 100-500 kPa, ϕ' = 30-45°, E = 80-160 MPa	
Tunnelman's Soft Ground Classification: Firm	
Construction Procedure: Heading and bench - round length 1.5m for heading and 4.0m for bench	
Initial Support: 15-20cm of shotcrete with 1 external wire mesh (Q221) light steel ribs (21kg/m) spaced 1.0-1.5m	
Remarks: Some localized blasting used to loosen rock.	

Table A.4 Data from case history No. 4

Case #4: Lorenzkirche (Section #1)
<p>References:</p> <p>Müller and Bauernfeind (1977) Bauernfeind et al. (1978)</p>
<p>Location: Nürnberg, F.R.G. Year of Completion: 1976</p> <p>Environment: Urban sensitive</p> <p>Purpose: subway station (1 track + platform)</p> <p>Excavation scheme: T1b</p> <p>Excavated Area (m²): 65 Width (m): 9.6 Height (m): 8.4</p> <p>Soil Cover (m): 9.0</p>
<p>Ground Type: Stiff coherent homogeneous</p> <p>Ground Description: soft sandstone, no significant ground-water</p> <p>Ground Properties:</p> <p>$c' = 100-500$ kPa, $\phi' = 37.5-40^\circ$, $E = 80-120$ MPa $K_0 < 0.5$ Bulk density = 22-23 kN/m³</p> <p>Tunnelman's Soft Ground Classification: Firm</p>
<p>Construction Procedure:</p> <p>Heading, bench and invert (L_{max}=2.6m) - round length max. 1.6m for heading</p>
<p>Initial Support:</p> <p>20cm of shotcrete with 1 external wire mesh (Q257) light steel ribs spaced 0.8m except at invert</p>
<p>Remarks:</p> <p>Synchronous excavation of twin large tunnels, data refers to a single unit. Presence of historical sensitive buildings nearby.</p>

Table A.5 Data from case history No. 5

Case #5: Lorenzkirche (Section #2)
References: Müller and Bauernfeind (1977) Bauernfeind et al. (1978)
Location: Nürnberg, F.R.G. Year of Completion: 1976 Environment: Urban sensitive Purpose: subway station (1 track + platform) Excavation scheme: T1b Excavated Area (m ²): 65 Width (m): 9.6 Height(m): 8.4 Soil Cover (m): 9.0
Ground Type: Stiff coherent heterogeneous Ground Description: soft sandstone, weaker clayey layers locally very soft due to groundwater infiltration Ground Properties: c'=100-500 kPa, ϕ' =37.5-40°, E= 80-120MPa Ko<0.5 Bulk density = 22-23kN/m ³ Tunnelman's Soft Ground Classification: ?
Construction Procedure: Heading, bench and invert (Lmax=2.6m) - round length max. 1.6m for heading
Initial Support: 25cm of shotcrete with 2 wire meshes (Q257) light steel ribs spaced 0.8m full circle
Remarks: Synchronous excavation of twin large tunnels, data refers to a single unit. Presence of historical sensitive buildings nearby.

Table A.6 Data from case history No. 6

Case #6: Rothenburgerstrasse	
References: Bauernfeind (1984) Bauernfeind et al. (1986) E.Gartung (personal communication)	
Location: Nürnberg, F.R.G.	Year of Completion: 1979
Environment: Urban	
Purpose: 2 track subway	
Excavation scheme: T1b	
Excavated Area (m ²): 85	Width (m): 13.2 Height(m): 7.5
Soil Cover (m): 7.5	
Ground Type: Stiff coherent homogeneous	
Ground Description: soft sandstone, no significant ground-water but presence of weaker clayey layers	
Ground Properties: $c' = 100-500$ kPa, $\phi' = 37.5-40^\circ$, $E \approx 80-120$ MPa $K_0 < 0.5$ Bulk density = 22-23 kN/m ³	
Tunnelman's Soft Ground Classification: Slow ravelling	
Construction Procedure: Heading, bench and invert ($L_{max} = 12$ m) - round length max. 3.0 m for heading and 6.0 m for bench	
Initial Support: 20 cm of shotcrete with 1 external wire mesh (Q257) TH 29/58 steel ribs spaced 0.8 m full circle	
Remarks:	

Table A.7 Data from case history No. 7

Case #7: Grigny Tunnel (Section #1)
References: Egger (1975), Steiner and Einstein (1980)
Location: near Paris, France Year of Completion: 1974 Environment: Urban Purpose: 2 track railway Excavation scheme: T1b Excavated Area (m ²): 80 Width (m): 10.4 Height (m): 9.3 Soil Cover (m): 8-16
Ground Type: Stiff coherent homogeneous Ground Description: Tertiary marls Ground Properties: qu=2.5kg/cm ² , c'=0.9-15kg/cm ² ϕ' =8-23° Tunnelman's Soft Ground Classification: Slow Ravelling
Construction Procedure: Heading, bench and invert with support core
Initial Support: 20cm of shotcrete - 2 layers of welded wire mesh (4kg/m ²) steel ribs spaced 0.8 - 1.2m
Remarks: 4m long grouted bolts spaced 2m circumferentially

Table A.8 Data from case history No. 8

Case #8: Grigny Tunnel (Section #2)	
References: Egger (1975), Steiner and Einstein (1980)	
Location: near Paris, France Environment: Urban Purpose: 2 track railway Excavation scheme: T2a Excavated Area (m ²): 80 Soil Cover (m): 8-16	Year of Completion: 1974 Width (m): 10.4 Height (m): 9.3
Ground Type: Stiff coherent heterogeneous Ground Description: Tertiary marls, locally weak Ground Properties: qu=2.5kg/cm ² , c'=0.9-15kg/cm ² ϕ' =8-23° Tunnelman's Soft Ground Classification: Fast Ravelling	
Construction Procedure: Heading with temporary invert and support core + bench and invert	
Initial Support: 30cm of shotcrete - 2 layers of welded wire mesh (4kg/m ²) steel ribs spaced 0.8 - 0.9m	
Remarks: 4m long grouted bolts spaced 1.0-1.5m circumferentially and 0.5m longitudinally	

Table A.9 Data from case history No. 9

Case #9: Butterberg Tunnel	
References: Meister and Wallner (1977) Duddeck et al. (1979) Duddeck et al. (1981)	
Location: Osterode, F.R.G. Environment: Urban Purpose: Highway Excavation scheme: T1b Excavated Area (m ²): 90 Soil Cover (m): 13	Year of Completion: 1978 Width (m): 11.7 Height (m): 10.1
Ground Type: Coarse grained coherent	
Ground Description: Sandy silty bouldery gravel, no significant groundwater	
Ground Properties: $c' = 20 \text{ kPa}$, $\phi' = 33^\circ$, $E = 215 \text{ MPa}$, Bulk density = 22 kN/m^3	
Tunnelman's Soft Ground Classification: Running	
Construction Procedure: Heading, bench and invert with central support core + forepoling at crown	
Initial Support: 30cm of shotcrete with 2 welded wire meshes GI 100 steel ribs spaced 1.0m except at invert	
Remarks:	

Table A.10 Data from case history No. 10

Case #10: Sinnberg Tunnel - South Portal
References: Harpf and Gais (1983)
Location: near Würzburg, F.R.G. Year of Completion: 1981 Environment: Non urban Purpose: 2 track railway Excavation scheme: T1a Excavated Area (m ²): 138 Width (m):15.5 Height(m):11.0 Soil Cover (m): H/D < 1.5
Ground Type: Coarse grained coherent Ground Description: Quaternary silty sandy gravels, locally cohesionless, no significant groundwater Ground Properties: N.A. Tunnelman's Soft Ground Classification: Running
Construction Procedure: Heading precedes bench by 20-50m. Central support core forepoling at crown
Initial Support: 30cm of shotcrete with 2 welded wire meshes (Q 188) GI 100 steel ribs spaced 0.75m
Remarks: Grouted anchors 4.0m long, 6 per steel rib at springline level. Elephant feet used at heading.

Table A.11 Data from case history No. 11

Case #11: Martinstrasse Tunnel	
References: Stadt Essen (1981) Author's personal files	
Location: Essen, F.R.G. Environment: Urban Purpose: Subway Station Excavation scheme: T3 Excavated Area (m ²): 132 Soil Cover (m): = 4.0m	Year of Completion: 1983 Width (m):15.9 Height(m):10.1
Ground Type: Stiff coherent homogeneous Ground Description: Sandy marl underlain by coal, no significant groundwater Ground Properties: $\phi' = 30^\circ$, $E = 50 \text{ MPa}$, Bulk density = 21 kN/m^3 , m.c. = 17% $C_u = 50 - 125 \text{ kPa}$ Tunnelman's Soft Ground Classification: Firm	
Construction Procedure: In mid section: heading with 2 benches + invert. Round length at top heading 1.0m. Invert closed at about 20m from face	
Initial Support: 25cm of shotcrete with 2 welded wire meshes (Q188) TH 21/29 steel ribs spaced 1.0m except at invert	
Remarks: Top heading in mid section excavated with sliding beam.	

Table A.12 Data from case history No. 12

Case #12: São Paulo North Extension
References: Celestino et al. (1985), Cruz et al. (1985) Kochen et al. (1985), Eisenstein et al. (1986), Negro (1988)
Location: São Paulo, Brazil Year of Completion: 1984 Environment: Urban Purpose: 2 track subway Excavation scheme: T2a Excavated Area (m ²): 77 Width (m): 11.5 Height (m): 8.5 Soil Cover (m): = 4.0m
Ground Type: Stiff coherent homogeneous Ground Description: Stiff fissured tertiary clay underlying a fine clayey sand deposit Ground Properties: Bulk density=21kN/m ³ , Cu=110kPa, E=70MPa Tunnelman's Soft Ground Classification: Slow Ravelling/Firm
Construction Procedure: Heading w. temporary shotcrete invert precedes bench by 12-40m. Round length averages 1.0m for heading and 2.5- 3.0m for bench. Temp. invert closed at ≈8m from face.
Initial Support: 25cm of shotcrete with 2 welded wire meshes (Q283) 18" steel ribs spaced 0.6-1.0m in upper half only
Remarks: Central support core in upper heading. Dewatering + grouting near portals. Quoted as being the first soil sub- way tunnel where shotcrete used as final support.

Table A.13 Data from case history No. 13

Case #13: Munich - Baulos 9/18.2
References: Laabmayr and Weber (1978)
Location: Munich, F.R.G. Year of Completion: 1976 Environment: Urban Purpose: 2 track subway Excavation scheme: T3 Excavated Area (m ²): 106 Width (m): 11.4 Height (m): 8.2 Soil Cover (m): H/D = 0.7-1.7
Ground Type: Stiff coherent homogeneous Ground Description: Tertiary clayey marl overlain by quaternary sands and gravels. Groundwater significant but dewatering undertaken far in advance. Ground Properties: Bulk density=21kN/m ³ , E=100-200MPa c'=40-80kPa, ϕ' =20-25° Ko=0.5-0.8 Tunnelman's Soft Ground Classification: Firm
Construction Procedure: In mid section: heading with bench + invert. Round length at top heading 1.0m. Invert closed at about 10m from face
Initial Support: 30cm of shotcrete with 2 welded wire meshes light steel ribs spaced 1.0m at crown and sides
Remarks:

Table A.14 Data from case history No. 14

<p>Case #14: Munich - Unidentified T3 Tunnel</p>
<p>References: Krischke and Weber (1981) Heinz (1984) Hochmut et al. (1987) Laabmayr and Swoboda (1986)</p>
<p>Location: Munich, F.R.G. Year of Completion: 1979 Environment: Urban Purpose: 2 track subway Excavation scheme: T3 Excavated Area (m²): 88 Width (m):13.1 Height(m):8.3 Soil Cover (m): H/D <2.5</p>
<p>Ground Type: Stiff coherent homogeneous. Ground Description: Tertiary clayey marl overlain by quaternary sands and gravels.</p> <p>Ground Properties: Bulk density=21kN/m³, E=100-200MPa c'=40-80kPa, ϕ'=20-25° Ko=0.5-0.8</p> <p>Tunnelman's Soft Ground Classification: Firm</p>
<p>Construction Procedure: In central portion heading precedes bench by 2-4m. Round length 0.8-1.0m for heading. 1.6-2.0m for bench. side galleries precede central portion by at least 10m.</p>
<p>Initial Support: 20-30cm of shotcrete (12cm for temporary walls). Generally double wire mesh full circle. Steel ribs GI100 spaced 0.8-1.0m in upper half of tunnel.</p>
<p>Remarks:</p>

Table A.15 Data from case history No. 15°

Case #15: Munich - Unidentified T2b Tunnel	
References: Krischke and Weber (1981) Heinz (1984) Hochmut et al. (1987)	
Location: Munich, F.R.G.	Year of Completion: 1979
Environment: Urban	
Purpose: 2 track subway	
Excavation scheme: T2b	
Excavated Area (m ²): 88	Width (m): 13.1 Height (m): 8.3
Soil Cover (m): H/D < 2.5	
Ground Type: Stiff coherent, heterogeneous	
Ground Description: Tertiary clayey marl overlain by quaternary sands and gravels. Numerous water bearing sand lenses at section in question.	
Ground Properties: Bulk density = 21 kN/m ³ , E = 100-200 MPa c' = 40-80 kPa, ϕ' = 20-25° Ko = 0.5-0.8	
Tunnelman's Soft Ground Classification: Firm/Running	
Construction Procedure: Heading, bench and invert. Average round length 1.0m for heading and 2.0m for bench. First cell precedes second one by at least 10m.	
Initial Support: 20cm of shotcrete (15cm for temporary wall). Single wire mesh full circle. Steel ribs GI 110 spaced 0.8-1.0m in upper half of tunnel.	
Remarks: Forepoling used when sand at crown made it unstable.	

Table A.16 Data from case history No. 16

Case #16: Munich - Generic T2b Tunnel
References: Hochmut et al. (1987)
Location: Munich, F.R.G. Year of Completion: 1986 Environment: Urban Purpose: 2 track subway Excavation scheme: T2b Excavated Area (m ²): 64 Width (m): 9.0 Height(m): 8.5 Soil Cover (m): H/D < 2.5
Ground Type: Stiff coherent heterogeneous Ground Description: Tertiary clayey marl overlain by quaternary sands and gravels. Occasional water bearing sand lenses. Ground Properties: Bulk density=21kN/m ³ , E=100-200MPa c'=40-80kPa, ϕ' =20-25° Ko=0.5-0.8 Tunnelman's Soft Ground Classification: Firm/Running
Construction Procedure: Heading, bench and invert. Average round length 1.0m for heading and 2.0m for bench. First cell precedes second one by at least 10m.
Initial Support: 20cm of shotcrete (15cm for temporary wall). Single wire mesh full circle. Steel ribs GI 110 spaced 0.8-1.0m in upper half of tunnel.
Remarks: Forepoling used when sand at crown made it unstable, also grouting and freezing of this area discussed in paper.

Table A.17 Data from case history No. 17

Case #17: Vivenotgasse Tunnel	
References: Pelz and Deix (1985) Deix and Gebeshuber (1987) Welzig (1986) Döllnerl et al. (1976)	
Location: Vienna, Austria.	Year of Completion: 1987
Environment: Urban Sensitive	
Purpose: 2 track subway	
Excavation scheme: T2b	
Excavated Area (m ²): 64 Width (m): 9.5 Height (m): 8.3	
Soil Cover (m): 7.0	
Ground Type: Stiff coherent heterogeneous	
Ground Description: Clayey silts, sands and gravels, very heterogeneous. Pervious material is generally water bearing.	
Ground Properties: E = 20-50MPa, m.c. 22%, Cu variable (up to 250kPa)	
Tunnelman's Soft Ground Classification: Runni	
Construction Procedure: Heading precedes bench by 3-4m. Average round length 1.0m for heading and 2.0m for bench. First cell precedes second by about 20m. Very short invert closure.	
Initial Support: 25-28cm shotcrete. 2 layers of wire mesh (AQ60) full circle. Light steel ribs spaced 1.0m in average.	
Remarks: Compressed air used.	

Table A.18 Data from case history No. 18

Case #18: Hiraiashi No.1 Tunnel
<p>References:</p> <p>Golser (1981) Mussger (1981) Tobishima Co. (1982)</p>
<p>Location: 230km N of Tokyo, Japan Year of Completion: 1978 Environment: Non Urban Purpose: 2 track railway Excavation scheme: Tlb Excavated Area (m²): 90 Width (m):11.4 Height(m):10.0 Soil Cover (m): 1.5-7.0m</p>
<p>Ground Type: Stiff coherent heterogeneous Ground Description: Weathered granite with weaker clayey layers. No significant groundwater.</p> <p>Ground Properties: Bulk density = 13-17kN/m³; c'=20-40kPa; ϕ'=30-34° E=9-13MPa, m.c.=16-23%</p> <p>Tunnelman's Soft Ground Classification: Ravelling</p>
<p>Construction Procedure: Heading, bench and invert. Round length 0.8-1.2m for top heading and 2.0-2.5m for bench. Invert closed at about 2.5D behind face.</p>
<p>Initial Support: 25cm shotcrete. Single layer of Q188 mesh. Light steel ribs (H25: A=30cm², W=23.8kg/m), spaced 0.8-1.2m.</p>
<p>Remarks: Additional ground control: forepoling at crown, central support core at top heading, anchors.</p>

Table A.19 Data from case history No.19

<p>Case #19: Kokubu Tunnel</p>
<p>References: Fujimori et al. (1985)</p>
<p>Location: Matsudo, Japan Year of Completion: 1984 Environment: Non Urban Purpose: drainage Excavation scheme: T1b Excavated Area (m²): 60 Width (m):8.6 Height(m):8.3 Soil Cover (m): 5.0-20.0m</p>
<p>Ground Type: Sandy cohesionless Ground Description: Fine quaternary uniform sand. GW level ≈@ tunnel crown level. Impervious clay layer 2m below invert confines a second GW level. Ground Properties: Bulk density =18kN/m³; ϕ'=37° E=45MPa, N(SPT)=30-40, %clay+silt ≈ 6% Tunnelman's Soft Ground Classification: When m.c.<11%: running; when m.c.>20%:>stability due to capillarity (as described by authors)</p>
<p>Construction Procedure: Heading precedes bench by 18m.</p>
<p>Initial Support: 20cm shotcrete. 2 layers of welded wire mesh (1st Ø3.2- 50x50mm; 2nd Ø6.0-150x150mm (≈Q188). steel ribs H-125 spaced 90cm at crown and walls.</p>
<p>Remarks: Additional ground control: forepoling at crown, central support core at top heading, anchors, dewatering prior to excavation.</p>

Table A.20 Data from case history No.20

Case #20: Kuriyama - Yagiri No. 1 Tunnel
References: Horiuchi et al. (1986)
Location: Tokyo, Japan Year of Completion: 1984 Environment: Urban Purpose: 2 track railway Excavation scheme: T2a Excavated Area (m ²): 73 Width (m):10.2 Height(m):8.7 Soil Cover (m): 10.0m
Ground Type: Sandy cohesionless Ground Description: Uncemented horizontal layers of fine uniform sand. Highly permeable and deformable. Ground Properties: $\phi' = 31^\circ$, $e = 0.84 - 1.05$, m.c. = 15-35% Tunnelman's Soft Ground Classification: ?
Construction Procedure: Heading and bench. Length of top heading \approx 15m
Initial Support: 20cm shotcrete, 2 layers of wire mesh (?), H-shaped steel ribs (150mm) except at invert
Remarks: Main heading further subdivided in 11 stages, each one advanced 1.0m with immediate application of chemical coating before shotcreting.

Table A.21 Data from case history No.21

Case #21: Kuriyama - Yagiri No. 2 Tunnel
References: Horiuchi et al. (1986)
Location: Tokyo, Japan Year of Completion: 1984 Environment: Urban Purpose: Station Excavation scheme: T3 Excavated Area (m ²): 90 Width (m): 12.4 Height (m): 8.9 Soil Cover (m): 8.5-10.5m
Ground Type: Sandy cohesionless Ground Description: Uncemented horizontal layers of fine uniform sand. Highly permeable and deformable. Ground Properties: $\phi' = 31^\circ$, $e = 0.84-1.05$, $m.c. = 15-35\%$ Tunnelman's Soft Ground Classification: ?
Construction Procedure: Heading with more than one bench in each cell.
Initial Support: 20cm shotcrete (15cm in side drifts), 2 layers of wire mesh (?), 150mm H-shaped steel ribs spaced 1.0m
Remarks: Top heading of central portion further subdivided into 5 smaller steps with immediate application of chemical coating before shotcreting.

Table A.22 Data from case history No.22

Case #22: Narita airport Tunnel (Section 9)
<p>References:</p> <p>Horiuchi et al. (1986)</p>
<p>Location: Tokyo, Japan Year of Completion: 1984</p> <p>Environment: Urban</p> <p>Purpose: 2 track railway</p> <p>Excavation scheme: T2a</p> <p>Excavated Area (m²): 130. Width (m):13.4 Height(m):11.2</p> <p>Soil Cover (m): = 9.0m</p>
<p>Ground Type: Sandy cohesionless</p> <p>Ground Description: Uncemented uniform sandy soils</p> <p>Ground Properties:</p> <p> N (SPT) = 10-40</p> <p> % silt+clay < 10%</p> <p>Tunnelman's Soft Ground Classification: ?</p>
<p>Construction Procedure:</p> <p>Upper half (69.5m²) further subdivided into heading and bench. Temporary invert closed at about 12.5m from face.</p>
<p>Initial Support:</p> <p>20cm shotcrete on roof and walls (15cm? in temporary walls)</p>
<p>Remarks:</p> <p>Top heading of central portion further subdivided into 5 smaller steps with immediate application of chemical coating before shotcreting.</p>

Table A.23 Data from case history No.23

Case #23: Hokushin Tunnel (#1)
References: Matsusita and Shimizu (1986)
Location: Kobe, Japan Year of Completion: 1985 Environment: Urban Sensitive Purpose: 2 track railway Excavation scheme: T1b Excavated Area (m ²): 70 Width (m):10.4 Height(m):8.5 Soil Cover (m): ≈ 12.0m
Ground Type: Coarse grained coherent. Ground Description: Quaternary gravel fan deposits and dense sands (SPT>50) Ground Properties: N.A. Tunnelman's Soft Ground Classification: ?
Construction Procedure: Heading, bench and invert. Round length for heading=0.8m.
Initial Support: 20cm shotcrete, 1 layer of wire mesh (Ø3.2x100x100mm in upper half section only)
Remarks: Additional ground control: central support core, anchors and forepoling. Pre-construction grouting of sensitive areas.

Table A.24 Data from case history No.24

Case #24: Hokushin Tunnel (#2)
References: Matsusita and Shimizu (1986)
Location: Kobe, Japan Year of Completion: 1985 Environment: Urban Sensitive Purpose: 2 track railway Excavation scheme: T2a Excavated Area (m ²): 70 Width (m):10.4 Height(m):8.5 Soil Cover (m): = 12.0m
Ground Type: Coarse grained coherent Ground Description: Quaternary gravel fan deposits and dense sands (SPT>50) Ground Properties: N.A. Tunnelman's Soft Ground Classification: ?
Construction Procedure: Heading, bench and invert. Round length for heading=0.8m. Temporary shotcrete invert adopted (Scheme T2a) after interpretation of field measurements)
Initial Support: 20cm shotcrete, 1 layer of wire mesh (Ø3.2x100x100mm in upper half section only)
Remarks: Additional ground control: central support core, anchors and forepoling. Pre-construction grouting of sensitive areas. One section under river.

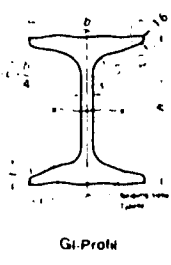
Table A.25 Data from case history No.25

Case #25: Ran-Hokke Tunnel
<p>References:</p> <p>Miyazaki (1982)</p> <p>Gomi and Higo (1984)</p>
<p>Location: Noboribetsu, Japan Year of Completion: 1981</p> <p>Environment: Non Urban</p> <p>Purpose: 2 track railway</p> <p>Excavation scheme: T1a</p> <p>Excavated Area (m²): 70 Width (m): 9.7 Height(m): 8.5</p> <p>Soil Cover (m): ≈ 20.0m</p>
<p>Ground Type: Coarse grained cohesionless</p> <p>Ground Description: Volcanic deposits</p> <p>Ground Properties:</p> <p>N(SPT)=30-35</p> <p>c'=0.5kg/cm², φ'=35-45°</p> <p>20% gravel, 62% sand</p> <p>Tunnelman's Soft Ground Classification: ?</p>
<p>Construction Procedure:</p> <p>Heading and 2 benches. Invert closed @ 40-60m from face</p>
<p>Initial Support:</p> <p>25cm shotcrete, 1 layer wire mesh (Ø4x150x150mm)</p> <p>steel ribs H125 spaced 1.00-1.20m, grouted anchors (Ø24mm, l=4.0m) at crown and sides</p>
<p>Remarks:</p> <p>Additional ground control: central support core, forepo- ling.</p>

Table A.26 Commonly used welded wire steel mesh sizes
(adapted from Beton-Kalender, 1981)

Länge Breite	Randeinsparung (Langrichtung)	Matten- be- zeichnung	Mattenaufbau in Langrichtung Querichtung				Quer- schnitte lang quer	Gewichte	
			Stab- ab- stände	Stabdurchmesser Innen- bereich	Stabdurchmesser Rand- bereich	Anzahl der Langrandstäbe links		Anzahl der Langrandstäbe rechts	je Matte
m			mm	mm		cm ² /m	kg		
5,00 2,15	ohne	Q 131	150 · 5,0 150 · 5,0			1,31 1,31	22,5	2,09	
		Q 188	150 · 6,0 150 · 6,0			1,88 1,88	32,4	3,01	
	mit	Q 221	150 · 6,5 / 5,0 - 4 / 4 150 · 6,5			2,21 2,21	33,7	3,14	
		Q 257	150 · 7,0 / 5,0 - 4 / 4 150 · 7,0			2,57 2,57	38,2	3,55	
		Q 377	150 · 8,0d / 6,0 - 4 / 4 150 · 8,5			3,77 3,78	56,0	5,21	
		Q 513	150 · 7,0d / 7,0 - 4 / 4 100 · 8,0			5,13 5,03	90,0	6,97	
6,00 2,15									

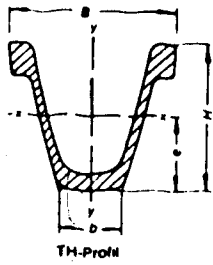
Table A.27 Commonly used steel sets (modified after Maidl, 1984:354)



Stahlbögen Technische Daten der GI-Profile

GI-Profile	h	b	s	t	r ₁	r ₂	Nerigung %	Querschnitt F cm ²	Gewicht (7,85 kg/dm ³) kg/m	Statische Werte für die Biegeachse					
										J _x cm ⁴	J _y cm ⁴	W _x cm ³	W _y cm ³	i _x cm	i _y cm
GI 100	100	80	9	12,5	15			26,4	20,7	403	80,7	3,91	80,5	20,1	1,75
GI 110	110	84	10	14	14			31,1	24,5	570	103	4,28	103	24,5	1,82
GI 120	120	92	11	15,5	14		33	37,6	29,5	816	136	4,66	150	32,6	2,00
GI 130	130	100	12	17	14			44,8	35,0	1130	175	5,05	211	42,3	2,18
GI 140	140	110	12	19	14			53,0	41,6	1586	227	5,47	315	57,3	2,44

Stahlbögen Technische Daten der TH-Profile



TH-Profile	kg/m	Typ	13	16	21	25	29	36	44
			48	48	58	58	58	58	58
Höhe	H	mm	85	89	108	118	124	138	147,8
Breite	B	mm	98	98	124	135	151	171	172
Breite	b	mm	36	36	35	38	44	51	50
Fläche	A	cm ²	16	20	27	32	37	46	56
Gewicht	G	kg/m	13	16	21	25	29	36	44
Trägheitsmoment	J _x	cm ⁴	137	176	341	484	616	972	1265
	J _y	cm ⁴	150	196	398	560	775	1264	1564
Widerstandsmoment	w _x	cm ³	32	40	61	80	94	137	174
	w _y	cm ³	31	40	64	83	103	148	182
Abstand der neutr. Faser	e	mm	41,9	44,35	52,4	57,5	58,2	66,8	72,3

Appendix B - Settlement Points Readings

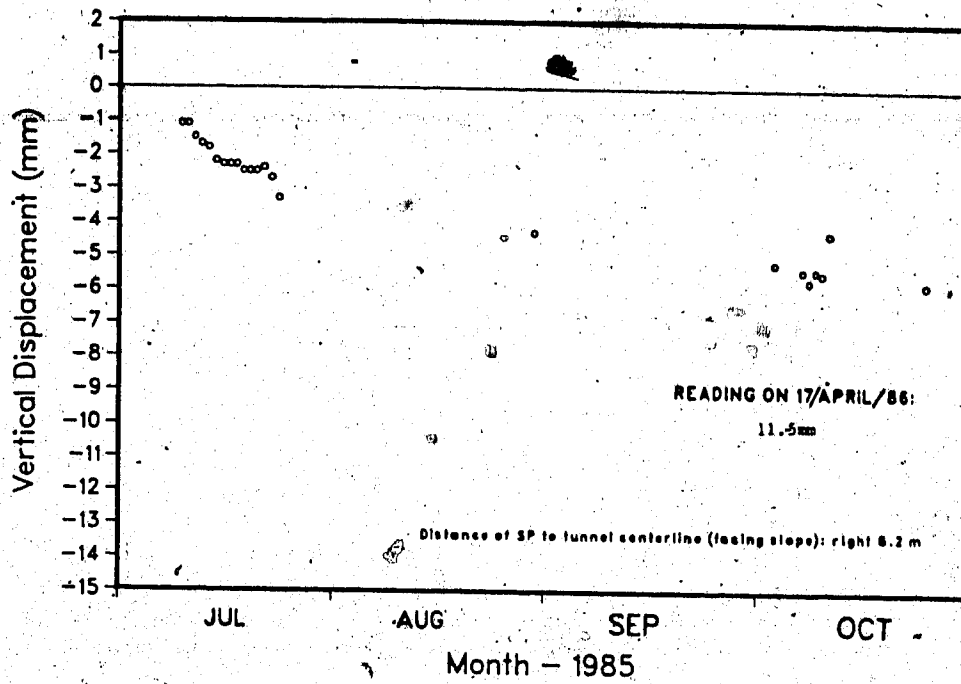


Figure B1 - Evolution of surface settlement with time - SP1

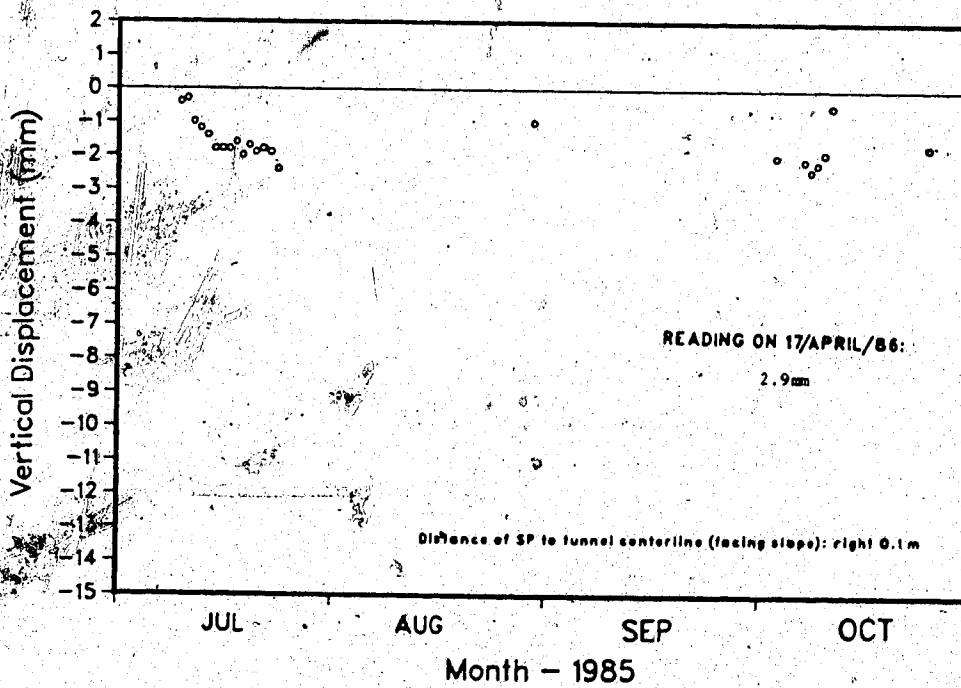


Figure B2 - Evolution of surface settlement with time - SP2

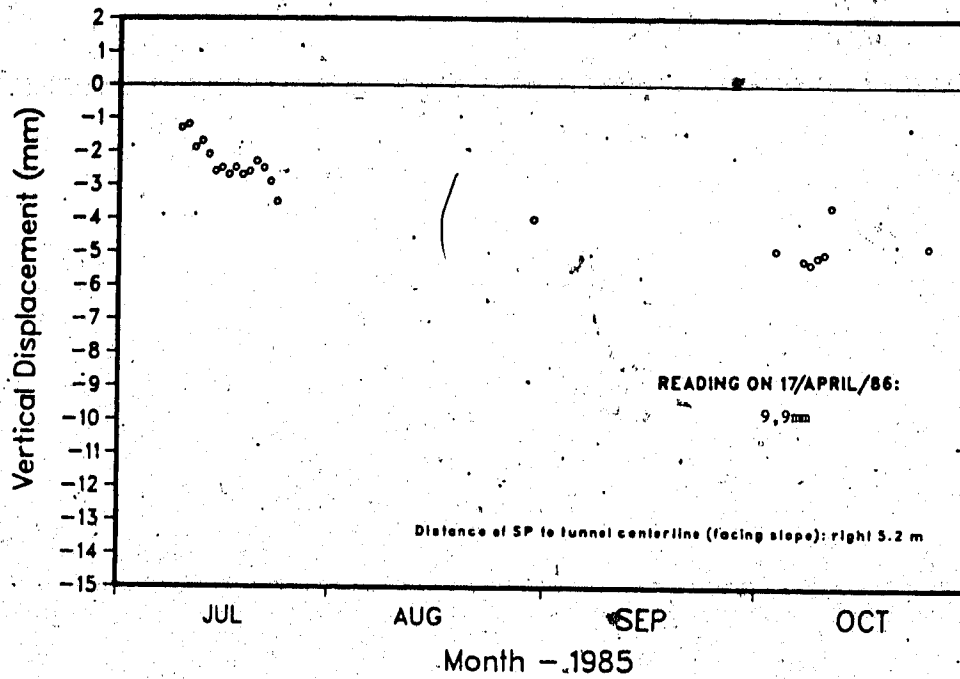


Figure B3 - Evolution of surface settlement with time - SP3

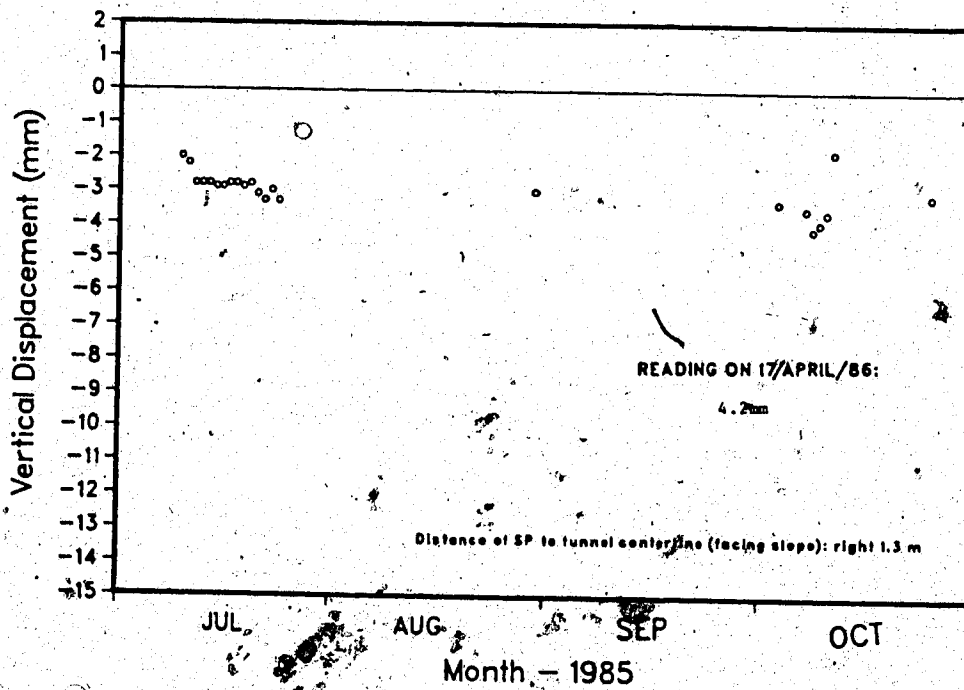


Figure B4 - Evolution of surface settlement with time - SP4

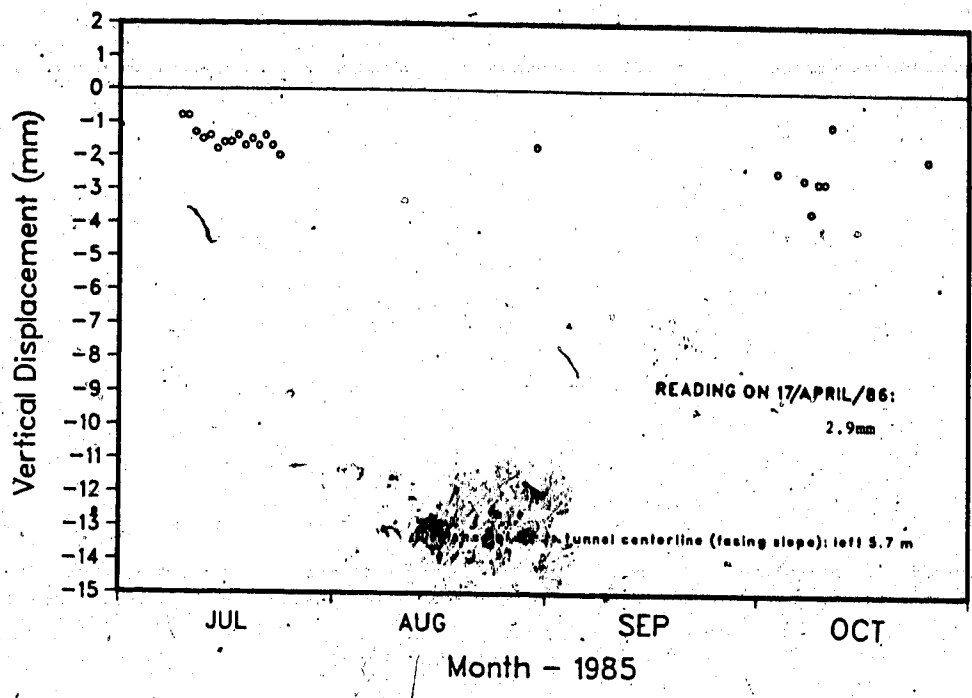


Figure B5. - Evolution of surface settlement with time - SP5

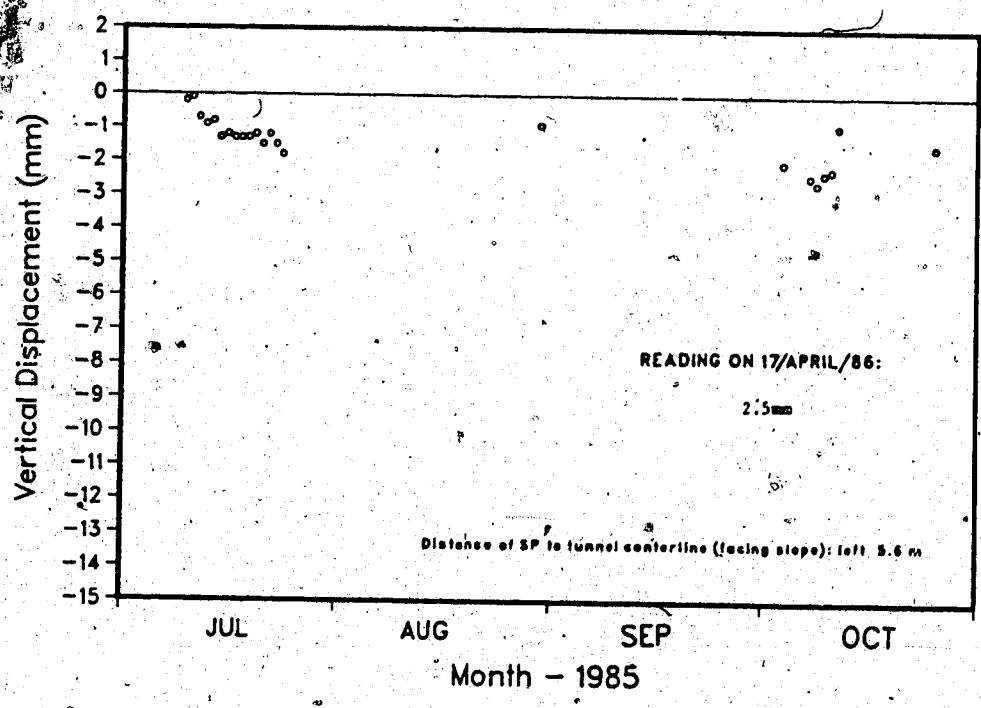


Figure B6 - Evolution of surface settlement with time - SP6

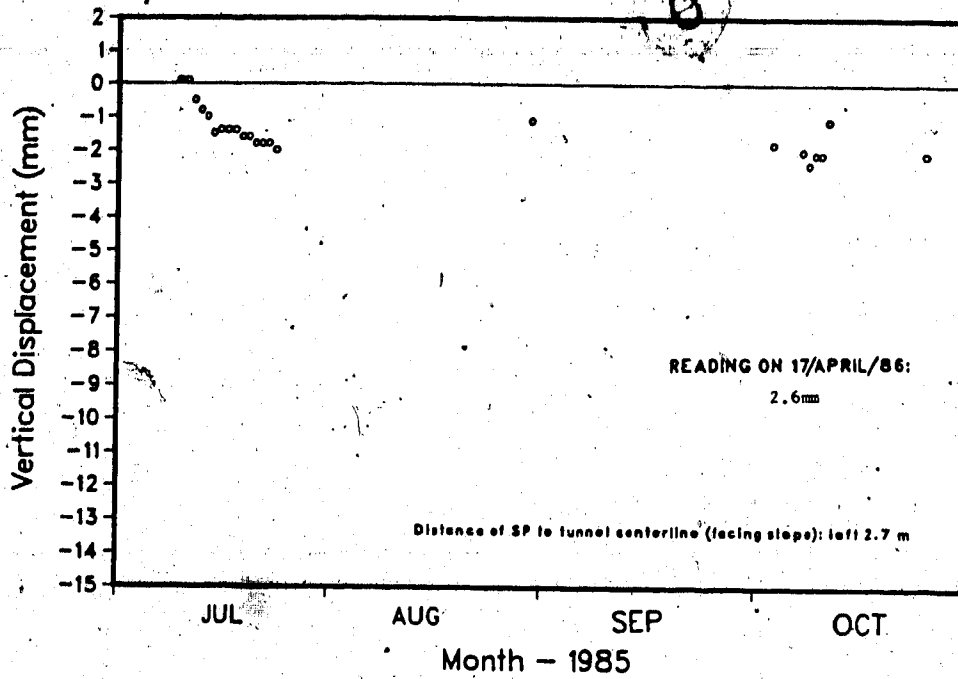


Figure B7 - Evolution of surface settlement with time - SP7

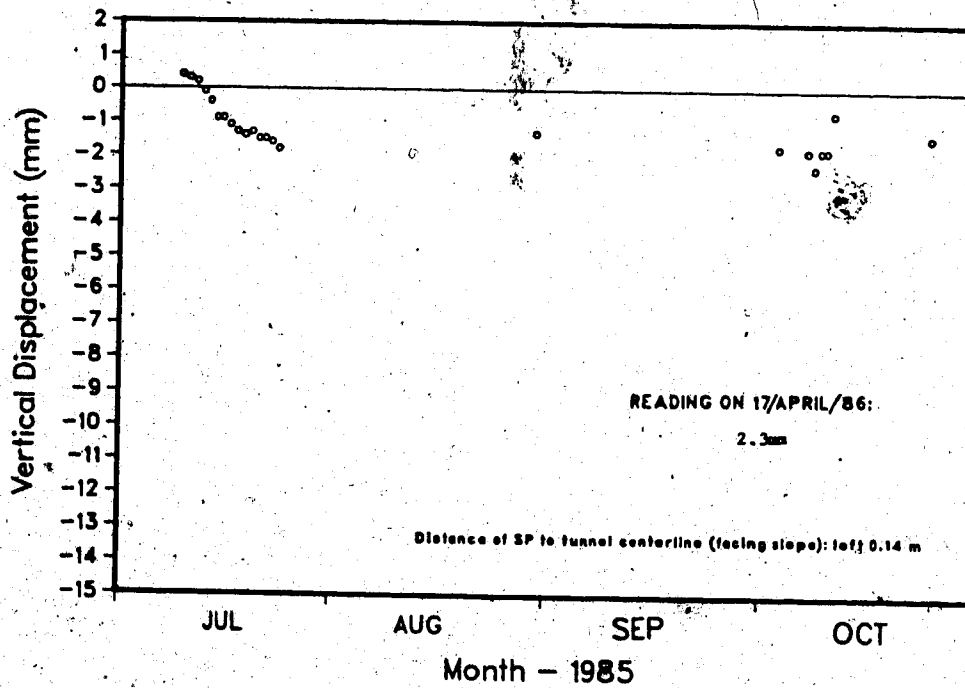


Figure B8 - Evolution of surface settlement with time - SP8

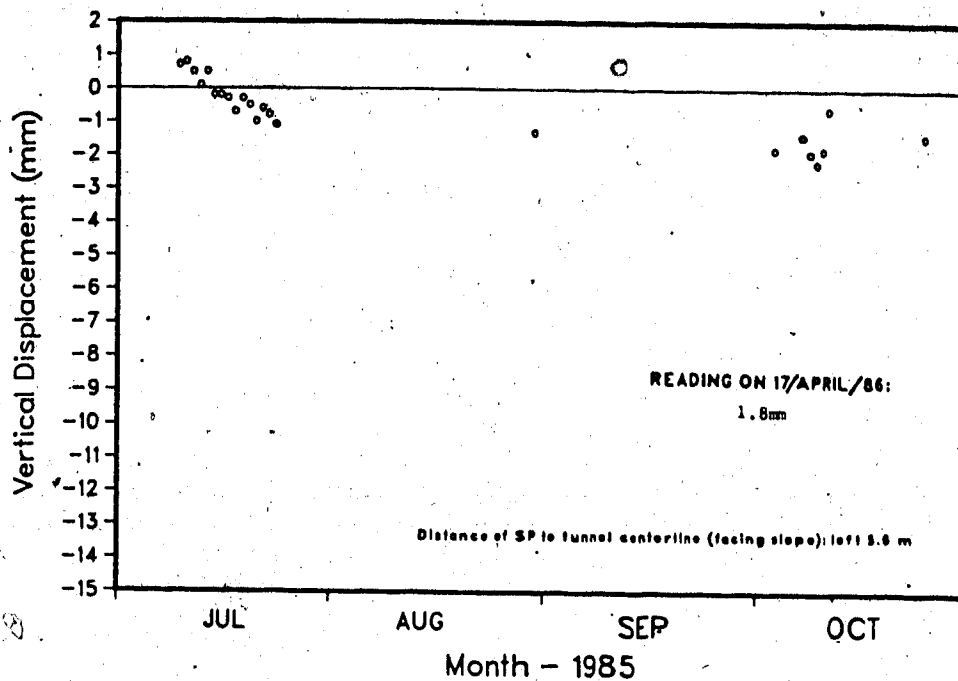


Figure B9 - Evolution of surface settlement with time - SP9

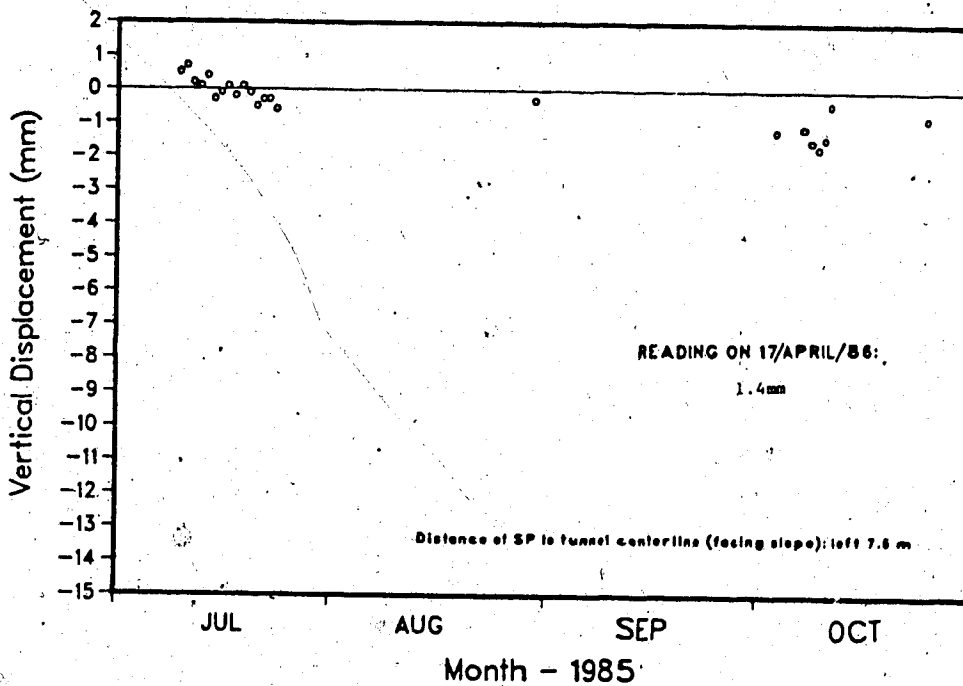


Figure B10 - Evolution of surface settlement with time - SP10

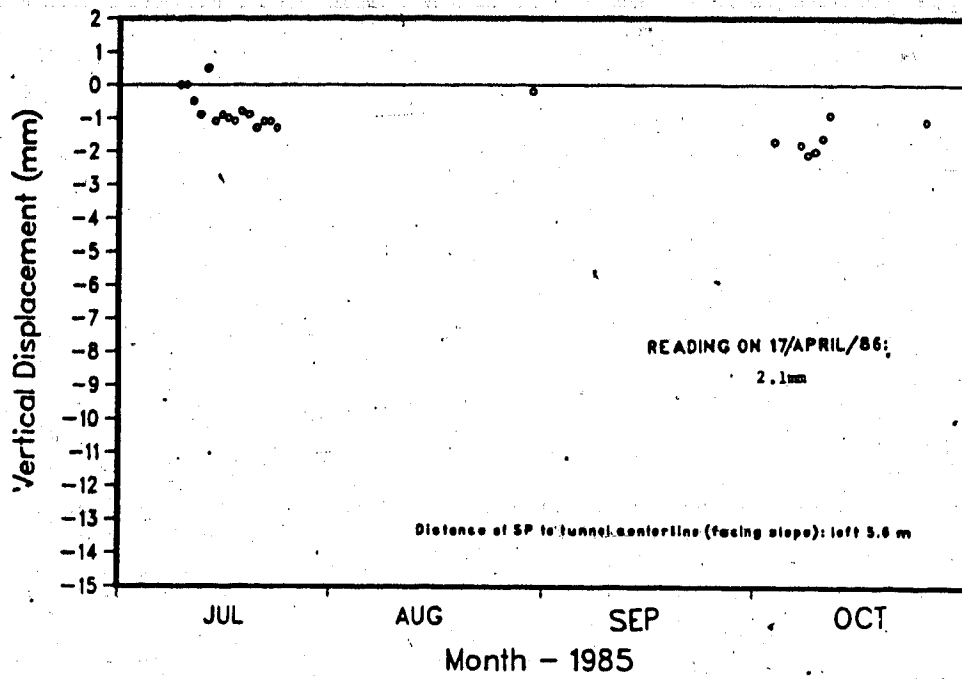


Figure B11 - Evolution of surface settlement with time - SP11.

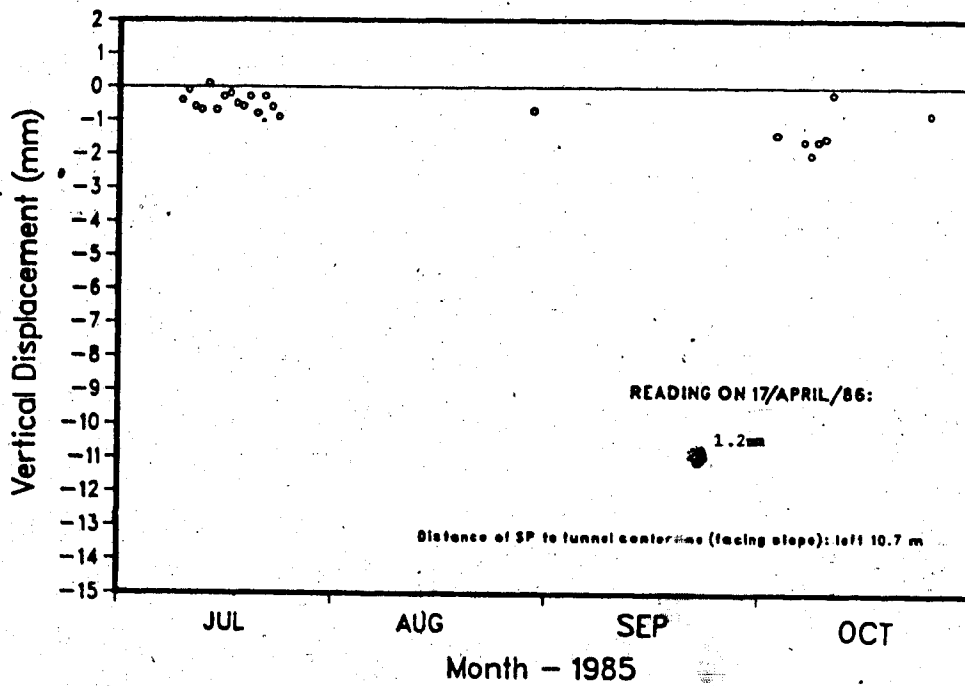


Figure B12 - Evolution of surface settlement with time - SP12

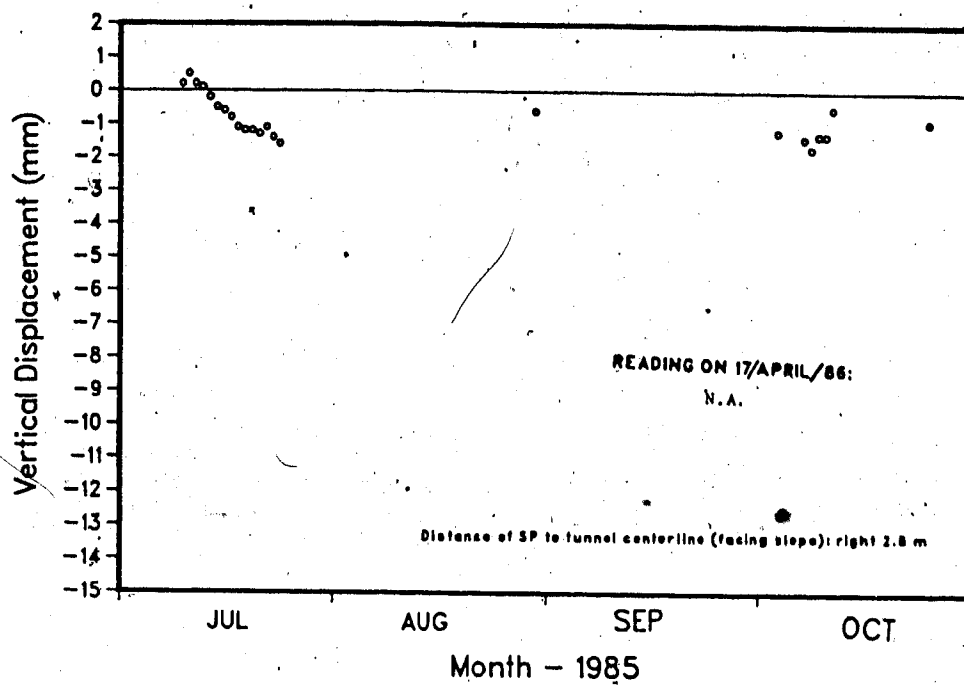


Figure B13 - Evolution of surface settlement with time - SP13

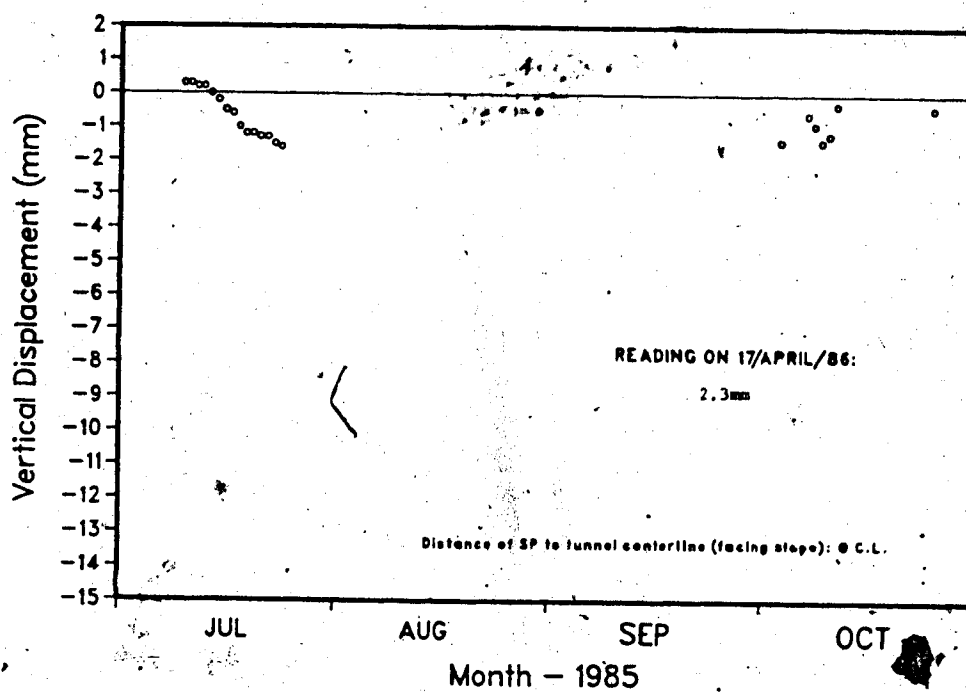


Figure B14 - Evolution of surface settlement with time - SP14

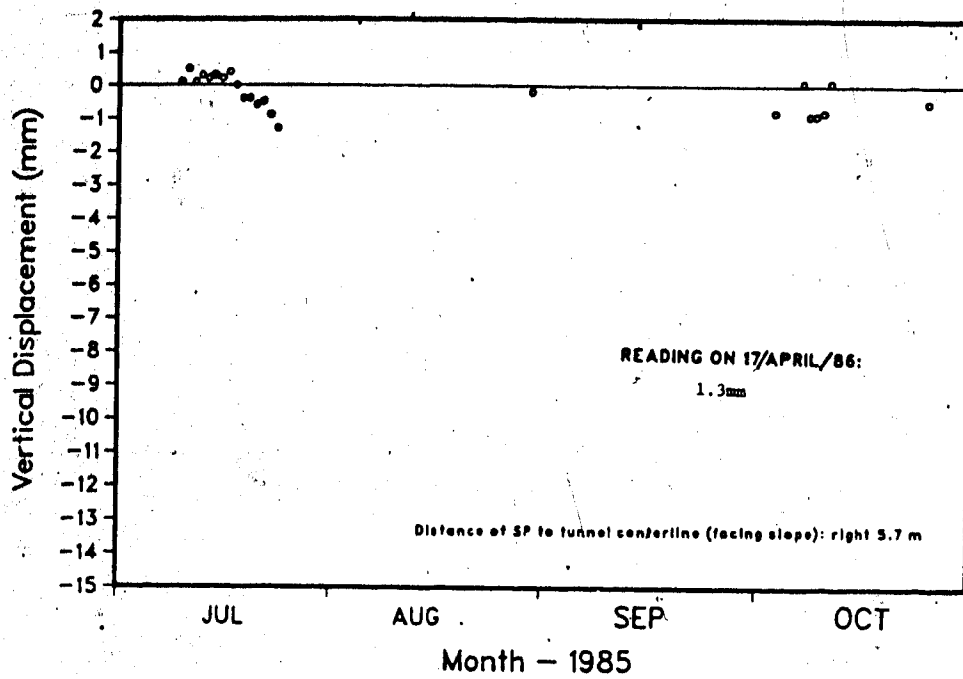


Figure B15 - Evolution of surface settlement with time - SP15

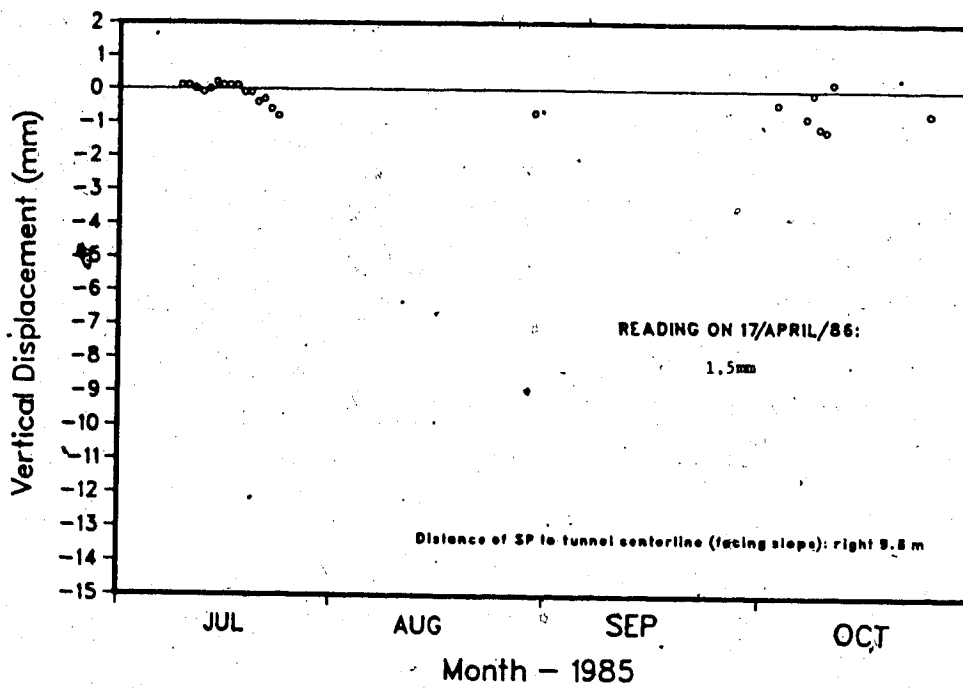


Figure B16 - Evolution of surface settlement with time - SP16

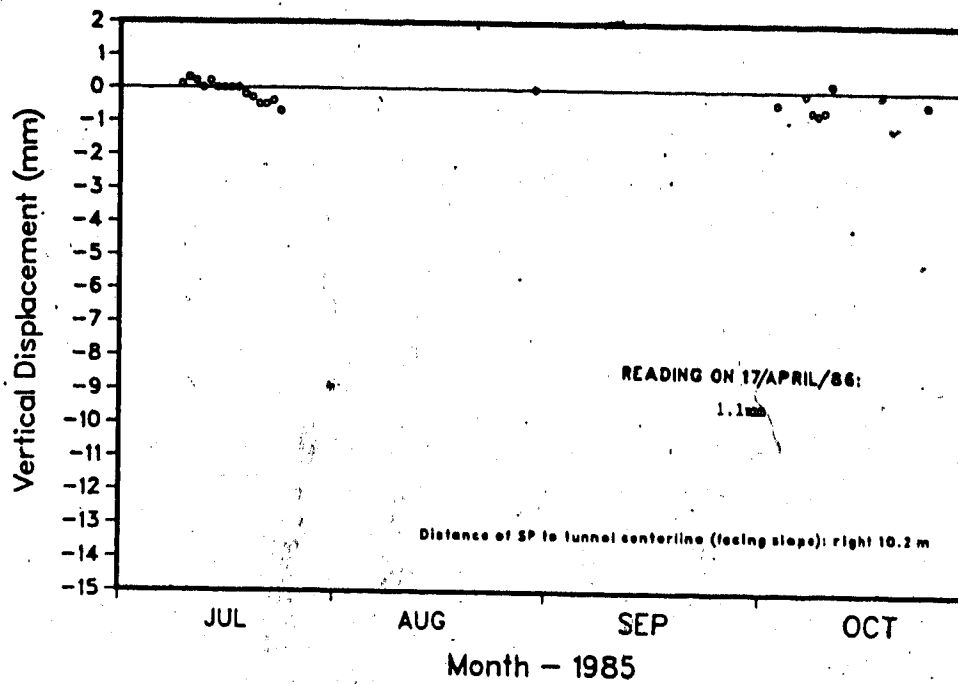


Figure B17 - Evolution of surface settlement with time - SP17

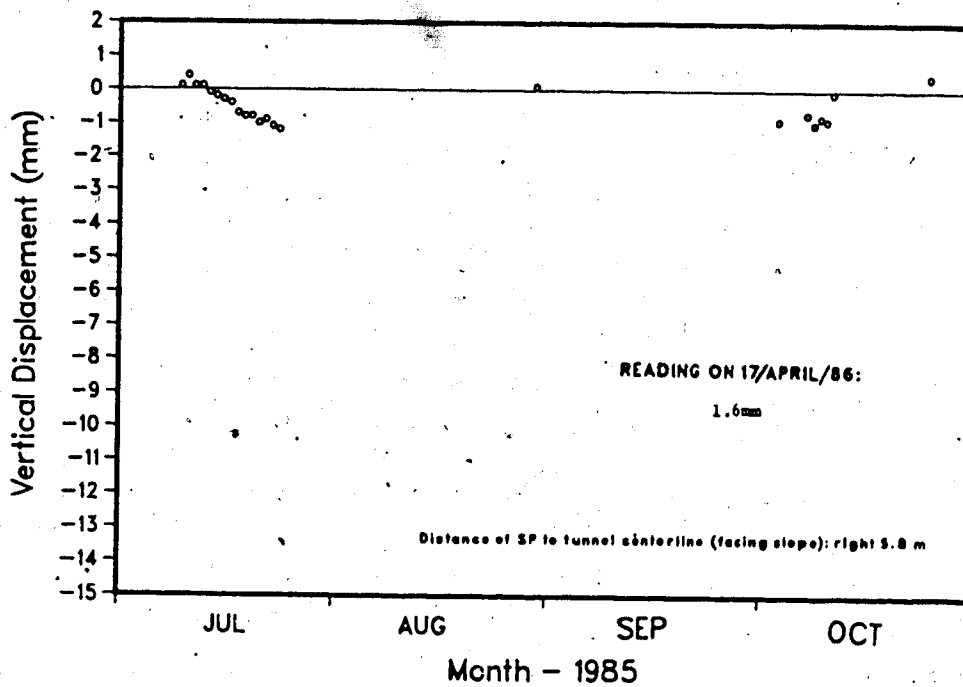


Figure B18 - Evolution of surface settlement with time - SP18

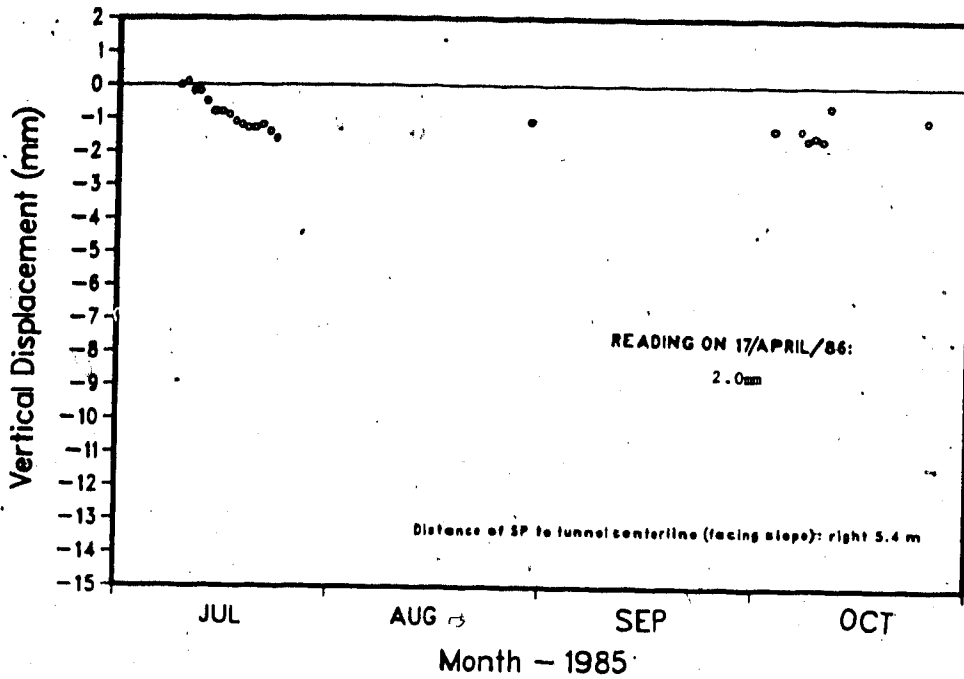


Figure B19 - Evolution of surface settlement with time - SP19

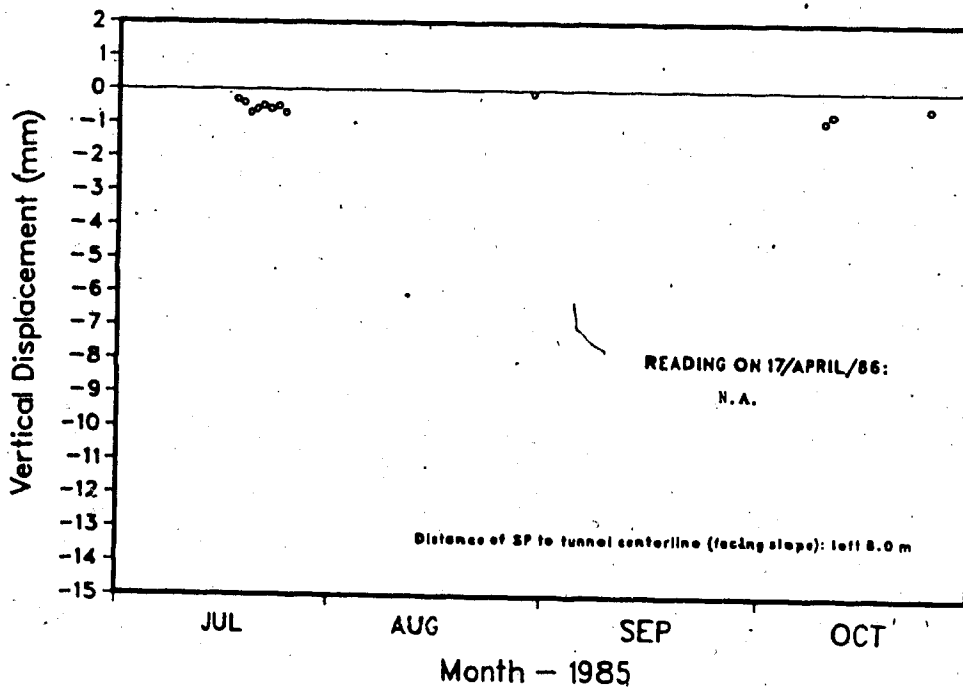


Figure B20 - Evolution of surface settlement with time - SP20

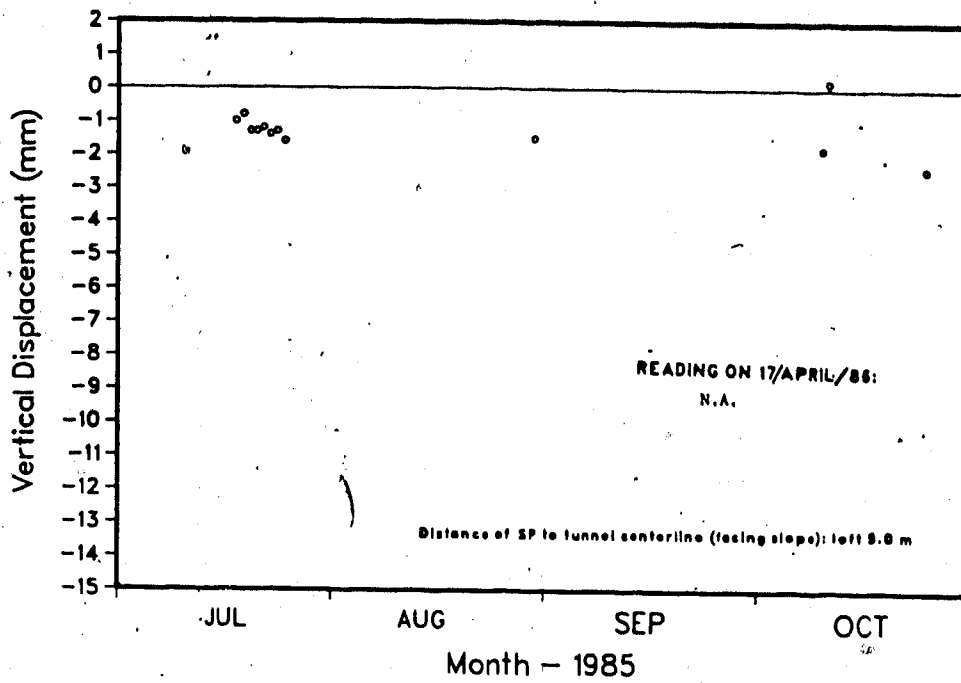


Figure B21 - Evolution of surface settlement with time - SP21

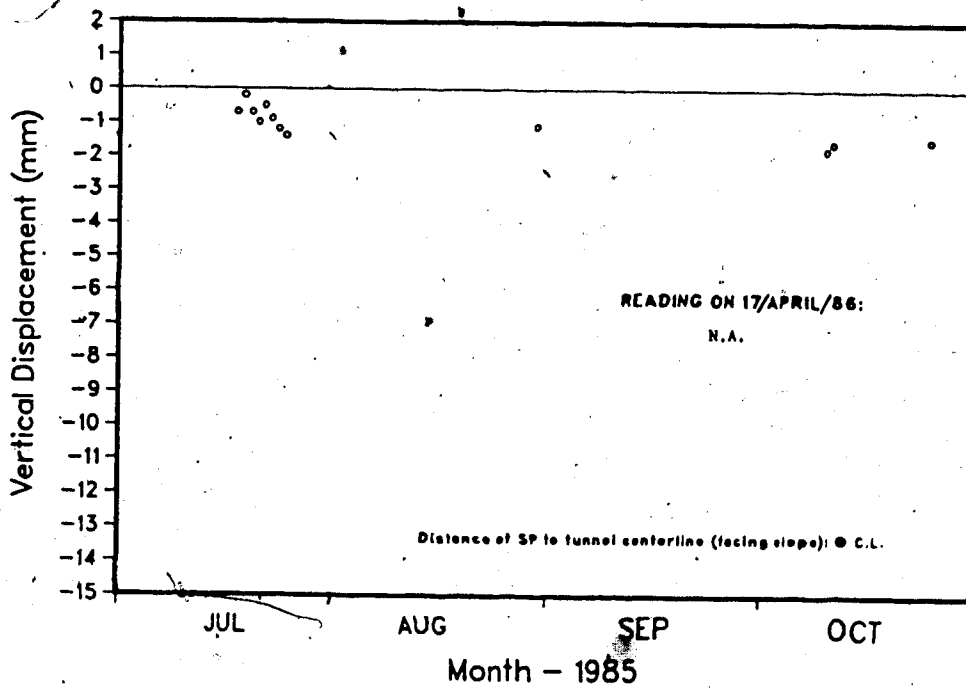


Figure B22 - Evolution of surface settlement with time - SP22

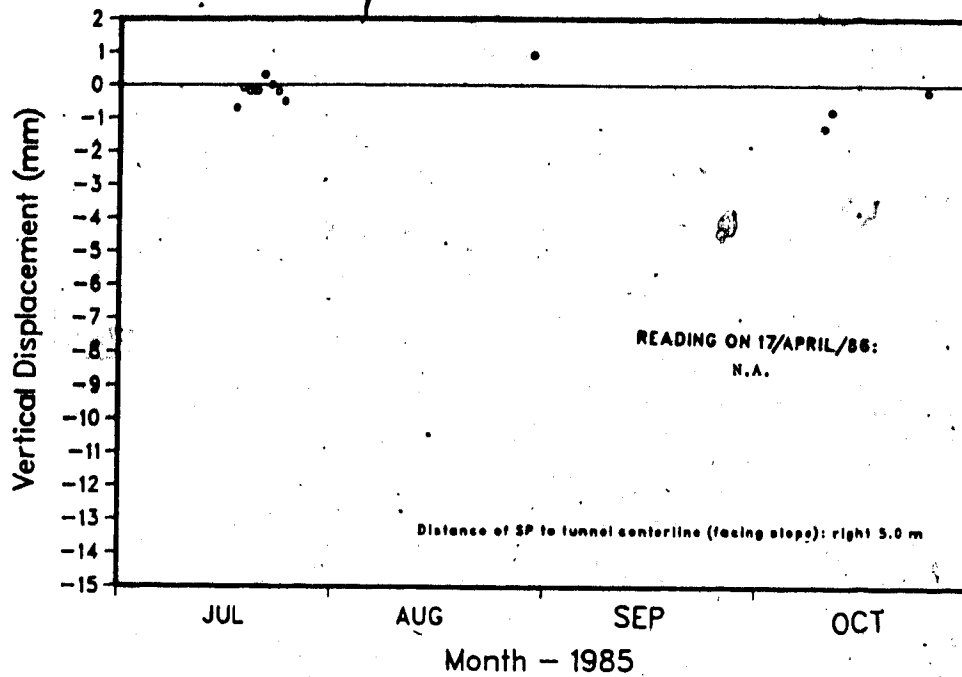


Figure B23 - Evolution of surface settlement with time - SP23

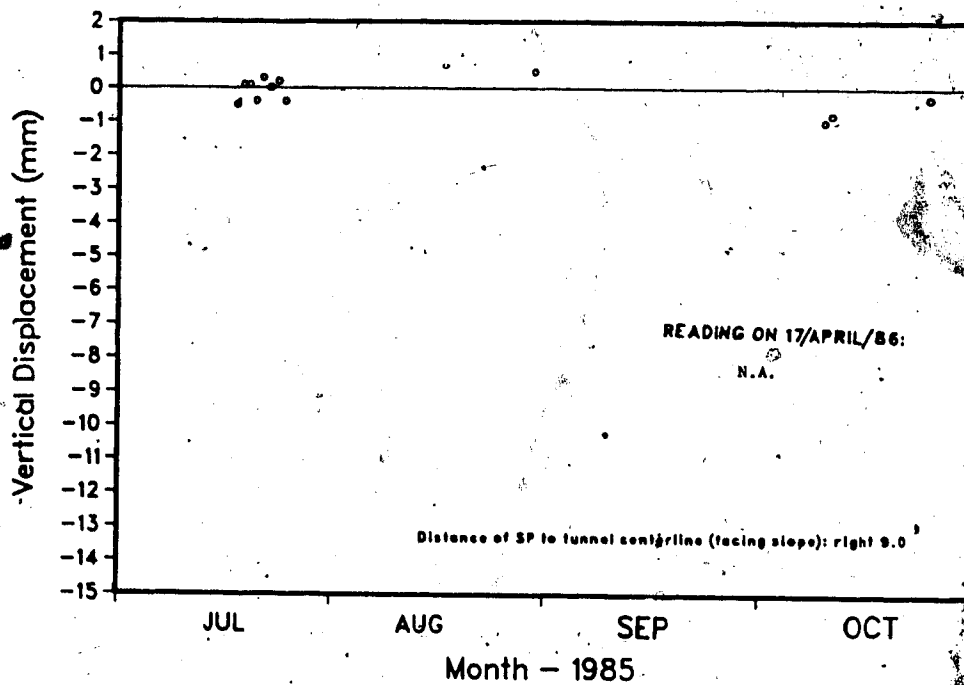


Figure B24 - Evolution of surface settlement with time - SP24

Appendix C - Multipoint Extensometers Readings

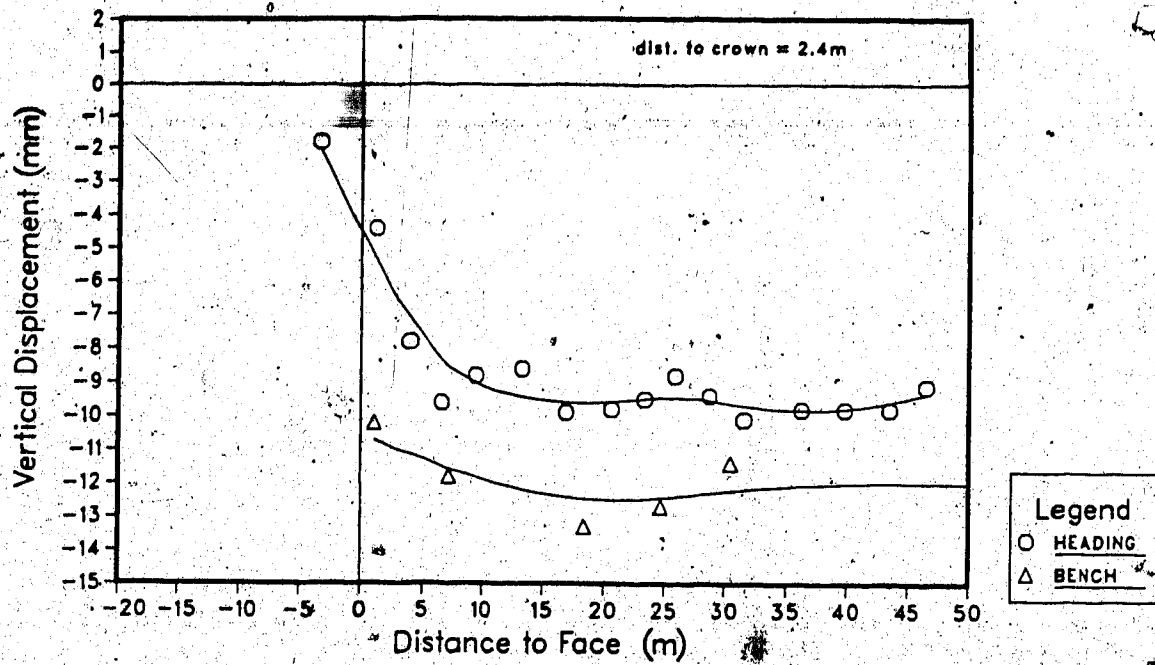


Figure C1 - Longitudinal distribution of displacements ME1 #1

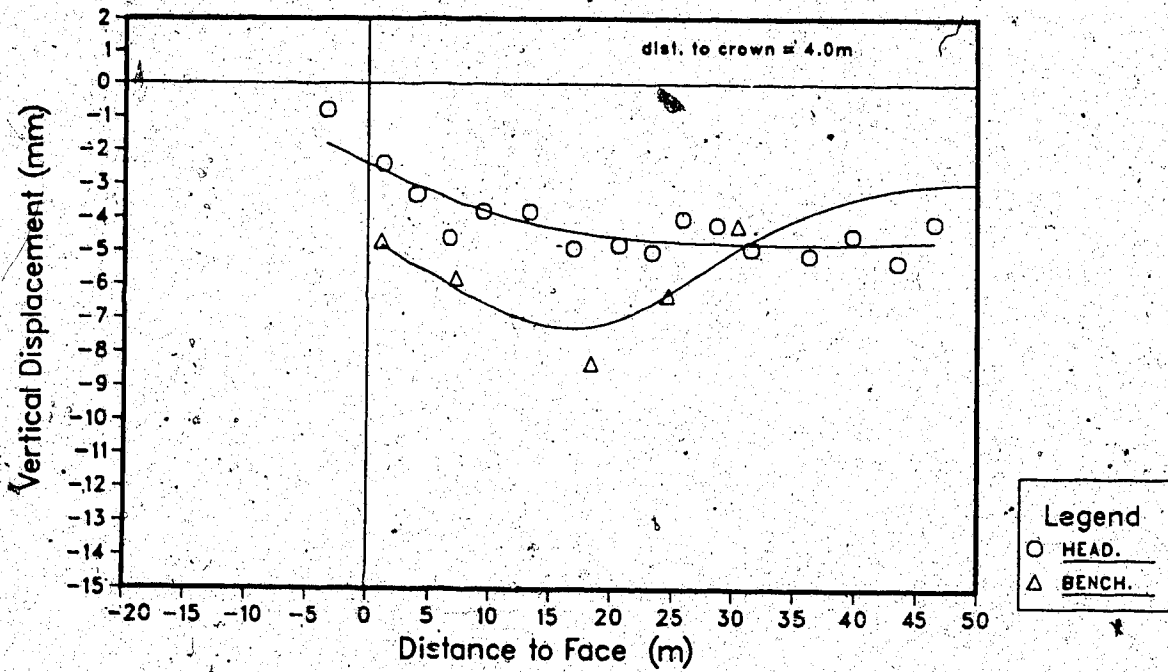


Figure C2 - Longitudinal distribution of displacements ME1 #2

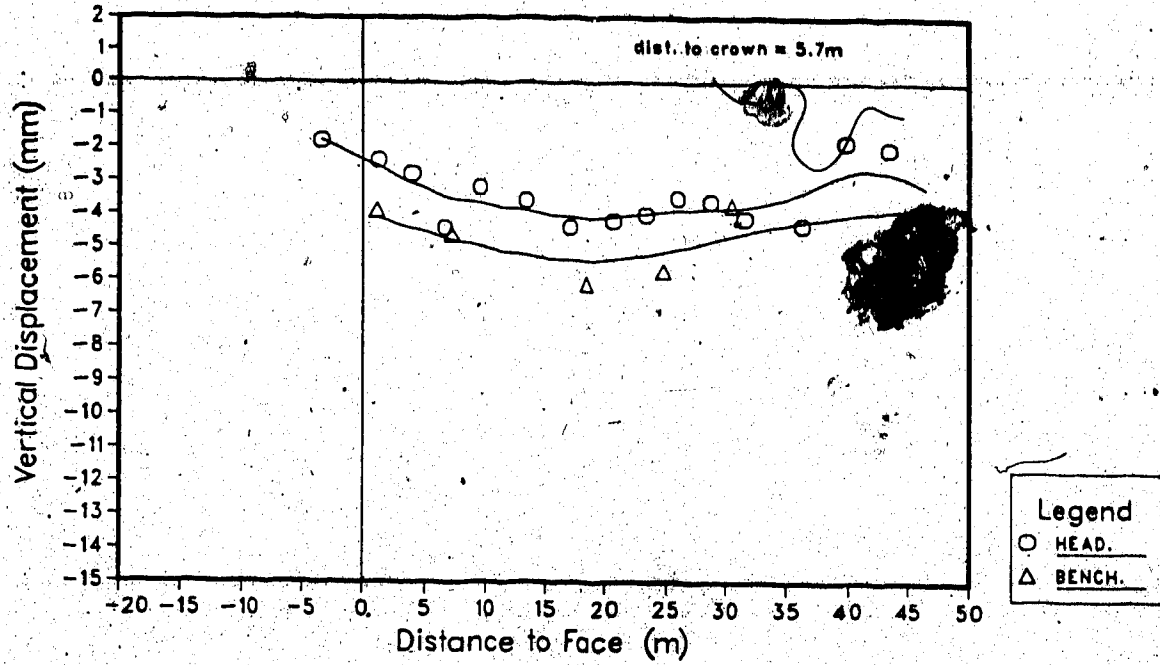


Figure C3 - Longitudinal distribution of displacements ME1 #3

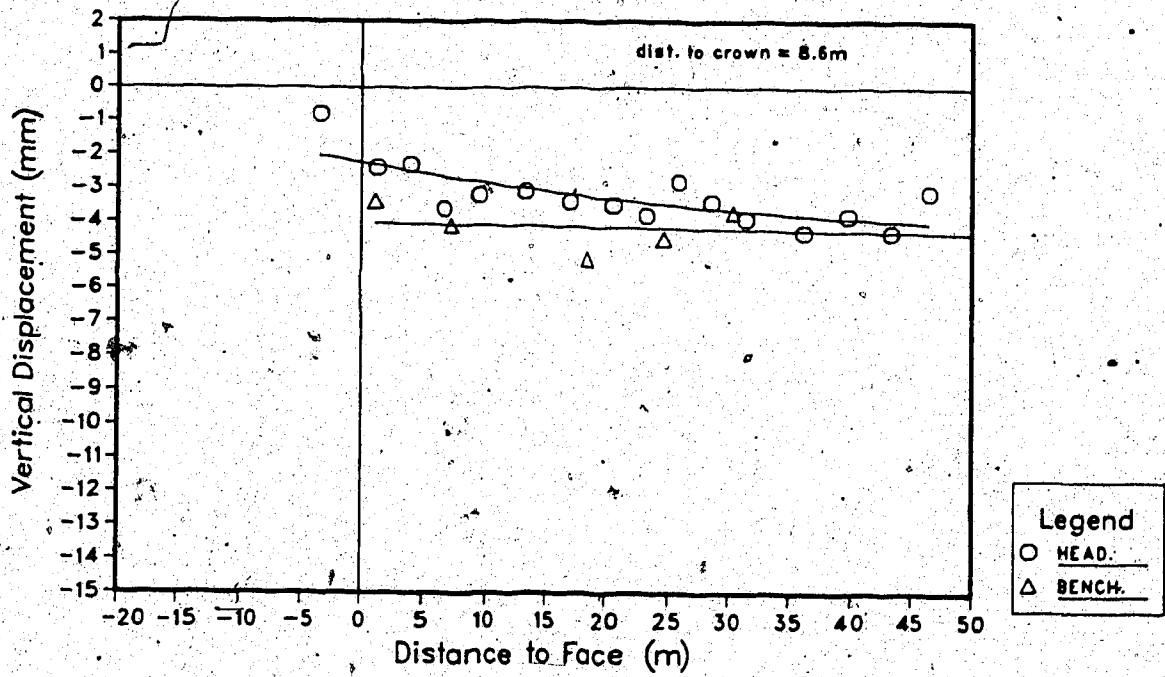


Figure C4 - Longitudinal distribution of displacements ME1 #4

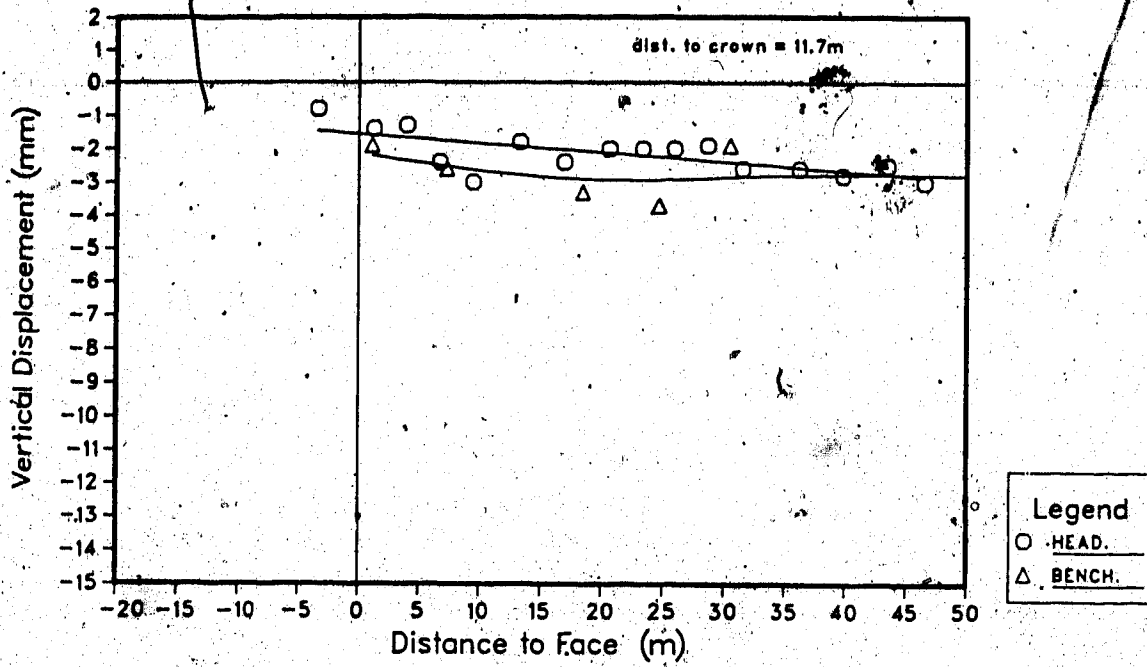


Figure C5 - Longitudinal distribution of displacements ME1 #5

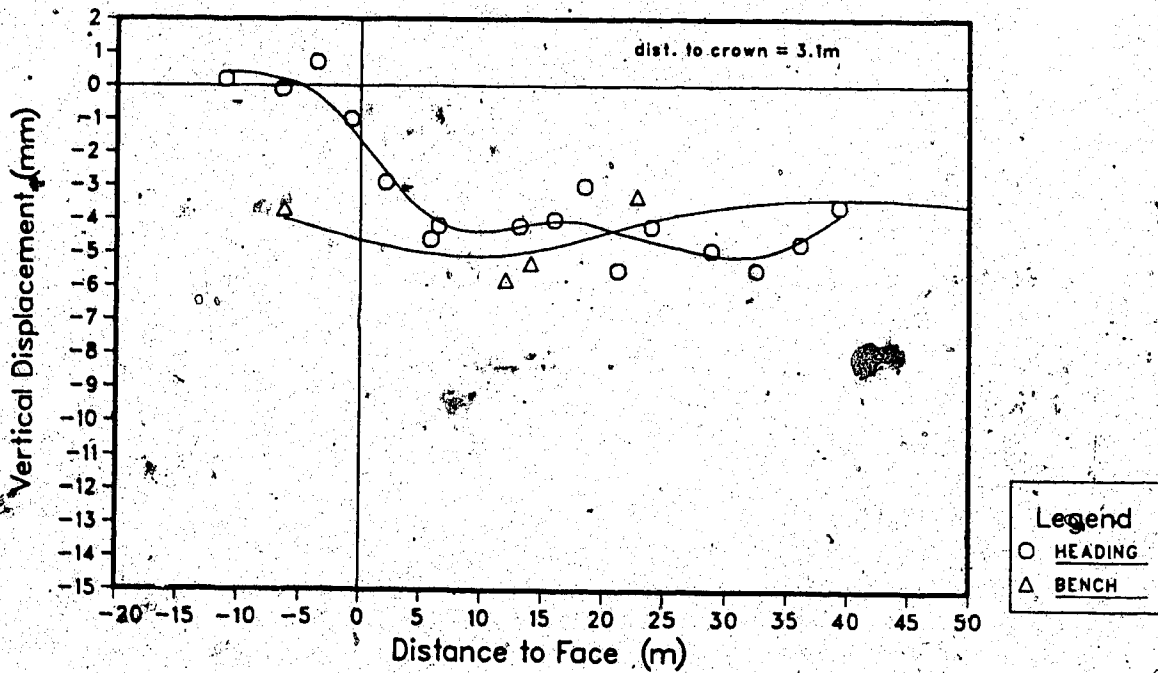


Figure C6 - Longitudinal distribution of displacements ME2 #1

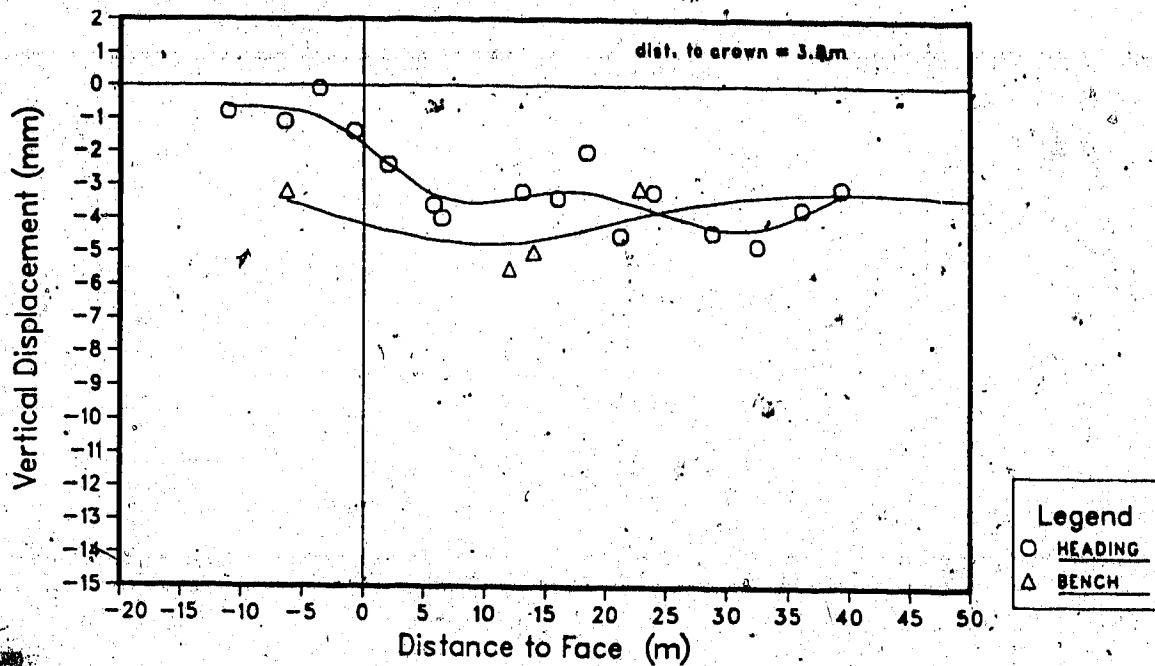


Figure C7 - Longitudinal distribution of displacements ME2 #2

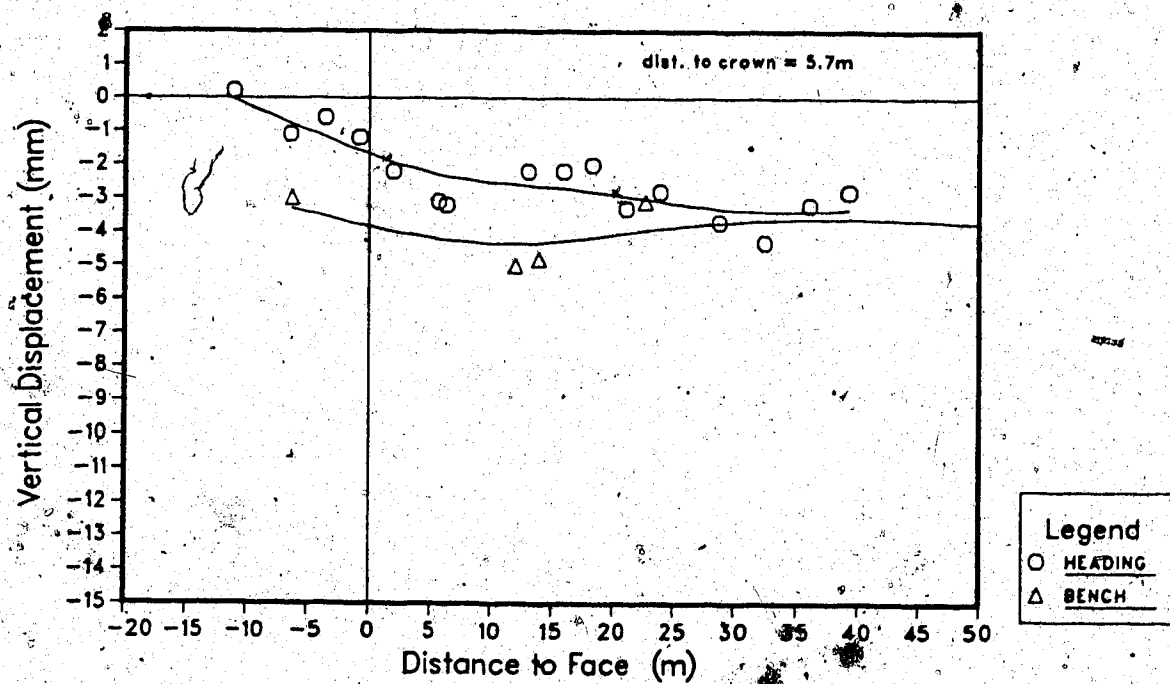


Figure C8 - Longitudinal distribution of displacements ME2 #3

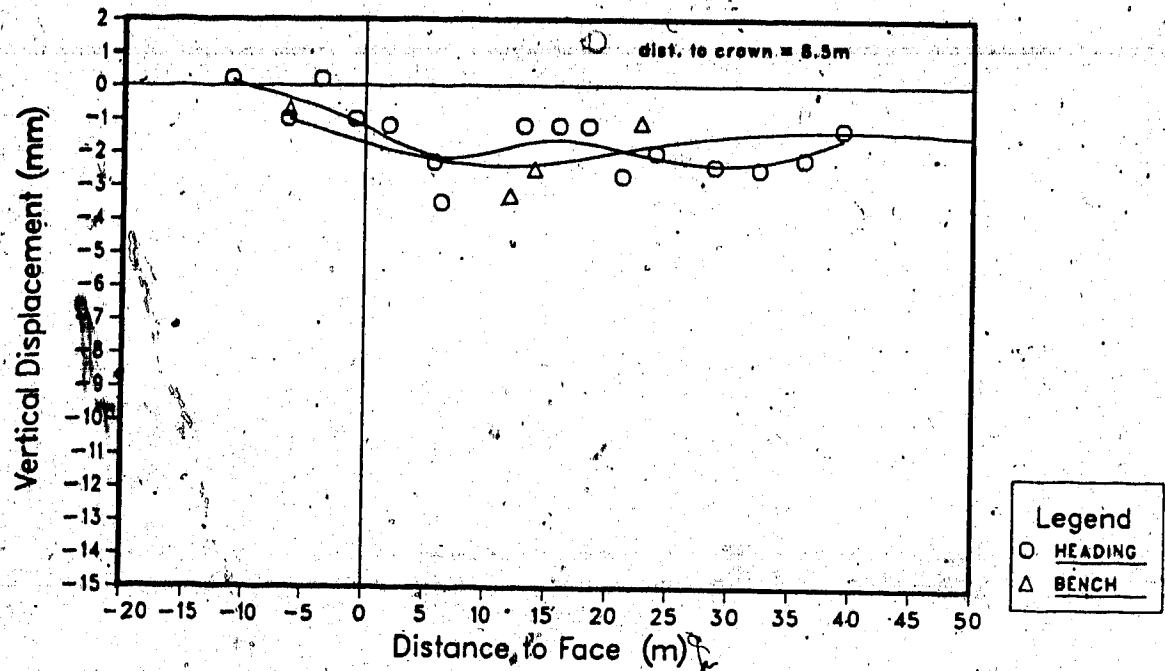


Figure C9 - Longitudinal distribution of displacements ME2 #4

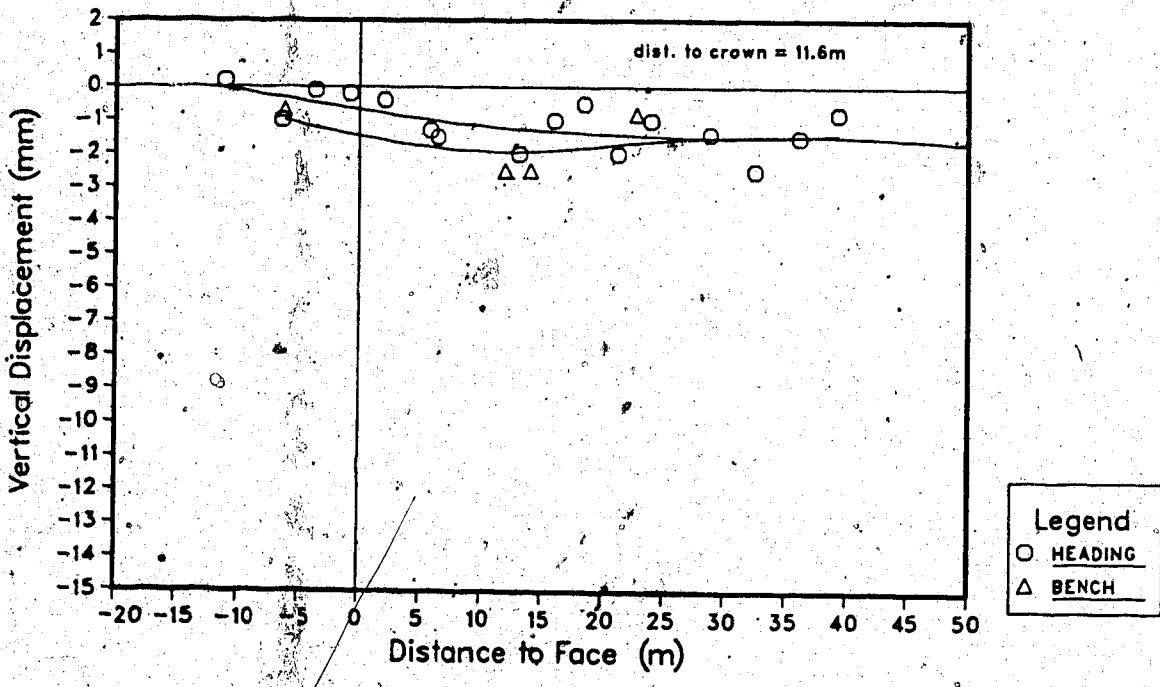


Figure C10 - Longitudinal distribution of displacements ME2 #5

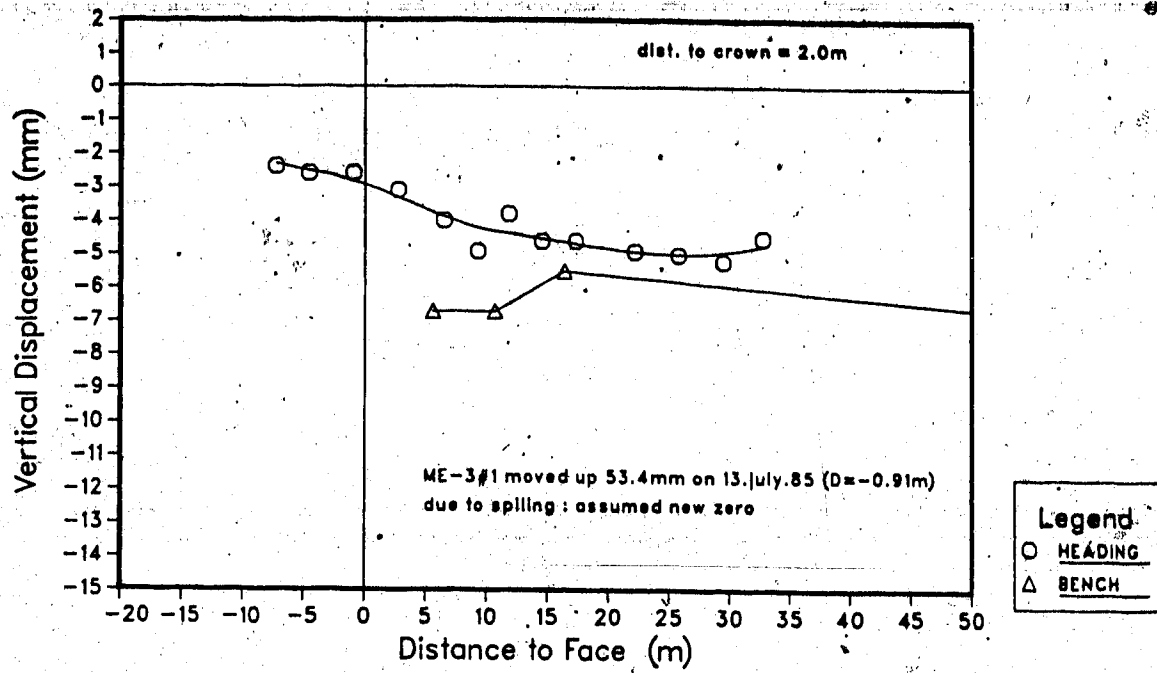


Figure C11 - Longitudinal distribution of displacements ME3 #1

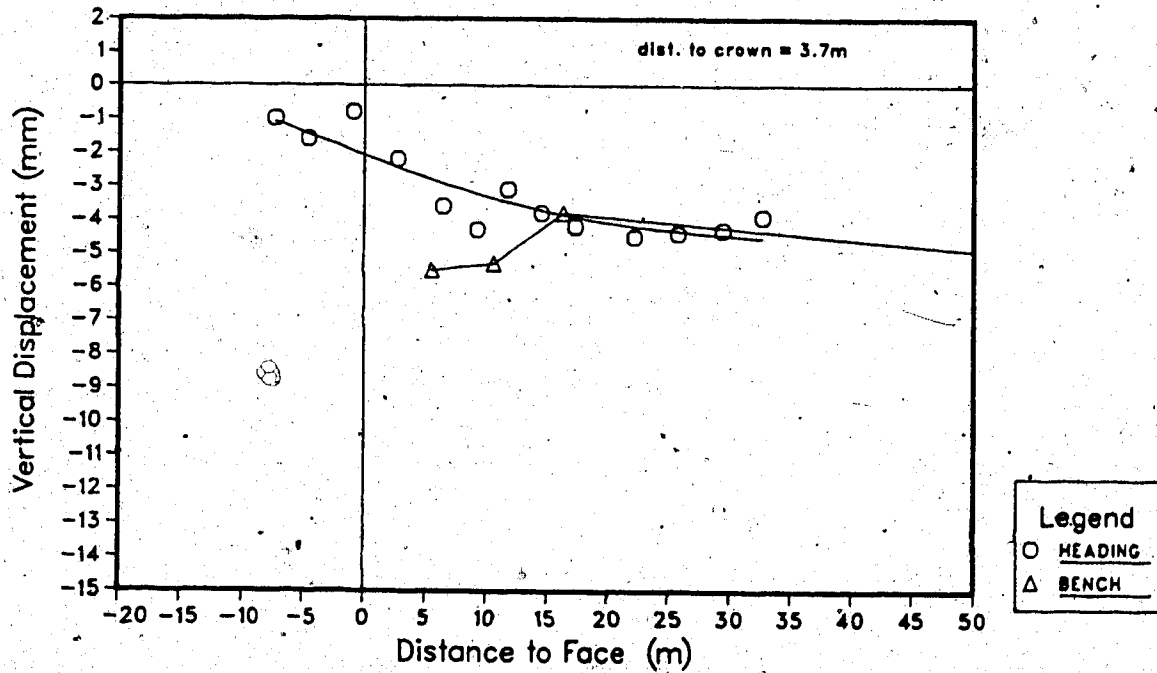


Figure C12 - Longitudinal distribution of displacements ME3 #2

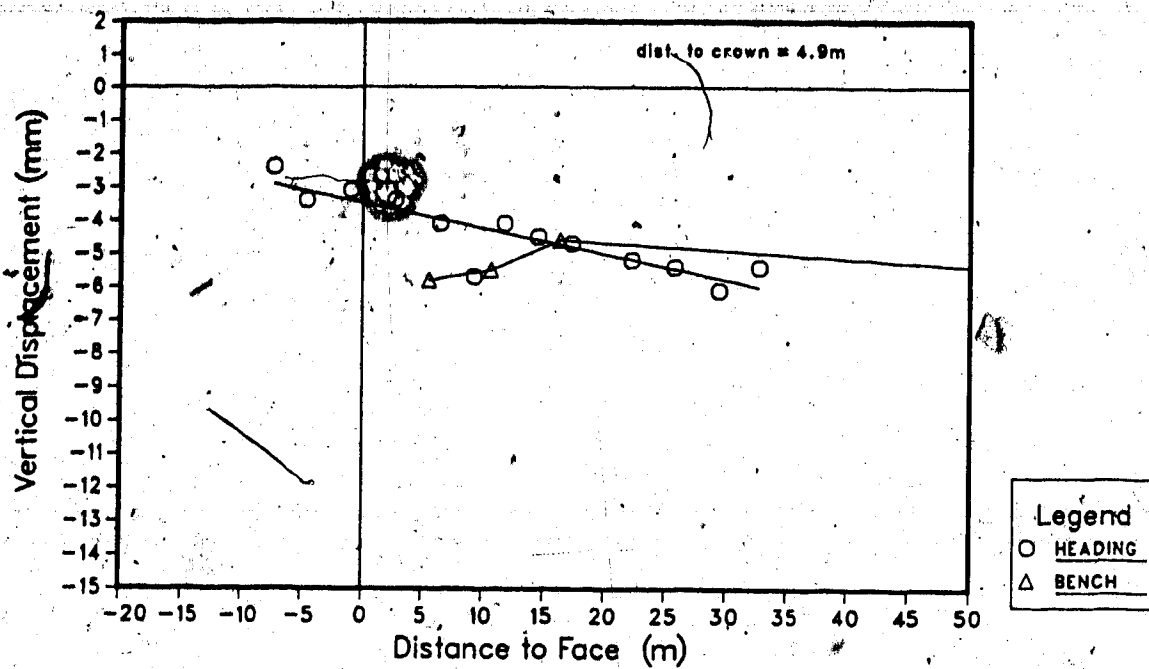


Figure C13 - Longitudinal distribution of displacements ME3 #3

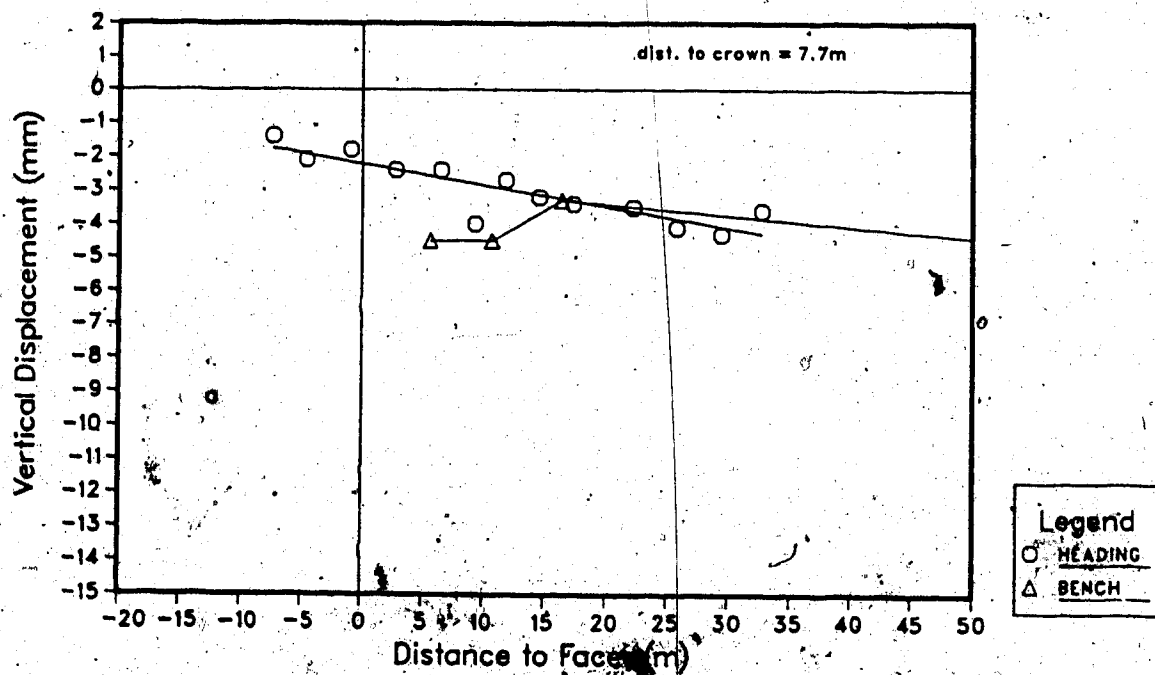


Figure C14 - Longitudinal distribution of displacements ME3 #4

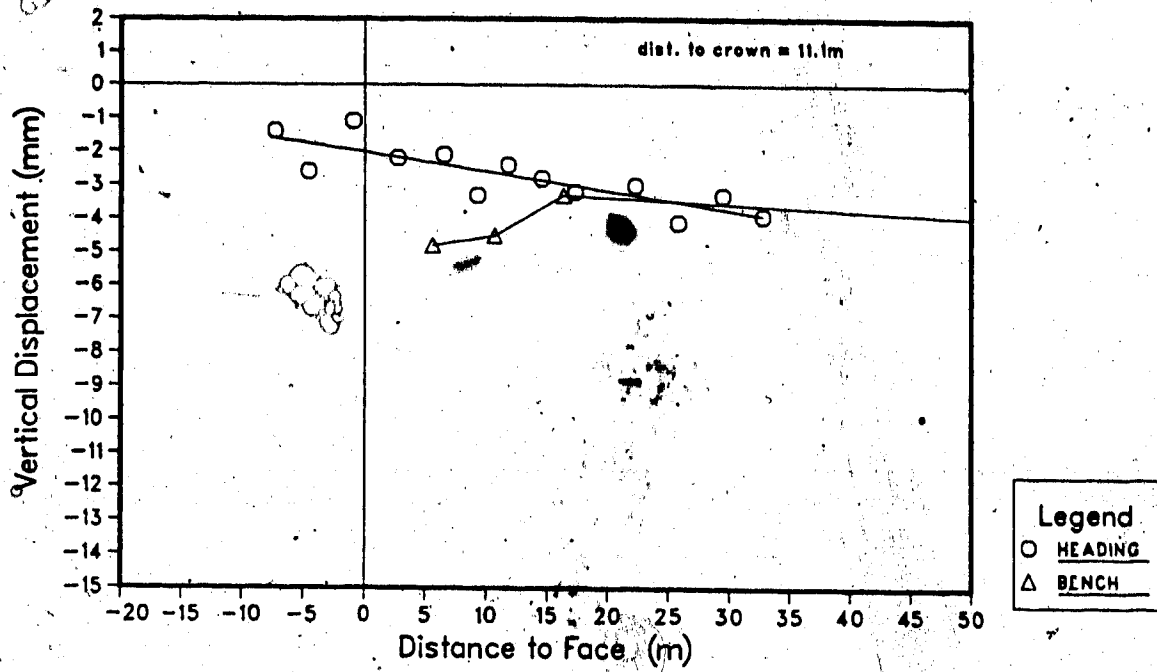


Figure C15 - Longitudinal distribution of displacements ME3 #5

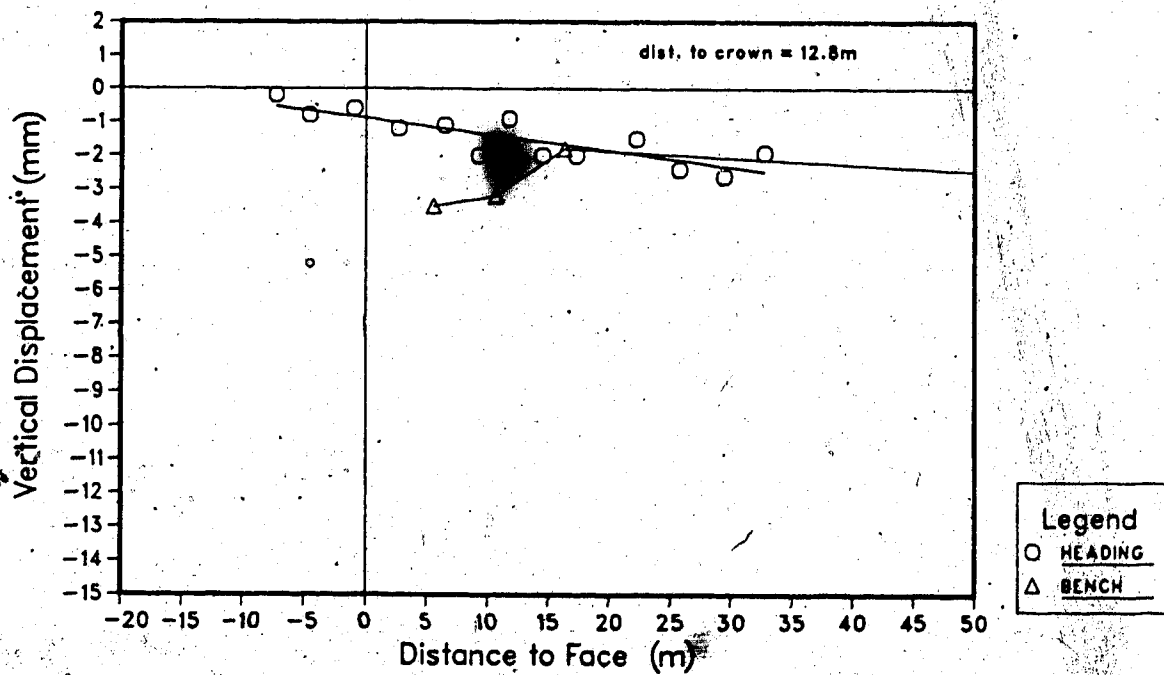


Figure C16 - Longitudinal distribution of displacements ME3 #6

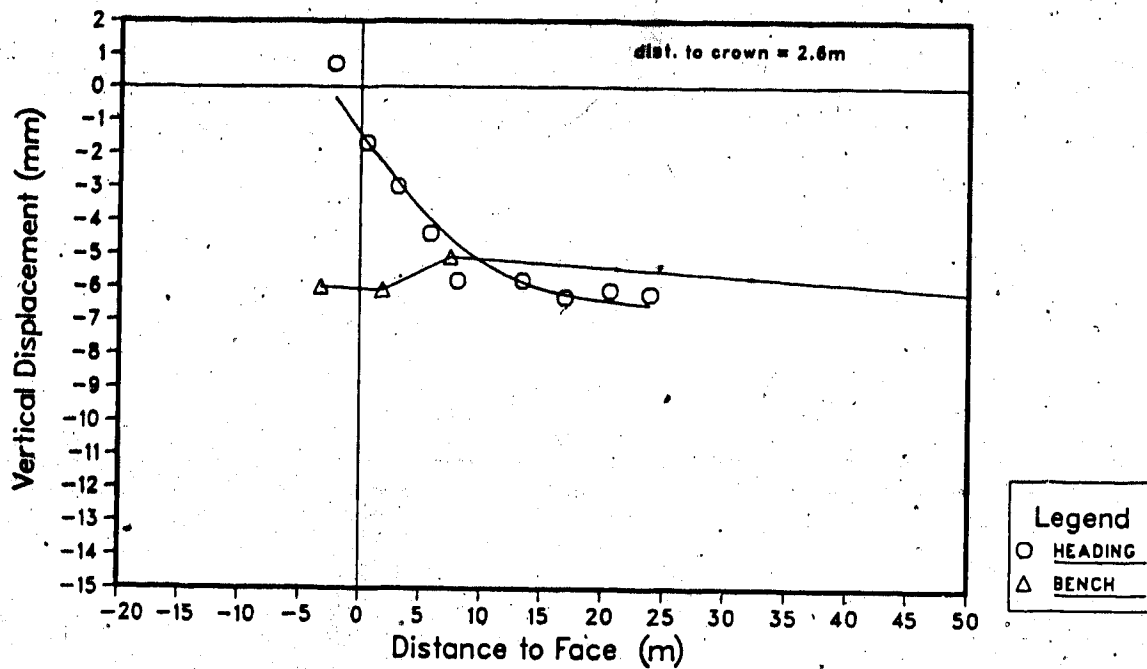


Figure C17 - Longitudinal distribution of displacements ME4 #1

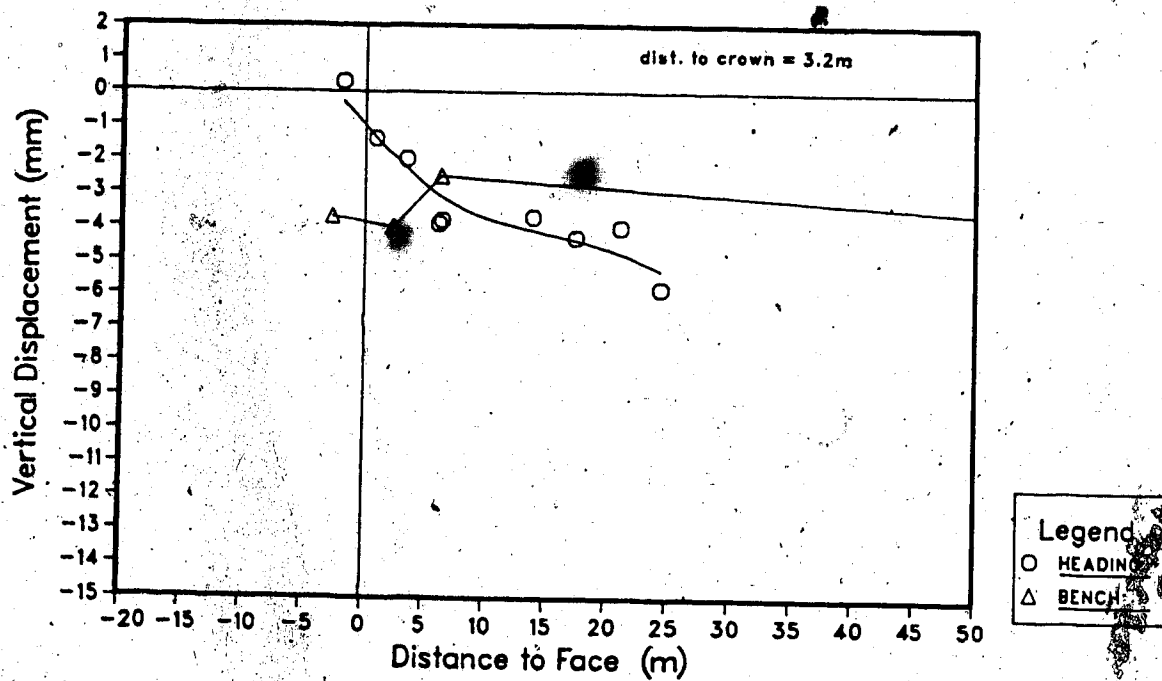


Figure C18 - Longitudinal distribution of displacements ME4 #2

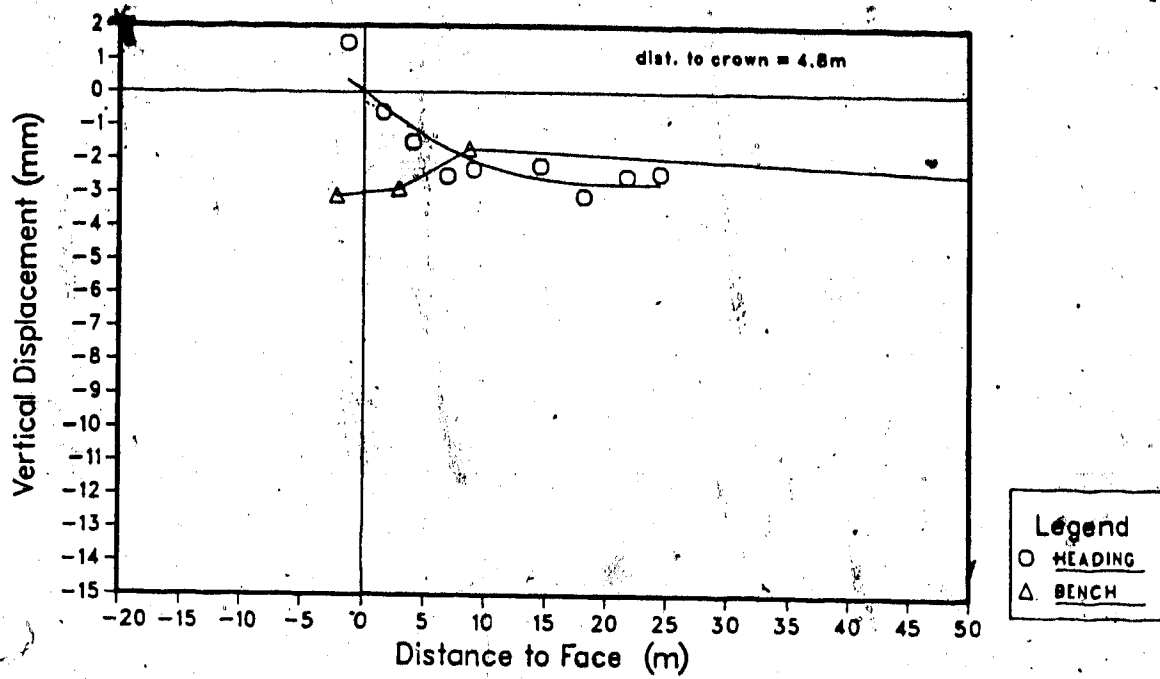


Figure C19 - Longitudinal distribution of displacements ME4 #3

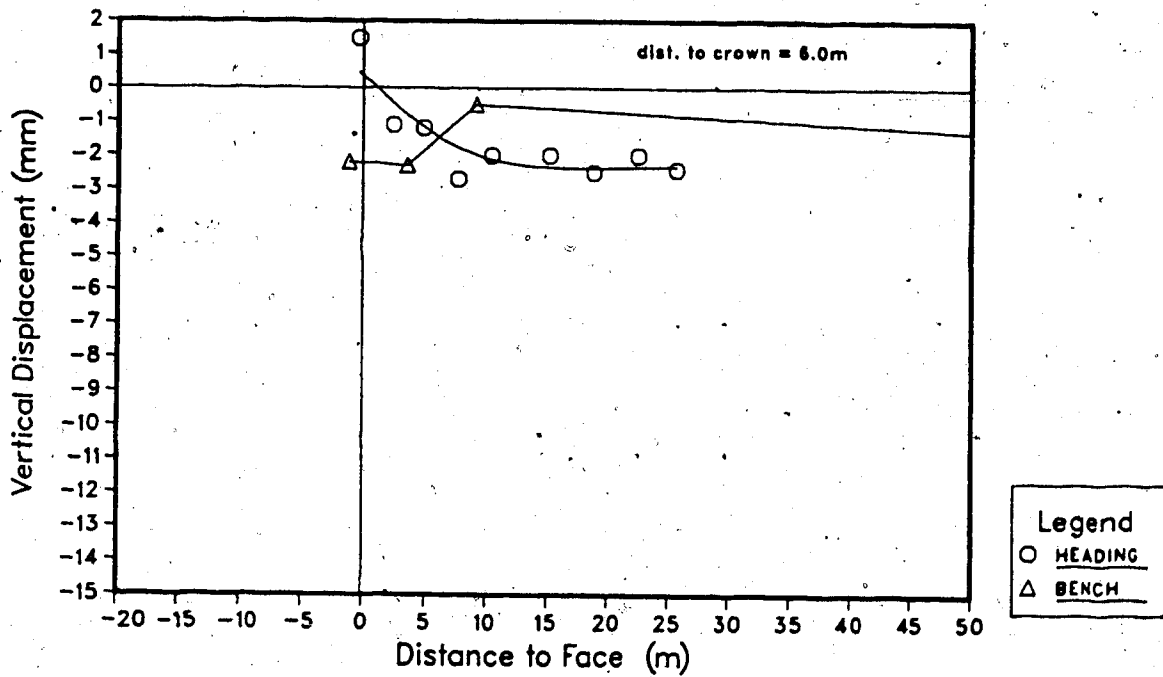


Figure C20 - Longitudinal distribution of displacements ME4 #4

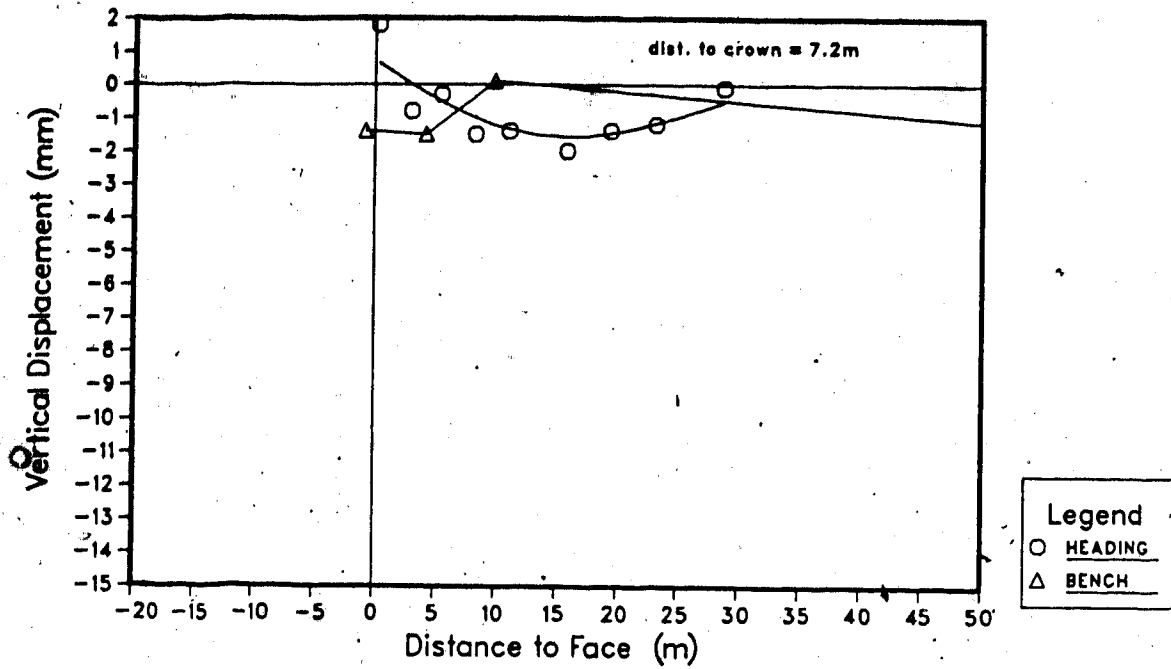


Figure C21 - Longitudinal distribution of displacements ME4 #5

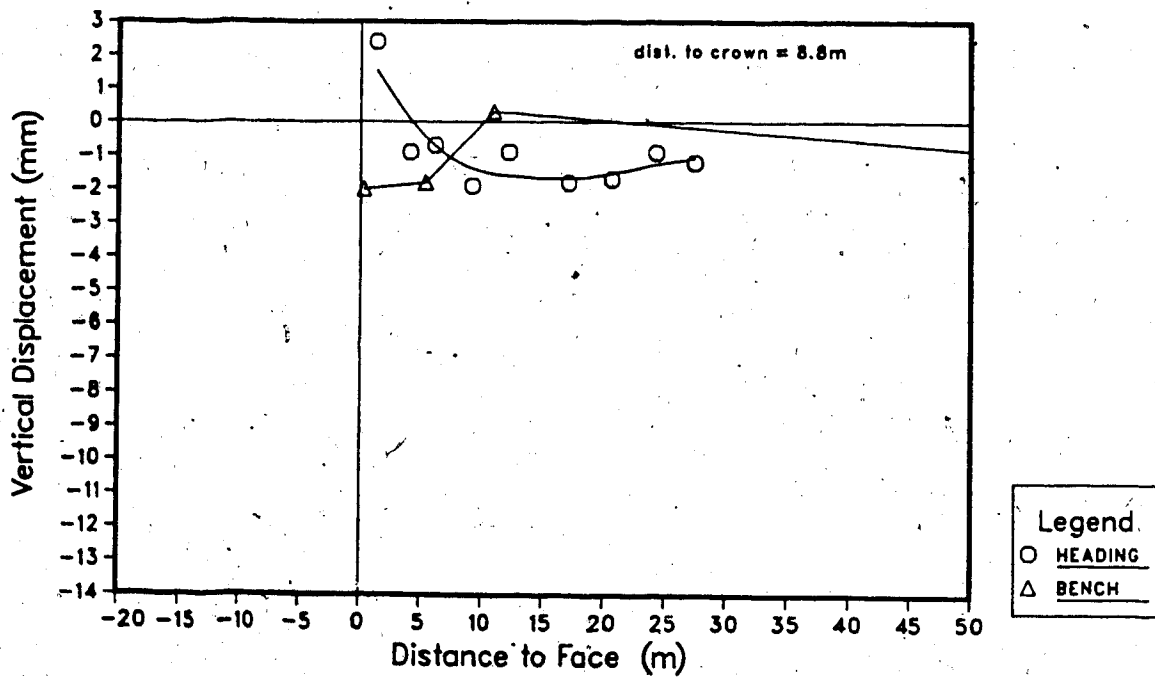


Figure C22 - Longitudinal distribution of displacements ME4 #6

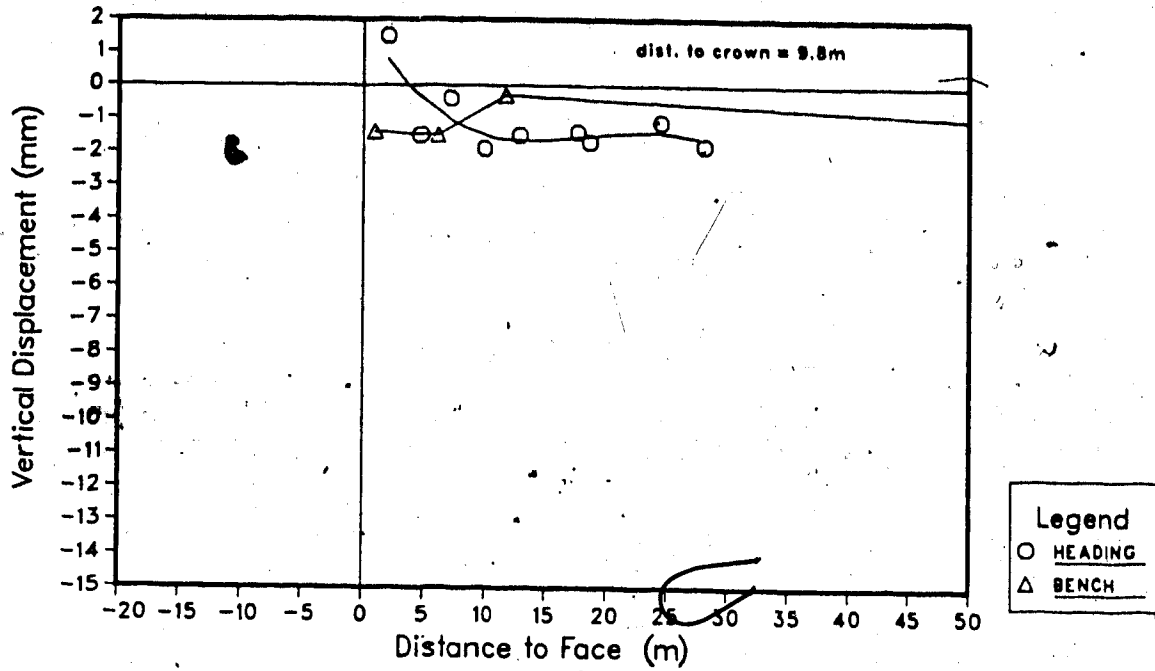


Figure C23 - Longitudinal distribution of displacements ME4 #7

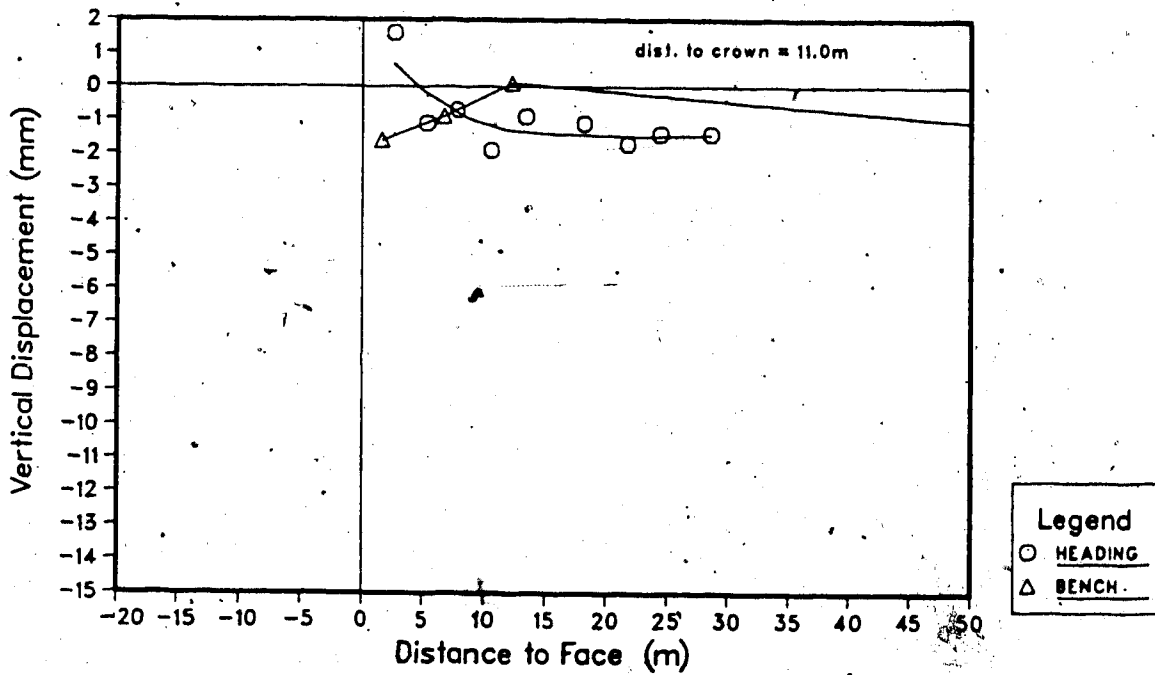


Figure C24 - Longitudinal distribution of displacements ME4 #8

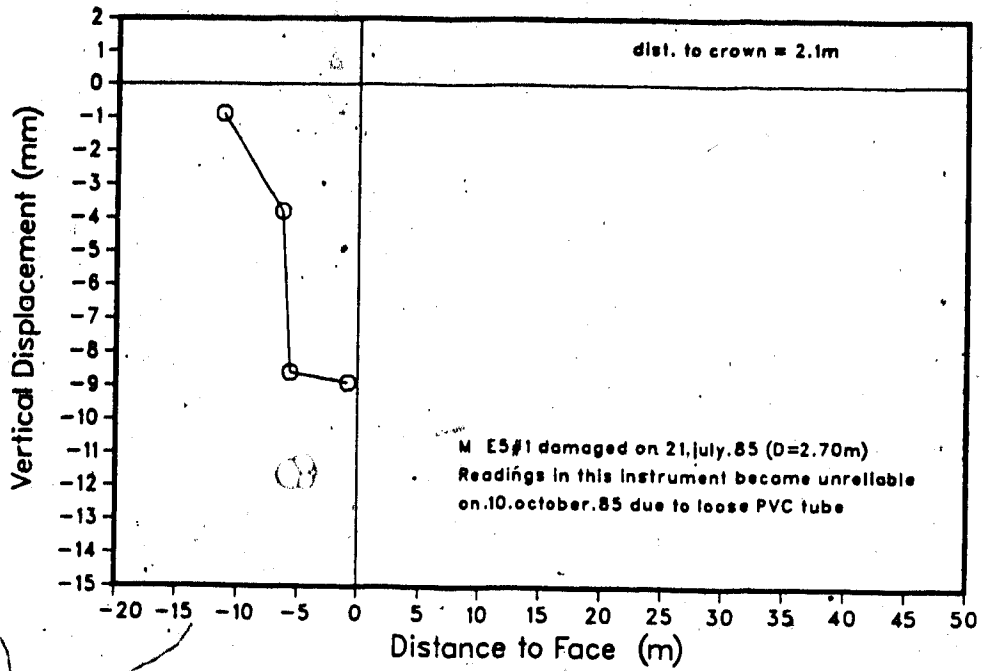


Figure C25 - Longitudinal distribution of displacements ME5 #1

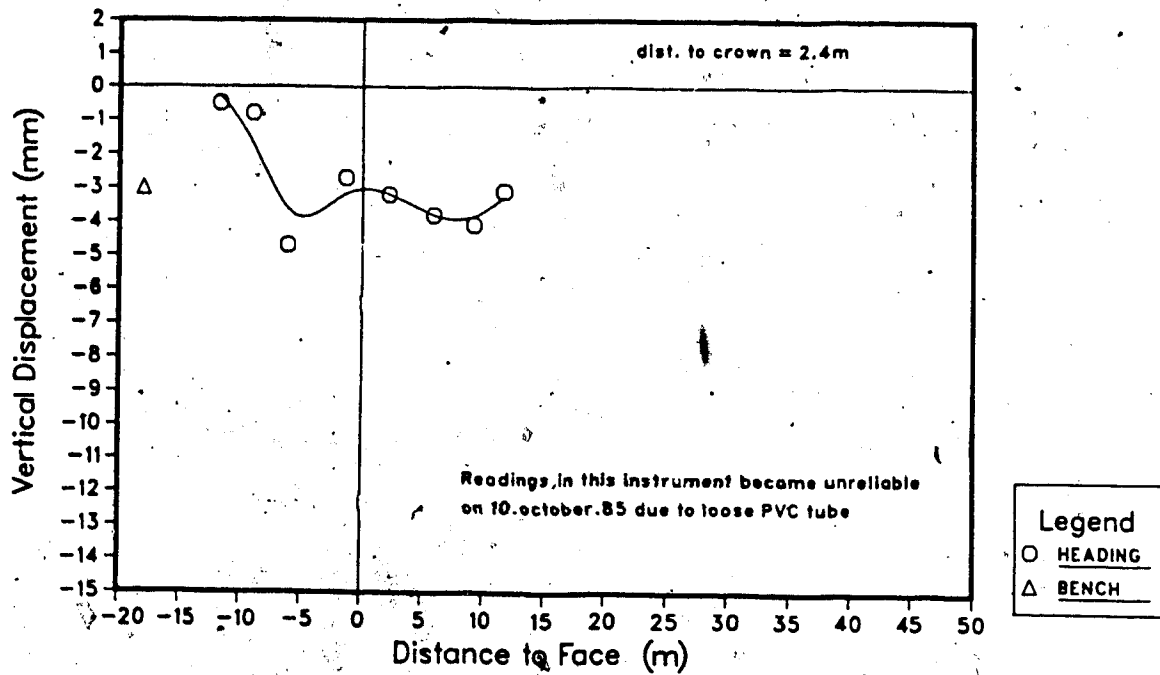


Figure C26 - Longitudinal distribution of displacements ME5 #2

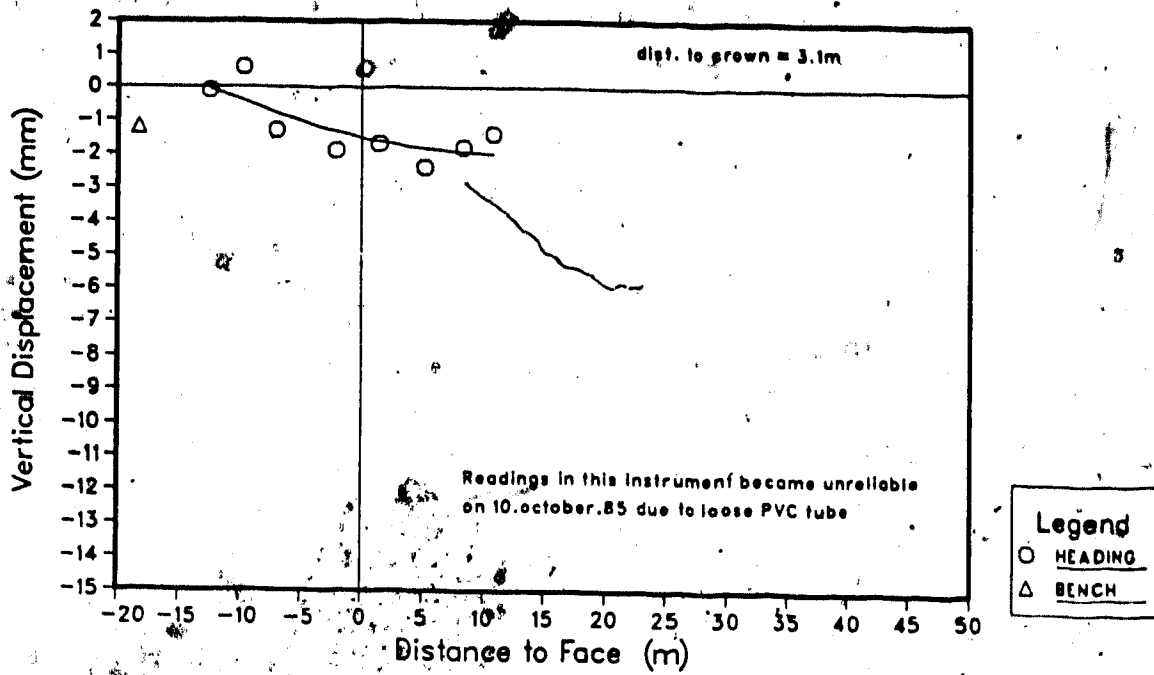


Figure C27 - Longitudinal distribution of displacements ME5 #3

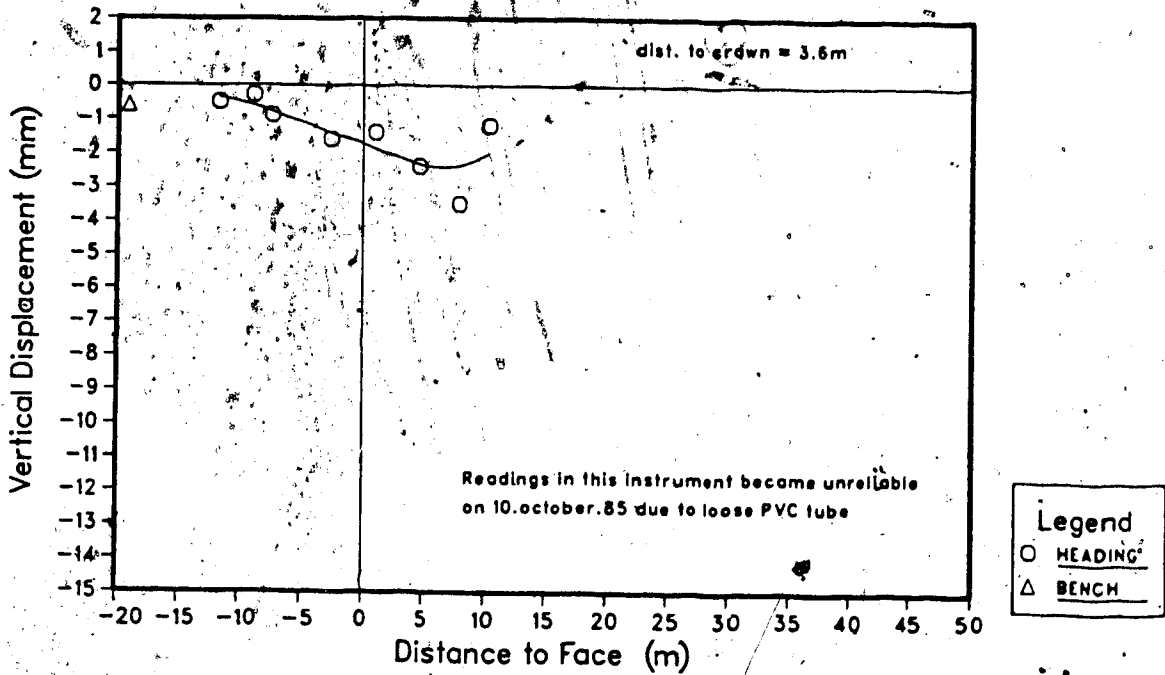


Figure C28 - Longitudinal distribution of displacements ME5 #4

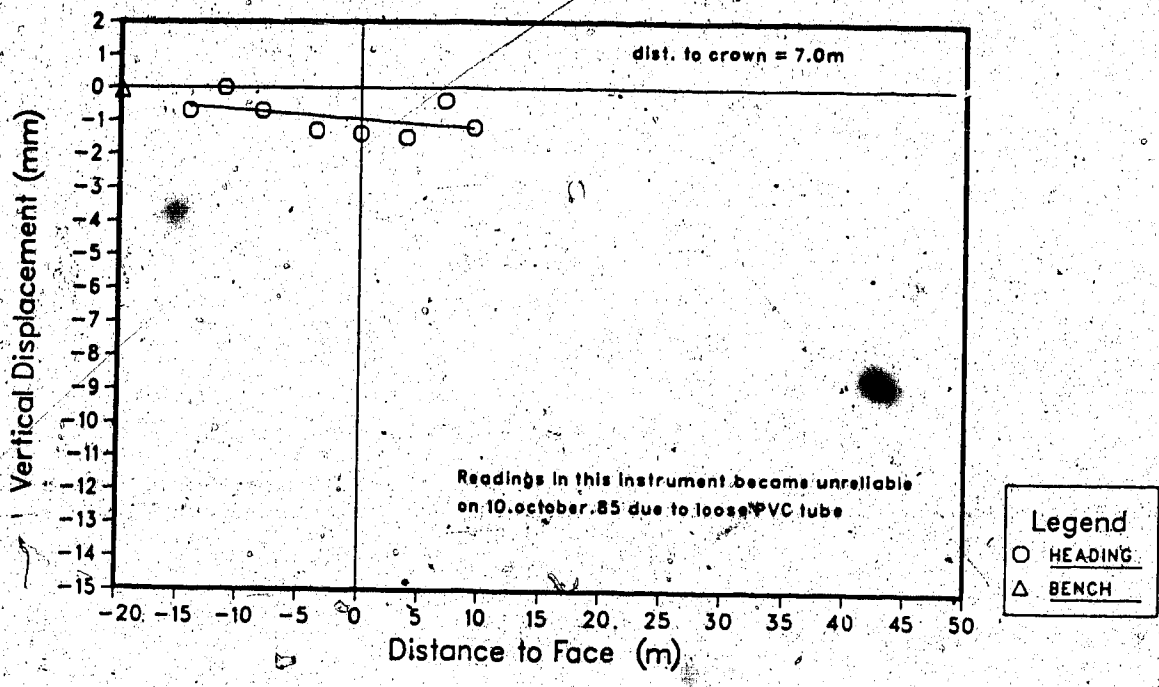


Figure C29 - Longitudinal distribution of displacements ME5 #5

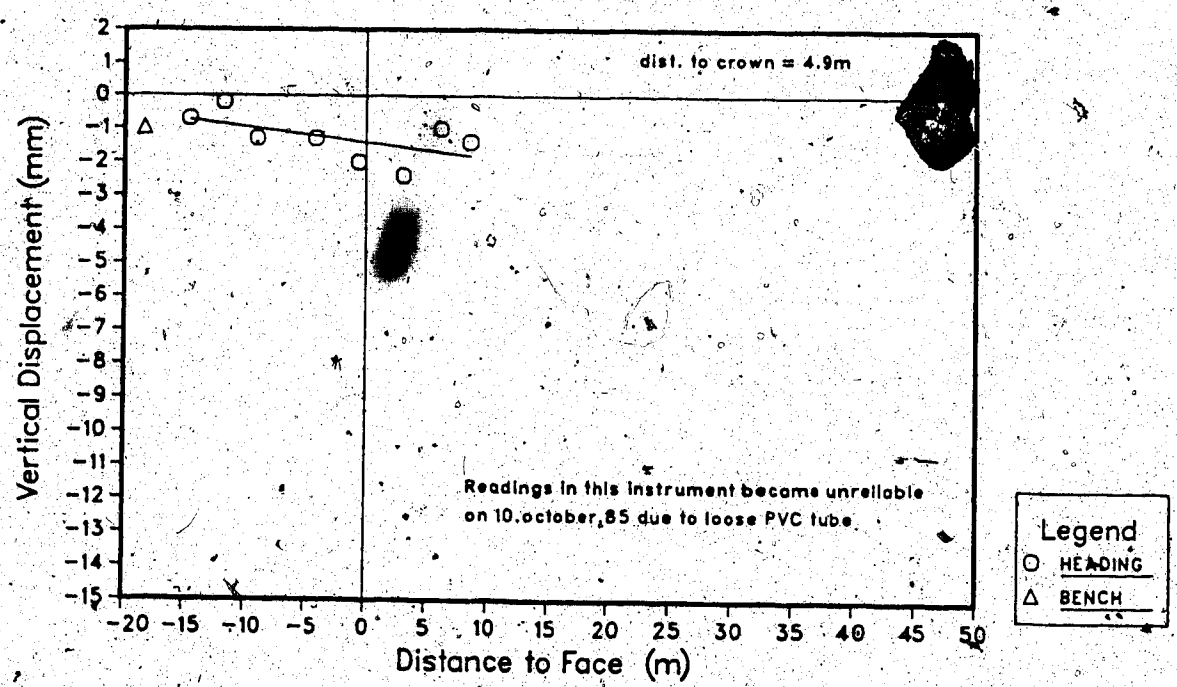


Figure C30 - Longitudinal distribution of displacements ME5 #6

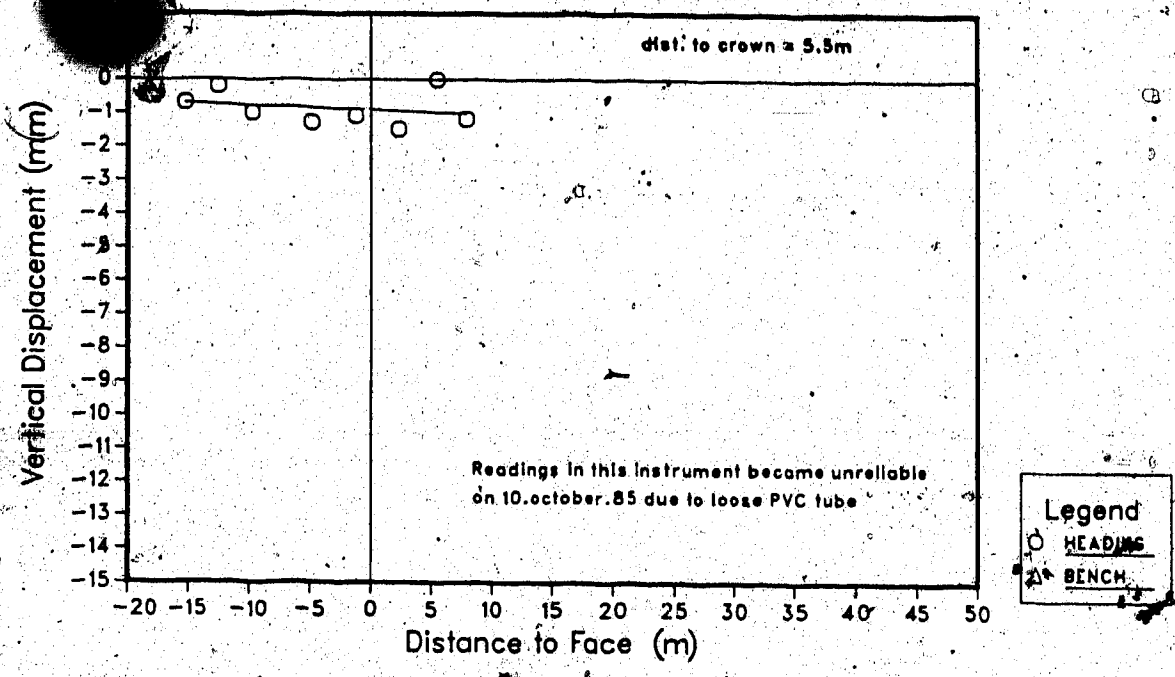


Figure C31 - Longitudinal distribution of displacements ME5 #7

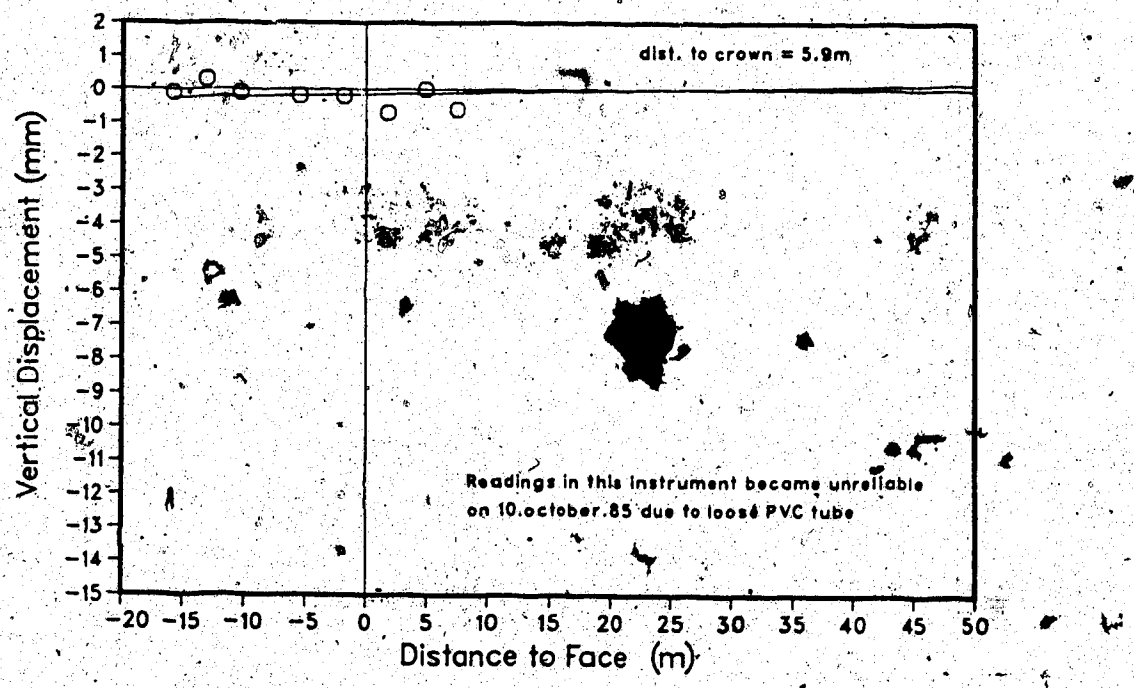


Figure C32 - Longitudinal distribution of displacements ME5 #8